A LABORATORY STUDY ON THE USE OF LIME COLUMNS TO IMPROVE EXPANSIVE SOILS

A THESIS SUBMITTED TO
THE GRADUATE SCHOOL OF NATURAL AND APPLIED SCIENCES
OF
MIDDLE EAST TECHNICAL UNIVERSITY

BY

İLYAS ÖZKAN

IN PARTIAL FULFILLMENT OF THE REQUIREMENTS
FOR
THE DEGREE OF DOCTOR OF PHILOSOPHY
IN
CIVIL ENGINEERING

SEPTEMBER 2021

Approval of the thesis:

A LABORATORY STUDY ON THE USE OF LIME COLUMNS TO IMPROVE EXPANSIVE SOILS

submitted by **İLYAS ÖZKAN** in partial fulfillment of the requirements for the degree of **Doctor of Philosophy** i**n Civil Engineering, Middle East Technical University** by,

Prof. Dr. Halil Kalıpçılar
Dean, Graduate School of **Natural and Applied Sciences** _____

Prof. Dr. Ahmet Türer
Head of the _____

Prof. Dr. Erdal Çokça
Civil Engineering Dept., METU _____

Examining Committee Members:

Prof. Dr. Erdal Çokça
Civil Engineering Dept., METU _____

Prof. Dr. Bahadır Sadık Bakır
Civil Engineering Dept., METU _____

Prof. Dr. Nihat Sinan Işık
Civil Engineering Dept., Gazi Uni. _____

Prof. Dr. Seyhan Fırat
Civil Engineering Dept., Gazi Uni. _____

Assoc. Prof. Dr. Nejan Huvaj Sarıhan
Civil Engineering Dept., METU _____

Date: ...

I hereby declare that all information in this document has been obtained and presented in accordance with academic rules and ethical conduct. I also declare that, as required by these rules and conduct, I have fully cited and referenced all material and results that are not original to this work.

Name Last name : İlyas Özkan

Signature :

ABSTRACT

A LABORATORY STUDY ON THE USE OF LIME COLUMNS TO IMPROVE EXPANSIVE SOILS

Özkan, İlyas
Doctor of Philosophy, Civil Engineering
Supervisor : Prof. Dr. Erdal Çokça

September 2021, 228 pages

Expansive soils are well-known for their cyclic shrink-swell behavior due to seasonal moisture changes. These cyclic movements of expansive soils are due to physico-chemical changes at the particle level that are dependent on mineralogical composition of these soils. The soil depths susceptible to moisture changes are known as active depths and based on previous studies vary from shallow to deep depths. Movements from these depths reflect to the surface leading to considerable deformation to overlying infrastructures. Therefore, it is necessary to improve the expansive soils prior to any construction activity on these soils. Since several available methods are unsuitable for deep soil stabilization, soil improvement with lime column technique is studied in this research. Lime column technique has been applied for stabilizations of expansive soil. However, lime column which contains lignosulfonate has not been studied in the literature. The main objective of this study is that investigation of influence of lignosulfonate on lime column technique. Laboratory testing program is conducted with a high plasticity clay specimen consisting of kaolinite and bentonite mixed in laboratory. The change of unconfined compressive strength, swelling potential, coefficient of permeability, CEC and SSA of the treated specimen during the

stabilization process is studied. The effect of scale of specimens on the test results were studied using different size boxes.

Lime diffusion into the soil is a considerable factor in this technique. Lignosulfonate as an additive material is added to the lime column to accelerate lime diffusion into the soil. The effectiveness of the lime column technique in both minimizing swell behaviour and changing the strength of expansive soils up to considerable depths are investigated in the present research by conducting comprehensive laboratory studies. The effectiveness of lignosulfonate lime column (LLC) treatment method is evaluated in terms of reducing heave movements of underlying expansive soils. A new method is proposed in this study: the combined improvement method (CIM) which includes three techniques that are prewetting, lignosulfonate lime columns, and geotextile+anchor. While the treated specimens with LLC included 37 pieces column, the number of the columns installed in treated specimen with CIM is only 19. The change of soil parameters are analyzed by testing both treated samples and untreated samples. The results of the free swell test, CBR test showed that both improvement methods strengthen the soil properties with the curing period. Besides, the change of properties of specimens taken from a region placed between the columns was observed by using the free swell test, unconfined compressive strength test, SEM-EDX analysis. The outputs of these tests and analyses indicated that the soil properties improved with these methods as follows:

The height of the lime column should be the depth of the active zone during the lime column stabilization. The swelling potential of the treated specimen with the lime column method decreases as the water content of the lime columns increase. The addition of the lignosulfonate to lime columns increases the diffusion rate of the lime particles into the expansive soil specimen prepared in this study. The calcium lignosulfonate type is more effective than the sodium lignosulfonate for stabilization. The unconfined compressive strengths of the treated specimens with lignosulfonate lime columns are greater than the untreated specimens.

The treated specimen with CIM is more stable and resistant to volumetric change than both the other treated specimens and untreated specimens prepared in this study. Also, the improvement process of the CIM method is faster than the other methods applied in this study.

In this study, a design method (CIM) was developed and it has been shown that the high swelling potential of subgrade clay layers, in the active depth, can be reduced to low swelling potential values by this method.

Keywords: Expansive soil, stabilization, lime column, lignosulfonate

ÖZ

ŞİŞEN ZEMİNLERİ İYİLEŞTİRMEK İÇİN KİREÇ KOLONLARI KULLANILMASI ÜZERİNE LABORATUVAR ÇALIŞMASI

Özkan, İlyas
Doktora, İnşaat Mühendisliği
Tez Yöneticisi: Prof. Dr. Erdal Çokça

Eylül 2021, 228 sayfa

Şişen zeminler, mevsimsel nem değişikliklerinden dolayı oluşan döngüsel büzüşme-şişme davranışlarıyla tanınırlar. Şişen zeminlerde meydana gelen döngüsel hareketler, bu zeminlerin mineralojik yapısına bağlı olarak parçacık düzeyindeki fiziko-kimyasal değişimlerinden ileri gelmektedir. Su içeriği değişimine yatkın zemin derinliği, aktif derinlik olarak bilinir ve önceki çalışmalara göre bu derinlik değişiklik gösterir. Bu derinliklerdeki hareketler, altyapıları örten zeminlerdeki önemli deformasyonları yüzeyde yansıtır. Sonuç olarak, bu tür zeminler üzerinde herhangi bir yapı çalışmasından önce şişen zeminlerin iyileştirilmesi gerekmektedir. Mevcut yöntemlerin birçoğu derin zemin stabilizasyonuna uygun olmadığı için bu araştırmada kireç kolon tekniği ile zemin iyileştirilmesi çalışılmıştır. Şişen zeminlerin stabilizasyonu için kireç kolon tekniği uygulanmıştır. Bununla birlikte lignosülfonat içeren kireç kolon, literatürde çalışılmamıştır. Bu çalışmanın esas amacı, kireç kolon tekniği üzerindeki lignosülfonat etkisinin araştırılmasıdır. Kaolinin ve bentonitin karıştırılmasıyla oluşturulan yüksek plastisiteli bir kil numunesi üzerinde laboratuvar çalışmaları yürütülmüştür. Stabilizasyon süresi boyunca iyileştirilmiş numunelerin serbest basınç mukavemeti, şişme potansiyeli, permeabilite katsayısı, CEC, SSA değişimi araştırılmıştır. Boyut etkisinin test sonuçları üzerindeki etkisi farklı ölçekler-

deki kalıplar kullanılarak araştırılmıştır.

Zemin içerisindeki kireç difüzyonu, bu teknikte önemli bir faktördür. Zemin içerisindeki kireç difüzyonunu artırmak için kireç kolonlara katkı malzemesi olarak lignosülfonat ilave edilmiştir. Kireç kolonu tekniğinin, hem şişme davranışını en aza indirmedeki hem de zeminin mukavemetini önemli derinliklere kadar değiştirmedeki etkinliği kapsamlı laboratuvar çalışmaları yürüterek araştırılmıştır. Lignosülfonatlı kireç kolon metodunun etkisi, şişen zeminlerin kabarma hareketi bakımından değerlendirilmiştir. Bu çalışmada yeni bir metod tasarlanmıştır: Birleştirilmiş iyileştirme metodu, ön ıslatma, lignosülfonatlı kireç kolon ve geotextile+ankraj tekniklerini içermektedir. LLC ile iyileştirilen numuneler 37 adet kolondan oluşurken, CIM ile iyileştirilen numunelerde kolon sayısı yalnızca 19 adettir. Zemin parametrelerindeki değişim, iyileştirilmiş ve iyileştirilmemiş numuneler test edilerek araştırılmıştır. Serbest şişme ve CBR deney sonuçları, her iki iyileştirme metodunun, zemin özelliklerini kür etkisi ile güçlendirdiğini göstermektedir. Ek olarak, kolonlar arasındaki bir bölgeden alınan numunelerin özelliklerindeki değişim, serbest şişme deneyi, tek eksenli basınç deneyi, SEM-EDX analizi gibi testlerle gözlemlenmiştir. Bu test ve analizlerin sonuçları, zemin özelliklerinin bu metodlar ile iyileştiğini aşağıda belirtildiği gibi göstermiştir:

Kireç kolon stabilizayonunda, kireç kolonun yüksekliği aktif bölgenin derinliği kadar olmalıdır. Kireç kolonun su muhtevası arttığında, kireç kolon metodu ile iyileştirilen numunelerin şişme potansiyeli azalmaktadır. Kireç kolona lignosülfonat ilavesi, bu çalışmada hazırlanan şişen zemin içerisindeki kireç parçacıklarının difüzyon hızını artırmıştır. Stabilizasyon için kalsiyum lignosülfonat, sodyum lignosülfonata göre daha etkilidir. Lignosülfonat kireç kolon ile iyileştirilen numunelerin serbest basınç mukavemeti, iyileştirilmemiş numunelerinkinden daha büyüktür.

Birleştirilmiş iyileştirme metodu (CIM) ile iyileştirilen numuneler, bu çalışmada hazırlanan iyileştirilmemiş ve diğer iyileştirilen numunlere göre hacimsel değişikliğe karşı daha rijit ve dayanıklıdır. Aynı zamanda CIM metodunun iyileştirme süreci, bu çalışmada uygulanan diğer metodlara göre daha hızlıdır.

Bu çalışmada bir tasarım yöntemi (CIM) geliştirilmiş ve alt temel kil tabakalarının aktif derinlikteki yüksek şişme potansiyelinin bu yöntemle düşük şişme potansiyeli değerlerine indirilebileceği gösterilmiştir.

Anahtar Kelimeler: Şişen zeminler, stabilizasyon, kireç kolon, lignosülfonat

To My family

ACKNOWLEDGMENTS

I would like to express sincere appreciation to my supervisor, Prof. Dr. Erdal Çokça for his guidance, continuous understanding, invaluable patience and support throughout this research.

The author would like to thank Prof. Dr. Nihat Sinan Işık and Assoc.Prof. Dr. Nejan Huvaj Sarıhan for their valuable supports and contributions during the progress of the thesis.

I also wish to express my special thanks Mr. Ulaş Nacar, technician Mr. Kamber Bilgen and technician Mrs. Gülşah Bilici for their support and friendly approach throughout the laboratory works.

Finally, I express my sincere thanks to my father Bahattin Özkan, to my mother Zekiye Özkan, my brother Ramazan Özkan for their endless supports throughout my life.
The author is grateful to his wife Hacer, for her continuous support, encouragement and patience.

TABLE OF CONTENTS

ABSTRACT v

ÖZ viii

ACKNOWLEDGMENTS xii

TABLE OF CONTENTS xiii

LIST OF TABLES xviii

LIST OF FIGURES xxii

LIST OF ABBREVIATIONS xxxiii

LIST OF SYMBOLS xxxiv

CHAPTERS

1 INTRODUCTION 1

1.1 General Background of the Study 1

1.2 Research Methodology and Objectives 2

1.3 Thesis Outline 3

2 LITERATURE REVIEW 5

2.1 Introduction 5

2.2 Expansive Soil 5

2.1.1 Clay Mineralogy 9

2.1.2 Active Zone 12

2.1.3 Expansive Soil Treatment Methods 14

2.3 Lime Stabilization of Expansive Soil 14

2.3.1 Lime Stabilization Mechanism 15

2.3.2 Lime Column Method 22

2.4 Lignosulfonates 26

2.4.1 Interaction mechanism of lignosulfonates with soil particles 30
2.4.2 Applications 31
2.5 Design Approaches and Treatment Alternatives for Highway Constructed on Expansive Soil 34
2.5.1 Subgrade Design and Construction 36
2.5.2 Lime Stabilization of Subgrade/Subbase Layer of Highway pavement 39
3 INDEX AND ENGINEERING PROPERTIES OF EXPANSIVE SOIL SPECIMEN AND LIME COLUMNS 43
3.1 Expansive Soil Specimen 43
3.1.1 Properties of Specimen A 44
3.1.2 Physical Properties 45
3.1.3 Engineering Properties 50
3.1.4 SEM-EDX Analysis 59
3.1.5 Classifications of Specimen A 61
3.2 Lime Columns 62
3.2.1 Selection of Column Installation Model 63
3.2.2 Factors Affecting the Achievement of the Lime Column Technique 69
3.2.3 Effect of Scale of the Specimens on the Test Results 83
4 LABORATORY MODEL TESTS FOR SCALE EFFECT BY USING 30 CM X 30 CM BOX 91
4.1 Introduction 91
4.2 Engineering Properties 91
4.2.1 Unconfined Compressive Strength 96
4.2.2 Swelling Potential 97
4.2.3 Coefficient of Permeability 98

4.2.4 California Bearing Ratio 98
4.3 Physical Properties 103
4.3.1 Methylene Blue Test 103
4.4 SEM-EDX analysis 107
5 COMBINED IMPROVEMENT METHOD 111
5.1 Combined Improvement Method 111
5.2 Free Swell Test On The Oedometer Ring 116
5.2.1 Test Specimens In Oedometer Ring 116
5.2.2 Effect of Scale of the Specimens 118
5.3 The Strength of the Specimens for Combined Improvement Method ... 120
6 DISCUSSION ON TEST RESULTS 123
6.1 Effect of Different Lime Column Installation Models on Swell Potential Test Results 123
6.1.1 Column Installation Model 124
6.1.2 The Height of the Column 125
6.1.3 The Surrounding Area of all Columns 127
6.1.4 The Water Percentages of the Water-Lime Mixture 128
6.1.5 Lignosulfonate Added to the Water-Lime Mixture 133
6.1.6 Effect of Scale of the Specimens 137
6.2 The Change of Unconfined Compressive Strength, Swelling Potential, Coefficient of Permeability, CEC And SSA of the Treated Specimen During The Stabilization Process 145
6.2.1 Unconfined Compressive Strength 145
6.2.2 Swelling Potential 147
6.2.3 Coefficient of Permeability 148

6.2.4 California Bearing Ratio 149
6.2.5 Physical Properties 154
6.3 SEM-EDX analysis 156
6.3.1 SEM Analysis 156
6.3.2 EDX Analysis 160
6.4 Comparison of the Effect of Sodium Lignosulfonate and Calcium lignosulfonate Addition to the Lime Columns 167
6.4.1 The Change of the Swelling Potentials, CBR Swell, and CBR Values of the Stabilized Block Soil Specimens with both Sodium and Calcium Lignosulfonate Lime Columns 168
6.4.2 The Change of the Unconfined Compressive Strength, Swell Potential and CBR Values of the Stabilized Soil Specimens (between the lignosulfonate lime columns) 173
6.4.3 The Correlation Between The Soil Bearing Capacity (CBR) and Unconfined Compressive Strength (UCS) of Specimens 175
6.5 Combined Improvement Method 178
6.5.1 Free Swell Test on the Oedometer Ring 179
6.5.2 Effect of Scale of the Specimens 180
6.5.3 California Bearing Ratio 184
6.6 Comparison of the Lignosulfonate Lime Columns method and Combined Improvement Method 189
6.6.1 The change of the swelling potential of the treated specimens 190
6.6.2 The Change of the Strength Properties of the Treated Specimens 191
7 CONCLUSIONS 195
REFERENCES 199

APPENDICES

A. Swelling Potential Versus Time Graphs For Treated Specimen In This Study 206

B. The Calculation of the Improvement Percentages of the Treated Specimens that are M1-2/3h, M1-h, M2-2/3h, and M2-h under 7 kPa surcharge pressure 209

C. The Graph Used To Calculate The Coefficient Permeability Of Both Specimen A And Treated Specimen 213

D. The Calculation of the Area Ratio of Combined Improvement Method 218

E. The Calculation of the Amount of the Water-Lignosulfonate Mixture for Each Column 219

F. The Calculation of the Improvement Percentages of the Correlation Treated Specimens 221

G. EDX diagrams 223

CURRICULUM VITAE 227

LIST OF TABLES

TABLES

Table 2.1 Some types of cracking of asphalt pavements due to the expansive soil subgrade (Dafalla and Shamrani, 2011)..... 7
Table 2.2 Microchemical properties of clay minerals (Nelson and Milner, 1992). 10
Table 2.3 Guidelines for estimating the depth of the active zone (Za) (From EM 1110-1-1904, 1990)..... 13
Table 2.4 The treatment intent and the implications for lime addition and time-dependent reactions (Beetham et al., 2015) 19
Table 2.5 The formations of both ettringite and thaumasite minerals (Hunter, 1988) 21
Table 2.6 The chemical analysis of pulverized calcium and sodium lignosulfonates (%)..... 29
Table 2.7 Suitability of soils type for subgrade applications (arrangement from Schaefer et al. (2008))..... 38
Table 2.8 Rating of both Subgrade and Subbase materials with respect to CBR values Schaefer et al. (2008)..... 39
Table 2.9 Physical and chemical properties of lime used at stabilization process (HTS, 2013) 40
Table 2.10 Properties of stabilized soil with lime after 7 days curing (HTS, 2013)41
Table 2.11 The classification of expansive soil in terms of the swelling potential 42
Table 3.1 Properties of Specimen A investigated in this study 45
Table 3.2 Classification of soil (Seed et al. 1962) 63
Table 3.3 Alterations of area ratio with respect to the number of a circular orbit.. 67
Table 3.4 The lime column properties of treated specimens prepared in this step of the study..... 75
Table 3.5 The improvement percentages and total column surrounding area of treated specimens in this step of the study..... 75

Table 3.6 The percentage of lignosulfonate-water-lime in regards to their weight 80
Table 3.7 The swelling potentials of treated specimens prepared in each step of this improvement process 82
Table 3.8 The properties of lime columns installed in oedometer ring 84
Table 3.9 The properties of lime columns installed in correlation moulds..... 85
Table 3.10 The distance between the two lime columns of the treated specimen in this study 86
Table 4.1 Unconfined compressive strength value of treated and untreated specimens 97
Table 4.2 The swelling potential of treated and untreated specimens under both 7 kPa and 25 kPa 97
Table 4.3 The change of volume compressibility and consolidation coefficient of ... untreated and treated specimens ..……...98
Table 4.4 The treated specimens prepared in this step 102
Table 4.5 The test data obtained from the soaked CBR tests 102
Table 4.6 The properties of the stabilized specimens used for the methylene blue tests 104
Table 4.7 The swelling potentials of treated specimens under 7 kPa surcharge pressure 108
Table 4.8 The specimens prepared for SEM-EDX analysis 108
Table 5.1 Parameters of both lignosulfonate lime columns and combined improvement method 112
Table 5.2 The parameters of correlation specimen prepared in this study 118
Table 5.3 The test data obtained from the soaked CBR tests done on the specimen treated with CIM 121
Table 6.1 The swelling potentials of treated specimens with lime column and untreated specimen under 7 surcharge pressure..... 125
Table 6.2 The lime column properties of treated specimens that are M1-2/3h, M1-h, M2-2/3h, and M2-h 127

Table 6.3 Improvement percentages of treated specimens in this step under 7 kPa 128
Table 6.4 The swelling potentials of M2-h treated specimens under 7 kPa surcharge pressure 129
Table 6.5 The improvement percentages of M2-h treated specimens under 7 kPa surcharge pressure 129
Table 6.6 Specimens selected for SEM analysis 130
Table 6.7 The swelling potentials of M2-h (30%), NaLS, and CaLS specimens under both 7 kPa surcharge pressure 133
Table 6.8 The swelling potentials of M2-h (30%), NaLS, and CaLS specimens under both 25 kPa surcharge pressure 133
Table 6.9 The classification of both untreated and treated specimens according to Seed et al. 1962 134
Table 6.10 The specimens used for the SEM analysis 135
Table 6.11 The properties of specimens prepared in this step 138
Table 6.12 Correlation specimens classification with respect to Seed et. al. (1962) 141
Table 6.13 The soil properties examined in this step 145
Table 6.14 The coefficient permeability values of untreated and treated specimens with curing period 148
Table 6.15 The evaluation of the treated specimens in regards to both HTS (2013) and Schaefer et al. (2008) 154
Table 6.16 Test specimens and final readings of methylene blue test done in this step 155
Table 6.17 The microchemical properties of both untreated and treated specimen used in this study 155
Table 6.18 The swelling potentials of the treated specimens used for SEM analysis 158
Table 6.19 Specimens are used for EDX analysis in this study 160

Table 6.20 The microchemical compositions of test specimens obtained from EDX analysis 160
Table 6.21 The diffusion coefficient of the ions of the slaked lime 161
Table 6.22 The parameters of the concentration equations 163
Table 6.23 The solution of concentration equation..... 163
Table 6.24 The swelling potential of the specimens treated with the combined improvement method 179
Table 6.25 The classification of treated specimens with CIM according to Seed et al. 1962.....180
Table 6.26 Correlation specimens classification with respect to Seed et. al. (1962) 182

LIST OF FIGURES

FIGURES

Figure 2.1 Global distribution of reported expansive soil sites (Nelson et al., 2015)6
Figure 2.2 Road damages due to the expansive soils (Dafalla and Shamrani, 2011) 7
Figure 1.1 Road damages types due to the expansive soils (Dafalla and Shamrani, 2011) 8
Figure 2.4 The structure of both octahedral and tetrahedral sheet Murray (2007) ... 9
Figure 2.5 Structure of 1:1 and 2:1 clay minerals (Sivakugan, 2001) 9
Figure 2.6 The SEM images of clay minerals (Murray, 2006) 11
Figure 2.7 Water content profiles in the active zone (Nelson and Miller, 1992).... 12
Figure 2.8 Lime- clay stabilization (Prusinski and Bhattacharja, 1999)..... 17
Figure 2.9 Cation exchange (Prusinski and Bhattacharja, 1999)..... 17
Figure 2.10 Flocculation and agglomeration (Prusinski and Bhattacharja, 1999).. 18
Figure 2.11 SEM views, a- natural soil, b- lime treated soil with 10000ppm sulfate concentration (Celik, 2014)..... 20
Figure 2.12 Column-supported embankment 22
Figure 2.13 Top view of lime column application..... 22
Figure 2.14 Representative structure of calcium lignosulfonate by JECFA in 2008 28
Figure 1.2 a) Binding Units of the LS molecule (After Sulphite Pulp manufacturers' Research League 1963); b) Chemical Structure of LS (After Vinod et al. 2009)... 28
Figure 2.16 Schematic diagram of lignosulfonate stabilization on clay soil (Vinod et al. 2010) 31
Figure 1.3 Erosion rate versus hydraulic shear stress of lignosulfonate treated / untreated silty sand (Indraratna et al., 2010)..... 32
Figure 2.18 UCS value of low plasticity clay improved by additive materials such as lignosulfonates, petroleum emulsion, tree resin, acid (Tingle and Santoni 2003) 33
Figure 2.19 Parts of the pavement system and the properties of materials consisted of these parts (FHWA NHI-05-037, 2006) 35

Figure 2.20 The selection of stabilizer material with respect to soil properties 40
Figure 2.21 The properties of soils stabilized with lime (HTS, 2013)..... 41
Figure 3.1 Kaolinite (left side) and Bentonite (right side)..... 43
Figure 3.2 Grain Size Distribution Curve of Specimen A 46
Figure 3.3 Compaction Curve of Specimen A..... 46
Figure 3.4 The suspension consisted of Specimen A and distilled water..... 47
Figure 3.5 Methylene blue addition to the suspension 48
Figure 3.6 Methylene blue test data obtained from Specimen A..... 48
Figure 3.7 Equipment used for both free swell test and one-dimensional consolidation test 51
Figure 3.8 The change of swelling potential of specimen A with respect to pressures..... 51
Figure 3.9 The steps of flexible wall permeability test..... 53
Figure 3.10 A graph of the cumulative outflow water volume versus time for the vertical permeability of Specimen A 54
Figure 3.11 sA graph of the cumulative outflow water volume versus time for the horizontal permeability of Specimen A 55
Figure 3.12 The unconfined compressive strength of specimen A with respect to water content..... 56
Figure 3.13 The test results of Unsoaked CBR and Soaked CBR 58
Figure 3.14 The CBR value for both unsoaked condition and soaked condition ... 58
Figure 3.15 SEM image of Specimen A (magnification factor=40000)..... 59
Figure 3.16 EDX Diagram of Sample A..... 60
Figure 1.4 Methylene blue activity diagram (modified from both Lautrin 1989 and Chiappone et al, 2004) 62
Figure 3.18 Circular orbit and distance between two columns..... 64
Figure 3.19 Assumption sample for area ratio..... 65
Figure 3.20 Column installation models with respect to the number of the circular orbit..... 66
Figure 3.21 The first model consisted of two circular orbits and 19 columns had a 6.5 mm diameter 68

Figure 3.22 Second model consisted of two circular orbits and 37 columns which have 4.5 mm diameter 68
Figure 3.23 Bishop load frame 69
Figure 3.24 Test program followed at this step of the study 70
Figure 3.25 Oedometer ring dimensions 71
Figure 3.26 Top view and A-A cross-section of M1-2/3h, M1-h, M2-2/3h, and M2-h 72
Figure 3.27 Swelling potentials of treated specimens under 7 kPa 73
Figure 3.28 Improvement percentages of treated specimens in this step under 7 kPa 74
Figure 3.29 Lime-water mixture to water percentage 76
Figure 3.30 The swelling potential of M2-h treated specimens that stabilize with water-lime mixtures (0%, 18%, 30%) without curing and with curing 77
Figure 3.31 The improvement percentages of M2-h treated specimens that stabilize with water-lime mixtures (0%, 18%, 30%) without curing and with curing 77
Figure 3.32 The lignosulfonate used in this study 79
Figure 3.33 The mixture involved lignosulfonate and water 79
Figure 3.34 The mixtures consisted of lime, water, and lignosulfonate 79
Figure 3.35 The swelling potential of M2-h treated specimens that stabilize with lignosulfonate-water-lime mixture without curing and with curing 80
Figure 3.36 The swelling potential of M2-h treated specimens that stabilize with lignosulfonate-water-lime mixture without curing and with curing 81
Figure 3.37 The moulds used in this step of the study 83
Figure 3.38 The example of the bigger specimens 84
Figure 3.39 The swelling potential of the treated specimen with sodium lignosulfonate lime column under 7 kPa 87
Figure 3.40 The swelling potential of the treated specimen with calcium lignosulfonate lime column under 7 kPa 88
Figure 3.41 The swelling potential of the treated specimen with sodium lignosulfonate lime column under 25 kPa 89

Figure 3.42 The swelling potential of the treated specimen with calcium lignosulfonate lime column under 25 kPa 90
Figure 4.1 A big mould used in this study 92
Figure 1.5 Specimen is used in previous work had 6.35 cm diameter (Left side), The specimen is prepared in the big mould (Right side) 92
Figure 4.3 Compaction process…..... 94
Figure 4.4 Scratch process 94
Figure 4.5 A drilling machine, drilling bit and boreholes..... 94
Figure 4.6 Tubes used for undisturbed sampling..... 95
Figure 4.7 The pushing process 95
Figure 4.8 Location of undisturbed samples..... 96
Figure 4.9 The dimensions of both a plunger and a CBR mould..... 99
Figure 4.10 Top view of both a specimen which has 271 columns and a specimen which has 61 columns..... 100
Figure 4.11The soaking step of the CBR test 101
Figure 4.12 The specimens in the CBR machine..... 101
Figure 4.13 The example of the location of the specimen for these tests..... 103
Figure 1.14 Methylene blue test data obtained from NaLS specimen had 7 mm diameter lime column 104
Figure 4.15 Methylene blue test data obtained from CaLS specimen had 7 mm diameter lime column 1045
Figure 1.16 Methylene blue test data obtained from NaLS specimen had 14 mm diameter lime column 1045
Figure 4.17 Methylene blue test data obtained from CaLS specimen had 14 mm diameter lime column 1046
Figure 1.18 Methylene blue test data obtained from NaLS specimen had 21 mm diameter lime column 1046
Figure 4.19 Methylene blue test data obtained from CaLS specimen had 21 mm diameter lime column 1047
Figure 4.20 The test specimens for SEM-EDX analysis 109

Figure 5.1 Nineteen columns instead of thirty-seven columns installed into the untreated soil 112
Figure 5.2 A circular orbit and hexagonal structure 113
Figure 5.3 A flexible crystal tulle used as a geotextile 114
Figure 5.4 Pins 115
Figure 5.5 A plan of the lignosulfonate lime column + pin in this study 115
Figure 5.6 The top view of the treated specimens with the CIM stabilization method..... 116
Figure 5.7 The swelling potential of treated specimens that stabilize with CIM with curing under 7 kPa surcharge pressure 117
Figure 5.8 The swelling potential of treated specimens that stabilize with CIM with curing under 25 kPa surcharge pressure 117
Figure 1.6 The swelling potentials of treated specimens with CIM under both 7 kPa and 25 kPa surcharge pressures 119
Figure 5.10 The specimen used in this step 120
Figure 6.1 Triangle and square column installation model..... 124
Figure 6.2 M2 model..... 124
Figure 6.3 Stabilized area..... 125
Figure 1.7 The heights of both column and non-column part of M1-2/3h specimens before/after test 126
Figure 6.5 Top view of the treated specimens 127
Figure 6.6 SEM image of Specimen A (magnification factor=40000)..... 131
Figure 6.7 SEM image of M2-h (30%) 28 days curing (magnification factor = 40000) 131
Figure 6.8 SEM image of M2-h (30%) 180 days curing (magnification factor = 40000) 132
Figure 6.9 SEM image of Specimen A (magnification factor=40000)..... 135
Figure 6.10 SEM image of M2-h (30%) 180 days curing (magnification factor = 40000) 136
Figure 6.11 SEM image of NaLS specimen 180 days curing (magnification factor = 40000) 136

Figure 6.12 SEM image of CaLS specimen 180 days curing (magnification factor = 40000) 137
Figure 6.13 The swelling potentials of the treated specimen with sodium lignosulfonate lime column under 7 kPa with respect to curing period..... 138
Figure 6.14 The swelling potentials of the treated specimen with calcium lignosulfonate lime column under 7 kPa with respect to curing period..... 1389
Figure 6.15 The swelling potentials of the treated specimen with sodium lignosulfonate lime column under 25 kPa with respect to curing period..... 1389
Figure 6.16 The swelling potentials of the treated specimen with calcium lignosulfonate lime column under 25 kPa with respect to curing period..... 13840
Figure 6.17 The improvement percentages of the treated specimen with sodium lignosulfonate lime column under 7 kPa with respect to both curing period and distance between the boreholes..... 143
Figure 6.18 The improvement percentages of the treated specimen with calcium lignosulfonate lime column under 7 kPa with respect to both curing period and distance between the boreholes..... 143
Figure 6.19 The improvement percentages of the treated specimen with calcium lignosulfonate lime column under 25 kPa with respect to both curing period and distance between the boreholes..... 144
Figure 6.20 The improvement percentages of the treated specimen with calcium lignosulfonate lime column under 25 kPa with respect to both curing period and distance between the boreholes..... 144
Figure 6.21 The unconfined compressive strength for untreated specimen and treated specimens 146
Figure 6.22 Stress-strain relationship for untreated specimen and treated specimens 146
Figure 6.23 The swelling potential of the treated and untreated specimen under 7 kPa..... 147
Figure 6.24 The swelling potential of the treated and untreated specimen under 25 kPa..... 148

Figure 6.25 CBR swell values of treated specimens under 7 kPa surcharge pressure 149
Figure 6.26 CBR swell values of treated specimens under 25 kPa surcharge pressure 150
Figure 1.8 The curves of the load-penetration of the treated specimens under 7 kPa surcharge pressure after the soaked CBR test 151
Figure 1.28 The curves of the load-penetration of the treated specimens under 25 kPa surcharge pressure after the soaked CBR test 151
Figure 6.29 The soaked CBR values for treated specimens under 7 kPa surcharge pressure 152
Figure 6.30 The soaked CBR values for treated specimens under 25 kPa surcharge pressure 153
Figure 6.31 SEM image of Specimen A (magnification factor=20000)..... 156
Figure 6.32 SEM image of LC (30%) 28 days curing (magnification factor=20000) 157
Figure 6.33 SEM image of LC (30%) 180 days curing (magnification factor = 40000) 157
Figure 6.34 SEM image of NaLS (30%) 180 days curing (magnification factor = 40000) 159
Figure 6.35 SEM image of CaLS (30%) 180 days curing (magnification factor = 40000) 159
Figure 6.36 The top view of the treated specimens consists of thirty-seven calcium lignosulfonate lime columns 161
Figure 6.37 The improvement percentages of treated specimens with calcium lignosulfonate lime columns 162
Figure 6.38 The graph of the ω versus curing periods 163
Figure 6.39 The EDX analysis of Specimen A 165
Figure 6.40 The EDX analysis of treated specimen with calcium lignosulfonate lime columns 180 days curing 166

Figure 6.41 The swelling potentials of the stabilized soil specimens with both sodium and calcium lignosulfonate lime columns under 7 kPa surcharge pressure 169
Figure 6.42 The swelling potentials of the stabilized soil specimens with both sodium and calcium lignosulfonate lime columns under 25 kPa surcharge pressure 169
Figure 6.43 Effect of Curing Time on the CBR swell value for both NaLS and CaLS specimens under 7 kPa surcharge pressure 170
Figure 6.44 Effect of Curing Time on the CBR swell value for both NaLS and CaLS specimens under 25 kPa surcharge pressure 171
Figure 6.45 Effect of Curing Time on the CBR for both NaLS and CaLS specimens under 7 kPa surcharge pressure 172
Figure 6.46 Effect of Curing Time on the CBR for both NaLS and CaLS specimens under 25 kPa surcharge pressure 172
Figure 6.47 Effect of Curing Time on the UCS for specimens treated with both NaLS and CaLS lime columns 173
Figure 6.48 Effect of Curing Time on the swelling potential for specimens stabilized with both NaLS and CaLS lime columns under 7 kPa surcharge pressure 174
Figure 6.49 Effect of Curing Time on the swelling potential for specimens stabilized with both NaLS and CaLS lime columns under 25 kPa surcharge pressure 174
Figure 6.50 CBR test under 7 kPa pressure (NaLS) 175
Figure 6.51 CBR test under 25 kPa pressure (NaLS) 176
Figure 6.52 CBR test under 7 kPa pressure (CaLS) 176
Figure 6.53 CBR test under 25 kPa pressure (CaLS) 177
Figure 6.54 NaLS ve CaLS samples together (under 7 kPa) 177
Figure 6.55 NaLS ve CaLS samples together (under 25 kPa) 178
Figure 6.56 The swelling potentials of the treated specimen with CIM under 7 kPa surcharge pressure 181

Figure 6.57 The swelling potentials of the treated specimen with CIM under 25 kPa surcharge pressure 181
Figure 6.58 The improvement percentages of the treated specimen with CIM under 7 kPa with respect to both curing period and distance between the boreholes 183
Figure 6.59 The improvement percentages of the treated specimen with CIM under 25 kPa with respect to both curing period and distance between the boreholes ... 184
Figure 6.60 CBR swell values of treated specimens under 7 kPa surcharge pressure 185
Figure 6.61 CBR swell values of treated specimens under 25 kPa surcharge pressure 185
Figure 6.62 The curves of the load-penetration of the treated specimens under 7 kPa surcharge pressure after the soaked CBR test 186
Figure 6.63 The curves of the load-penetration of the treated specimens under 25 kPa surcharge pressure after the soaked CBR test 187
Figure 6.64 The CBR values for treated specimens under 7 kPa surcharge pressure 188
Figure 6.65 The CBR values for treated specimens under 25 kPa surcharge pressure 188
Figure 6.66 The swelling potentials of the stabilized soil specimens with both CaLS and CIM under 7 kPa surcharge pressure 190
Figure 6.67 The swelling potentials of the stabilized soil specimens with both CaLS and CIM under 25 kPa surcharge pressure 190
Figure 6.68 Effect of Curing Time on the CBR swell value for both CaLS and CIM specimens under 7 kPa surcharge pressure 192
Figure 6.69 Effect of Curing Time on the CBR swell value for both CaLS and CIM specimens under 25 kPa surcharge pressure 192
Figure 6.70 Effect of Curing Time on the CBR for both NaLS and CaLS specimens under 7 kPa surcharge pressure 193
Figure 6.71 Effect of Curing Time on the CBR for both NaLS and CaLS specimens under 25 kPa surcharge pressure 193

Figure A.1 Swelling potential versus Time Graph for Treated Samples with lime column..... 206
Figure A.2 Swelling potential versus Time Graph for Treated Samples with lime column..... 206
Figure A.3 Swelling potential versus Time Graph for Treated Samples with both lime column and lignosulfonate lime column under 7 kPa..... 207
Figure A.4 Swelling potential versus Time Graph for Treated Samples with both lime column and lignosulfonate lime column under 25 kPa..... 207
Figure A.5 Swelling potential versus Time Graph for Treated Samples with CIM under 25 kPa 208
Figure A.6 Swelling potential versus Time Graph for Treated Samples with CIM under 7 kPa 208
Figure C.1 Void ratio versus consolidation pressure graph for Specimen A and treated specimen with NaLS 213
Figure C.2 Void ratio versus consolidation pressure graph for Specimen A and treated specimen with CaLS 213
Figure C.3 Displacement versus time graph for Specimen A under 25 kPa..... 214
Figure C.4 Displacement versus time graph for treated specimen with NaLS (7 days curing) under 25 kPa..... 214
Figure C.5 Displacement versus time graph for treated specimen with NaLS (28 days curing) under 25 kPa..... 215
Figure C.6 Displacement versus time graph for treated specimen with NaLS (90 days curing) under 25 kPa..... 215
Figure C.7 Displacement versus time graph for treated specimen with CaLS (7 days curing) under 25 kPa..... 216
Figure C.8 Displacement versus time graph for treated specimen with CaLS (28 days curing) under 25 kPa..... 216
Figure C.9 Displacement versus time graph for treated specimen with CaLS (90 days curing) under 25 kPa..... 217
Figure G.1 EDX diagram of Specimen A 223

Figure G.2 EDX diagram of treated specimen with lime columns consists of 70% lime and 30% water 224
Figure G.3 EDX diagram of treated specimen with sodium lignosulfonate lime columns with 180 days curing period 225
Figure G.4 EDX diagram of treated specimen with calcium lignosulfonate lime columns with 180 days curing period 226

LIST OF ABBREVIATIONS

ABBREVIATIONS

AASHTO	American Association of State Highway and Transportation Officials
ASTM	American Society for Testing and Materials
CaLS	Treated specimen with calcium lignosulfonate lime columns
CBR	California Bearing Ratio
CEC	Cation exchange capacity
CIM	Combined improvement method
COR	Correlation specimens
EDX	Energy Dispersive X-Ray
FHWA	Federal Highway Administration
HTS	Highways Technical Specification
L	Lime
LC	Lime column
LLC	Lignosulfonate lime column
LVDT	Linear variable differential transducer
M	Model
METU	Middle East Technical University
NaLS	Treated specimen with sodium lignosulfonate lime columns
NLA	National Lime Association
SEM	Scanning Electrom Microscope
TS	Turkish Standard
UCS	Unconfined Compressive Strength
USCS	Unified Soil Classification System

LIST OF SYMBOLS

SYMBOLS

Al_2O_3	Aluminium oxide
CAH	Calcium aluminate hydrate
CaO	Unslaked lime
$Ca(OH)_2$	Calcium hydroxide
CH	Clay with high plasticity
CL	Clay with low plasticity
CSH	Calcium silicate hydrate
c_v	Coefficient of consolidation
D	Diameter of the column
D^*	Effective diffusion coefficient
D^0	Free diffusion coefficient
GC	Clayey gravel
h	Initial height of the specimen
H_2O	Water
h_f	Final height of the specimen
J_D	Diffusive mass flow per unit area
k	Coefficient of permeability
LL	Liquid limit
MH	Silt with high plasticity
ML	Silt with low plasticity
m_v	Coefficient of volume compressibility
OH	Hydroxide
PI	Plasticity index
PL	Plastic limit
SC	Clayey sand
SiO_2	Silicon dioxide
SP	Swelling potential
t	Time

V_s	Seepage velocity
w	Water content
x	Diffusion distance
Za	Active zone
ω	Coefficient related to the effective porosity and tortuosity
γ_w	Unit weight of the water

CHAPTER 1

INTRODUCTION

1.1 General Background of the Study

The performance of the soil affects the service life of any superstructure. When a lightweight structure, which is built on expansive soils, the service life of this structure is not too long due to volume change in response to variations in moisture content of the soil. Water molecules are absorbed by these soil minerals when they are subjected to moisture. The damage which is from minor cracking to irreparable destruction on this structure comes into existence because of the swell pressure resulted from this process.

Expansive soils are problematical soils all around the world as they generally exist in every part of the globe. These soil deposits are located in the tropical and temperate climate zones in all five continents (Chen, 1988). Turkey is a rich country in terms of the expansive soil deposits as these deposits exist in some parts of the Central Anatolia region, West Anatolia region, Southeast Anatolia region, and East Anatolia region (Çokça, 1991). Ankara, which is the capital city of Turkey, is located in the Central Anatolia region. Some part of the city settlement is founded on expansive soil deposits. The damage resulted from these soils forms on the lightweight structures such as light one-story buildings, garden walls, roads, and buried utilities such as water pipes (Erguler and Ulusay, 2003). Although the damage of this soil does not end up with the loss of life, the substantial monetary problem forms the result of the damage caused by this soil. For this reason, this soil is called a “hidden disaster” (Snethan, 1986).

Expansive soil is stabilized with additive materials such as lime, cement, fly ash, etc. by geotechnical engineers. The addition of these chemical additives to soil triggers the change of soil properties. The soil improvement technique consists of three parts which are mechanical, thermal, and chemical components (Ashok and Reddy, 2015). Treatment of this soil by using lime could be two different applications. The first application is that lime and soil mix homogeneously. The second one is that hole opened in the ground is filled with lime. This operation is called the lime column technique (Tonoz et al., 2003). Ion migration through the soil is derived from some factors such as chemical flow, electrical flow, hydraulic flow, and thermal flow. For instance, the ion migration starts with the chemical flow at the lime pile applications. After this process, ion migration continues utilizing electrical flow, hydraulic flow. The soil which is far from the lime is stabilized as a consequence of these flows (Barker and Roger 2006). As lime is a low solubility material, it remains at the bottom of the borehole or does not diffuse into the surrounding soil during the lime pile method. Thus, lime migration in the surrounding soil takes a long time. This condition is defined as a disadvantage of this method (Bhuvaneshwari, 2010).

Lignosulfonate is a waste material that is an inexpensive chemical. This material is an additive material that is used as a concrete plasticizer. This material has a property that reduces surface tension, it is easily absorbed from cement particles. In this way, cement particles have the same electrostatic charge and repel each other. Eventually, cement particles disperse homogeneously into the concrete (Ekinci et al., 2016). The addition of this material in the lime column is envisaged that the velocity of lime migration into the expansive soil will be increased.

1.2 Research Methodology and Objectives

The addition of lime to soil triggers the change of soil properties. Tonoz et al. (2003) stated that treatment of expansive soil by using lime could be two different applications;

a) Lime and soil are mixed homogeneously.
b) A hole opened in the ground is filled with lime.

In this research, the properties of expansive soils by using lime column is studied in detail. The achievement of this study is based on lime diffusion through the expansive soil. The main obstacle of lime diffusion through the soil is that lime is a low solubility material. For this reason, sodium lignosulfonate and calcium lignosulfonate are added to the lime column built in the expansive soil within the scope of this study.

In this study, lignosulfonate that is a waste material obtained from the paper industry is added to the lime column for increasing and accelerating lime diffusion into the soils. In addition to this, a combined improvement method mentioned below has been developed to shorten the time of the improvement process. The specific objectives of this research are as follows:

1- To investigate the efficiency of both lime column and some of its properties in controlling the swell potential of expansive soil in the laboratory.
2- To research the lignosulfonates addition on other engineering properties (e.g. swelling potential, unconfined compressive strength, compaction, consolidation, and permeability) of the expansive soil.
3- To investigate and identify the mechanisms by which expansive soil is modified or altered by the lignosulfonate lime column using analytical techniques such as energy dispersive x-ray diffraction (EDX), scanning electron microscope (SEM), specific surface area (SSA), and as well as cation exchange capacity (CEC) tests.
4- To study the curing effect of both lime column and lignosulfonate lime column on the swelling potentials of treated specimens.
5- To determine a more suitable lignosulfonate lime column application for stabilization of the expansive soil.
6- To search the effect of a combined improvement method that consists of prewetting, lignosulfonate lime column, and geotextile-anchor technique on expansive soil specimen.

1.3 Thesis Outline

This thesis related to an expansive soil stabilized with the lignosulfonate lime column method consists of seven parts to explain this study. Each part is briefly summarised below;

1- The introduction part includes general information about this study.

2- The literature part contains a review of the previous literature published related to expansive soil, the stabilization methods of this soil, lime column method, and lignosulfonate and applications in civil engineering.

3- The expansive soil specimen and lime column part involves properties of both expansive soil specimen and treated specimen prepared in this study.

4- Stabilized soil specimen part contains some outputs of laboratory tests such as unconfined compressive strength, one-dimensional consolidation, methylene blue tests, and the images obtained from SEM analysis.

5- The combined improvement method contains those studies relevant to the combined technique consisted of prewetting, lignosulfonate lime column, and geotextile+anchor.

6- The discussion on test results part involves some assesments that are related to test data obtained from experimental study done in this study.

7- The conclusion part contains some evaluations related to outputs obtained from this study.

CHAPTER 2

LITERATURE REVIEW

2.1 Introduction

The lime column technique has been applied for stabilizations of expansive soil. However, the lime column which contains lignosulfonate has not been studied in the literature. The main objective of this study is to investigate the influence of lignosulfonate on lime column technique in highway subgrade (expansive soil).

2.2 Expansive Soil

Expansive soils are problematic soils that have volume change properties when they get in contact with water. While these soils swell with the increase of the water content, these soils shrink with the reduction of the water content. The volume changes of these soils resulted from the alteration of their water contents trigger unpredicted upward movements of the lightweight structures or cracks in the pavements, roads (Masia et al., 2004).

These soils can be found in many parts of the world as they are located in semi-arid regions of the tropical and temperate climate zones. In addition to this, Nelson et al. (2015) stated that this soil type was found in many parts of the world and they map the general distribution of expansive soil in the world concerning some studies in the literature (Figure 2.1). Turkey is a substantial country in terms of expansive soil. For instance, two-thirds of the settlement of the capital city of this country, Ankara is established on the Ankara Clay that has medium to highly plastic properties (Erguler and Ulusay, 2003).

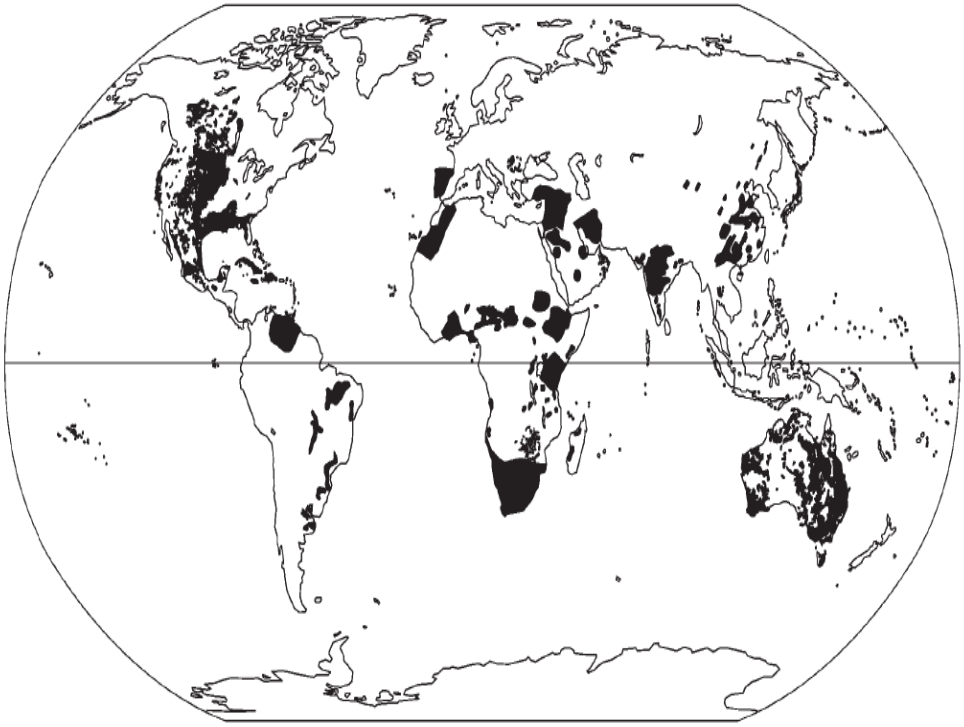

Figure 2.1 Global distribution of reported expansive soil sites (Nelson et al., 2015)

Parhi et al. (2017) stated that expansive soils take place in many parts of the world. Damages of some structures such as roads, pipelines, one-story buildings, etc. resulted from these soils are greater than the other disasters. Although these damages do not lead to the loss of life, they annually give rise to a significant economic loss in the whole world.

Dafalla and Shamrani (2011) stated that some problems resulted from the expansive soil subgrade may occur in both rigid (concrete) and flexible (asphalt) pavements. In addition to this, asphalt pavements that are flexible and tolerant materials are more resistant to these problems than concrete pavements. Figure 2.2 illustrates two examples of problems that arise from expansive soil subgrade. Besides, Table 2.1 explains some types of cracking of asphalt pavements due to the expansive soil subgrade. Figure 2.3 shows the examples of these types of cracks mentioned in Table 2.1.

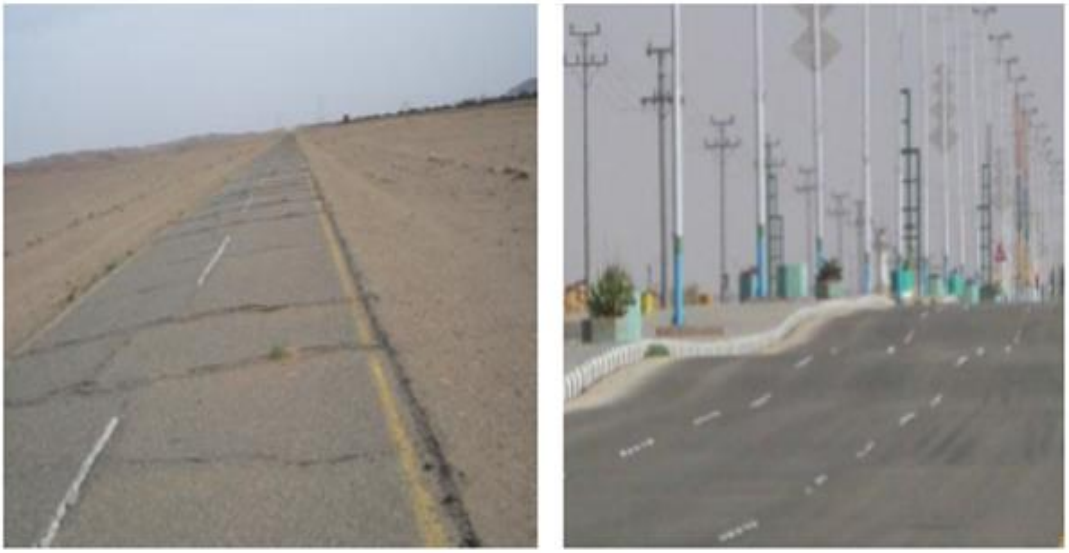

(a) Tayma-Tabuk Road (b) King Abdulaziz Road- AlGhatt

Figure 2.2 Road damages due to the expansive soils (Dafalla and Shamrani, 2011)

Table 2.1 Some types of cracking of asphalt pavements due to the expansive soil subgrade (Dafalla and Shamrani, 2011)

Types of cracking of asphalt pavements	Explanations
Longitudinal Crack	This crack occurs either parallel to the edge or along the asphalt joint between lanes.
Transverse Crack	Subgrade of the road is medium to high swelling potential and the durability of pavements is lower than the heave.
Block Crack	This crack may develop a large patch area when it is exposed to moisture changes.
Yield Crack	Frequent cyclic movements resulted from subgrade and repetitive heavy tire pressure causes this type of cracks.
Spot Ridge Crack	This crack is a center of excessive damages.
Green Zone Crack	A landscaped area triggers this crack.

a) Longitudinal crack

b) Transverse crack

c) Block crack

d) Yield crack

e) Spot ridge crack

f) Green zone crack

Figure 2.3 Road damages types due to the expansive soils

(Dafalla and Shamrani, 2011)

2.1.1 Clay Mineralogy

Clay soils generally have three mineral groups such as kaolinite, illite, and montmorillonite. The layer of the clay minerals comprised of two basic units that are tetrahedral sheet and octahedral sheet. Figure 2.4 illustrate the structure of these sheets.

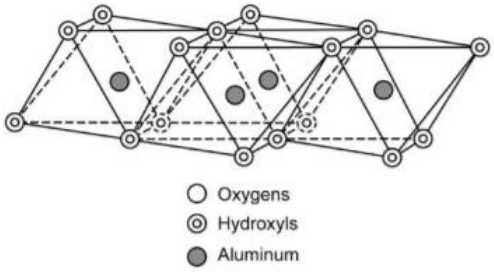

a) Octahedral sheet

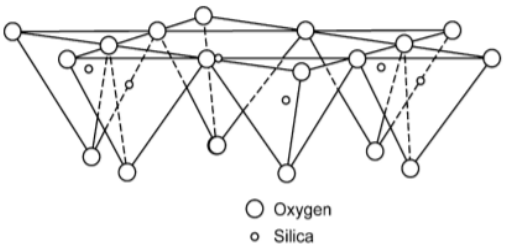

b) Tetrehedral sheet

Figure 2.4 The structure of both octahedral and tetrahedral sheet Murray (2007)

The silica tetrahedral sheet and the octahedral sheet are connected after either oxygens or hydroxyls ions are shared with each other. Thus, either the 1:1 clay mineral layer (kaolinite) or the 2:1 clay mineral layer (illite, montmorillonite) forms (Figure 2.5).

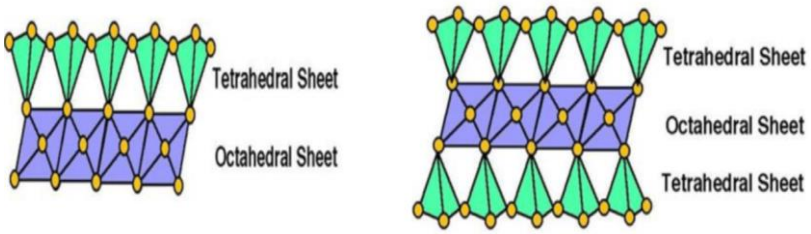

Figure 2.5 Structure of 1:1 and 2:1 clay minerals (Sivakugan, 2001)

The both physical and chemical properties of these minerals based on the arrengement and composition of these sheets.

Murray (2007) briefly explained these minerals groups as follows:

- Kaolinite: The basic structure of the kaolinite mineral consists of two parts that are of a single tetrahedral sheet and a single octahedral sheet. The structural formula for kaolinite is $Al_4Si_4O_{10}(OH)_8$ and the theoretical chemical composition is SiO_2, 46.54%; Al_2O_3, 39.50%; and H_2O, 13.96%.
- Illite: This mineral, which is named as a clay mineral mica by Grim et al. (1937), includes two tetrahedral sheets and a single octahedral sheet. In addition to this, potassium ions are placed between the layers as an interlayer cation.
- Montmorillonite: Two silica tetrahedral sheets with a central octahedral sheet form the structure of this mineral. The space between montmorillonite layers is occupied with water. The structural formula of this mineral is $(OH)_4Si_8Al_4O_{20}$-NH_2O and the chemical composition of this mineral without interlayer is SiO_2, 66.7%; Al_2O_3, 28.3%; and H_2O, 5%.

The swelling capacity of the montmorillonite is the highest than the other types of the clay minerals. Their properties, which are index, engineering, and microchemical, change with respect to their mineral compositions. Some properties of these minerals are given in Table 2.2.

Table 2.2 Microchemical properties of clay minerals (Nelson and Milner, 1992)

Properties	*Kaolinite*	*Illite*	*Montmorillonite*
Liquid limit (%)	30-100	60-120	100-900
Plastic limit (%)	25-40	35-60	50-100
Activity	0.33-0.46	0.9	1.5-7.2
Interlayer bonding	Strong hydrogen bonds	Strong potassium bonds	Very weak van der Waals bonds
Basal Spacing (A)	14.4	10	9.6
Specific surface area (m^2/g)	10-20	65-100	700-840
Cation exchange capacity (meq/100g)	3-15	10-40	80-150

The SEM images of these mineral types are shown in Figure 2.6.

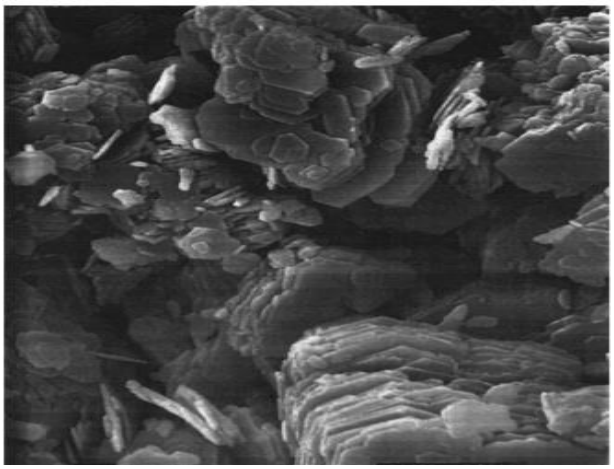

a) Kaolinite

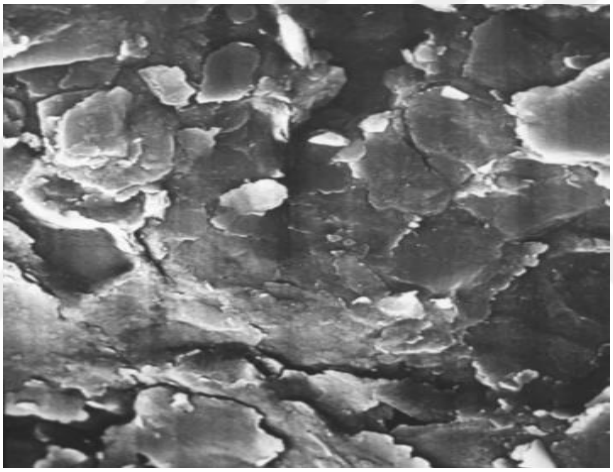

b) Illite

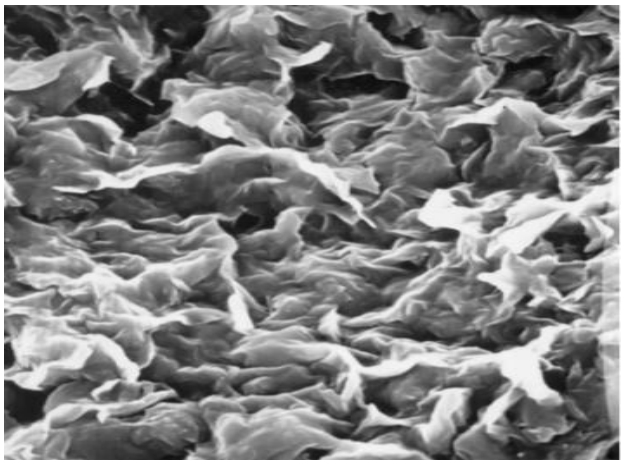

c) Montmorillonite

Figure 2.6 The SEM images of clay minerals (Murray, 2006)

2.1.2 Active Zone

The problems originated from the expansive soils occur as a result of the water content variation. These problems can arise at any depth of the expansive soil layers. However, the probability of the existence of these problems decreases with the depth of the soil. Since the water content of the upper part of the expansive soil layer is more affected by climatic environmental factors. This part is mostly named as either the zone of seasonal fluctuation or the active zone in Figure 2.7 (Nelson and Milner, 1992).

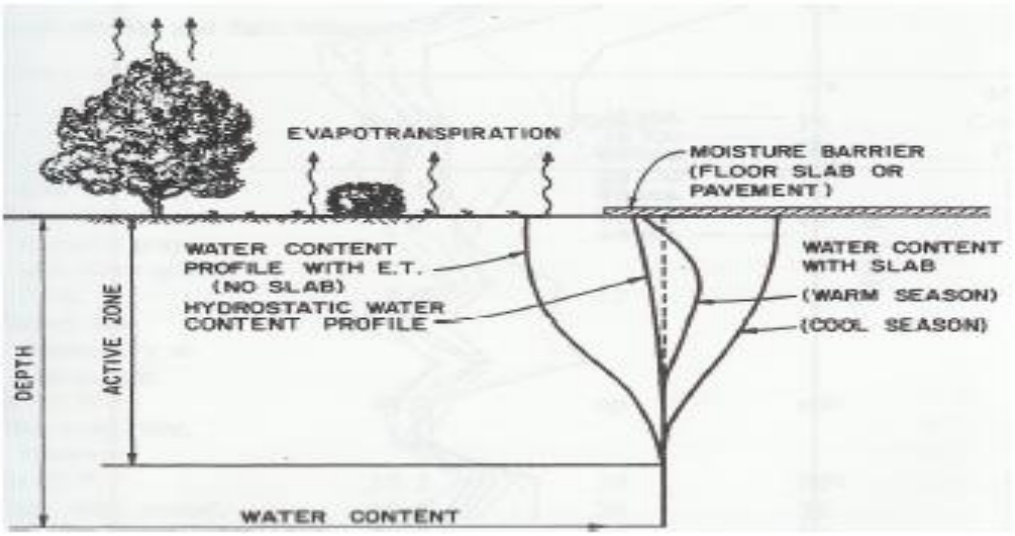

Figure 2.7 Water content profiles in the active zone
(Nelson and Miller, 1992)

This term, which is defined as an active zone, can involve a variety of meanings. For this reason, four subtitles are generated by Nelson et al. (2001) to make clear this term:

a. Active zone: The region of soil which swells at any specific time and causes the volume expansion of soil.
b. Zone of seasonal moisture fluctuation: The region below the ground surface is affected by climatic changes. The water content of this region fluctuates as a result of this change.
c. Depth of wetting: The water content of this region raises when water originated from external sources goes into the soil.
d. Depth of potential heave: A swelling pressure of soil and overburden vertical stress are keystone parameters that determine this depth. This depth can be defined as both the depth that has overburden vertical stress equal to the swelling pressure of soil and the maximum depth of the active zone.

Some estimation methods for determining the depth of the active zone (***Za***) have been advanced in the literature. According to the U.S. Army Corps of Engineers, the change of water content of soil influenced by environmental conditions is a substantial parameter of estimation of the active zone. The water content of soil should not remarkably alter with time at any depth of soil that is under the depth of the active zone. Some approach methods prepared by the U.S. Army Corps of Engineers are given in Table 2.3.

Table 2.3 Guidelines for estimating the depth of the active zone (Za)

(From EM 1110-1-1904, 1990)

Relative to	*Guideline*
Water table	Za will extend to depths of shallow groundwater levels $\leq 20\ ft$, $(6.10\ m)$.
Swell pressure	Za will be located within depths where $\sigma_{sj} - \sigma_{fj} \geq 0$,σ_{sj} =average swell pressure of stratum j and σ_{fj}= total average vertical overburden pressure after construction in stratum j.
Fissures	Za will be within the depth of the natural fissure system caused by seasonal swell/shrinkage
Climate	<u>Za, m</u> Humid 3,05 Semi-Arid 4,57 Arid 6,10

The water content, plasticity index, and liquidity index of expansive soil are essential parameters for determining active zone depth in some areas which had several strata. In these cases, the active zone depth should be specified by plotting either water content divided by plasticity index $(w - PI)$ or liquidity index $(LL - w/PI)$ (Nelson and Miller, 1992).

Erguler and Ulusay (2003) studied the engineering characteristics of Ankara clay and swelling maps of central parts of Ankara. According to this study, this clay has both a

high liquid limit and high swelling pressure that disserves a lightweight structure. Moreover, the depth of the active zone in this region is approximately 2 m below the ground surface.

2.1.3 Expansive Soil Treatment Methods

Nelson et al. (2015) summarized that some techniques are preferred for either improvement of soil or stabilization of moisture regime around the structures such as pavement, foundation, etc. These techniques are listed below;

- ✓ Removal and replacement
- ✓ Prewetting
- ✓ Water content control
- ✓ Chemical admixtures

As the techniques mentioned above may be applied either alone or combined for the project. When the project is a treatment of expansive soil subgrade, the most preferable techniques in the field are given below.

- ✓ Replacement with nonexpansive soil after the removal process
- ✓ Replacement with moisture-conditioned on-site soils after the removal process
- ✓ Chemical admixtures

Goud et al. (2017) mentioned that some soils that have a low bearing capacity and high swelling potential should be improved before pavement construction. Even though many differential techniques such as removal-replacement, mechanical modification, chemical admixtures, using geotextile have been applied in the field, chemical admixtures, that is especially lime, are the most favored method in the world.

2.3 Lime Stabilization of Expansive Soil

Stabilizer materials that contain calcium such as lime, cement have been preferred and utilized for the improvement of subgrade materials contain clay soil. The main factor

is the amount of calcium in these materials indicates at the first period of this stabilization stabilization method. The decision of stabilizer material applied is based on the requirement of the project such as strength, durability, time, etc. (Prusinski and Bhattacharja, 1999).

A hydrated high calcium lime, which is one of the product types in the market, has more free calcium ions. Besides, the particle size of lime affects the dissolution of lime during the stabilization process. Since finer particles have more surface area and this condition accelerates the solution process. As the stabilization of lime needs a high pH environment to form cementitious material, the addition of lime increases the pH value of the environment (Prusinski and Bhattacharja, 1999).

The lime content and number of freeze-thaw cycles are important parameters that influence both strength and durability of expansive soils treated with lime. Optimum lime content in terms of freeze-thaw durability of these soils was found as 6%. The lime treatment method enforces the durability of these soils against freeze-thaw action and is a suitable improvement method in cold regions (Shaqour et al., 2017).
Nelson et al. (2015) stated that some soil properties affect the reaction between lime and soil. These properties are listed below;

- ✓ pH value: Soils that had greater than 7 pH are more reactive than others.
- ✓ Organic carbon: A reaction between lime and soil considerably retards due to this material.
- ✓ Drained properties: Soils had poorly drained properties are more suitable than soils that possess well-drained for lime stabilization.
- ✓ Soil type: Calcareous soil is a good reactivity for this stabilization.
- ✓ Soluble sulfate salts: Ettringite minerals occur as a result of the reaction between soils contain these salts and lime.

2.3.1 Lime Stabilization Mechanism

Several different chemical reactions occur as a result of the lime addition to cohesive soil. The formation of calcium silicates and aluminates which are the result of the reaction between the lime and clay minerals binds the soil particles. This reaction is

called a pozzolanic reaction. This reaction lasts a very long time such as many months or years. In surface stabilization the carbon dioxide in the soil and the air reacts with

the calcium hydroxide when the stabilized soil is poorly compacted; the calcium carbonate retards the pozzolanic reactions in the soil. The soil physical properties such as grain size distribution, Atterberg limits change as a result of this reaction by the time of progress. These alterations in the soil end up with the enhancement of shear strength of the soil. The rate of enhancement of shear strength of the soil depends on many factors which are soil type, lime content, type of lime, the density of the compacted material, and the curing conditions. The soil which is stabilized with lime can be affected by frost condition while the expansive soil is not a frost susceptible soil. The organic materials in the soil affect negatively pozzolanic reactions and shear strength (Broms and Boman, 1975).

A highly exothermic hydration reaction occurs during the addition of unslaked lime into the clay soil. The results of these reactions are that both the formation of slaked lime and the release of heat energy (Eq. 2.1). Besides, this heat energy causes the temperature increase of the mixture and the evaporation of some water in the soil. Thus, the soil workability is considerably improved with this process that is called dewatering.

$$CaO + H_2O \rightarrow Ca(OH)_2 + 15.6\frac{Kcal}{mol} \qquad (Eq.\,2.1)$$

The concentration of calcium ions (Ca^{2+}) and hydroxyl ions (OH^-) in the pore water of soil increases after the hydration process. A series of reactions that change concerning some parameters such as soil composition, mineralogy, and pore water chemistry forms the results of the disintegration of these ions. A modification process that the cations exchange reactions between the calcium ions and the cations on the negative charges area of clay mineral surface develop at the first step of these series. As the existence of hydroxyl ions increase the pH of the mixture, the affected area of the clay mineral surface could rise as far as these ions increase. Thus, the improvement of both the flocculation mineral particles and plasticity properties of the soil materializes as a result of this step. Besides that, the sample becomes a superficially drier, more friable material in terms of physical properties after this step (Boardman et al., 2001).

The chemical change of clay structure takes place with long-term cementing reactions due to the addition of chemical substances such as cement, lime, etc. to the clay soil.

The lime stabilization of clay is firstly based on the cations exchange that occurred before the reaction between the lime and siliceous components of clay. This process lasts 24-72 hours after the mixture. After the clay particle flocculates rapidly during this process, the cohesive properties of clay particles convert into breakable and granular properties (Rogers and Glendinning, 1996a). In addition to this, the improvement process continues with a step that is identified as a pozzolanic reaction period. The curing period and temperature are essential parameters of this period (Sudhakar and Shivananda, 2005). The change between the clay particles and compounds made up of this step is demonstrated in Figure 2.8.

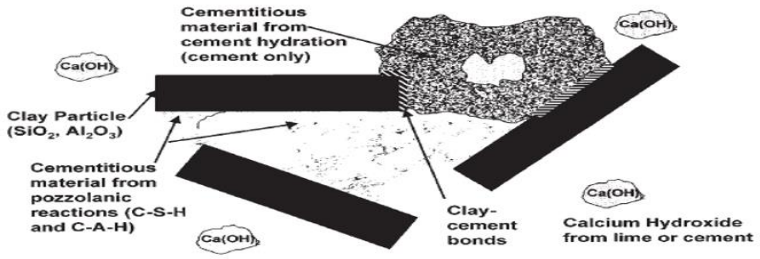

Figure 2.8 Lime- clay stabilization (Prusinski and Bhattacharja, 1999)

The three steps of the improvement process mentioned above are comprehensively explained in these subtitles;

a) Cation exchange: This step starts with a replacement between the ions of clay particles surface and the calcium ions of stabilizer materials. An adequate amount of calcium ions presented from them is exchanged with monovalent cations within the first few hours of this improvement method. At this period, the thickness of a layer that is called a double layer confines the clay particles decreases because of the alteration of the electrical charge density around the clay particles immediately after the ion exchange process. This process is illustrated in Figure 2.9. (Muntohar, 2005).

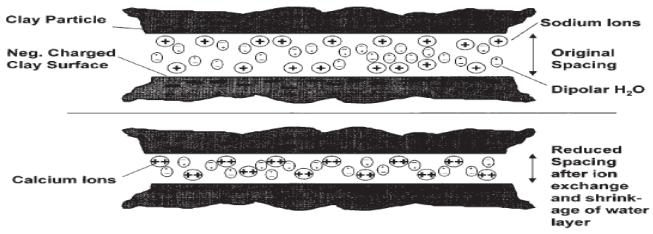

Figure 2.9 Cation exchange (Prusinski and Bhattacharja, 1999)

b) Flocculation and agglomeration: The structure of clay particles, which are generally flat, parallel, convert to a more random edge-to-face orientation after the flocculation process. The clay texture improves and bigger particles obtained from fine particles occur after this process. Therefore, an internal friction angle of particles develops due to this alteration and occurrence. In addition to this, some results of this process and cation exchange process come out of that are high electrolyte content, the high pH, and the declination in the double-layer thickness. This process is completed in the first several hours as well as the cation exchange process (Prusinski and Bhattacharja, 1999). The figure is related to this process is given in Figure 2.10.

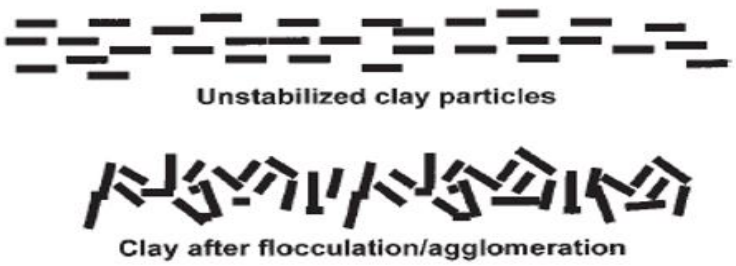

Figure 2.10 Flocculation and agglomeration (Prusinski and Bhattacharja, 1999)

c) Pozzolanic reaction: Final step is named a pozzolanic reaction process that is different from other steps in terms of time because this process occurs slowly. There is a high pH environment resulted from the previous step of the chemical stabilization. The solubility and reactivity of compounds existing in clay particles such as silica and alumina improve with this environment. Thus, calcium ions from the stabilizer materials tie up with these compounds, and some compounds such as calcium silicate hydrate, and calcium aluminate hydrate come into being (Narasimha and Rajasekaran, 1996). These reactions are shown below (Eq. 2.2 and Eq. 2.3).

$$Ca^{++} + 2(OH)^{-} + SiO_2 \rightarrow CSH \qquad (Eq.\,2.2)$$

$$Ca^{++} + 2(OH)^{-} + Al_2O_3 \rightarrow CAH \qquad (Eq.\,2.3)$$

The lime stabilization process, which starts with the hydration step and ends up with the pozzolanic reaction step is generally explained for decades in the literature. Beetham et al. (2015) investigated the literature that is related to this topic before they stated that two terminologies which are called lime improvement and lime stabilization are utilized in the literature for the lime stabilization process. Furthermore, many aspects of this stabilization process were searched and grouped in detail. The stabilization process is briefly summarised in Table 2.4.

Table 2.4 The treatment intent and the implications for lime addition and time-dependent reactions (Beetham et al., 2015)

Treatment intent	*Physico-chemical process*	*Common terminology*	*Indicative lime requirements*	*Typical time required*
Lower the moisture content of a wet/low-strength soil towards OMC. Either for compaction as general fill or to enhance trafficability	Removal of free moisture by reaction with quicklime. Cation exchange/clay mineral aggregation effectively increasing the OMC	Lime improvement	Low, e.g. 0.5–4 % (initial moisture content/clay content dependent)	1.Immediate 2. Rapid (0–72 h)
Reduced plasticity/potential for volume change.	Cation exchange/clay aggregation reduces clay mineral effective surface area and affinity for water. Early pozzolanic reactions restrict subsequent dispersion of aggregations	Lime improvement		Rapid (0–72 h)
Substantially improved engineering properties, i.e. strength, stiffness and durability.	Pozzolanic reaction between lime–clay soil system	Lime stabilization	Above the ICL value, e.g. 2–10% (actual binder addition determined by site-specific mix design)	Ongoing improvement from 72 h continuing for months/years

2.3.1.1 Effect of Sulfate on Lime Stabilized Soils

The pH value of soils increases during the lime stabilization of soil. An alumino-hydroxides come out of the dissolution of clay minerals in this high pH environment. Then, ettringite minerals form the result of the reaction between lime and sulfates with these compounds. To sum up, the ettringite mineral usually forms the lime stabilizations of soils that contain soluble sulfates. The volume of stabilized soil increases due to this mineral contains 26 molecules of water. Thus, this volume increase leads to considerable heaving of soil. This phenomenon has also been observed by some researchers. It is referred to as sulfate-induced heave (Mitchell and Soga 2005), lime-induced heave (Hunter 1988), or ettringite-induced heave (Puppala et al., 2014).

The National Lime Association (NLA 2004) reported that sulfate concentrations of soils influence the formation of ettringite minerals. For example, the probability of the formation of this mineral is very low for soil that has a 3,000 ppm sulfate concentration. However, if this concentration is between 3,000 and 5,000 ppm, this probability is very high during the lime stabilizations.

The growth of ettringite minerals is affected by temperature. If a temperature is higher than 60˚F, the growth of this mineral continues. If a temperature is higher than 60˚F, this mineral transforms the thaumasite mineral (Nelson et al., 2015).

A SEM image of both untreated soil and lime-treated soil is given in Figure 2.11. A SEM image ettringite mineral can be seen in the SEM image of treated soil with lime.

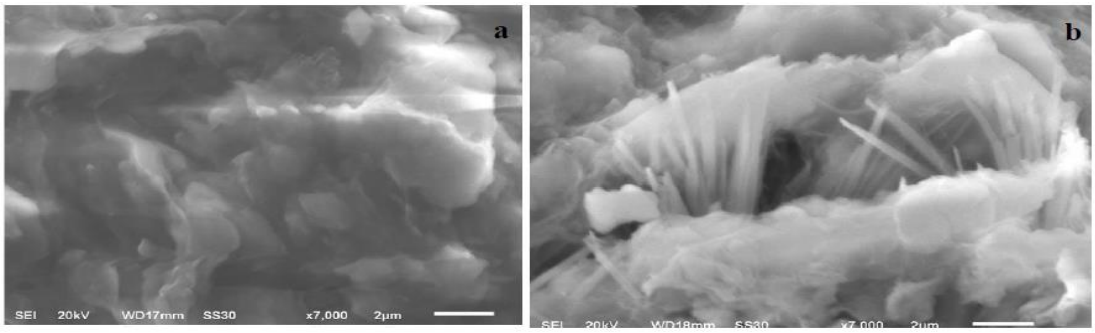

Figure 2.11 SEM views, a- natural soil, b- lime treated soil with 10000ppm sulfate concentration (Celik, 2014)

The formations of both ettringite and thaumasite minerals were explained by Hunter (1988). The reactions during these formations are given in Table 2.5.;

Table 2.5 The formations of both ettringite and thaumasite minerals (Hunter, 1988)

Reaction	**Explanation**	**Notes**
$CaO+H_2O \rightarrow Ca(OH)_2$	Hydration of quicklime	Pozzolanic reactions that cause the siliceous cementation of lime–treated soils
$Ca(OH)_2 \rightarrow Ca^{2+}+2(OH)^-$	Ionization of calcium hydroxide; pH rises to 12.3	
$Al_2Si_4O10(OH)_2.\ nH_2O+2(OH)^- + 10H_2O \rightarrow 2Al(OH)4^- + 4H_4SiO_4+ nH_2O$	Dissolution of clay mineral, at pH>10.5	
$2H_4SiO_4 \rightarrow 2H_3SiO_4^- +2H+ \rightarrow 2H_2SiO_4 + 2H^+$	Dissociation of silicic acid	
$5Ca^{2+}+2H_3SiO_4+4OH^- \rightarrow Ca_5(Si_6O_{18}H_2).4H_2O+6H_2O$		Finish reaction due to the presence of excessive sulfate
$M_XSO_4.\ nH_2O \rightarrow XM_Y+ + SO_4^{2-} + nH_2O$	Dissolution of sulfate minerals; x=1, y=2 or x=2, y=1)	
$6Ca^{2+} + 2Al(OH)_4^- + 4OH^- + 3(SO_4)^{2-} + 26H_2O \rightarrow Ca_6\ (Al(OH)_6)_2.\ (SO_4)_3.\ 26H_2O$	Formation of ettringite	Temperature is higher than 60˚F
$CO_2 + H_2O \rightarrow H_2CO_3$	Formation of carbonic acid	Temperature is lower than 60˚F
$CaCO_3 + H_2CO_3 \rightarrow Ca^{2+} + 2H^+ + 2CO_3^{2-}$	Dissolution of calcite in carbonic acid	Temperature is lower than 60˚F
$Ca_6(Al(OH)_6)_2.\ (SO_4)_3.\ 26H_2O + 2H_2SiO_4^{2-} 2CO_3^{2-} + O_2 \rightarrow Ca_6(Si(OH)_6)_2.\ (SO_4)_2.\ (CO_3)_2.\ 24H_2O + 2Al(OH)_4^- + SO_4^{2-}\ 4OH^- + 2H_2O$	Formation of thaumasite	Temperature is lower than 60˚F

2.3.2 Lime Column Method

The method of the lime column which improves the physical and mechanical properties of the soils divided into two parts which are dry lime application and wet lime application. This method should be preferred for the remediation of soft soil by the virtue of the development of soil strength parameters (Muntohar, 2010). Some images of the lime column method are illustrated in Figures 2.12, and 2.13.

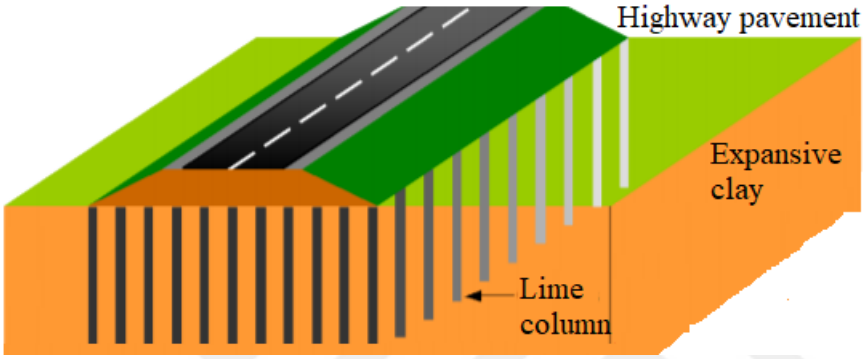

Figure 2.12 Column-supported embankment

Figure 2.13 Top view of lime column application

Two different stabilization mechanisms about the lime column technique are stated by previous researchers in the literature. The first group of researchers was interested in the strength and settlement of the soft soil. Their idea was that both the water content of soil reduced and the strength of soil increased throughout the stabilization process because of the lime addition. Thus, this method results in that the water content reduces significantly while the density of soil increases. The researcher's interest was soil under the foundation. The other group was concentrated the lime diffusion into clay soil. These researchers thought that lime diffused into the soil and the reaction between the clay and lime occurred with time. Some failing slopes in problematic soils were studied by them. In addition to this, the lime pile technique is widely used for different missions in the world. For instance, the lime pile technique is chosen as slope stability in the USA, Austria, and Sweden while this technique is applied to recover the soft soil in Russia, China, and Japan (Rogers and Glendinning, 1997).

The lime column method increases bearing capacity. The temperature of the ground could be reached the boiling point due to the lime slaking process when the dry weight of lime is 10-20% of the weight of the soil (Broms and Boman, 1975).

2.3.2.1 Lime diffusion

Lime migration, which is referred to instead of calcium migration and diffuse cementation, is a term that is defined as calcium ions of stabilizer materials diffuse into the clay soil. Portland cement and lime, which are applied as stabilizer materials for soil, contain sufficiently calcium ions to conclude the migration process (Prusinski and Bhattacharja, 1999).

Ion transportation in clay soil based on diffusion process is defined as that the ions pass from high concentration to low concentration because of the electro-chemical differences in the soil. The other description of this term is that consists primarily of the migration of both anion and cation for the charge balance of the soil. The most essential parameter from the point of ion transport mechanism into the low plasticity soil is an advection that is identified as a horizontal flow of water, air into this soil (Jungnickel et al., 2004).

Barker et al. (2006) explained that the mechanism of ion migration for lime piles into clay soil Firstly, an electrical cell forms between the lime pile and surrounding soil as the lime pile acts as an anode and the surrounding soil acts as a distributed cathode. Then, a primary step of lime migration is that three types of flows through the clay listed below initially occurs;

- ✓ Chemical flow resulted from diffusion
- ✓ Electrical flow due to the electrical conduction
- ✓ Hydraulic flow due to chemical osmosis and electrical osmosis

A secondary step of this migration that resulted from these flows has formed for curing time. As the pH value of surrounding soil increases the result of these flows, the dissolution of minerals and the gradient of chemical and electrical occurs. Further, hydraulic gradient forms that water flows due to electro-osmosis.

Rogers and Glendining (1997) stated that some factors such as soil water content, soil mineralogy, hydraulic gradient, lime moisture content affect the migration rate of calcium (Ca^{+2}) and hydroxyl (OH^{-}) ions during lime column stabilization.

The performance of lime diffusion into the soil is affected considerably by the initial water content. In other words, the initial water content is a considerable factor that qualifies both the amount of lime diffusion into the clay soil and reaction with this soil type. Therefore, the bigger value of this factor means that the more influential stabilization process in terms of lime diffusion. For instance, the molecular warming in saturated soil is more rapid than in unsaturated soil due to the thermal conductivity. As a result, the acceleration of OH^{-} ions replacement significantly increases at the higher water content (Barker et al., 2007).

Subbarao (2011) stated that the migration of lime placed in both lime piles and lime slurry pressure injection is very slow. For example, lime particles migrate 50 mm for four years in soil that including no extensive cracks and fissures.

Most of the previous studies related to the lime piles method focused on two subjects that are lime migration rate and an alteration of soil properties. In addition to this, some researchers have investigated that soil properties such as mineralogy, temperature, ions influence lime migration. Although lime migration is mainly dependent on two important properties that are soil fabric and pore structures, they have not been

examined in detail by these researchers (Cherian and Arnepalli, 2013).

The diffusion of lime particles into the expansive soils is evaluated as the movement of contaminants in soils that is the transport of the dissolved and immiscible contaminants in porous media. A generalized advection-diffusion model obtained from mass equilibrium is applied for dissolved contaminants. This model is based on the mechanical dispersion, sorption, and biodegradation of pollutants during mass transport mechanisms. When the transport of the immiscible contaminants is related to the displacement of liquids that affect the viscosity ratio, specific surface area of particles, soil fabric, and hydraulic conductivity.

The transportation of the lime particles into the expansive soil occurs by either concentration or hydraulic gradient. The first case is that the dissolved particles diffuse from high concentration to low concentration areas due to the thermal vibrations that are related to their inner thermal energy. This process is named molecular diffusion. The second one is that dissolved contaminants move with liquid movement that occurs due to the different total pressure between two points.

Diffusive transport may occur in some conditions that are either no water flows or in the opposite direction to the hydraulic flow. When there is no difference in concentration between mediums, the diffusion process will merely stop.

Fick's first law relates the concentration gradient with the contaminant mass flow (1D-flow) as follows (Eq. 2.4):

$$J_D = -D^* \frac{\partial C}{\partial x} \qquad (Eq.\,2.4)$$

Where J_D [kg/(m^2/s)] is the diffusive mass flow per unit area and time, D* [m^2/s] is the effective diffusion coefficient and $\partial C/\partial x$ [kg m^{-3}/m] is the concentration gradient.

Longitudinal and transverse mechanical dispersion occurs during mass transport due to differences in flow path lengths, spatial variability of pore sizes, and friction between fluid and soil particles. D_L and D_T are the longitudinal and transverse mechanical dispersion coefficients, respectively, and α_L and α_T are the longitudinal and transverse dispersivities. In general, molecular diffusion and mechanical dispersion take place simultaneously; for this reason, their effects are considered as cumulative. These mechanisms affect the advancing solute front and produce mechanical dispersion which can be computed as (Eq. 2.5 and Eq. 2.6):

$$D_L^* = \alpha_L v_s + D^* \qquad (\text{Eq. } 2.5)$$

$$D_T^* = \alpha_T v_s + D^* \qquad \text{(Eq. 2.6)}$$

Boundary conditions of this concentration problem and an equation of this problem are given below (Eq. 2.7).

$$C(x,0) = 0 \qquad x \geq 0 \; initial\; condition$$

$$C(0,t) = C_0 \qquad t \geq 0 \; boundary\; condition$$

$$C(\propto, t) = 0 \qquad t \geq 0 \; boundary\; condition$$

$$\frac{C(x,t)}{C_0} = 0.5\left[erfc\left(\frac{x - v_s t}{2\sqrt{D_L^* * t}}\right) + \exp\left(\frac{v_s x}{D_L^*}\right) erfc\left(\frac{x + v_s t}{2\sqrt{D_L^* * t}}\right)\right] \qquad \text{(Eq. 2.7)}$$

Contaminant transport in low permeable soils is provided by the diffusion process due to the low value of the v_s .When there is no water flow in the medium, this equation is simplified (Eq. 2.8);

$$\frac{C(x,t)}{C_0} = erfc\left(\frac{x}{2\sqrt{D_L^* * t}}\right) \qquad \text{(Eq. 2.8)}$$

Where t is time in terms of seconds, x (m) is the distance from the surface.

D^0 is the free solution diffusion coefficient that is no soil present. The effective diffusion coefficient (D^*)is related to the molecular diffusion coefficient D^0 [m^2/s] by the following relation (Eq. 2.9):

$$D^* = \omega D^0 \qquad \text{(Eq. 2.9)}$$

Where ω is a coefficient related to the effective porosity and tortuosity of the porous media. According to Perkins and Johnston (1963), $\omega \approx 0.7$ for sands, whereas Freeze and Cherry (1979) suggest values between 0.5 and 0.01 for different geomaterials. In general, ω is highly variable and should be experimentally determined for each soil condition (Rowe *et al*. 1988). The molecular diffusion coefficient varies according to the nature and size of the diffusive element, the solvent type, and the temperature.

2.4 Lignosulfonates

Lignosulfonates are obtained from the trees which can be classified into two groups such as softwood and hardwood. The trees are consist of wood substances that are formed with different cells include primarily cellulose, hemicellulose, and lignin. Wood can be grouped into two categories in terms of the molecule. The first group is macromolecule substances which are cellulose (45%), hemicellulose (20-25%), and

lignin (softwood 27-37%, hardwood 16-29%). The properties and chemical composition of lignin and hemicellulose vary to wood types, whereas cellulose is a uniform component for all wood types. Low molecular weight substances are extractives which are terpenes, alcohol, etc. Lignosulfonates can be classified as sodium, calcium, and magnesium for chemical composition. In other words, this classification is based on the complex polymer of the wood (Vincent et al., 2017). Lignosulfonate, which is a water-soluble material derived from lignin, is a by-product of the paper industry. This material is preferred material in numerous fields such as petrol industry, construction industry, etc. (Rana et al., 2002).

Lignosulfonates are sold in two different types that are pulverized form and liquid form. A liquid form of lignosulfonate has black or yellow color, 3-7 pH, 1.17 kg/m^3 density. However, lignosulfonates are only formed 40%-60% of this type of them. The other type of them is pulverized lignosulfonates that have yellow or tan color, 0.45 kg/m^3 density. This type is a thinner and water-soluble material. The specific surface area of this type is between 0.5 and 1 m^2/g. The chemical structure of this type is very complex and the molecules of them are very long. An edge of these molecules is a hydrophile that has water interaction properties, the other edge of them is a hydrophobe that has oil and air interaction properties. Lignosulfonates are considered as a polymer that consists of hydroxyl (OH), metoxil (OCH_3), phenyl radical (C_6H_5), sulfonic acid (SO_3H). Pearl (1967) stated that lignosulfonate was a highly acidic material that had molecules that included the strongly disassociated sulfonic acid groups. Sulphite Pulp Manufacturers Research League (1963) reported that their pH value is usually between 2 and 4 and they had cations such as Ca, Na, and Mg that could be formed complexes. These conditions result in that lignosulfonates were absorbed by clay soil.

The structural formula of lignosulfonate is undetermined although many structural formulae of them have been offered in the literature. The example chemical structure of lignosulfonate was suggested by JECFA (2008) in Figure 2.14. The other structure of them was proposed by Sulphite Pulp Manufacturers' Research League (1963) and Vinod et al. (2010), respectively in Figure 2.15.

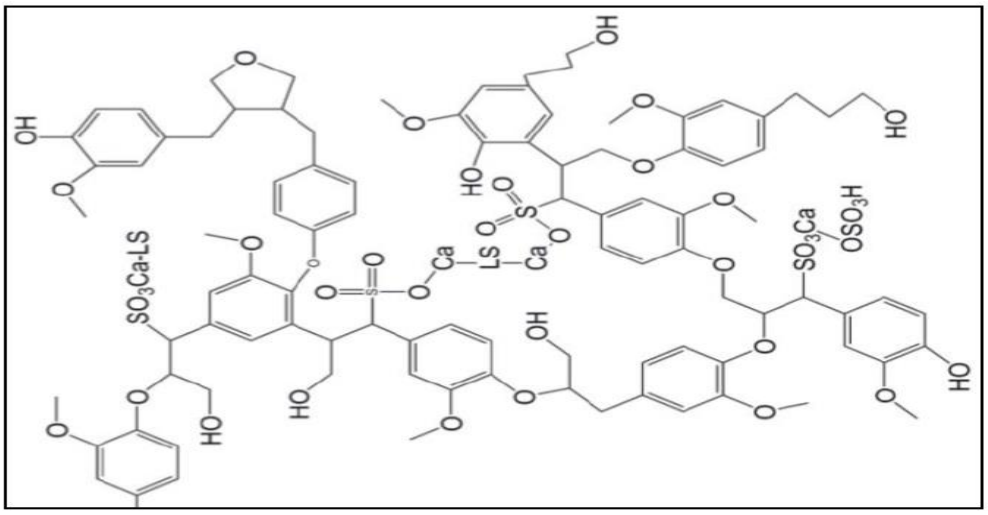

Figure 2.14 Representative structure of calcium lignosulfonate by JECFA in 2008

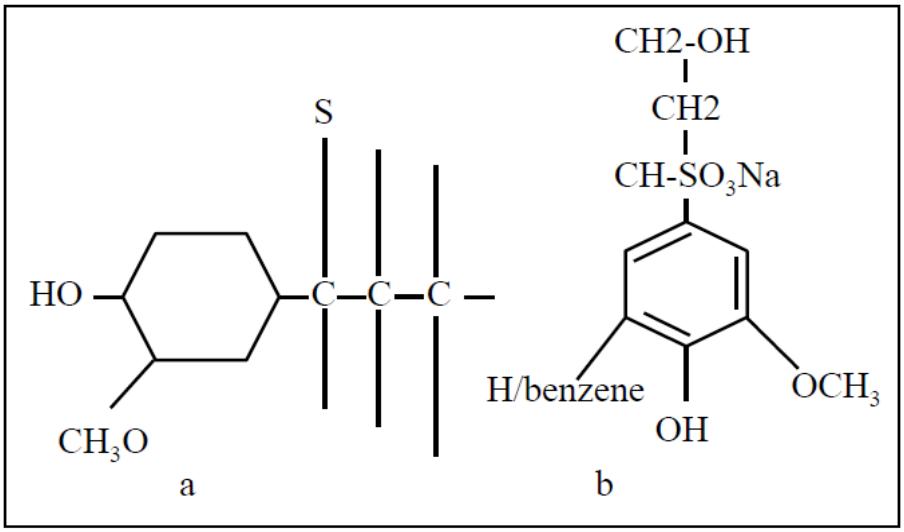

Figure 2.15 a) Binding Units of the LS molecule (After Sulphite Pulp manufacturers' Research League 1963); b) Chemical Structure of LS (After Vinod et al. 2009)

Lignosulfonate is a waste material that is an inexpensive and extensive chemical. This material is an additive material that is used as a concrete plasticizer. Although 50 million tonnes of lignin is produced annually, only six percent of this quantity is used as an additive such as agriculture chemical, industrial binder. Though the usage of lignin as a raw material in any applications has been studied for several decades, these studies have not been sufficient due to the gap between theory and practice (Yang et al., 2007).

The net potential of lignosulfonate is negative although the surface of lignosulfonates contains both negative and positive potentials (Theng, 1979; Adam, 1988). As

lignosulfonates included negative and positive charges, both positive ions and negative ions in soil solution may be absorbed by them. Besides, intramolecular hydrogen bonds, which lignosulfonate includes, can react with divalent or multivalent metal ions to form covalent coordinate bonds (Pearl 1967).

The chemical compositions of lignosulfonates were based on some parameters that were the process of neutralization and fermentation, the type and age of tree used as a raw material. Lignosulfonates used as a water reducer in the market contained carbohydrates that caused the hardening of concrete for a long time. The chemical compositions of some different pulverized lignosulfonates were shown in Table 2.6.

Table 2.6 The chemical analysis of pulverized calcium and sodium lignosulfonates (%)

	Calcium Lignosulfonates			*Sodium Lignosulfonates*	
Humidity	5	10.2	3.6	6	7.2
Ash	17	16.8	18.2	18.1	16.3
Unslaked lime	9	21	8.3	0.1	0.2
Sulfonate	3.2	-	3.4	-	-
Reducing agent	4.5	12.5	4	4.1	3.7
Sulphur	11.8	9	12.3	11.2	7.5
Nitrogen	-	0.2	-	-	-
Methoxyl	7.2	-	-	-	-
pH	6.4	-	6.2	6.8	6.9

Lignosulfonates were utilized for different purposes that were only retarder agents or both retarder agents and water reducer agents. As some materials, which are triethanolamine, calcium chloride, and salts, were added to these materials, the strength increased in a short time.

Tegin and İsfendiyaroğlu (1967) explained that the lignosulfonates could be used in four different areas owing to their active anionic surface. These areas were listed below;

1. The effect of dispersion: The main impact of them was dispersion by the virtue of their molecular structure. The lignosulfonates selected for this purpose were clarified from carbohydrate and was fairly pure. The amount of them in the suspension

was enough between 1% and 3% for the dispersion process. The amount of them in the suspension was changed about an activity such as petrol industry, concrete industry, and textile industry. The lignosulfonates selected in the concrete industry provided some benefits for users. These benefits are that the reduction of the amount of water in concrete, the interception of flocculation, and the homogenous mixture. As a result of them, the more durable concrete was manufactured.

2. The effect of physical bonding: The lignosulfonates could be employed as a physical binder and they gained adhesion properties by adding carbohydrates. This process resulted from the contraction of humidity by sugar. This material was preferred from road stabilizations, fabrications of ceramic.

3. The effect of chemical bonding: Lignosulfonates were materials that form chelate bonding between the molecules. They were handled for water softening, flotation, agricultural chemistry.

4. The other effects: Lignosulfonates were chosen for the leather industry.

2.4.1 Interaction mechanism of lignosulfonates with soil particles

Vinod et al. (2010) studied that the interaction mechanism of lignosulfonate with soil particles was done on dispersive clay soil. The result of the X-Ray Diffraction (XRD) analysis was that there was no change in crystalline orientation in treated dispersive clay. The crystalline size reduction of this soil, which resulted in the electrostatic reaction between the clay and lignosulfonate, changed concerning the type of clay mineral. For example, montmorillonite had a more reduced rate than others groups such as illite, kaolinite. During the electrostatic reaction process, the surface negative charges of clay minerals were decreased and the interlayer bonding between the clay minerals formed, respectively. A mixture, which consisted of lignosulfonate and water, was prepared and added to this soil. Hydrogen (H^+) and hydroxyl (OH^-) ions came out of the result of the disintegration of water at this step. Lignosulfonate gained H^+ ions and altered positively charged compounds. Thus, the negatively surface charged of clay mineral was neutralized by this nascent positively charged compound end of the process (Figure 2.16).

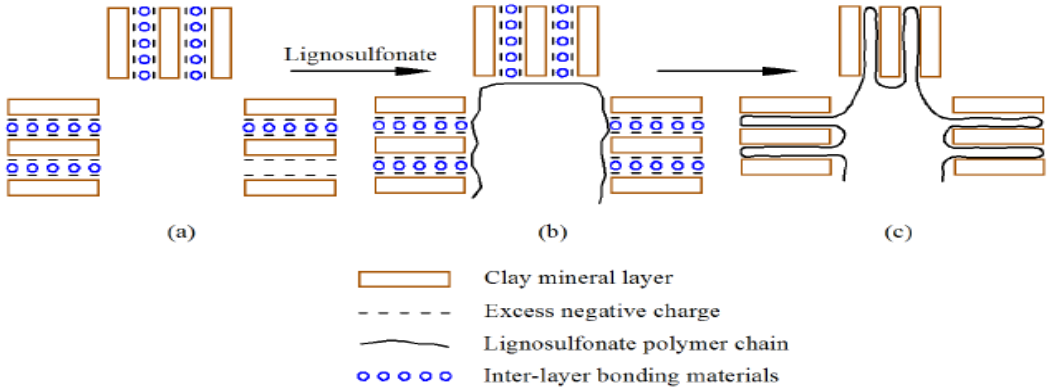

Figure 2.16 Schematic diagram of lignosulfonate stabilization on clay soil

(Vinod et al. 2010)

Vakili et. al. (2018) explained that while the attractive forces between the individual clay particles significantly rise, the repulsion forces between the individual clay particles go down during the lignosulfonate stabilization process. Then, this process ends up with both the substantial reduction in thickness of the diffuse double layer and the dropping off soil dispersivity.

2.4.2 Applications

Lignosulfonate can be used in soil stabilization applications. Although this material has not any negative effect on the environment, this waste material gives rise to improved durability and strength of soil (Chen & Indraratna 2014a).

Orszulik (2013) mentioned that lignosulfonate was used at the stage of oil drilling muds in the petroleum industry. The viscosity of muds diminished with the addition of lignosulfonates. This process provided lower energy requirements needed for drilling.

Lignosulfonates are derived from two different methods. The first one is that is obtained from sulfite pulping spent liquor and the second one is that prepared from sulphonation of alkali lignin. These materials are utilized as water reducers additives in concrete mixtures. When these materials are added to the concrete mixture, it can generate electrostatic repulsion, steric hindrance, and lubrication layer between cement particles in mixtures. Thus, both the water content of concrete is reduced and the strength of concrete increased for a given fluidity (Yu et al., 2013).

Lignosulfonates are classified into different groups which are calcium, sodium, potassium, and magnesium. This condition is a result of both the type of woods and the chemical process. The main function of lignosulfonate reduces the water of concrete without the loss of fluidity of concrete. As lignosulfonates have a property that reduces surface tension, they are easily absorbed from cement particles. In this way, cement particles have the same electrostatic charge and repel each other. Eventually, cement particles disperse homogeneously into the concrete (Ekinci et al., 2016).

Vinod et al. (2016) studied the microchemical analysis of lignosulfonate and stabilized soil. According to this study, the negative surface charges of clay particles are neutralized at the soil stabilization with lignosulfonate. After the neutralization process, the double layer thickness of clay particles reduces and the stable aggregations are formed. Thus, the properties of soil treated with lignosulfonates is better than untreated soil.

Lignosulfonates can be used as a stabilizer material for erodible soils since these materials bind soil particles together. It is reported that these additive materials both increased the critical shear stress of a silt clay soil and decreased the coefficient of this soil erosion (Figure 2.17). Besides, lignosulfonate was better additive material than Portland cement for these properties of soils (Indraratna et al., 2010).

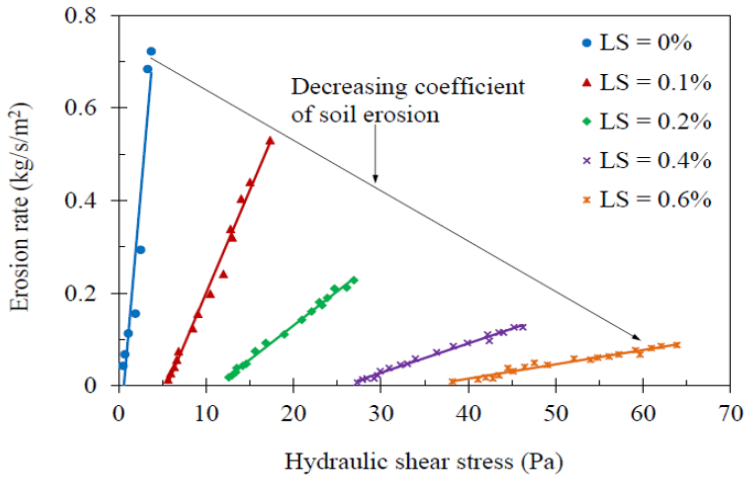

Figure 2.17 Erosion rate versus hydraulic shear stress of lignosulfonate treated/untreated silty sand (Indraratna et al., 2010)

Tingle and Santoni (2003) investigated the effectiveness of some additive materials such as lignosulfonates, petroleum emulsion, tree resin, acid on unconfined compressive strength (UCS) of low plasticity clay. At this study, the UCS of the treated specimen was tested under dry and wet conditions. The result of this study is that lignosulfonate was determined as a better additive material than others to improve the UCS of low plasticity clay (Figure 2.18). Also, the optimum amount of lignosulfonate was found as %5 for this soil type. Apart from this, the other output of this study, UCS of treated soil with %3.37 lignosulfonate was greater than UCS of treated soil with % 7 cement.

Tingle et al. (2007) studied that some admixtures, which were acid, enzymes, LS, a petroleum emulsion, polymers, and a tree resin, Type I Portland cement, and hydrated lime, were stabilized clay soil. Each sample was prepared under the same mixing, compaction, and curing process.

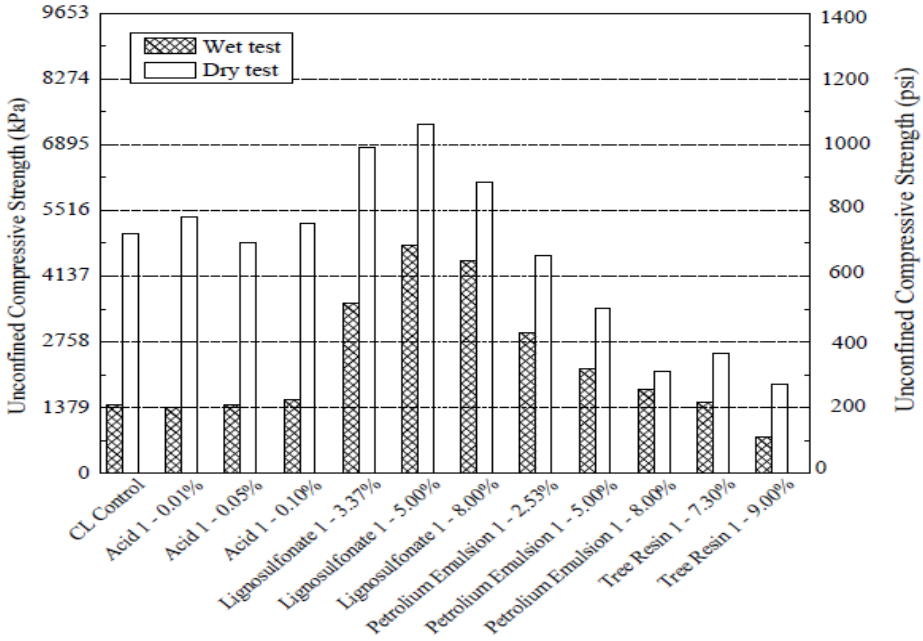

Figure 2.18 UCS value of low plasticity clay improved by additive materials such as lignosulfonates, petroleum emulsion, tree resin, acid (Tingle and Santoni 2003)

According to 28 days of curing test results, the treated sample with lignosulfonate had lower swelling potential than the other treated sample. In other words, the intake of water by treated sample with lignosulfonate was fewer than the other treated sample. Thus, lignosulfonate was the most suitable admixture in terms of the waterproofing properties of clay soil.

Lignosulfonate was used to investigate the deformation behavior of sandy silt under cyclic loading. According to this study, the service life of soil increased when lignosulfonate was added to untreated soil. The excess pore pressure of lignosulfonate treated soil declined steadily with the number of loading cycles. This step brought two outcomes that the deterioration of soil particle bonding and the dilation of treated specimen. The other conclusion was related to the resilient modulus of soil specimen. Although the resilient modulus of both untreated and treated soil specimen diminished with the number of cycles, the resilient modulus of the treated specimen was considerably greater than the resilient modulus of untreated soil specimen (Chen and Indraratna, 2015)

2.5 Design Approaches and Treatment Alternatives for Highway Constructed on Expansive Soil

The change of volume of expansive soil induces damages to pavements constructed on this soil. Since these structures are lightweight and spread over large areas. Then, this condition ends up with a financial loss. However, it is enough that this problematic soil is removed from construction areas and is a switch with the more stable soil to solve this condition. Unfortunately, this solution method in highway construction is more costly and is not suitable in terms of economy (Nelson and Milner, 1992).

Federal Highway Administration (FHWA) stated that a cross-section of pavement system consists of four parts such as surface, base, subbase, and subgrade. These parts are briefly explained below;

a) Surface: An uppermost part of the pavement system is constructed to compensate for traffic load. In addition to this, the surface layer endures many harmful effects resulted from vehicles and climate. This layer is installed by two different materials that are asphalt concrete and Portland cement concrete. While a surface layer consisted of asphalt concrete is named a flexible pavement, a term that is called a rigid pavement is used for a layer formed Portland cement concrete.
b) Base: An intermission part of the pavement system is a stable and uniform layer that is built for supporting the surface layer. Some specified materials, which are high-quality aggregates, such as crushed stone, crushed slag, gravel, and

sand, or combinations of them, are compacted at the designed thickness and form this layer. When a subbase layer is not constructed, this layer blocks the migration of subgrade soil to the upper part.

c) Subbase: This part is constructed between subgrade and base. Some pavement systems especially rigid pavement do not include this part. An evaluation of the subbase construction is made before the installation of this part due to the economic condition. Some factors that are frost action, fine-grained subgrade migration, drainage system, and subgrade stiffness are taken into account during this evaluation process.

d) Subgrade: A bottom part of the pavement system called a subgrade is made up of natural in-situ soil at the construction site. To improve these soil properties, the upper part of this soil layer is either compacted or stabilized. A construction target of this part is that the performance of the pavement system is improved with an installation of the platform that is blocked unexpected deflection formed at this system.

As a summary, the parts of a pavement system and the properties of materials formed these parts are given in Figure 2.19.

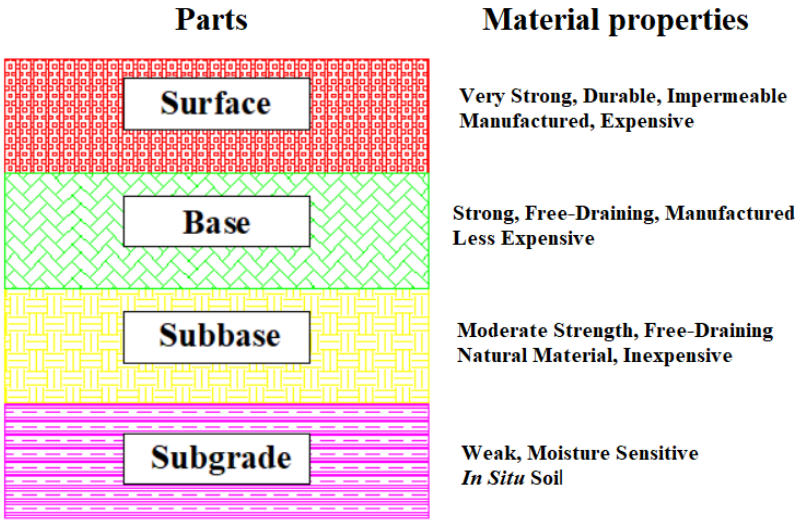

Figure 2.19 Parts of the pavement system and the properties of materials consisted of these parts (FHWA NHI-05-037, 2006)

This study is related to the improvement of a pavement subgrade that consists of expansive soil that had high swelling potential and low CBR value. For this reason, some information about the pavement subgrade is given below.

2.5.1 Subgrade Design and Construction

A subgrade is a layer that is placed under either base or subbase layer of the pavement system. Both the service life of the pavement and the design of pavement have considerably affected the quality of this layer.

An initial step of pavement construction is the removal or scraping of the uppermost part of the natural soil. Some particles such as organic materials, stones should be removed during this process. This process is done for not only the removal of problematic soil but also the preparation of the design line of the pavement system.

Schaefer et al. (2008) stated that some qualifications of subgrade soil influence the functionality of this layer. These qualifications are briefly explained below;

a) Moisture content: Many subgrades properties that are bearing capacity, shrinkage-swelling, and some factors infiltration, pavement porosity, groundwater table elevation, drainage depends on this parameter. For example, subgrade soils had high moisture content may easily deform under any loading.
b) Swelling/Shrinkage: Soils had volume change to moisture content cause some problems of pavement. Besides, soils that consist of mostly fine-grained particles may harm a pavement built in the northern climate zone. Damages resulted from these soils may come out of cracks of the pavement due to the volume changes.
c) Strength: Subgrade soils have to sustain loads on pavement systems. Some parameters such as compaction degree, moisture content, and soil type sometimes act upon the bearing capacity of this part. A CBR value of this soil placed in this part should be either 10 or greater than 10. Since unconscionable deformations originated from heavy loads and traffic loads generally occur at soil had lower CBR value.

A subgrade uniformity is another property that influences the performance of this layer. However, many factors such as temperature, installation operation, etc affect this property of the subgrade layer.

Natural soils used for subgrade material can be found as different types of soils. For this reason, these soil types have several properties and different reactions under any condition. Some information related to these soil types utilized for subgrade installation is given in Table 2.7.

Strength properties of subgrade materials considerably influence the design and serviceability of pavement structure. For this reason, stresses transmitted from a surface layer of pavement should be smaller than the elastic limit of subgrade material. Therefore, a laboratory test called the Soaked California Bearing Ratio test is done to calculate the CBR value of this material. After this test, an evaluation related to the suitability and stability of this material used as subgrade material is made for test results (Rakaraddi and Gomarsi, 2015).

Highways Technical Specification (HTS, 2013) prepared by Turkey Highways General Directorate stated that soil used as a subgrade material should have two important properties. Two properties of this material are;

- A CBR value of this material should be greater than 3% after the soaked CBR test. This parameter should be greater than 8% for subgrade material done by embankment during flexible pavement construction. However, this value should be greater than 10% for the protective layer of the highway.
- Material cannot have high swelling potential.

Table 2.7 Suitability of soils type for subgrade applications (arrangement from Schaefer et al. (2008))

Subgrade Soils for Design	*Unified Soil Classifications*	*Load Support*	*Drainage Characteristics*	*Frost action*	*Modulus of Subgrade Reaction (k), (MPa/m)*	*Resilient Modulus(MR), (MPa)*	*CBR Range (%)*
Clay	CL, LL >40 and PI >10	Very poor	Impervious	High	13.57 to 27.14	6.89 to 18.62	1 to 15
Silt	ML, >50% silt, LL <40, and PI <10	Poor	Impervious	Very high	13.57 to 27.14	6.89 to 18.62	1 to 15
Silty sand	SM, (PI) <10, and <35 % silt	Poor	Fair to Poor	Moderate to high	27.14 to 40.72	18.62 to 27.58	5 to 30
Silty sand	SM, non-plastic (NP), and >35% silt	Poor	Poor	Very high	27.14 to 40.72	18.62 to 27.58	5 to 30
Sand	SW, SP, GP-GM, and GM	Good	Excellent	Very slight	40.72 to 54.29	27.58 to 39.30	10 to 40
Silty gravel	GW-GM, GP-GM,and GM	Good	Fair	Moderate	40.72 to 54.29	27.58 to 39.30	20 to 60
Gravel	GW, GP, and GU	Excellent	Excellent	Very slight	54.29 to59.72	31.03 to39.30	30 to 80
Crushed Stone	GW, GP, and GU	Excellent	Excellent	None	59.72 to 68.76	>39.30	30 to 80

A classification related to both subgrade and subbase materials is made for their CBR values (Table 2.8).

Table 2.8 Rating of both Subgrade and Subbase materials with respect to CBR values Schaefer et al. (2008)

CBR (%)	*Materials*	*Rating*
>80	Subbase	Excellent
50-80	Subbase	Very good
30-50	Subbase	Good
20-30	Subgrade	Very good
10-20	Subgrade	Fair-Good
5-10	Subgrade	Poor-Fair
<5	Subgrade	Very poor

2.5.2 Lime Stabilization of Subgrade/Subbase Layer of Highway pavement

Natural soils placed on highway route is not always suitable for road construction. Two different procedures, which are either the removal step or stabilization step, are generally applied to these soils. The stabilization step is the most preferable method in highway construction. A stabilization type changes to a type of soil found in the construction area. For example, the U.S. Department of Transportation (1976) stated that a material used in the stabilization step is determined for some soil properties (Figure 2.20)

According to HTS (2013), some soils or materials used in highway construction have to be stabilized with lime. These soils placed in highway route are explained below;

- A soil utilized in road infrastructure has low engineering properties,
- The capacity of soil is lower than the capacity of embankment material,
- A CBR value of soil is low,
- Soil has high swelling potential,

A material used in either subgrade or subbase layer improves engineering properties.These soils and materials mentioned above have to be stabilized with lime. Both unslaked and slaked lime are powder materials and have certain physical and chemical properties to utilize during the stabilization process (Table 2.9).

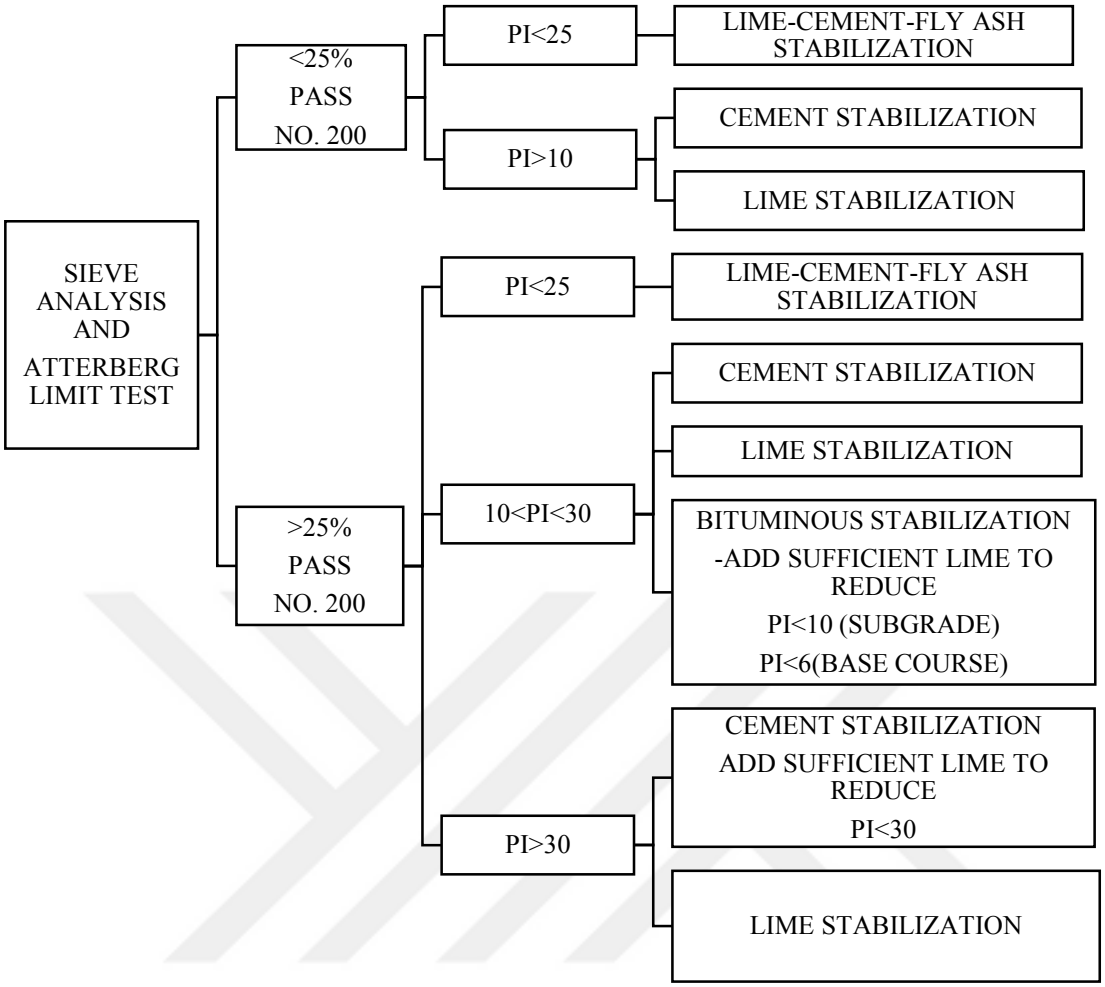

Figure 2.20 The selection of stabilizer material with respect to soil properties

Table 2.9 Physical and chemical properties of lime used at stabilization process (HTS, 2013)

Property	*Unslaked lime*	*Slaked lime*
CO_2 (%)	≤7	≤7
CaO+MgO (%)	≥80 ≤2	≥80 ≤2
SO_3 (%)	≤5	≤5
MgO (%)	≤2	-
Particle size (mm) Retained above sieve by weight (%)	-	0.09 mm ≤7 0.2 mm ≤2

According to HTS (2013), soils stabilized with lime are explained during highway construction in Figure 2.21.

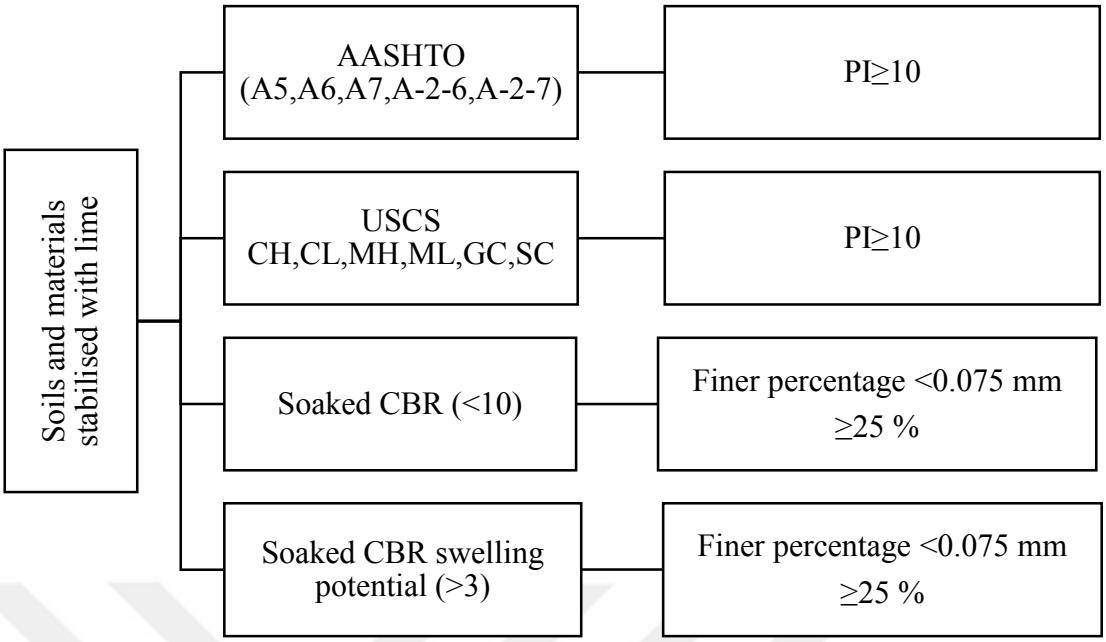

Figure 2.21 The properties of soils stabilized with lime (HTS, 2013)

Then, any type of soil explained in Figure 2.21, water and lime are homogenously mixed during the stabilization process. After the mixture process, this stabilized soil should wait in the curing room for 7 days. Then, a soaked CBR test is done on this soil to measure the both soaked CBR value and soaked CBR swelling potential. These properties change in terms of pavement layers (Table 2.10).

Table 2.10 Properties of stabilized soil with lime after 7 days curing (HTS, 2013)

Pavement layer	*Soaked CBR (%)*	*Soaked CBR swelling potential (%)*
Subbase	≥50	≤ 0.5
Subgrade	≥20	≤ 1
Embarkment	≥15	≤ 2

Seed et al. (1962) explained that the expansive soil is classified in terms of the swelling potential under the 7 kPa surcharge pressure (Table 2.11).

Table 2.11 The classification of expansive soil in terms of the swelling potential (Seed et al., 1962)

Degree of expansion	Swelling potential (%)
Low	≤ 1.5
Medium	1.5-5
High	5-25
Very high	>25

CHAPTER 3

INDEX AND ENGINEERING PROPERTIES OF EXPANSIVE SOIL SPECIMEN AND LIME COLUMNS

3.1 Expansive Soil Specimen

A comprehensive laboratory testing program is conducted with a high plasticity clay specimen consisted of kaolinite and bentonite to study the lignosulfonate lime column technique. In the preparation process, bentonite mineral, which has the highest swelling potential, activity, and liquid limit in clay soils, is used to obtain an expansive soil specimen having high swelling potential. Thus, it is easier to observe the influence of the stabilization process.

An expansive soil specimen that had swelling potential in this study is not natural soil. In other words, this soil that is named Specimen A has been prepared in laboratory condition. Specimen A is a mixture material that consists of kaolinite and bentonite. These materials are shown in Figure 3.1. Some information related to them is given below.

Figure 3.1 Kaolinite (left side) and Bentonite (right side)

Kaolinite: Kaolinite is taken from Kaolin Industrial Minerals Company in the form of gravel-sized grains. These grains are crushed and passed through the # 40 sieve before the study. The specific gravity was 2.57 and the liquid limit, plastic limit, and plasticity index were found as 46%, 28%, and 18%, respectively.

Bentonite: Bentonite is obtained from Karakaya Bentonite Factory which is situated in Esenboğa in Ankara. This material is pulverized and passed through the # 40 sieve before the study. The specific gravity was 2.53 and the liquid limit, plastic limit, and plasticity index were found as 410%, 34%, and 376% respectively.

Specimen A has been prepared with respect to dry weights. While a dry weight percentage of kaolinite into the mixture is selected as 85%, this percentage is taken as 15% for bentonite. The water content of this mixture is adjusted to 15%.

The following procedure was followed for the preparation of Specimen A. This procedure is explained below.

- Both kaolinite and bentonite were oven-dried for one day.
- They were passed through the No.40 sieve.
- They were mixed with the trowel in the cup.
- They were sieved two times through the No.20 sieve to obtain a homogeneous mixture at each mixture.

3.1.1 Properties of Specimen A

Soil properties are substantial parameters that are necessary for soil classification, estimation of soil behavior under any condition. For this reason, many properties related to soil are properly determined before their use in any engineering project. While some of them are very important for some soil types, some of them are not essential or are not determined for some soil types.

Some properties of Specimen A are determined in regards to standards and they are separated into three groups that are called index properties, engineering properties, and microchemical properties. In this study, properties analyzed in each group are listed in Table 3.1.

Table 3.1 Properties of Specimen A investigated in this study

Index properties	*Engineering properties*	*Microchemical properties*
Specific gravity Atterberg limits Grain size distribution Clay content Activity Maximum dry density Optimum water content	Unconfined compressive strength Swelling potential Swelling pressure Permeability coefficient CBR value	SEM images Chemical characterization CEC capacity Specific surface area Index of activity of the clay fraction

3.1.2 Physical Properties

Some index properties of Specimen A were found by doing some laboratory tests such as specific gravity, liquid limit, plastic limit, sieve analysis, hydrometer, and standard compaction. All tests except specific gravity were done to ASTM standards. A specific gravity test was done concerning Turkish standards.

Specific gravity test of specimen A was done by adding gas oil instead of water due to the reaction between the clay and water. This test was done for TS EN 196-2 (2013) in this study. The specific gravity of specimen A was found as 2.56.

The grain size distribution curve of specimen A was identified by using both the sieve analysis test and the hydrometer test (ASTM D422). The grain size distribution curve of specimen A was shown in Figure 3.2.

According to ASTM D4318, the Atterberg limits of this sample, which were the liquid limit, plastic limit, and plasticity index, were determined 95.2%, 23.2%, and 72%, respectively. The clay content of specimen A was found to a 57%. The activity of specimen A, that is the ratio between the plasticity index and clay content, was calculated as 1.27.

The maximum dry density and optimum water content were confirmed as 1.495 g/cm^3 and 26% with respect to ASTM D698. The compaction curve of specimen A is illustrated in Figure 3.3.

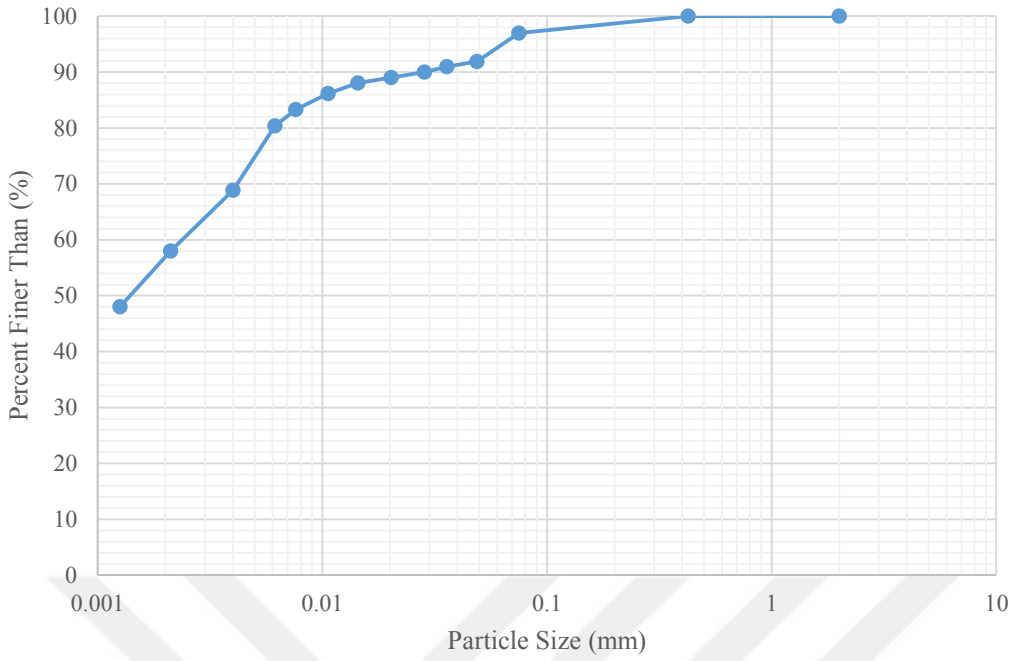

Figure 3.2 Grain Size Distribution Curve of Specimen A

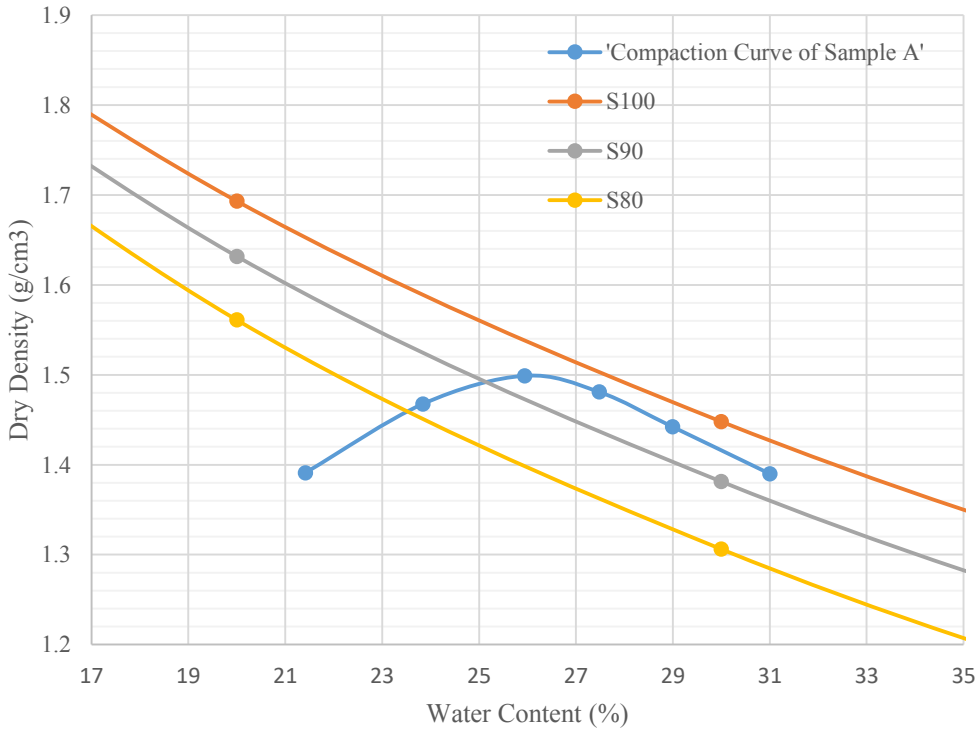

Figure 3.3 Compaction Curve of Specimen A

3.1.2.1 Methylene Blue Test

Two physical properties of clay soil such as cation exchange capacity and specific surface area are significant in terms of its behavior. A test called a Methylene Blue Test (MBT) is done to determine these properties. This test has been done concerning NF P 94-068 standard.

The first step of this test is the preparation of a solution consisted of 10 grams methylene blue and 1 liter distilled water. After two materials are put into the cylindrical cup, this solution is mixed with a mechanic mixer. This solution has waited in a closed bottle for one day.

Some amount of Specimen A (30 grams) is put into the 500 cm^3 distilled water (Figure 3.4). This suspension has been blended at 700 rpm for five minutes.

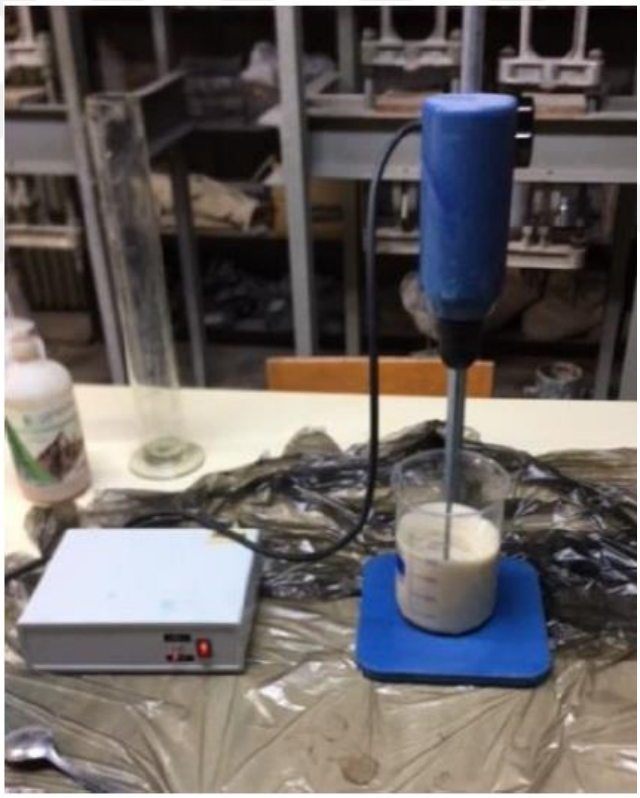

Figure 3.4 The suspension consisted of Specimen A and distilled water

Then, 5 cm^3 methylene blue solution is added to this suspension and a new composed suspension is mixed at 400 rpm for a minute (Figure 3.5).

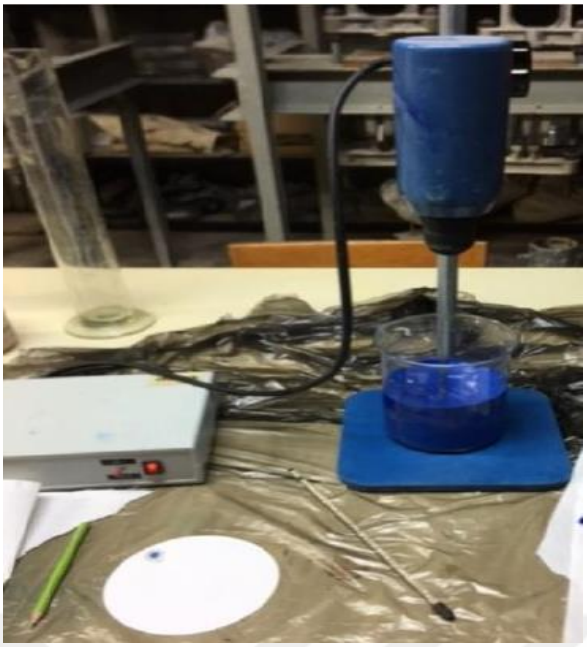

Figure 3.5 Methylene blue addition to the suspension

After a drop of the solution is removed with a glass rod and this drop is dripped on a sheet of filter paper. The addition of methylene blue solution to this suspension has been continued until the endpoint of this test. The endpoint of this test is explained that the edge of the dark blue circle appears fuzzy and/or is surrounding by a narrow light blue halo. Figure 3.6 shows the result of methylene blue test done on Specimen A in this study.

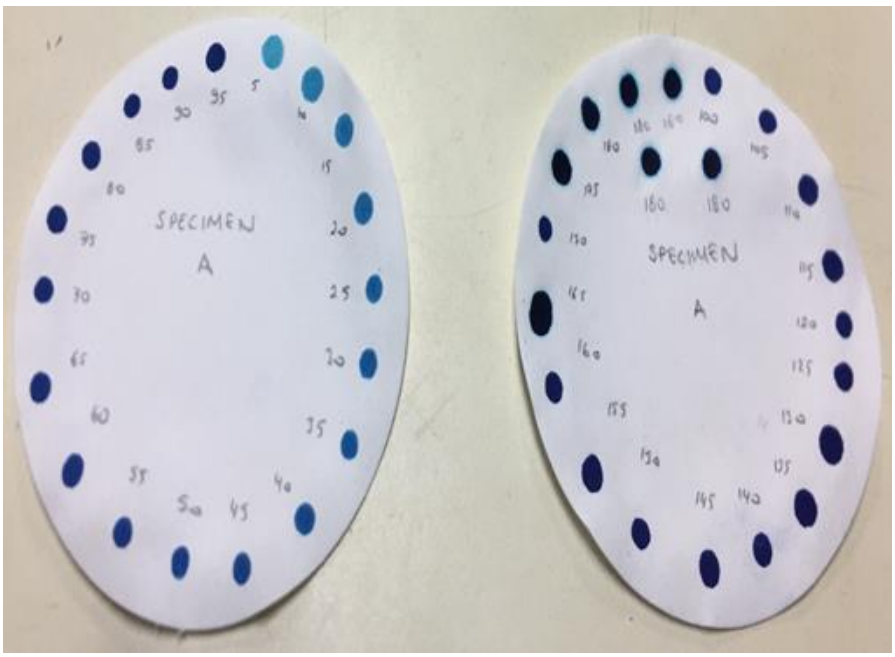

Figure 3.6 Methylene blue test data obtained from Specimen A

Some data obtained from this test was given below.

- WMB=The weight of dry methylene blue used for methylene blue solution (10 grams)
- VMBS=The volume of methylene blue solution (1 liter)
- VMB=The volume of methylene blue added to the sample until the endpoint is reached
- WS=The weight of the dry specimen used in this test (30 grams)
- NMB = The normality of methylene blue (NMB= WMB/320=10/320=0.03126)
- m(MB) = The mass of adsorbed methylene blue at the point of complete cation replacement (endpoint) (1.75 grams)
- AN=Avogadro's Number ($6.02*10^{23}$/mol)
- AMB = The area covered by one methylene blue molecule, typically assumed to be 130 Å2 ($130*10^{-20}$), according to Hang and Brindley (1970)

A test data Some parameters such as the blue value of the soil (V_B), index of activity of the clay fraction in soil (A_{CB}), specific surface (S_a), and cation exchange capacity (CEC) have been found for data mentioned below. These parameters have been found by using the equations given below (Eq. 3.1-3.3).

$$V_B = VMB \times 0.01 \times \frac{100}{WS} \qquad (Eq.3.1)$$

$$V_B = 180 * 0.01 * \frac{100}{30} = 6\frac{g}{100\ g}$$

$$CEC = \left(\frac{100}{WS}\right) X\ VMB\ X\ NMB \qquad (Eq.3.2)$$

$$CEC = \left(\frac{100}{30}\right) X180\ X\ 0.03126 = 18.75\frac{meq}{100\ g}$$

$$Sa = (V_B/100)(AN/WMB)(AMB) \qquad (Eq.3.3)$$

$$Sa = \left(\frac{6}{100}\right)\left(6.02 * \frac{10^{23}}{320}\right)(130 \times 10^{-20}) = 146.73\frac{m^2}{g}$$

In addition to these parameters, a parameter called an index of activity (A_{CB}) can be calculated by using both the blue value and clay content (CC) of soil. A formula related to this parameter is given below (Eq. 3.4).

$$A_{CB} = \frac{100V_B}{CC} \qquad (Eq.\,3.4)$$

$$A_{CB} = \frac{100 * 6}{57} = 10.52$$

3.1.3 Engineering Properties

Engineering properties of the soil are keystone parameters that generally determine its behavior under any engineering construction. The properties of Specimen A investigated in this step were divided into three groups those are volume change, permeability, and strength of soil specimen.

3.1.3.1 Properties of Specimen A related to volume change

Clay soil tends to volume change when it is not only exposed to water but also dried. The volume change should be estimated before the construction. A term named as a swelling potential is used when this soil is exposed to water. A free swell test was used for the measurement of the soil swelling potential. Specimen A has been compacted at maximum dry density (1.495 g/cm^3) and 15% water content with a hydraulic jack (Figure 3.7 (a)) before the free swell test. The sizes of the specimens prepared for both the free swell test and one-dimensional consolidation test are 6.35 cm diameter and 1.9 cm height. Bishop oedometer load frame (Figure 3.4 (b)) has been utilized for these tests in this study.

The swelling potential of a soil specimen under any pressures (SP) is that a ratio between the change in specimen height (h_f -h) and the initial specimen height (h). This calculation is given in Eq. 3.5.

$$SP(\%) = \frac{(h_f - h)}{h} \times 100\% \qquad (Eq.\,3.5)$$

a) Hydraulic jack b) Bishop load frame

Figure 3.7 Equipment used for both free swell test and one-dimensional consolidation test

The swelling potential of soil usually depends on the surcharge pressure applied to the soil. Therefore, some pressures were applied to the soil specimen for observation of any alteration of the soil swelling potential. These pressures applied in this step are 7 kPa, 25 kPa, 50 kPa, 100 kPa, 150 kPa, 200 kPa, 250 kPa, and 260 kPa.

The swelling potentials of soil under any pressures applied in this step are presented in Figure 3.8.

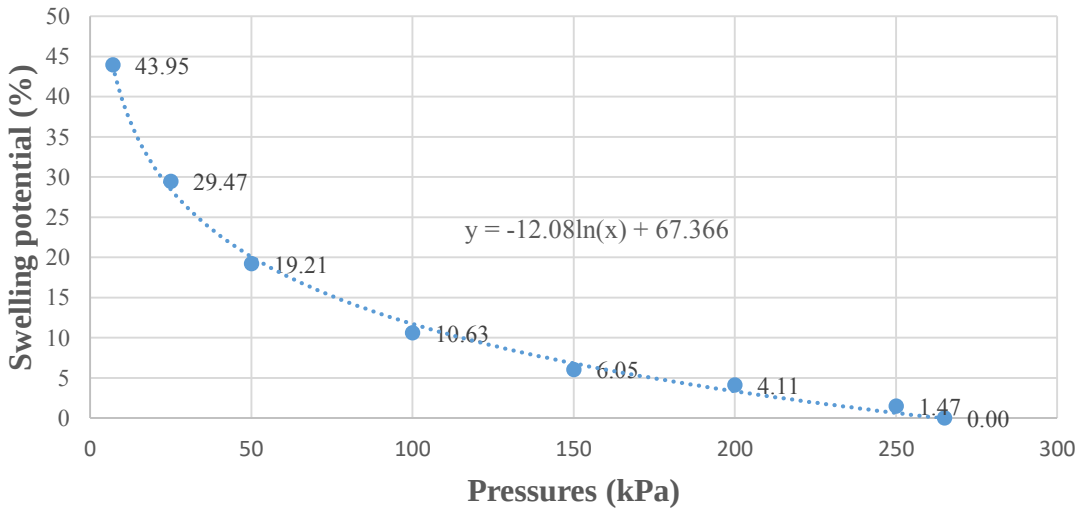

Figure 3.8 The change of swelling potential of specimen A with respect to pressures

Besides, the swelling potential of this specimen under any pressures up to swelling pressure could be estimated with the help of an equation, which was y = -12,08ln(x) + 67.366. Finally, an ultimate pressure applied to the specimen in this step, which corresponds to no volume change of soil, is called a swelling pressure of the specimen. This pressure was measured as 260 kPa for Specimen A.

Two surcharge pressures applied to Specimen A are 7 kPa and 25 kPa. Swelling potentials of Specimen A under 7 kPa and 25 kPa are respectively determined as 43.95% and 29.47%. These two values are reference points for the results of the next free swell tests.

3.1.3.2 Properties of Specimen A related to permeability

Two test methods have used to determine the coefficient of permeability of Specimen A. These are given below;

1- One-dimensional consolidation test

2- Flexible wall permeability test

3.1.3.2.1 One Dimensional Consolidation Test

The one-dimensional consolidation test can be used to determine the coefficient of the specimen permeability. An equation given below is used for the calculation of this parameter of soil (Eq. 3.6).

$$k = \gamma_w m_v c_v \qquad (Eq\ 3.6)$$

Both volume compressibility (m_v) and a coefficient of consolidation (c_v) are necessary for this calculation. These two parameters mentioned above are generally altered with respect to applied pressures in this test. As this study is focused on the expansive soil under the lightweight structure that had 25 kPa pressure, parameters obtained from the 25 kPa load increment of the specimen consolidation test were used for this calculation. A preparation procedure of the specimen in this step is identical to the specimen of the free swell test or one-dimensional consolidation test. The coefficient of permeability of specimen A was found as a $6.6 \times 10^{-10} cm/s$.

3.1.3.2.2 Flexible Wall Permeability Test

In this study, both vertical permeability and horizontal permeability of Specimen A have been determined by doing a flexible permeability test. The test specimens prepared in this step have been compacted at maximum dry density and optimum water content. The saturation of these specimens was found 94%. A procedure followed in this test is explained below;

- All equipment used in this test, which are valves, membrane, porous stone, were controlled before the test.
- A specimen was prepared (Figure 3.9 a). An initial reading of specimen dimensions was recorded.
- Porous stone and filter paper were soaked and placed at both base and top of the specimen. A membrane was placed around the specimen by using a membrane expander. Two O-rings were placed on the base and to the top cap for sealing the membrane (Figure 3.9 b).
- Permeameter cell was filled with de-aired water.
- 100 kPa back-pressure was applied to remove all air in the voids of the specimen.
- 200 kPa cell pressure was applied into the triaxial chamber to protect the specimen. Since the failure of the specimen results from an increase of pore pressure of the specimen(Figure 3.9 c).

a) Test specimen b) Placement of specimen c) Saturation process

Figure 3.9 The steps of flexible wall permeability test

- When outward drainage of water has reached the burette, the saturation process was completed.
- The readings were taken from volume change gage and burette after a chronometer was started. While the volume of water inflow into the specimen is measured by the volume change gage, the volume of water outflow from the specimen was determined by burette.
- When the inflow water volume equals the outflow water volume, a flow rate is steady. The test is finished.
- The final step is a calculation of both vertical permeability and horizontal permeability of Specimen A according to test data. Firstly, a graph of the cumulative outflow water volume versus time is plotted.

Two graphs of the cumulative outflow water volume versus time were drawn according to test data for both the vertical permeability and horizontal permeability of Specimen A (Figures 3.10-11).

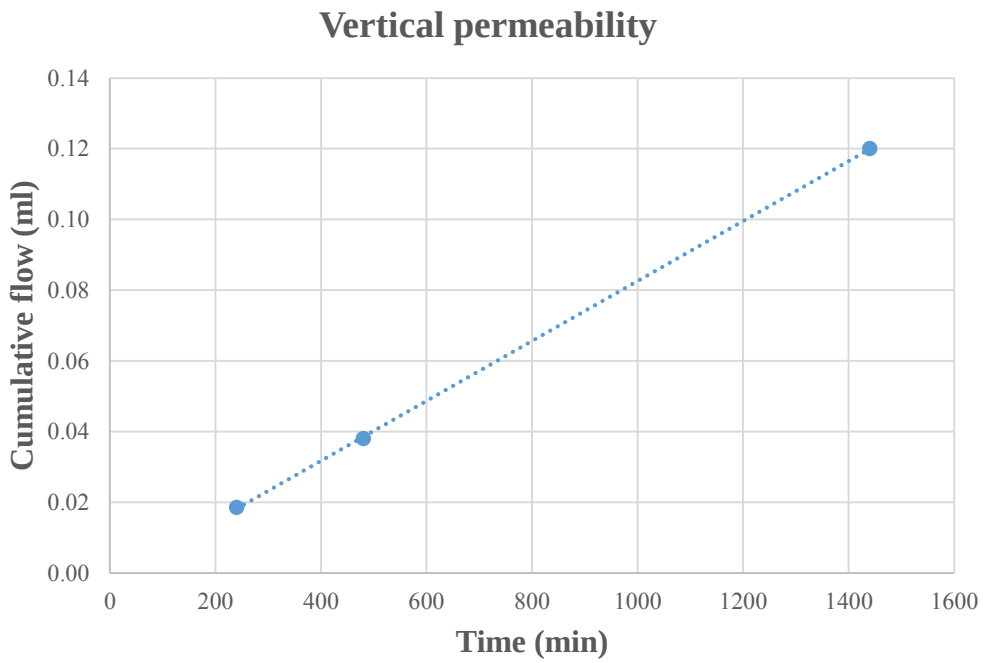

Figure 3.10 A graph of the cumulative outflow water volume versus time for the vertical permeability of Specimen A

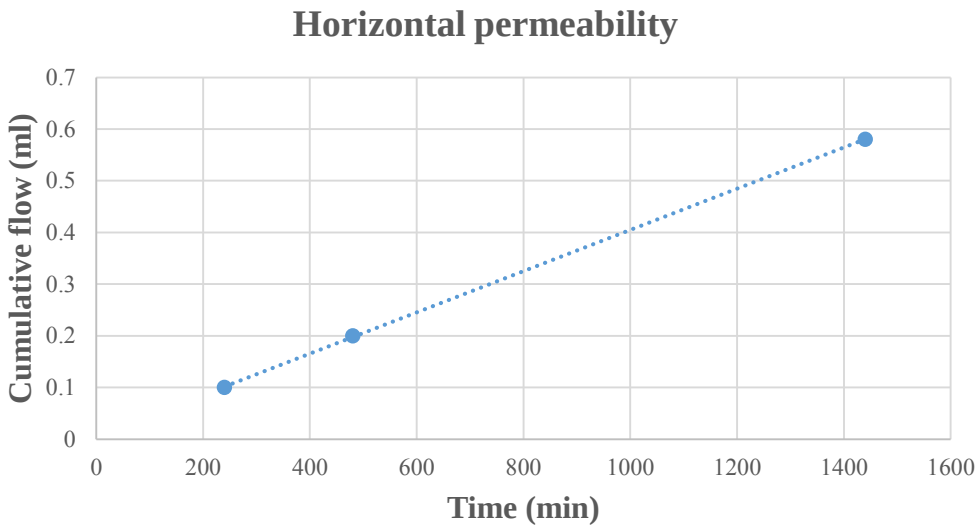

Figure 3.11 sA graph of the cumulative outflow water volume versus time for the horizontal permeability of Specimen A

The linear slope of the curve means a steady rate of flow. Then, the mean rate of flow (ml/min) is calculated from this linear part of the curve. In this study, both vertical permeability and horizontal permeability of Specimen A are calculated from this equation (Eq. 3.7).

$$k = \frac{qL}{6120Ap} \ m/s \qquad (Eq\ 3.7)$$

Where;

q: Mean rate of flow (ml/min)

L: Length of the specimen (mm)

p: Backpressure applied to the specimen (kPa)

A: Cross-sectional area of the specimen (mm^2)

According to these test results, the vertical permeability and horizontal permeability of Specimen A is determined $9.82 \times 10^{-10}\ cm/s$, $4.56 \times 10^{-9}\ cm/s$, respectively.

3.1.3.3 Properties of Specimen A related to strength

Strength parameters of Specimen A were found by doing two tests such as Unconfined Compressive Strength (UCS) and California Bearing Ratio (CBR). While the UCS test was done as to ASTM D2166, the CBR test was performed in regards to ASTM D1883.

3.1.3.3.1 Unconfined Compressive Strength

Two specimens had different water content were prepared for the UCS test. Although the dry densities of these specimens (1.495 g/cm^3) are the same, the water contents of these specimens are respectively selected as 15% and 26%.

A degree of saturation affects both the soil behaviour and the soil strength. For this reason, this parameter was found for two specimens prepared in this step. While this parameter of the specimen had 26% water content was calculated as 93.4%, this parameter is computed as 53.9% for the other specimen in this step.

The dimensions of all specimens for the UCS test are 3.8 cm in diameter and 7.6 cm in height. A mould for preparing specimens in this step has approximately 3.6 cm diameter and 10 cm height. The test specimen was put into the mould and compacted at three layers with a hydraulic jack.

The unconfined compressive strength of Specimen A had 15% water content was measured as an approximately 385 kPa. Specimen prepared at maximum dry density and optimum water content was determined as a 510 kPa. The stress-strain curves of these specimens after the unconfined compression test are given in Figure 3.12.

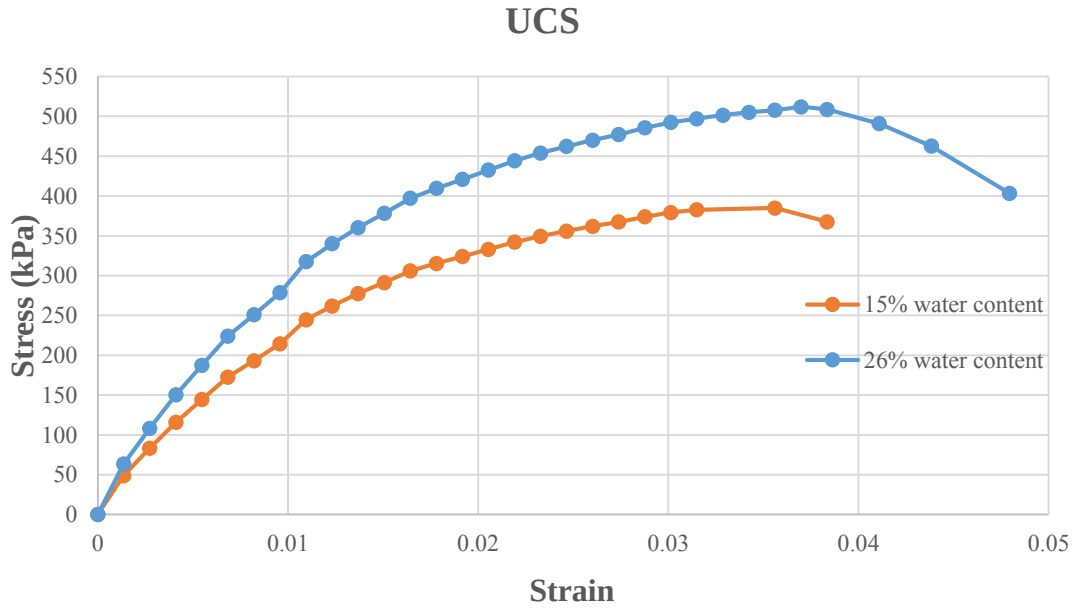

Figure 3.12 The unconfined compressive strength of specimen A with respect to water content

3.1.3.3.2 California Bearing Ratio Test

The preparation of the specimen was briefly explained for the soaked CBR test. The dry density and moisture content of Specimen A was 1.495 g/cm^3 and 15%. The soil was mixed thoroughly after adding the required amount of water corresponding to the moisture content. The soil was filled in the mould and then compacted to get the required dry density. This part, which was the preparation of unsoaked CBR, was valid for both unsoaked CBR and soaked CBR.

The shear strength of specimen A was specified by doing the CBR test. This test was done at two different conditions that were unsoaked condition (dry soil) and soaked condition (wet soil). The test procedure followed is explained below;

- For soaked CBR specimen, a filter paper and a perforated metallic disc with adjustable stem along with an annular surcharge load (weight 12.67 kg) were then placed on the top of the compacted soil specimen. The whole mould assembly was transferred to a soaking tank filled with water. After that, the swell measuring device was placed on the top edge of the mould to determine the swelling potential of the specimen. The initial dial gauge reading was recorded. The mould assembly was left undisturbed for 96 hours in the soaking tank to allow the soaking of water in the specimen. After 96 hours of soaking, the final dial gauge reading was recorded to measure the swelling potential of the specimen due to the soaking of water.

- Now the whole mould assembly was transferred to a motorized loading frame to conduct the CBR test. Initially, a seating load of 12.67 kg was applied through the penetration plunger at the center of the specimen. The load cell and LVDT were set to zero before the application of any further load. The load was then applied through the penetration plunger at a constant rate of strain (1.27 mm/minute) and the loads were carefully recorded up to a total penetration of 12.50 mm. Finally, load~penetration curves were drawn for each case and corrections were applied to the load~penetration curves wherever required using the standard procedure. This process was followed for all the specimens considered in the investigation.

The swelling potential of Specimen A was measured at 40.3% after 96 hours of soaking. The test results for unsoaked conditions and soaked specimens were illustrated in Figure 3.13.

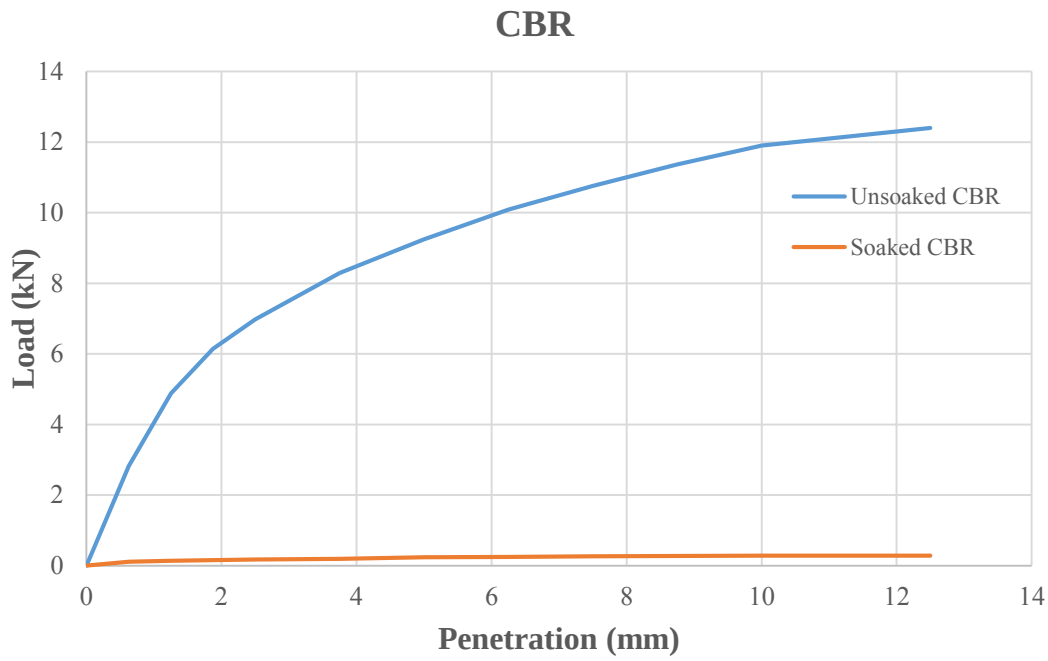

Figure 3.13 The test results of Unsoaked CBR and Soaked CBR

Although the CBR value of the unsoaked condition was found as 51.52 %, the CBR value of the soaked condition was found at 1.31 % (Figure 3.14).

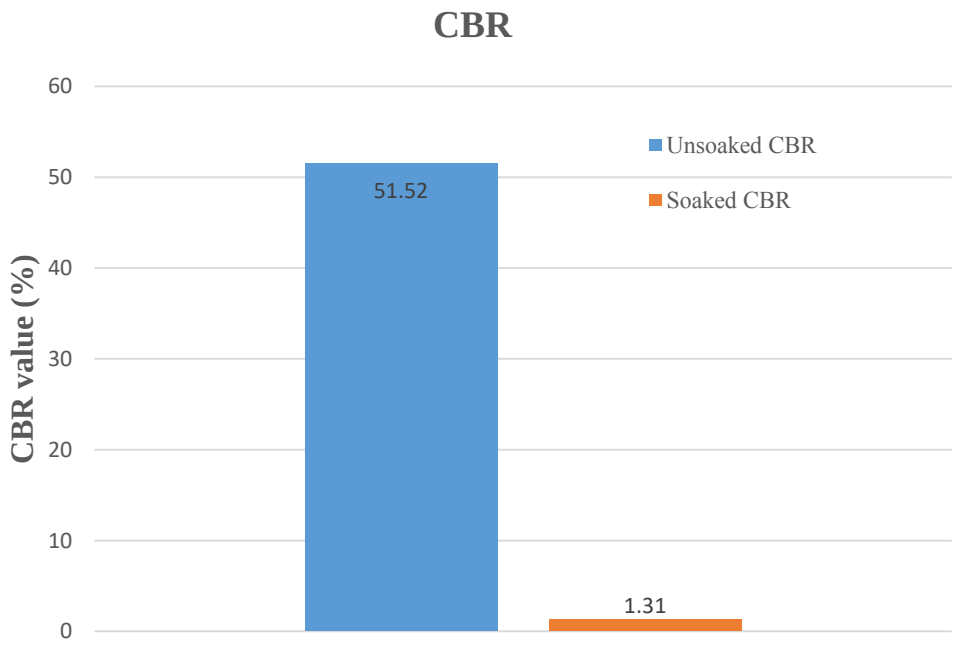

Figure 3.14 The CBR value for both unsoaked condition and soaked condition

3.1.4 SEM-EDX Analysis

The microchemical properties of clay soil give engineers some information about its behaviour, its interaction between water, its chemical composition, and its particle structure, etc. Some tests that are SEM analysis, and EDX analysis have been done to investigate these properties of Specimen A. Detailed information about these tests done in this study is given below.

SEM analysis was done at METU Central Laboratory. The name of the device used for SEM analysis in this study is QUANTA 400F Field Emission Scanning Microscope. Firstly, Specimen A was dried at 45°C and pulverized before the analysis. This process is done as water vapors that existed in soil particles do not harm the scanning electron microscope. After the samples were cupped, they were coated with gold and palladium for SEM Analysis.

SEM images of Specimen A are shown in Figure 3.15. In addition to this, Energy Dispersive X-Ray (EDX) analysis was performed to take information about chemical characterization of Specimen A during SEM analysis. EDX diagrams that were obtained from Specimen A are illustrated in Figure 3.16.

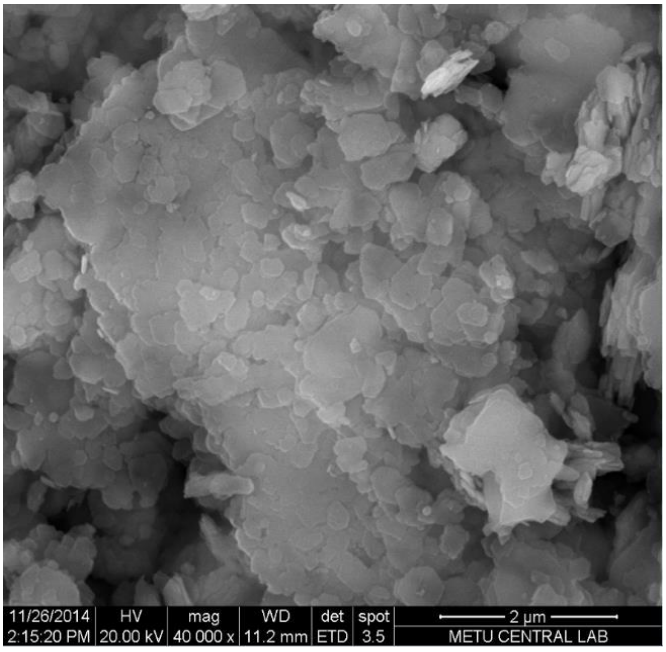

Figure 3.15 SEM image of Specimen A (magnification factor=40000)

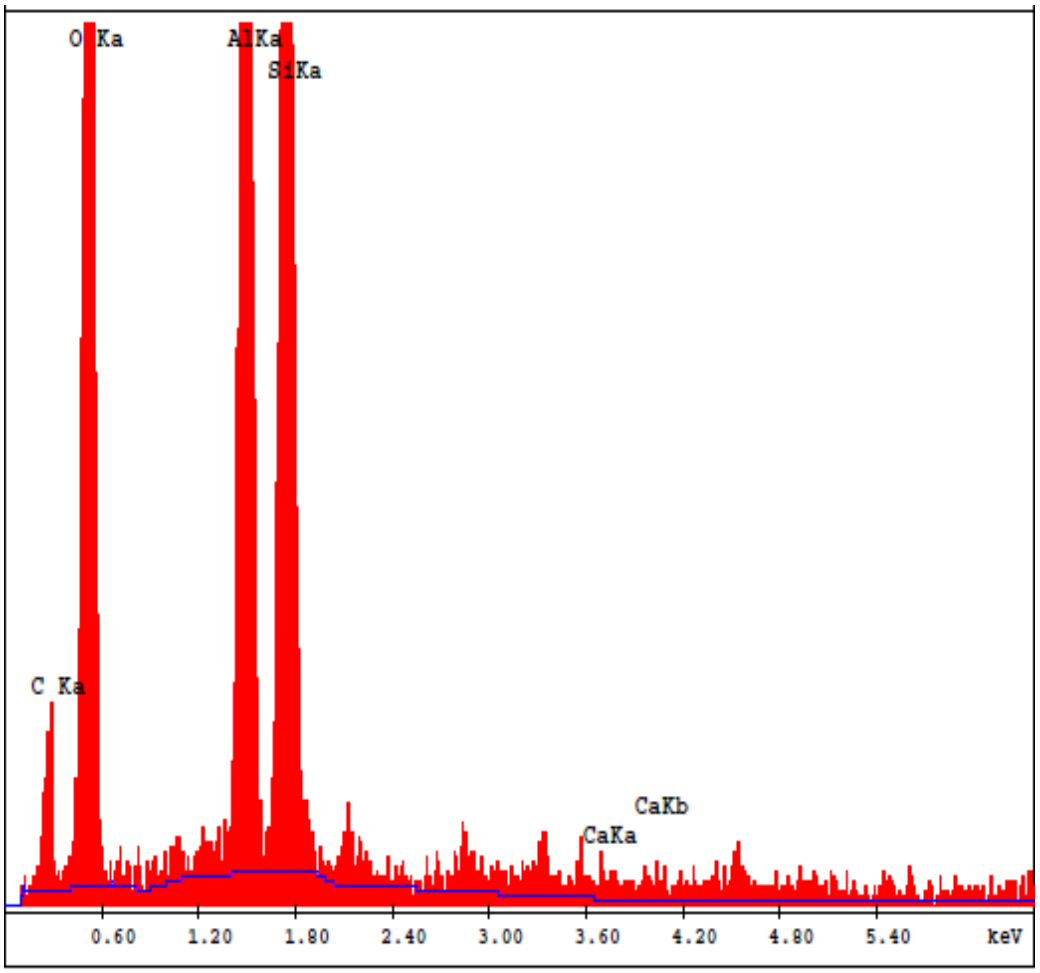

EDAX ZAF Quantification (Standardless)
Element Normalized
SEC Table : Default

Element	Wt %	At %	K-Ratio	Z	A	F
C K	15.97	23.53	0.0270	1.0334	0.1634	1.0005
O K	48.68	53.86	0.1543	1.0161	0.3119	1.0004
AlK	15.57	10.21	0.1084	0.9465	0.7307	1.0072
SiK	19.39	12.22	0.1284	0.9741	0.6796	1.0000
CaK	0.39	0.17	0.0035	0.9445	0.9493	1.0000
Total	100.00	100.00				

Element	Net Inte.	Bkgd Inte.	Inte. Error	P/B
C K	8.72	1.01	8.92	8.61
O K	130.62	1.35	2.10	96.79
AlK	130.39	3.15	2.13	41.41
SiK	143.89	3.54	2.02	40.62
CaK	2.42	0.73	19.32	3.31

Figure 3.16 EDX Diagram of Sample A

3.1.5 Classifications of Specimen A

Specimen A is classified by using both its Atterberg limits and particle sizes to some standards such as Unified Soil Classification System (USCS), American Association of State Highway and Transportation Officials (AASHTO), Turkish Soil Classification System (TS EN ISO 14688). While this specimen is a high plasticity clay (CH) in regards to both USCS and TS 1500, it is determined as an A-7-6 according to AASHTO.

In 2013, Highways Technical Specification was prepared by Turkey Highways General Directorate. According to this specification, some soils have to be stabilized with lime before a highway construction. These soils can be specified in two different ways;

- The first one is based on a soil classification system. The soil had to be stabilized with lime should be both A5, A6, A7, A-2-6, A-2-7 according to AASHTO or CH, CL, MH, ML, GC, SC according to USCS and its plasticity index should be greater than 10%.
- The second one uses data obtained from California Bearing Ratio (CBR) test. The soil had to be stabilized with lime should be both its Soaked CBR value (<10%) or its CBR swell (≥ 3%) and its fine grain particles percentage (≥ 25%)

In conclusion, Specimen A should be stabilized with lime to obtain more stable soils for highway construction for this specification.

According to the Highways Agency of the United Kingdom, Specimen A is not used as fill material in the earthworks since the liquid limit and plasticity index of suitable soil for earthworks should be lower than 90% and 65%, respectively.

According to this classification, Specimen A under both 7 kPa and 25 kPa surcharge pressures is soil that had very high volume changes according to the classification done by Seed et al. (1962). According to this classification system, the swelling potential of the soil had very high volume changes is greater than 25%.

A classification of the index activity is made by Lautrin (1989). This classification is based on clay content and index of activity and is shown in Figure 3.17. Detailed information about this classification is given in this figure.

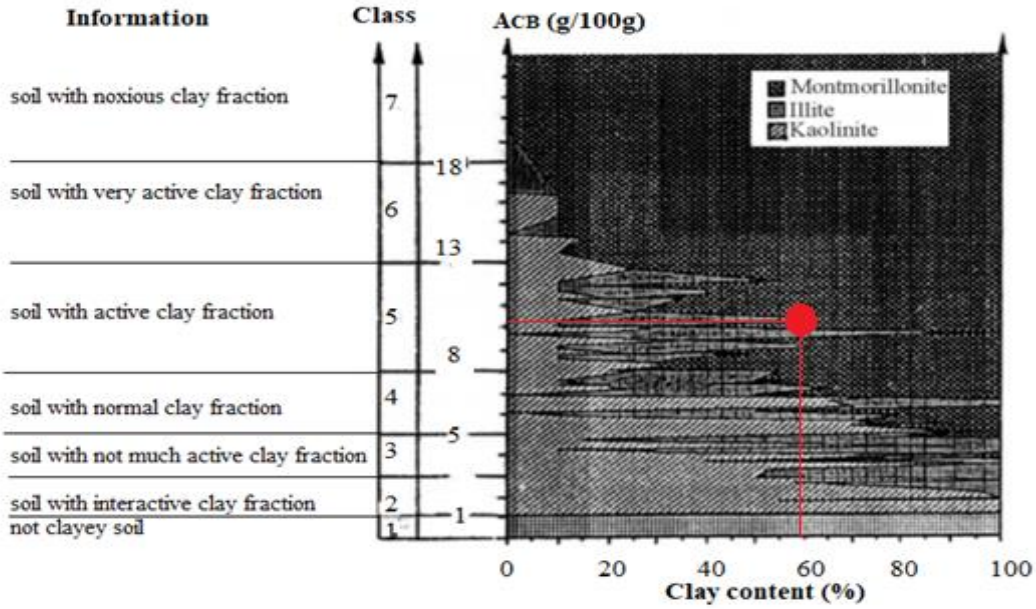

Figure 3.17 Methylene blue activity diagram

(modified from both Lautrin 1989 and Chiappone et al, 2004)

3.2 Lime Columns

The main objective of this step is that soil used as a highway subgrade is stabilized with the lime column technique. According to Highway Technical Specification (2013), a highway subgrade should have some properties after a stabilization process. The properties of this layer are swelling potential and soaked CBR value after 7 days curing period. However, this step of the study is focused on the swelling potential of the treated specimen with the lime column technique. The swelling potentials of this layer should be lower than 1% after soaked condition. In addition to this as proposed by Seed et al. (1962), the classification of expansive soil was done by using data obtained from the free swell test (Table 3.3).

Table 3.2 Classification of soil (Seed et al. 1962)

Degree of Expansion	*Swelling potential (%)*
Low	0-1.5
Medium	1.5-5
High	5-25
Very high	>25

Some parameters related to the lime column technique were comprehensively investigated in this step of the study. This study was based on the free swell test under two surcharge pressure such as 7 kPa and 25 kPa to determine the swelling potentials of treated soils prepared in this part of the study.

Specimens were prepared in an oedometer ring in this part of the study. The compacted specimens in this ring had 6.35 cm diameter and 1.9 cm height. Two subjects have been investigated in this step of the study. These are;

- Lime columns built into this specimen such as column diameter and a distance between the lime columns should be determined. Therefore, the first step of this study is about the column installation model.
- Lime diffusion into the soil is a significant parameter of this method. Some factors have generally influenced the achievement of lime diffusion into the soil. Some of them have been comprehensively searched at the second step of the study.

In addition to these, the most suitable model obtained from the previous two steps is going to be selected to use a correlation process. Then, these selected models had both different diameters and different heights are going to be prepared for the free swell test. Therefore, some outputs resulted from these tests are going to be used for the correlation process.

3.2.1 Selection of Column Installation Model

Many alternative installation models for lime columns in this step can be applied even though the sizes of the specimen are specific. For this reason, two parameters about the installation of the column into the untreated

specimen are fixed to obtain one installation model. The first parameter is that a model of the columns built into the specimen. This parameter has been determined as a circular orbit since this specimen shape is circular. The second one is that a distance between two columns and this parameter is indicated as 0.9 times the diameter of the column (D) in this step. These parameters are given in Figure 3.18.

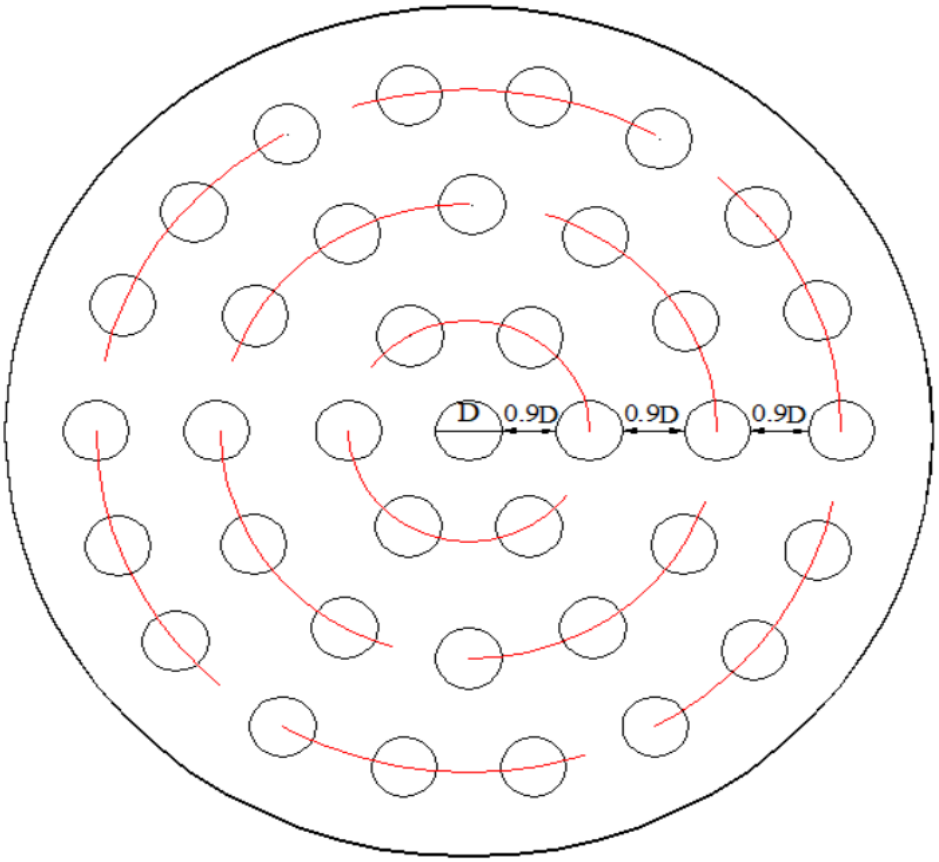

Figure 3.18 Circular orbit and distance between two columns

A number of the columns into the treated specimen changes to the diameter of the column. A parameter that is called an area ratio of the column is utilized to decide this piece. The area ratio is found that the area of columns are divided by the area of the specimen. In addition to this, a border of the specimen is drawn that is half of a column diameter extending from the outermost column because an untreated part of the specimen that existed in this distance is tried to treat by each column. Thus, this distance is forty-five percentages of the column diameter. To calculate the area ratio, an assumption that the treated specimen included seven columns is shown in Figure 3.19.

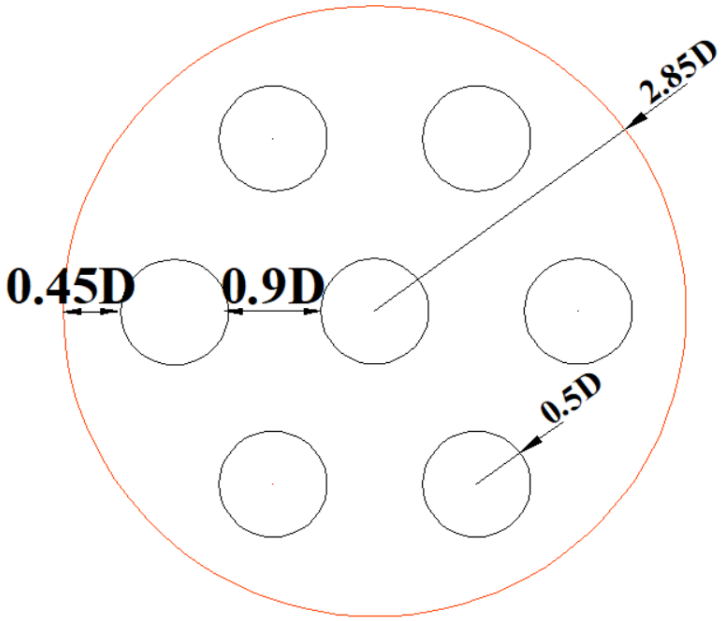

Figure 3.19 Assumption sample for area ratio

The area of the specimen and the area of columns are calculated in Eq 3.9 and Eq 3.10, respectively. Then, the area ratio is found as in Eq. 3.11.

$$Area\ of\ specimen = \pi * 2.85D^2 \qquad Eq.3.9$$

$$Area\ of\ columns = 7 * \pi * 0.5D^2 \qquad Eq.3.10$$

$$Area\ ratio = \frac{Area\ of\ columns}{Area\ of\ all\ specimen} = \frac{7 * \pi * 0.5D^2}{\pi * 2.85D^2} \qquad Eq.3.11$$

Some models of the column installation with respect to the number of circular orbits are illustrated in Figure 3.20. Even though the specimen area is constant for each model, the number of columns, the column area, and the area ratio alters in regards to the number of the circular orbit (Table 3.4). Besides this, these alteration percentages of area ratio to the specimen that is noninclusive circular orbit are given concerning the number of the circular orbit in Table 3.4.

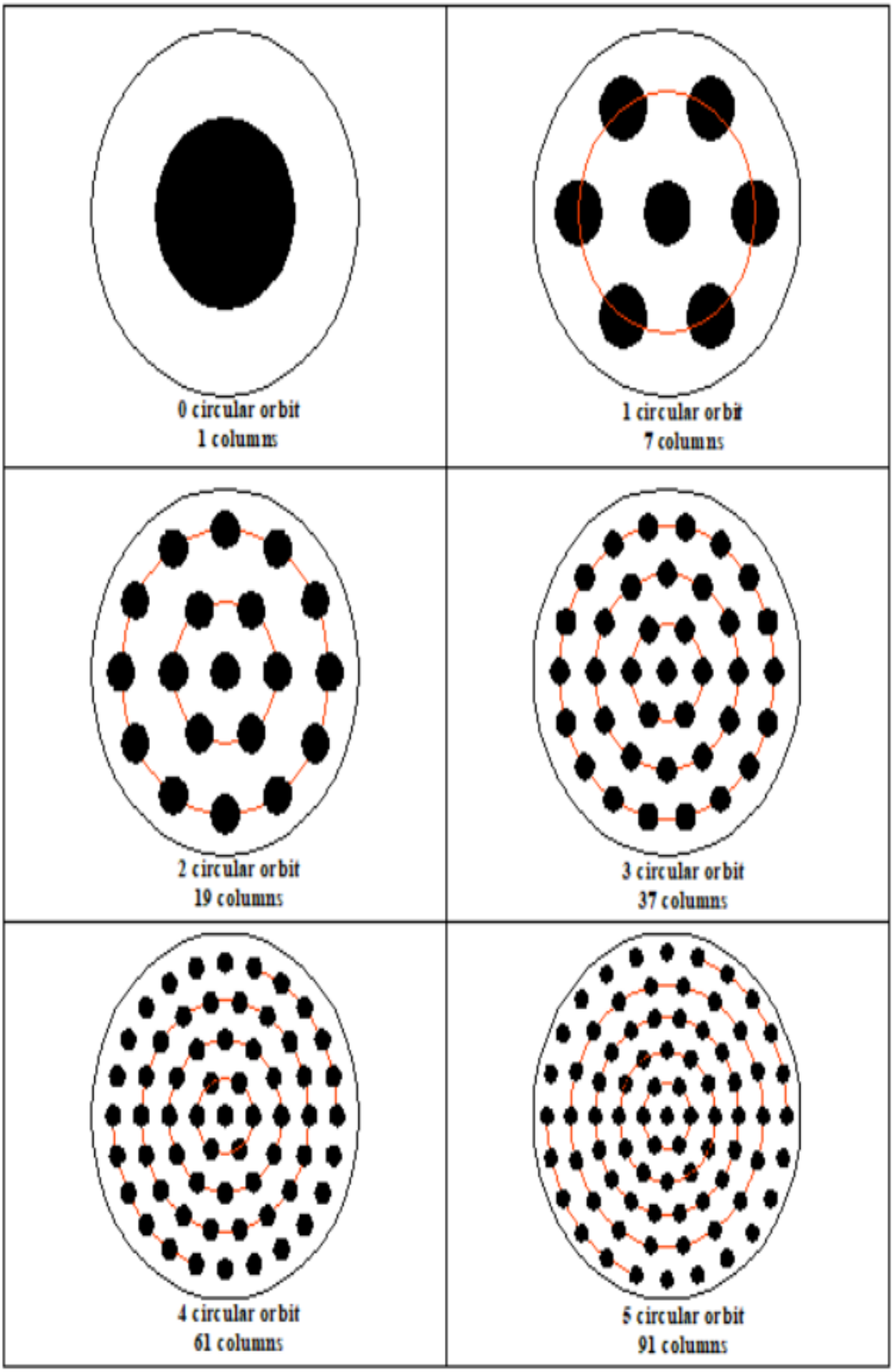

Figure 3.20 Column installation models with respect to the number of the circular orbit

Table 3.3 Alterations of area ratio with respect to the number of a circular orbit

The number of the circular orbit	*Number of Boreholes*	*Area of columns(cm^2)*	*Area of specimen(cm^2)*	*Area Ratio (%)*	*Alteration (%)*
0	1	$1 * \pi * (0.5D)^2$	$\pi * (0.95D)^2$	$100 * \frac{1 * \pi * (0.5D)^2}{\pi * (0.95D)^2} = 27.70$	$100 * \frac{27.7 - 27.7}{27.7} = 0$
1	7	$1 * \pi * (0.5D)^2$	$\pi * (2.85D)^2$	$100 * \frac{7 * \pi * (0.5D)^2}{\pi * (0.2.85D)^2} = 21.55$	$100 * \frac{27.7 - 21.55}{27.7} = 22.20$
2	19	$1 * \pi * (0.5D)^2$	$\pi * (4.75D)^2$	$100 * \frac{19 * \pi * (0.5D)^2}{\pi * (4.75D)^2} = 21.05$	$100 * \frac{27.7 - 21.05}{27.7} = 24$
3	37	$1 * \pi * (0.5D)^2$	$\pi * (6.65D)^2$	$100 * \frac{37 * \pi * (0.5D)^2}{\pi * (6.65D)^2} = 20.91$	$100 * \frac{27.7 - 20.91}{27.7} = 24.51$
4	61	$1 * \pi * (0.5D)^2$	$\pi * (8.55D)^2$	$100 * \frac{61 * \pi * (0.5D)^2}{\pi * (8.55D)^2} = 20.86$	$100 * \frac{27.7 - 20.86}{27.7} = 24.69$
5	91	$1 * \pi * (0.5D)^2$	$\pi * (10.45D)^2$	$100 * \frac{91 * \pi * (0.5D)^2}{\pi * (10.45D)^2} = 20.83$	$100 * \frac{27.7 - 20.83}{27.7} = 24.80$

An acceleration of the alteration percentages of area ratio continues with the number of circular orbits but this acceleration progressively decreases. This alteration percentage is under 1% after two circular orbits. Two installation models that had different column diameters are preferred in this step thereby the specimen diameter is constant. These models are explained below;

M1 models: The first model of the column installation is selected as a specimen consists of two circular orbit and 19 columns. Thus, column diameter and the distance between the two columns are respectively found as 6.5 mm, 5.85 mm as the diameter of the specimen included two circular orbits is 63.5 cm (Figure 3.21). Treated specimen prepared with respect to this model has been called an M1.

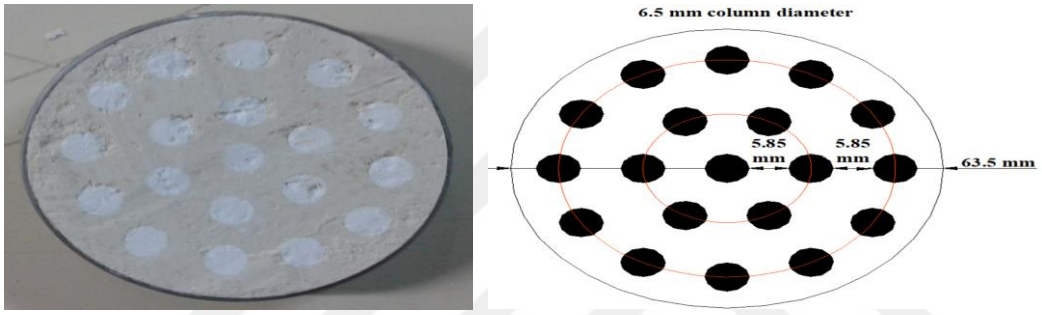

Figure 3.21 The first model consisted of two circular orbits and 19 columns had a 6.5 mm diameter

M2 models: The second model of the column installation is selected as specimen included three circular orbit and 37 columns. Thus, column diameter and the distance between two columns are respectively found as 4.5 mm, 4.05 mm due to the diameter of the specimen included three circular orbit (Figure 3.22). Treated specimen prepared with respect to this model has been called an M2.

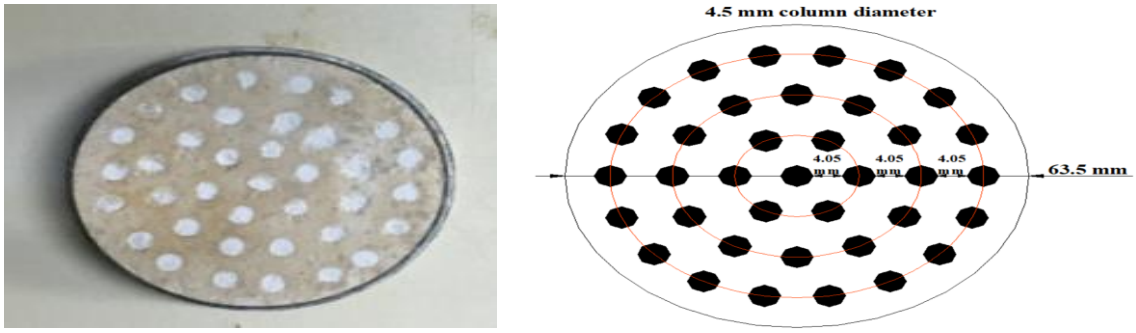

Figure 3.22 Second model consisted of two circular orbits and 37 columns which have 4.5 mm diameter

3.2.2 Factors Affecting the Achievement of the Lime Column Technique

A parameter related to expansive soils, which is called a swelling potential, gives civil engineers an idea about the volume changes. The lime column technique is commonly applied to reduce the volume change. However, many factors like height of the column, the surrounding area of all columns, water percentages of the water-lime mixture, material added to the water-lime mixture (Sodium Lignosulfonate or Calcium Lignosulfonate) generally affect the swelling potentials of these soils treated with lime column technique.

This part of the study was concentrated on these factors stated above. These factors were investigated in the subtitles given below.

- ✓ The height of the column
- ✓ The surrounding area of all columns
- ✓ The water percentages of the water-lime mixture
- ✓ Lignosulfonate added to the water-lime mixture

Although some information about the first three factors has existed in the literature, any information related to the last factor has not been studied until now.

Bishop oedometer load frame was used for all free swell tests under two surcharge pressures such as 7 kPa and 25 kPa (Figure 3.23). While the 7 kPa surcharge pressure is represented as a very lightweight structure such as a sidewalk, the 25 kPa surcharge pressure is represented as a lightweight structure such as pavement and embankment fill loading or one-story, one-two house loading.

Figure 3.23 Bishop load frame

Many free swell tests were done in this step of the study as two different models and two surcharge pressures have existed to investigate four factors. In addition to this, each factor consists of two or more groups. A test program followed at this step is shown in Figure 3.24.

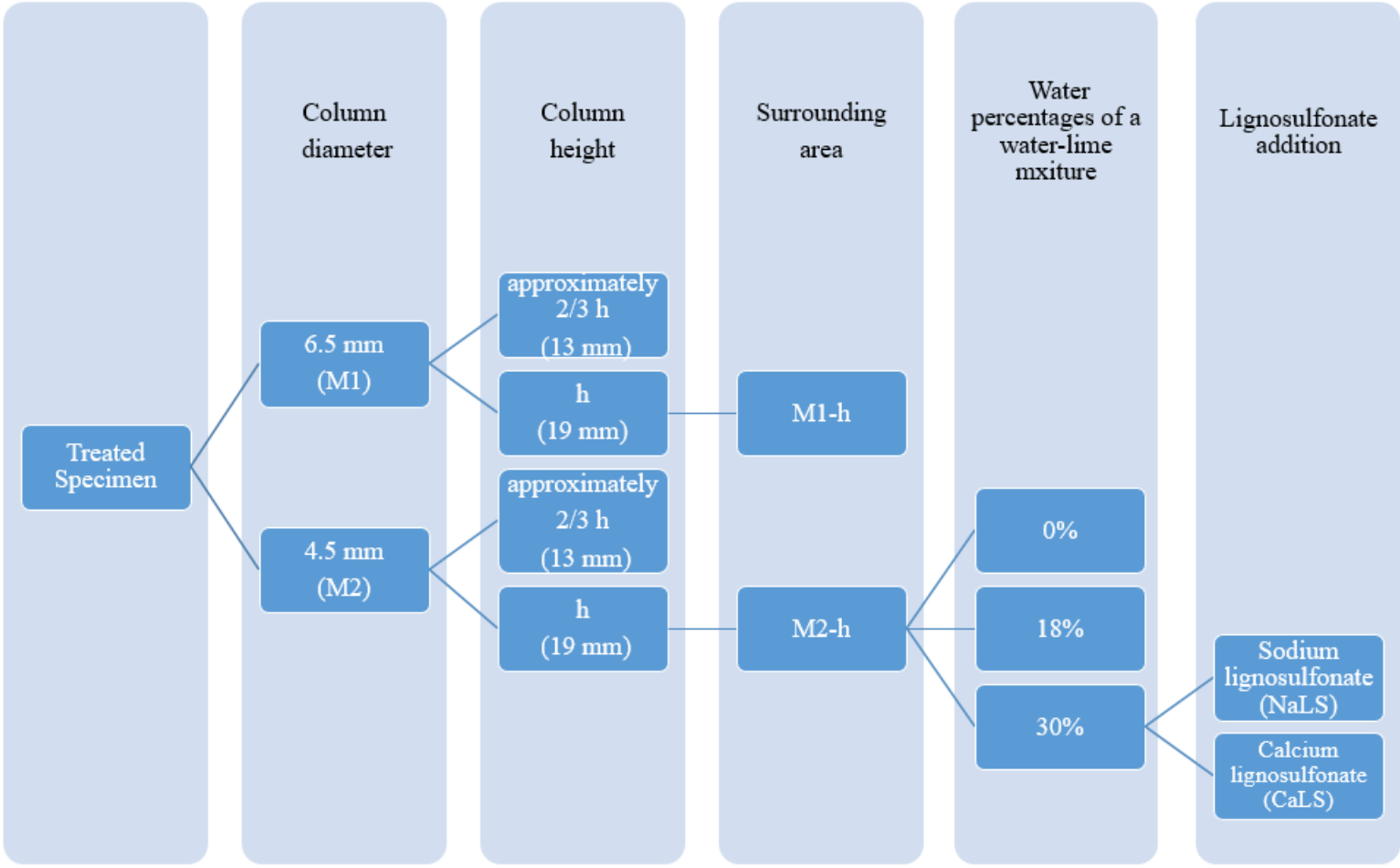

Figure 3.24 Test program followed at this step of the study

When this program is applied for each section, the more suitable specimen from the previous section is selected. Thus, the test program is made for the reduction in the number of free swell tests. In the subtitles, not only some information given in Figure 3.24 but also reasons related to the planning of this program are going to be explained in detail.

This test program is based on the swelling potential of treated specimens. The main goal of this test program is that the swelling potential of treated specimens should be 1% that is determined for HTS (2013). According to the classification done by Seed et al. (1962), the swelling potential of the soil had low volume change should be lower than 1.5%.

3.2.2.1 The Height of the Column

A volume changes of the expansive soils generally occur in the active zone of the soil. The problem about these changes is significantly solved when the soil in the active zone is improved with the lime column technique. Since all specimen particles swell when the water is added to this specimen. Therefore, the active zone of the specimen used in this step is the height of the specimen. The symbol of either specimen height or active zone in this study is h.

The height of the columns built into this zone should be determined to find out an effective column height before the installation process. Two different column heights, which are approximately 2/3h and h, are preferred for qualifying the effective column height. The first column height and second column height are respectively adjusted as 13 mm and 19mm due to the height of the oedometer ring (Figure 3.25).

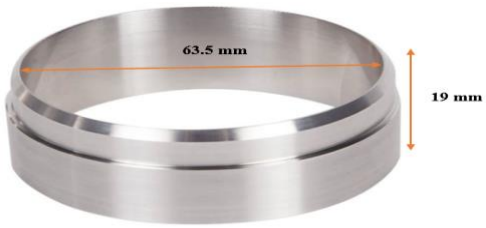

Figure 3.25 Oedometer ring dimensions

Treated specimens in this step have been separated into four groups as two-column installation models and two-column height have existed in this step.

The names of these groups are M1-2/3h, M1-h, M2-2/3h, and M2-h, respectively. A top view of both the M1-2/3h and M1-h are similar (Figure 3.26a.) but the A-A cross-section of these samples are different due to the column height (Figure 3.26c. and 3.26e.). This condition is valid for M2-2/3h and M2-h (Figure 3.26b, 3.26d, and 3.26f.)

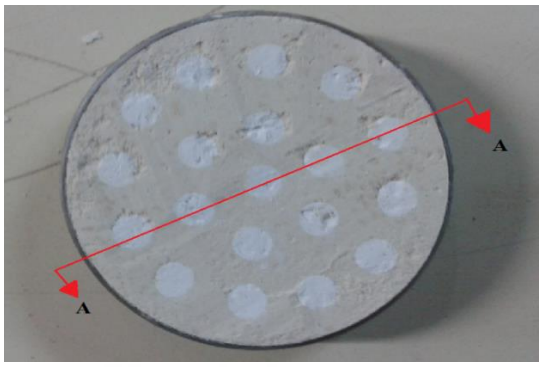

a) Top view of M1-2/3h and M1-h

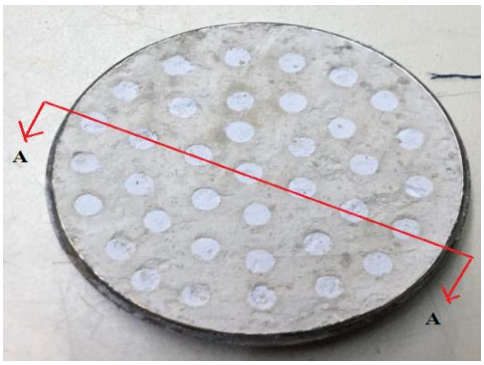

b) Top view of M2-2/3h and M2-h

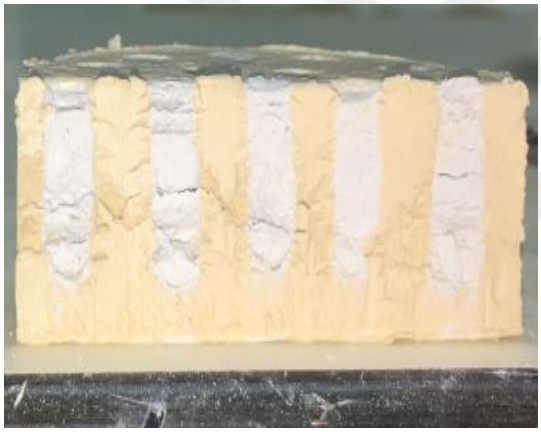

c)A-A cross-section of M1-2/3h

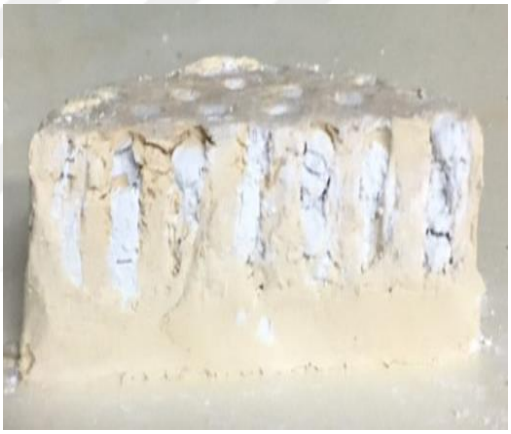

d) A-A cross-section of M2-2/3h

e)A-A cross-section of M1-h

f) A-A cross-section of M2-h

Figure 3.26 Top view and A-A cross-section of M1-2/3h, M1-h, M2-2/3h, and M2-h

Three different specimens have been prepared to investigate the curing effect of this method. While one specimen is tested as soon as it is prepared, the other two specimens have respectively waited for 7 days and 28 days in a humid room.

The swelling potentials of a treated specimen prepared in this study under one surcharge pressure, which is 7 kPa. The swelling potentials of these specimens prepared in this step under7 kPa are illustrated in Figure 3.27. Swelling potential vs. time graphs for treated specimens prepared in this step are presented in Appendix A.

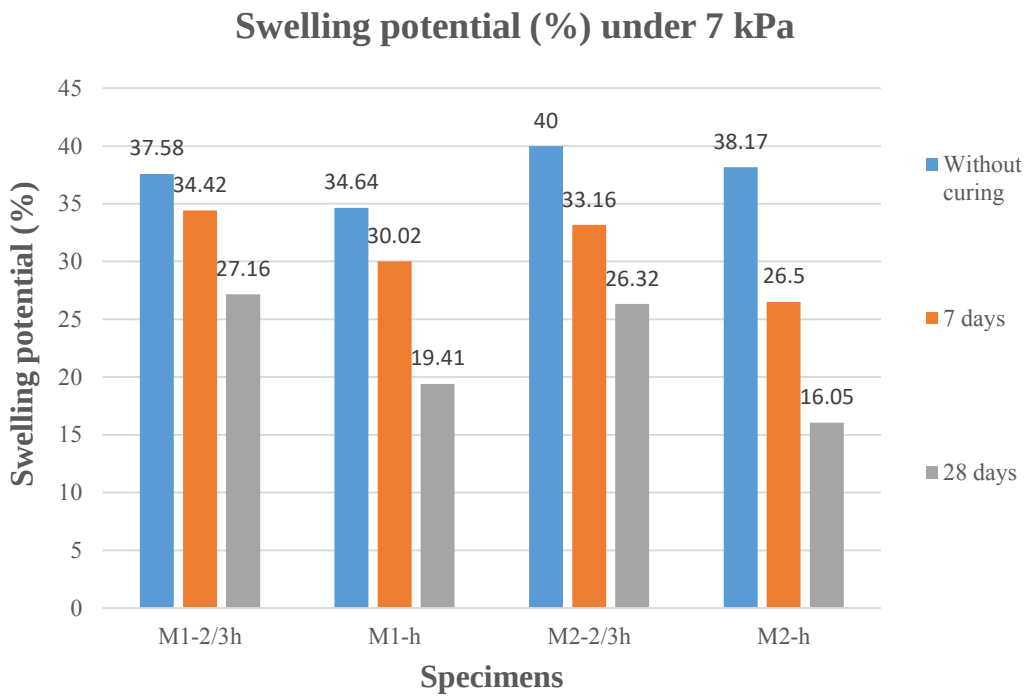

Figure 3.27 Swelling potentials of treated specimens under 7 kPa

Under 7 kPa surcharge pressure, while the swelling potential of Specimen A is 43.95%, the swelling potentials of treated specimens are lower than this value. The reduction of swelling potentials of them results from not only the lime column effect but also the volume reduction of Specimen A. Therefore, a parameter named an improvement percentage is developed for the effect of the lime column on the swelling potentials of the treated specimen. The improvement percentage of the treated specimen is a determinant parameter of this study. Since this parameter is that an effect of this treatment method onto the untreated specimen.

The improvement percentages of treated specimens are shown in Figure 3.28. Besides that, the calculation of improvement percentage is given in Appendix B.

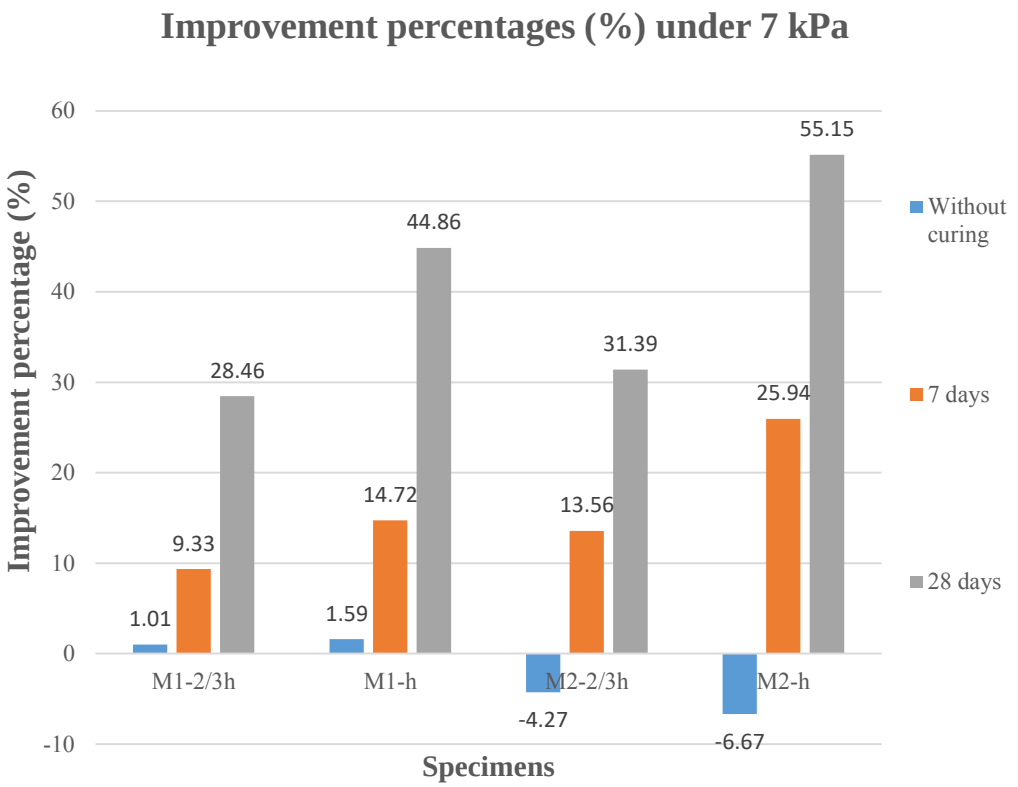

Figure 3.28 Improvement percentages of treated specimens in this step under 7 kPa

The values of improvement percentages of all treated specimens increase with the curing period. After 28 days of curing periods, while the improvement percentages of the M1 specimen reached 44.86%, this value has been determined 55.15% for the M2 specimen.

3.2.2.2 The Surrounding Area of All Columns

An interaction area of lime-soil particles increases the quantity of lime in the lime column method. The interaction area is a surrounding area that is between the columns and soil particles. In this step, four different specimens that are M1-2/3h, M1-h, M2-2/3h, and M2-h were prepared and tested. The lime column properties of treated specimens prepared in this step of the study are presented in Table 3.4.

In conclusion, the improvement percentage of the M2-h specimen is greater than the others as this specimen has more total surrounding area than the other. This specimen was suitable for forwarding studies of this study.

Table 3.4 The lime column properties of treated specimens prepared in this step of the study

Specimens	*Total Column Area (cm^2)*	*Area Ratio (%)*	*Total Column Volume (cm^3)*	*Total Columns Surrounding Area (cm^2)*
M1-h	$19 * \frac{\pi * 0.65^2}{4} = 6.30$	21.05	$6.30 * 1.9 = 11.97$	$(\pi * 0.65) * 1.9 * 19 = 73.7$
M1-2/3h	$19 * \frac{\pi * 0.65^2}{4} = 6.30$	21.05	$6.30 * 1.3 = 8.19$	$(\pi * 0.65) * 1.3 * 19 = 50.5$
M2-h	$37 * \frac{\pi * 0.45^2}{4} = 5.88$	20.91	$5.88 * 1.9 = 11.17$	$(\pi * 0.45) * 1.9 * 37 = 99.4$
M2-2/3h	$37 * \frac{\pi * 0.45^2}{4} = 5.88$	20.91	$5.88 * 1.3 = 7.64$	$(\pi * 0.45) * 1.3 * 37 = 68$

After 28 days of curing periods, both the improvement percentages and total column surrounding area of treated specimens in this step are given in Table 3.5.

Table 3.5 The improvement percentages and total column surrounding area of treated specimens in this step of the study

Specimens	*Improvement percentages (%)*	*Total columns surrounding area (cm^2)*
M1-2/3h	28.46	50.5
M2-2/3h	31.39	68
M1-h	44.86	73.7
M2-h	55.15	99.4

The improvement percentages of the treated specimens increase with the total column surrounding areas of the treated specimens. The most effective model in this step is the M2-h specimens.

3.2.2.3 The Water Percentages of the Water-Lime Mixture

The M2-treated specimen, which has not waited in a humid room, has more swelling potential than the expected swelling potential of this specimen. A reason for this situation is that while the water content of the lime column is zero, the water content of the specimen is 15%. To solve this problem, the boreholes drilled into the specimen were filled with a mixture consisting of water and lime. The water percentage of the water-lime mixture in the columns was 0% in the previous study (Figure 3.29a.). As the water content of the soil specimen is 15%, the second water percentage of this mixture was slightly greater than this value. The second one was 18% (Figure 3.29b.). The third one has specified a water percentage value that was in the plastic state of this mixture. The third one was selected as a 30% (Figure 3.29c.). When the water percentage of this mixture is greater than 30%, this mixture is not workable material due to its sticky structure. For this reason, three different mixtures were prepared and filled into the boreholes to determine the optimum water percentage of this mixture. As a result, the water percentages of this mixture selected in this step were 0%, 18%, and 30%, respectively.

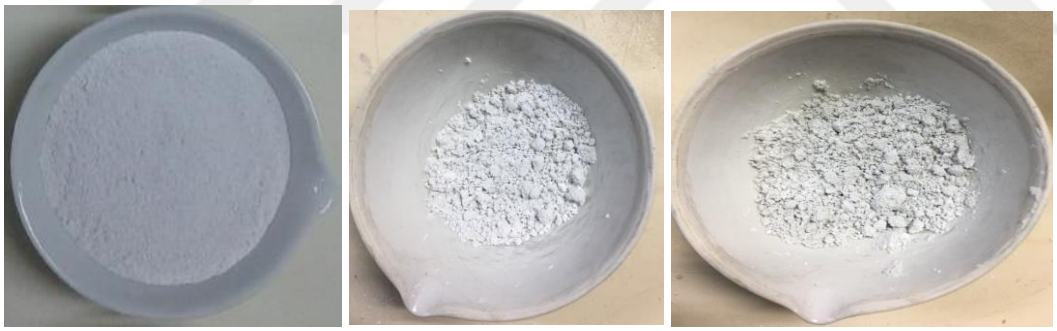

a) w/c=0% b) w/c=18% c) w/c=30%

Figure 3.29 Lime-water mixture to water percentage

Since this water content of these lime columns is selected for enhancing lime diffusion into the soil. Besides, when the water content of the lime column is greater than 30%, the workability of the lime column is notably hard because of its sticky structure.

Free swell tests were done for each specimen both with curing and without curing. The soil specimens prepared in this step were waited in the humid room for 7 days, 28 days, and 90 days to investigate the curing effect. The seating pressure was applied as 7 kPa to each specimen.

The swelling potentials of these specimens were illustrated in Figure 3.30 and the effect of these applications on the stabilization of swelling potential was shown in Figure 3.31. Swelling potential vs. time graphs for treated specimens prepared in this step are presented in Appendix A.

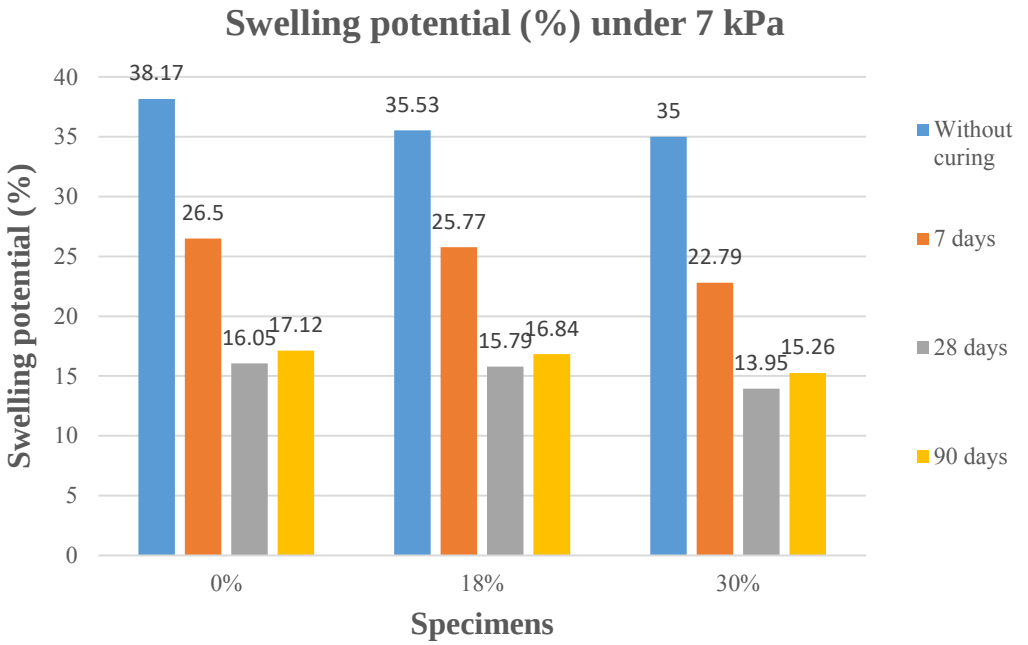

Figure 3.30 The swelling potential of M2-h treated specimens that stabilize with water-lime mixtures (0%, 18%, 30%) without curing and with curing

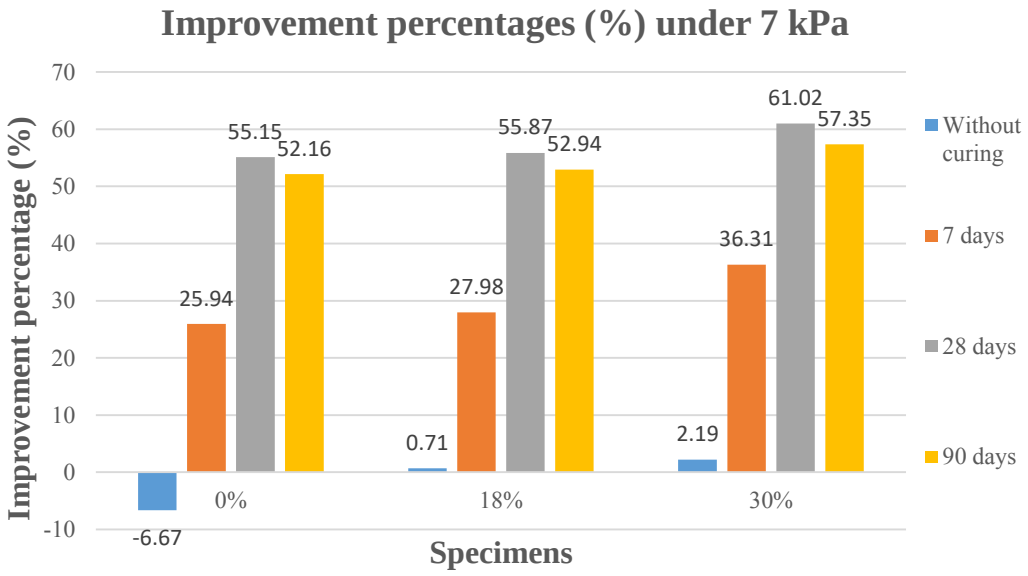

Figure 3.31 The improvement percentages of M2-h treated specimens that stabilize with water-lime mixtures (0%, 18%, 30%) without curing and with curing

The treated specimen with lime columns that had no water has the higher swelling potential of the untreated specimens since the improvement percentages of this treated specimen is a negative value. The reason of this case is that the water content of the lime column is lower than the water content of the untreated specimen. The swelling potentials of treated specimens in this step are lower than the swelling potential of the untreated specimen. In addition to this, the swelling potentials of treated specimens waited 90 days curing is greater than the swelling potentials of treated specimens waited 28 days curing. This condition may result from the ettringite mineral that occurs in the lime stabilization process of expansive soil. In conclusion, M2-h (30%) treated specimen waited 28 days curing improved the soil specimen than the other treated specimens.

3.2.2.4 Lignosulfonate Added to the Water-Lime Mixture

A new material, which is named lignosulfonate, is a waste material obtained from the paper industry. This material has been used as a water reducer and plasticizer in the concrete industry. Two reasons of the lignosulfonate addition to the water-lime mixture are;

1- An accelerating the lime diffusion into the soil specimen.
2- Either minimization or demolition the increase of swelling potentials of treated specimens after 28 days of curing period.

Two types of this waste material, which were sodium lignosulfonate and calcium lignosulfonate, were separately added to the water-lime mixture. These powder materials are used in this study even though they are found both powder and liquid in the market. While the specimen included sodium lignosulfonate lime column is called a NaLS specimen, the specimen included calcium lignosulfonate lime column is called a CaLS specimen. The images of both sodium and calcium lignosulfonate used in this study are given in Figure 3.32.

a) Sodium lignosulfonate b) Calcium lignosulfonate

Figure 3.32 The lignosulfonate used in this study

Specimen preparation of this step is similar to the previous specimen except for the preparation of the water-lime mixture. Since lignosulfonate was added to this mixture in this section. Firstly, some lignosulfonate was solved in the water (Figure 3.33).

Figure 3.33 The mixture involved lignosulfonate and water

An amount of lignosulfonate was determined as 12.5% of the water weight. When the amount of lignosulfonate increases, lignosulfonate particles are not solved in the water. Then, some lime was added to a water-lignosulfonate mixture. Thus, the mixture consisted of lime, water, and lignosulfonate was prepared (Figure 3.34).

a) Lime-water-sodium lignosulfonate b)Lime-water- calcium lignosulfonate

Figure 3.34 The mixtures consisted of lime, water, and lignosulfonate

The percentage of lignosulfonate-water-lime of the treated specimen prepared in this step according to their weight is given in Table 3.6.

Table 3.6 The percentage of lignosulfonate-water-lime in regards to their weight

Specimens	Percentage by weight (%)			
	Water	*Lime*	*NaLS*	*CaLS*
M2-h (30%)	30	70	-	-
NaLS	30	66.25	3.75	-
CaLS	30	66.25	-	3.75

These treated specimens have been waited in the humid room for 7 days, 28 days, 90 days, and 180 days These specimens have been tested under two pressures such as 7 kPa and 25 kPa to determine their swelling potentials. Both swelling potentials and improvement percentages of treated specimens prepared in this step are illustrated in Figure 3.35-3.36. Swelling potential vs. time graphs for treated specimens prepared in this step are presented in Appendix A.

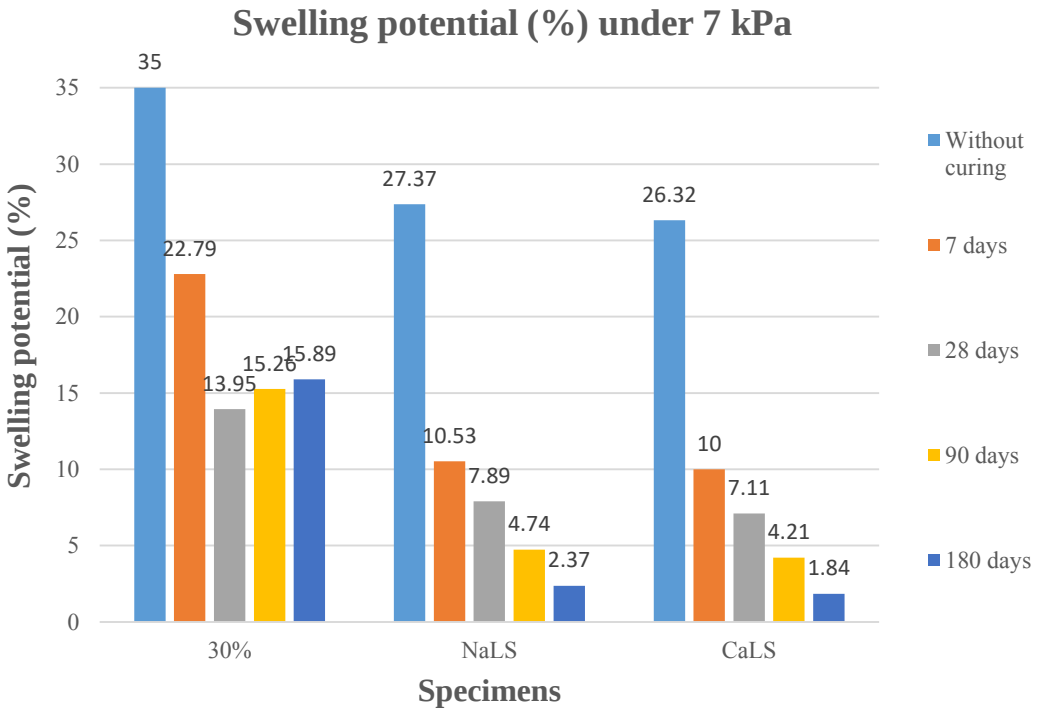

Figure 3.35 The swelling potential of M2-h treated specimens that stabilize with lignosulfonate-water-lime mixture without curing and with curing

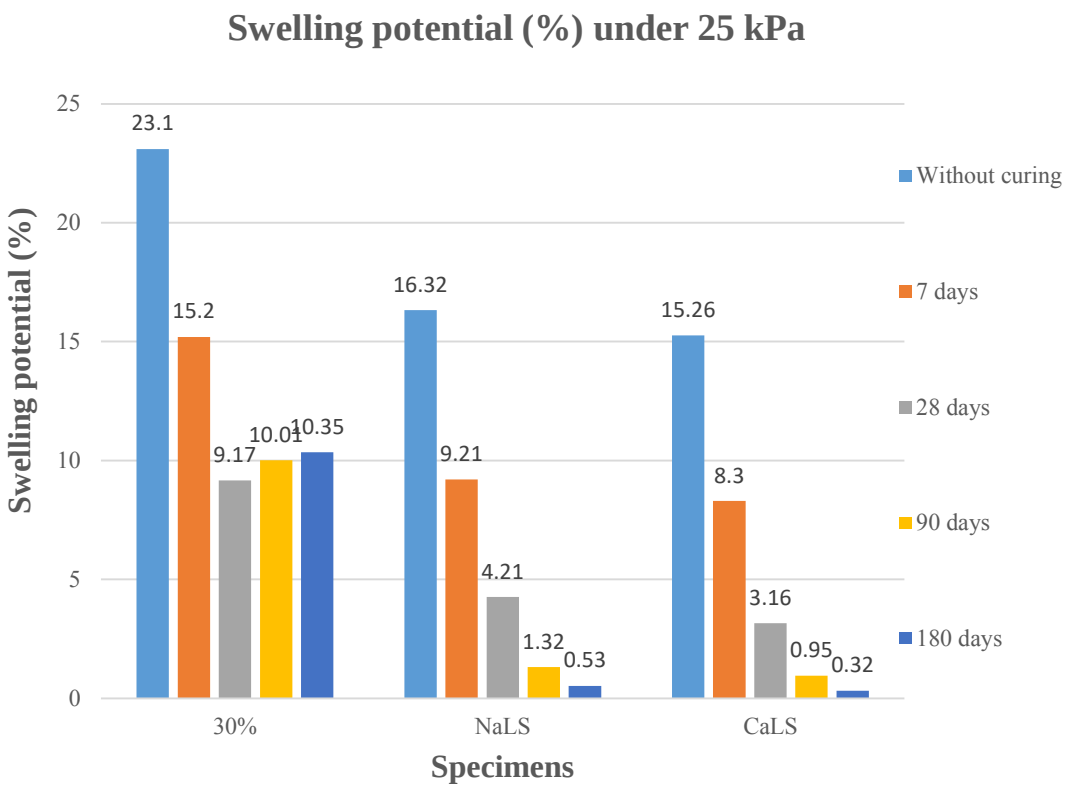

Figure 3.36 The swelling potential of M2-h treated specimens that stabilize with lignosulfonate-water-lime mixture without curing and with curing

Under 7 kPa surcharge pressure, the swelling potentials of the NaLS specimen and CaLS specimen, which have waited in a humid room for180 days, were measured at 2.37% and 1.84%, respectively. Under 25 kPa surcharge pressure, the swelling potentials of the NaLS specimen and CaLS specimen, which have waited in a humid room for180 days, were measured at 0.53% and 0.32%, respectively.

The main goal of this test program is that the swelling potential of the treated specimen is measured 0.5%. Under 25 kPa surcharge pressure, the swelling potential of CaLS specimen waited in the humid room for 180 days is lower than this value.

The swelling potentials of treated specimens prepared in each step of this improvement process are given in Table 3.7. Furthermore, these treated specimens are classified with respect to a classification made by Seed et al. (1962).

Table 3.7 The swelling potentials of treated specimens prepared in each step of this improvement process

Treated Specimen	*Curing Period (Days)*	*Surcharge Pressure (kPa)*	*Swelling Potential (%)*	*Seed et al. (1962) Classification*
Specimen A	-	7 kPa	43.95	Very high
Specimen A	-	25kPa	29.47	Very high
M1-2/3h	28	7 kPa	27.16	Very high
M1-h	28	7 kPa	19.41	High
M2-2/3h	28	7 kPa	26.32	Very high
M2-h (0%)	90	7 kPa	17.12	High
M2-h (18%)	180	7 kPa	16.84	High
M2-h (30%)	180	7 kPa	15.89	High
M2-h (30%)-NaLS	180	7 kPa	2.37	Medium
M2-h (30%)-CaLS	180	7 kPa	1.84	Medium
M2-h (30%)-NaLS	180	25kPa	0.53	Low
M2-h (30%)-CaLS	180	25kPa	0.32	Low

3.2.3 Effect of Scale of the Specimens on the Test Results

The specimen treated with the lignosulfonate lime column is the most effective stabilization method in the previous step of the study. However, the expansive soil specimen which includes lignosulfonate lime columns has been studied in an oedometer ring that has a 6.35 cm diameter. When the scale effect of this stabilization method is investigated, the test result of this previous work is not sufficient to research this subject. Since this previous work represents a point that is in any correlation. In conclusion, previous work is inadequate for the estimation of the swelling potentials of the specimens prepared in this study that have different scales.

This chapter is a laboratory work in which six different scale specimens for both a specimen contain sodium lignosulfonate lime columns and a specimen contain calcium lignosulfonate lime columns have been separately prepared. Each specimen represents one point that is on the correlation graph. Thus, the estimation process is based on six points obtained from this step. The diameters of these specimens are selected as 5 cm, 10 cm, 15 cm, 20 cm, 25 cm, and 30 cm, respectively. Besides, the diameter of lime columns is ranging 0.35 cm to 2.1 cm, respectively. The moulds used in this step of the study are illustrated in Figure 3.37.

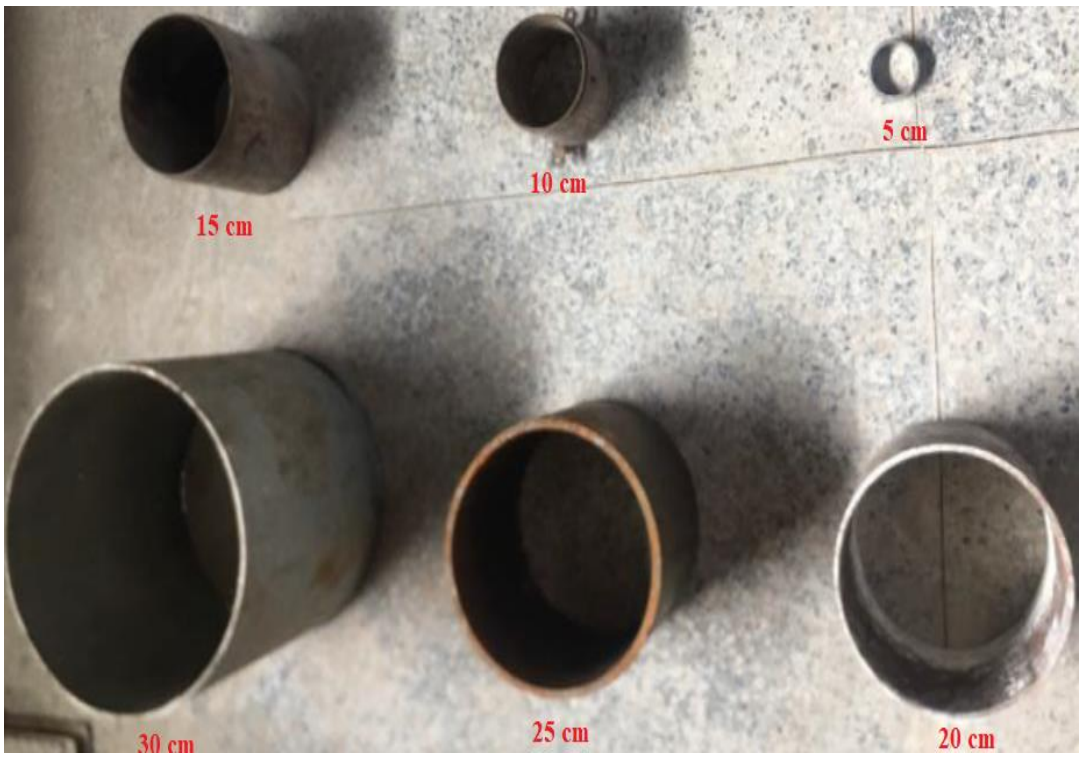

Figure 3.37 The moulds used in this step of the study

The preparation of the bigger specimens is the same as the preparation of the small specimens. Figure 3.38 illustrates one of the bigger specimens prepared in this study.

Figure 3.38 The example of the bigger specimens

In the previous chapter, the number of circular orbits and the number of columns are respectively 3, 37 for the most suitable models obtained from the previous step of this study. Besides, the diameter of lime columns is 0.45 cm and the area ratio is approximately 18.58% (Table 3.8).

Table 3.8 The properties of lime columns installed in oedometer ring

Specimen Diameter (cm)	Specimen Area (cm^2)	Borehole Diameter (cm)	Borehole Area (cm^2)	Area Ratio (%)
6.35	31.67	0.45	5.88	18.58

These treated specimens in this chapter are named COR1 to COR6 for treated specimen with both sodium lignosulfonate lime column and calcium lignosulfonate lime column as they were used for the correlation process. For instance, while the treated specimen had 5 cm diameter with sodium lignosulfonate lime column is named as a COR1-NaLS, while the treated specimen had a 5 cm diameter with calcium lignosulfonate lime column is named as a COR1-CaLS.

The properties of lime columns that are built in the improvement specimens that have a different diameter that is ranging from 5 cm to 30 cm are given in Table 3.9. Even though the area ratio of improvement specimens with lignosulfonate lime columns that

have 6.35 cm is 18.58%, the area ratio of improvement specimens with lignosulfonate lime columns prepared in this chapter is 18.13%. However, this difference is an acceptable value. In addition to this, the water content of both lignosulfonate lime columns is 30%, the water content of untreated specimen is 15%.

Table 3.9 The properties of lime columns installed in correlation moulds

Specimen Name	Specimen Diameter (cm)	Specimen Area (cm^2)	Borehole Diameter (cm)	Borehole Area (cm^2)	Area Ratio (%)
COR1	5	$\frac{\pi * 5^2}{4} = 19.63$	0.35	$37 * \frac{\pi * 0.35^2}{4} = 3.56$	$100 * \frac{3.56}{19.63} = 18.13$
COR2	10	$\frac{\pi * 10^2}{4} = 78.54$	0.7	$37 * \frac{\pi * 0.7^2}{4} = 14.24$	$100 * \frac{14.24}{78.54} = 18.13$
COR3	15	$\frac{\pi * 15}{4} = 176.71$	1.05	$37 * \frac{\pi * 1.05^2}{4} = 32.04$	$100 * \frac{32.04}{176.71} = 18.13$
COR4	20	$\frac{\pi * 20}{4} = 314.16$	1.4	$37 * \frac{\pi * 1.4^2}{4} = 56.96$	$100 * \frac{56.96}{314.16} = 18.13$
COR5	25	$\frac{\pi * 25^2}{4} = 490.87$	1.75	$37 * \frac{\pi * 1.75^2}{4} = 89$	$100 * \frac{89}{490.87} = 18.13$
COR6	30	$\frac{\pi * 30^2}{4} = 706.86$	2.1	$37 * \frac{\pi * 2.1^2}{4} = 128.15$	$100 * \frac{128.15}{706.86} = 18.13$

A distance between the two lime columns is a critical parameter that affects the achievement of this treatment method. Because this parameter covaries with the diameter of the lime column when the dimensions of the treated specimen either shrink or enlarge. This parameter is 4.05 mm for the treated specimen that had a 4.5 mm diameter lime column in the previous study. This parameter is calculated owing to a previous study and explained in detail in Table 3.10.

Table 3.10 The distance between the two lime columns of the treated specimen in this study

Specimens	Diameter of lime column (mm)	The distance between two lime columns (mm)
COR1	3.5	$(4.05 \div 4.5) * 3.5 = 3.15$
COR2	7	$(4.05 \div 4.5) * 7 = 6.3$
COR3	10.5	$(4.05 \div 4.5) * 10.5 = 9.45$
COR4	14	$(4.05 \div 4.5) * 14 = 12.6$
COR5	17.5	$(4.05 \div 4.5) * 17.5 = 15.75$
COR6	21	$(4.05 \div 4.5) * 21 = 18.9$

The swelling potentials of the correlation treated specimens tested under 7 kPa are illustrated in Figure 3.39 and Figure 3.40.

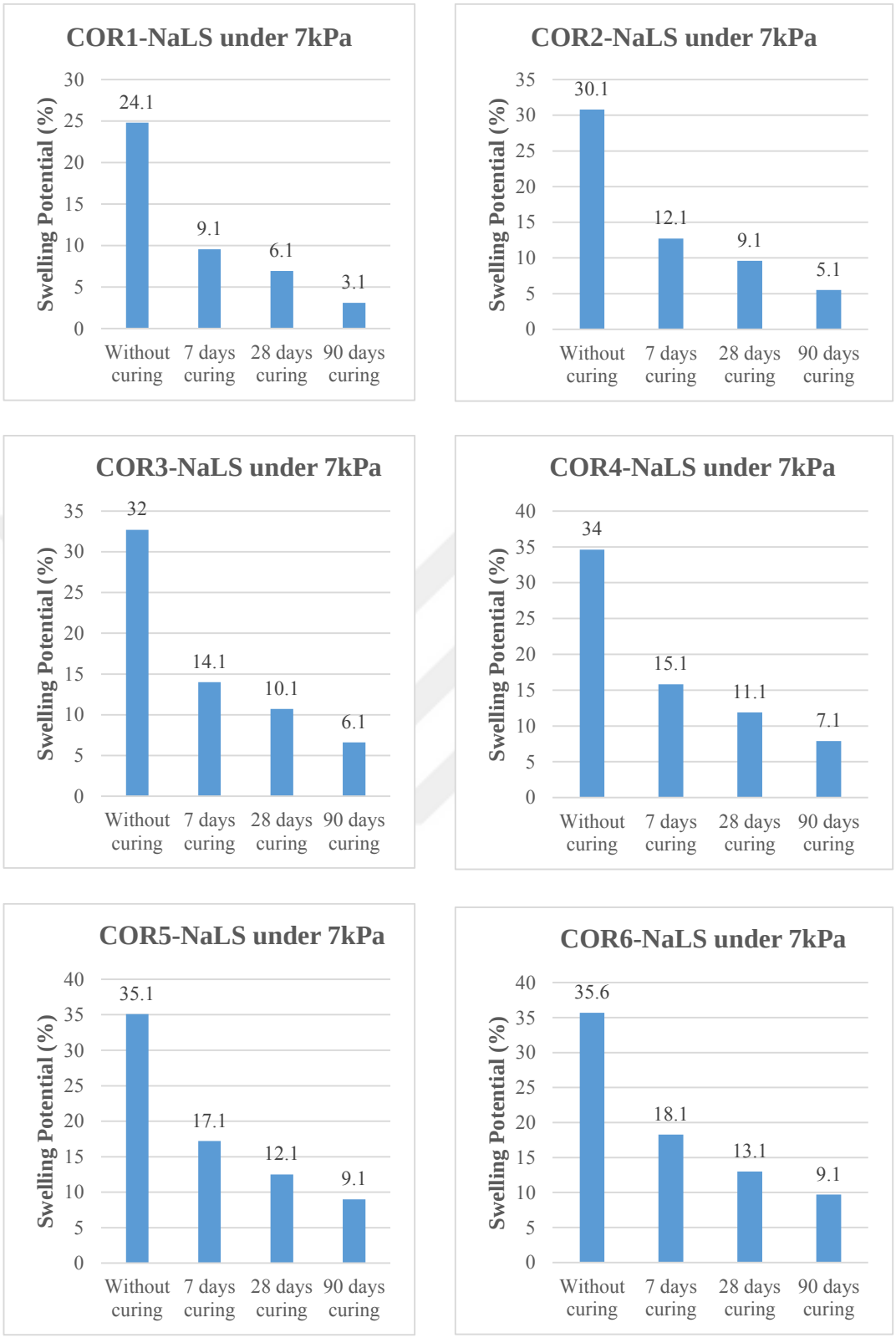

Figure 3.39 The swelling potential of the treated specimen with sodium lignosulfonate lime column under 7 kPa

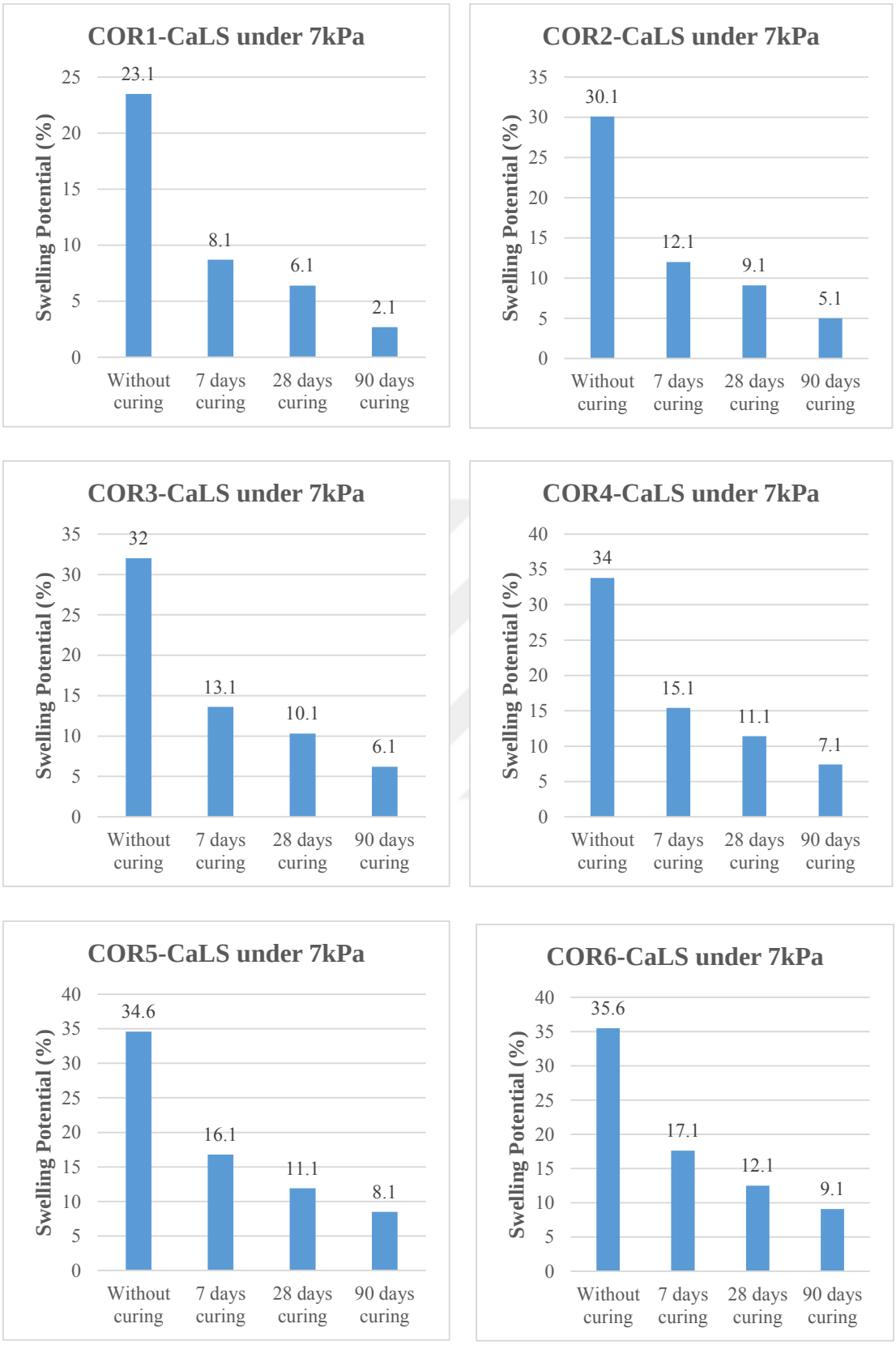

Figure 3.40 The swelling potential of the treated specimen with calcium lignosulfonate lime column under 7 kPa

The swelling potentials of the correlation treated specimens tested under 25 kPa are illustrated in Figure 3.41 and Figure 3.42.

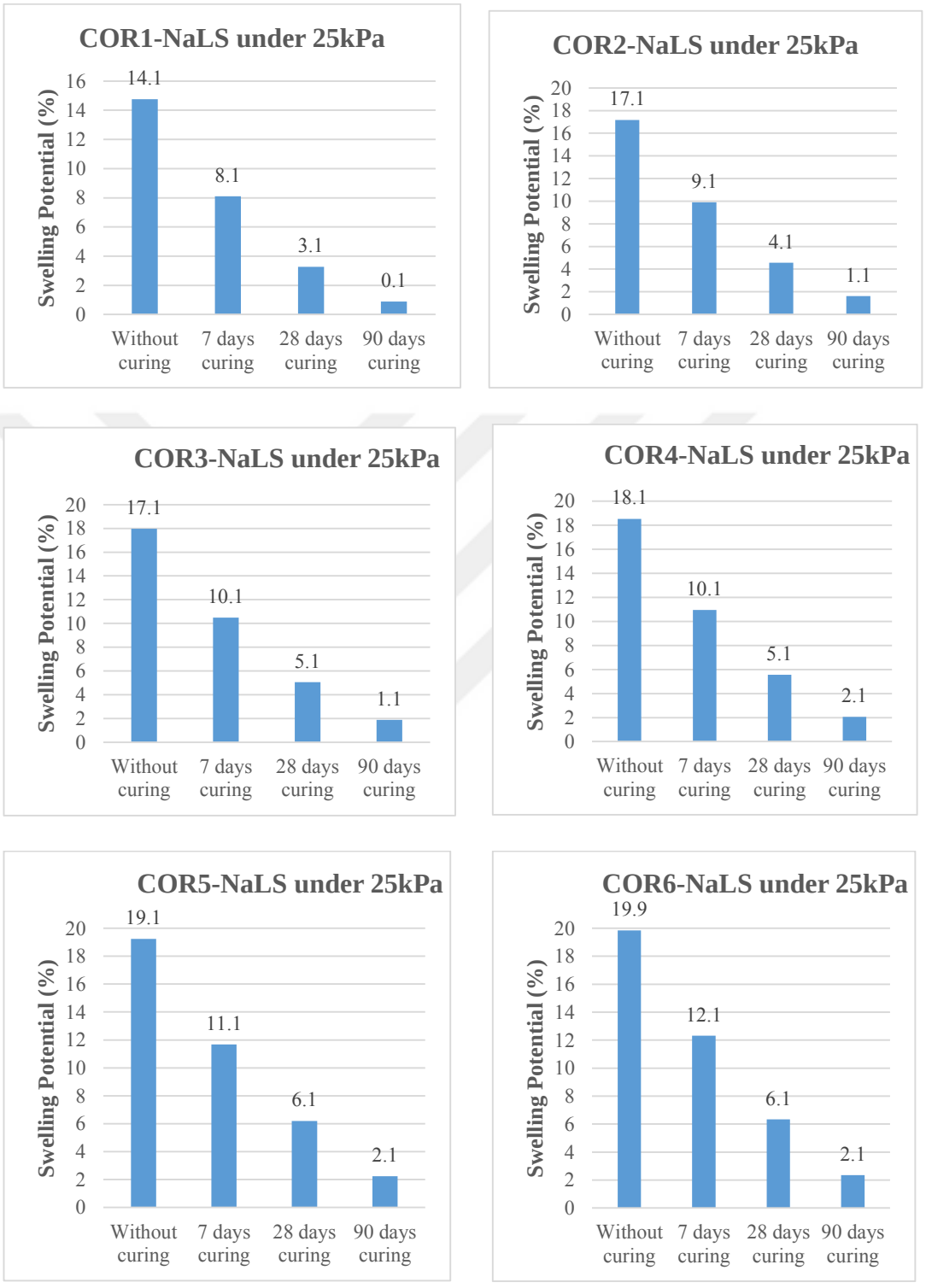

Figure 3.41 The swelling potential of the treated specimen with sodium lignosulfonate lime column under 25 kPa

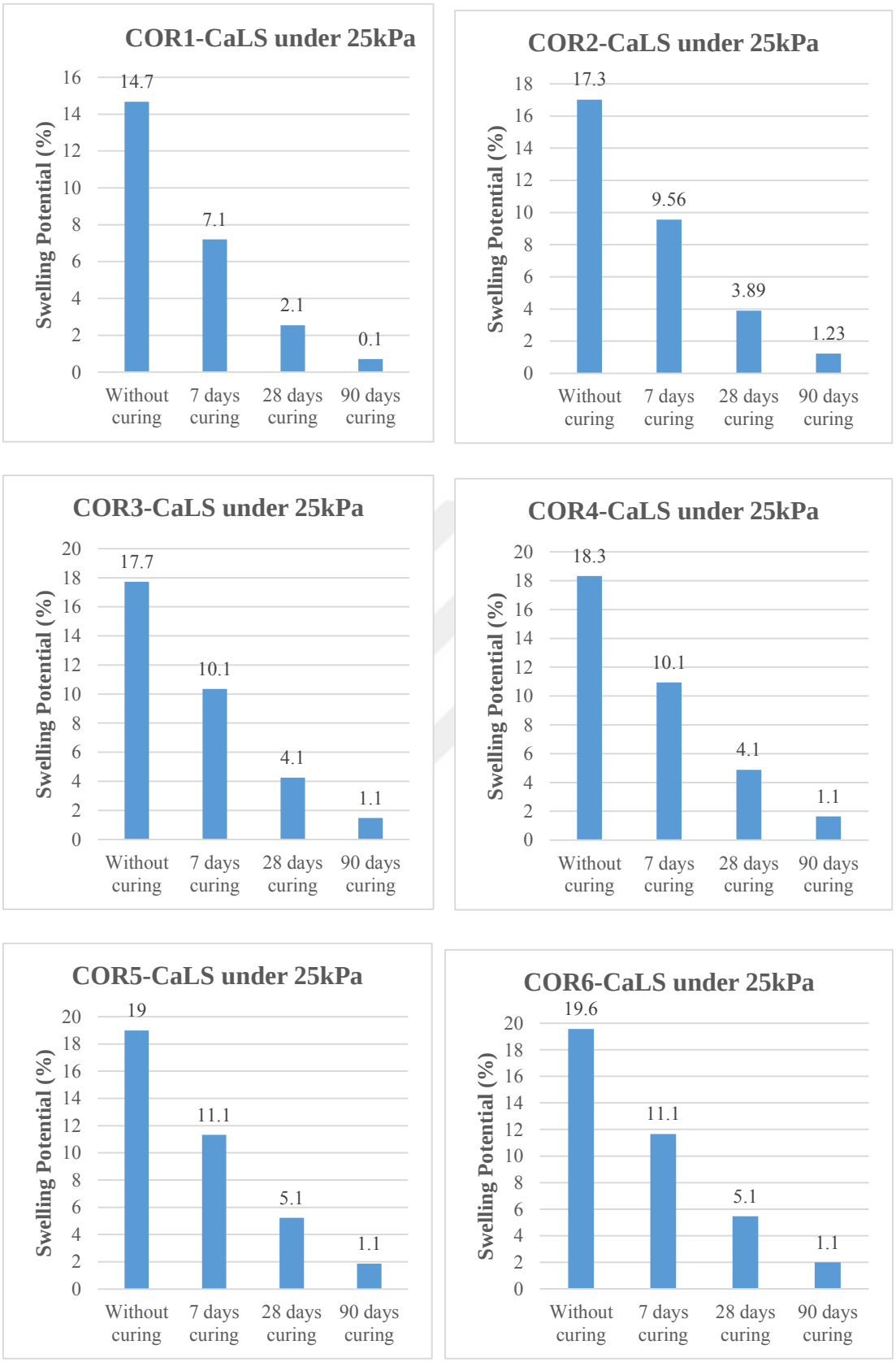

Figure 3.42 The swelling potential of the treated specimen with calcium lignosulfonate lime column under 25 kPa

CHAPTER 4

LABORATORY MODEL TESTS FOR SCALE EFFECT BY USING 30 CM X 30 CM BOX

4.1 Introduction

In the previous chapter, the lime column included lignosulfonate improved the swelling potential of the untreated specimen. However, the sizes of the treated specimen that had 6.35 cm diameter and 1.9 cm height were very small than the real project of civil engineering. In addition to this, the alteration of untreated soils between the columns in terms of both engineering and microchemical properties with curing should be determined for each lignosulfonate lime column type, which are sodium and calcium, to observe the stabilization process. This part is divided into two sections such as engineering properties and microchemical properties.

4.2 Engineering Properties

Lignosulfonate lime columns are based on lignosulfonate lime diffusion into the soil with time. Thus, the soil specimen placed between lignosulfonate lime columns has been stabilized with the curing period. Therefore, some soil engineering properties, which are unconfined compressive strength, coefficient of permeability, swelling potential, and CBR value, have been found.

Two different specimens with different sizes have been prepared for observation of the alteration of these properties. These specimens are;

- Big mould
- CBR mould

A big mould that had 30 cm width, 30 cm length, and 18 cm height was used to investigate the alteration of some engineering properties mentioned above (Figure 4.1).

Figure 4.1 A big mould used in this study

At this step of the study, seven columns instead of thirty-seven columns were installed into the big mould to take some undisturbed samples between the columns that were utilized for the free swell test, unconfined compression test, permeability test from oedometer test, and these seven columns were constructed as shown in (Figure 4.2).

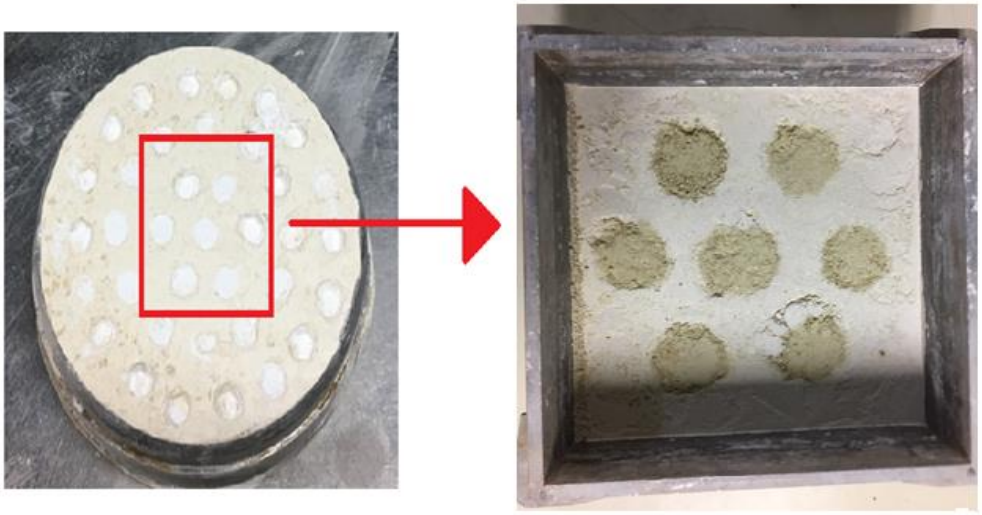

Figure 4.2 Specimen is used in previous work had 6.35 cm diameter (Left side),

The specimen is prepared in the big mould (Right side)

The diameter of these columns installed in the big mould is 4.5 cm. Thus, the distance between the columns is 40 mm. In addition to this, the three different big samples were prepared and waited separately for 7 days, 28 days, and 90 days in the humid room to observe the curing effect of the treatment method.

The term that is an untreated part of the specimen can be said for the part of the specimen placed between the columns at the beginning of the stabilization process. Since this untreated part of the specimen was treated progressively with the curing period. Thus, some studies for this part of the specimen were carried out. These studies were listed below;

1- The observation
2- The investigation of some engineering properties such as unconfined compressive strength, swelling potential, coefficient of permeability
3- The curing effect

Sample Preparation

The preparation of untreated specimens was presented in detail in the lime column chapter. After the preparation of the untreated specimen, the laying and the compaction of the specimen were done, respectively. Both two operations were made in layers due to the height of the specimen. In other words, these operations were done ten times. These operations were stated below;

1- The soil was prepared with specified unit weight and water content
2- This soil filled into the big mould.
3- Then, this soil was compacted with a hydraulic piston (Figure 4.3).
4- The top of the compacted layer was scratched to obtain a homogenous mixture and interrelating layers (Figure 4.4).
5- The drilling process was started after the compaction process. At this process, seven boreholes which have 45 mm diameter and 100 mm height opened in the compacted soil. The drilling boreholes were done by using a drilling machine and drilling bit (Figure 4.5).
6- The lignosulfonate lime column was prepared and filled into these boreholes.

Figure 4.3 Compaction process

Figure 4.4 Scratch process

Figure 4.5 A drilling machine, drilling bit and boreholes

7- Two different undisturbed samples obtained from treated soil with lignosulfonate lime columns were 50 mm diameter and 36 mm diameter. For this process, two different tubes which had 50 mm inner diameter and 36 mm

inner diameter were used at this stage (Figure 4.6). These undisturbed sample tubes were pushed into the compacted soil with a hydraulic jack (Figure 4.7).

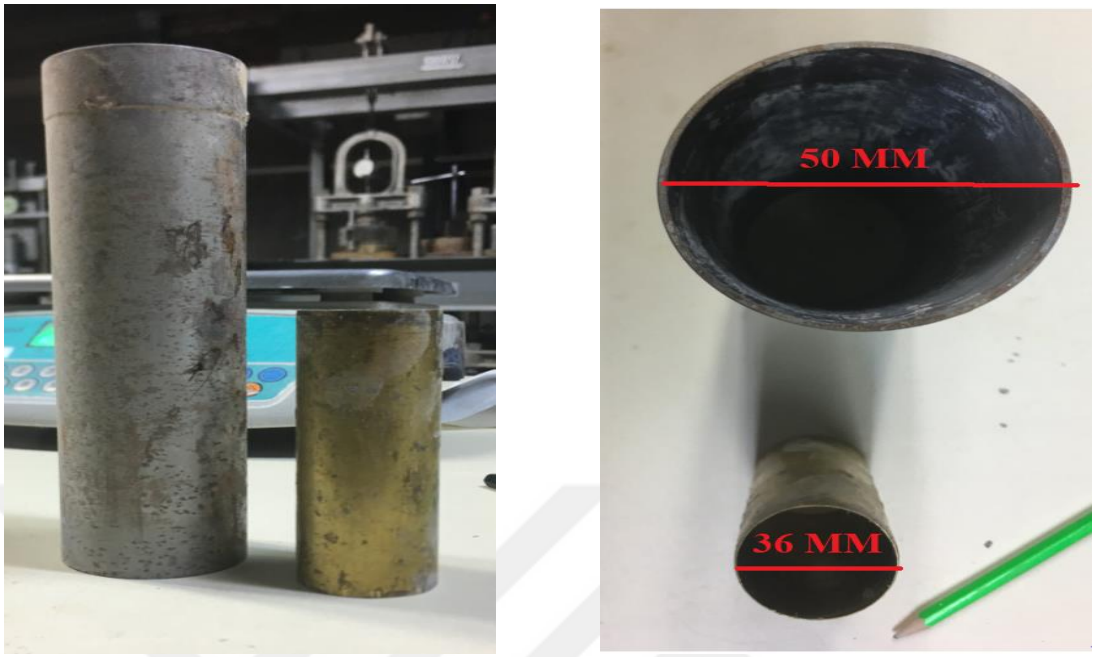

Figure 4.6 Tubes used for undisturbed sampling

Figure 4.7 The pushing process

The undisturbed samples were taken from this treated soil after the curing periods that were 7 days, 28 days, and 90 days in this step.

The undisturbed samples that had 50 mm diameter were used to determine the swelling potential and coefficient permeability of the treated specimen. The other undisturbed sample was utilized for the measurement of the unconfined compressive strength of the treated specimen. Meanwhile, the undisturbed sample had 50 mm diameter was taken between three columns, the undisturbed sample had 36 mm diameter was taken between two columns because of the distance between the columns (Figure 4.8).

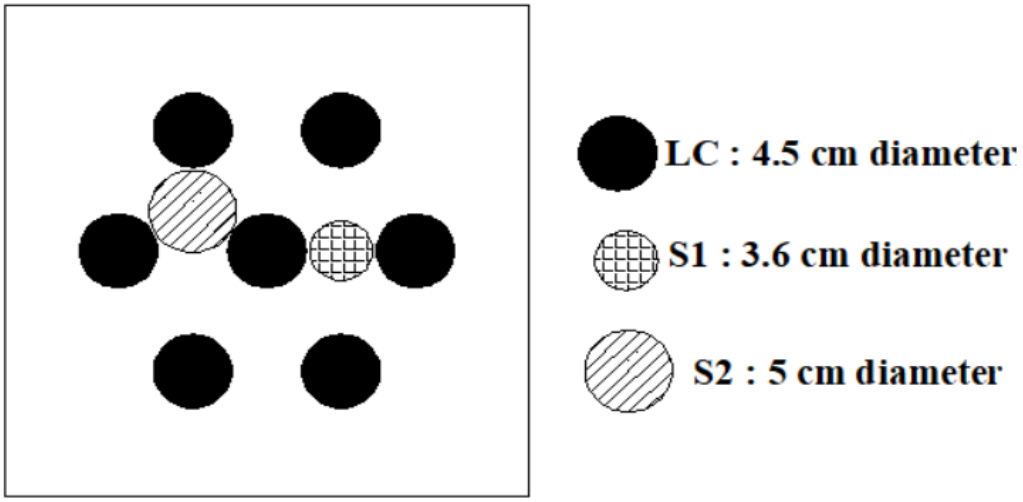

Figure 4.8 Location of undisturbed samples

The alteration of some engineering properties such as unconfined compressive strength, swelling potential, and coefficient of permeability of treated specimen was observed with the curing period. This observation process was separately made for untreated specimen stabilized with either calcium lignosulfonate lime columns or sodium lignosulfonate lime columns.

In the following subtitles, each engineering property studied in this step is explained in detail and the alteration of these properties was determined according to the untreated specimen.

4.2.1 Unconfined Compressive Strength

The undisturbed samples had 36 mm diameter and 72 mm height used for the only measurement of unconfined compressive strength. For both specimens treated by lignosulfonate lime columns, the unconfined compressive strengths of both untreated and the treated specimens are given in Table 4.1.

Table 4.1 Unconfined compressive strength value of treated and untreated specimens

Specimens	*Unconfined compressive strength (kPa)*
Specimen A	384.94
NaLS LC 7 Days	413.92
NaLS LC 28 Days	456.37
NaLS LC 90 Days	533.21
CaLS LC 7 Days	414.89
CaLS LC 28 Days	488.35
CaLS LC 90 Days	622.47

4.2.2 Swelling Potential

The swelling potentials of treated specimens obtained from 50 mm tubes were tested under both 7 kPa and 25 kPa. The swelling potential of the treated specimen decreased with the curing period (Table 4.2).

Table 4.2 The swelling potential of treated and untreated specimens under both 7 kPa and 25 kPa

Specimens	*Swelling Potential under 7 kPa (%)*	*Swelling Potential under 25 kPa (%)*
Specimen A	43.95	29.47
NaLS LC 7 Days	30.3	20.6
NaLS LC 28 Days	20.1	13.8
NaLS LC 90 Days	13.5	8.8
CaLS LC 7 Days	29.9	20.35
CaLS LC 28 Days	19.4	13.2
CaLS LC 90 Days	12.4	8.65

4.2.3 Coefficient of Permeability

The consolidation tests were done to obtain the coefficient of permeability of treated specimens. At this part, the pressure applied to the specimens increased from 25 kPa to 50 kPa. The equation given below was applied to determine the engineering properties of treated soil (Eq. 4.1).

$$k = \gamma_w m_v c_v \qquad Eq.4.1$$

The coefficient of permeability of untreated specimen was found as $6.6 * 10^{-10}\ cm/s$. The change of volume compressibility (m_v) and consolidation coefficient ($\boldsymbol{c_v}$) of treated specimens were presented in Table 4.3. Both void ratio versus consolidation pressure graph and displacement versus time graph for Specimen A and treated specimen prepared in this step are given in Appendix C.

Table 4.3 The change of volume compressibility and consolidation coefficient of untreated and treated specimens

Specimens	$m_v\ (m^2/kN)$	$c_v\ (m^2/s)$
Specimen A	$\mathbf{1.860 * 10^{-4}}$	$\mathbf{3.56 * 10^{-9}}$
NaLS LC 7 Days	$\mathbf{1.744 * 10^{-4}}$	$\mathbf{2.94 * 10^{-9}}$
NaLS LC 28 Days	$\mathbf{1.683 * 10^{-4}}$	$\mathbf{8.39 * 10^{-10}}$
NaLS LC 90 Days	$\mathbf{1.396 * 10^{-4}}$	$\mathbf{3.86 * 10^{-10}}$
CaLS LC 7 Days	$\mathbf{1.747 * 10^{-4}}$	$\mathbf{2.54 * 10^{-9}}$
CaLS LC 28 Days	$\mathbf{1.612 * 10^{-4}}$	$\mathbf{6.18 * 10^{-10}}$
CaLS LC 90 Days	$\mathbf{1.290 * 10^{-4}}$	$\mathbf{2.43 * 10^{-10}}$

4.2.4 California Bearing Ratio

Several soaked CBR tests have been done to determine the strength parameters of both untreated and treated specimens in this study.

The CBR value of the unsoaked condition was found as 51.52 %, the CBR value of the soaked condition was found at 1.31 %. As the untreated specimen is soaked, this specimen swells, and the strength of this specimen under the soaked condition is very

low than the unsoaked condition. Thus, the soaked CBR test is more significant than the unsoaked CBR test.

The first stage of this step is that a model of specimens prepared in this step is selected for measuring CBR values of them. The dimensions of both a plunger and a CBR mould are given in Figure 4.9.

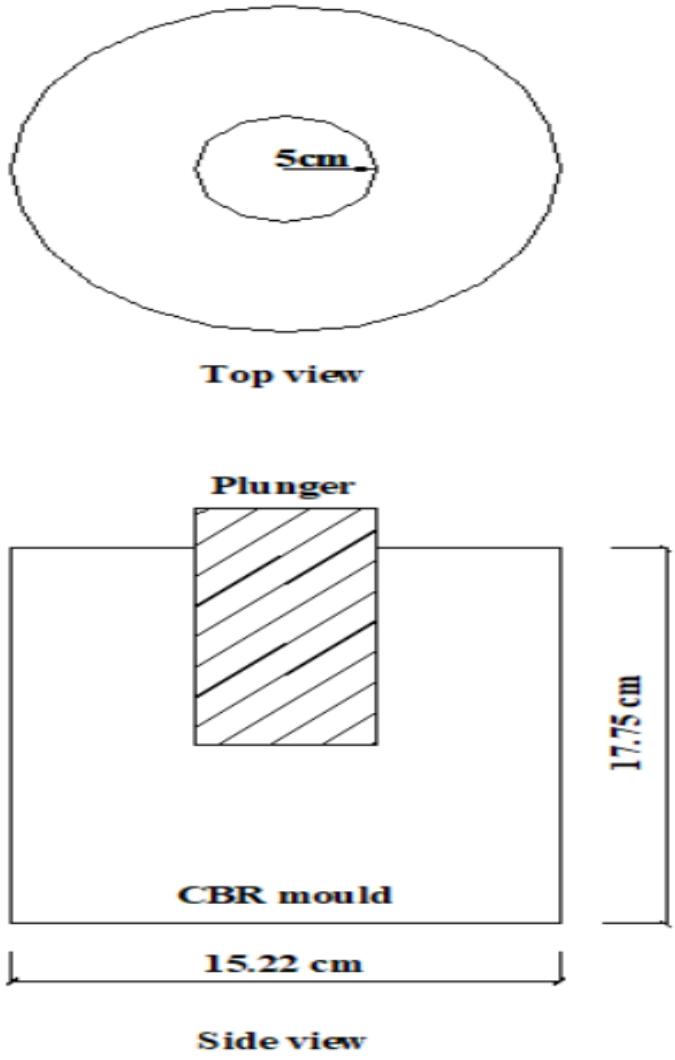

Figure 4.9 The dimensions of both a plunger and a CBR mould

Thirty-seven columns were installed in the best specimen model of this study. If this model is installed in CBR mould, 37 columns should be opened in a plunger area with had 5 cm diameter. Furthermore, 271 columns should be opened in an area of CBR mould (Figure 4.10). A model had 61 columns should be selected to simplify this problem. Therefore, 7 columns are opened in the plunger area and 61 columns are opened in the CBR mould area (Figure 4.10). After the curing period, these specimens are tested to both CBR swells and CBR values of them.

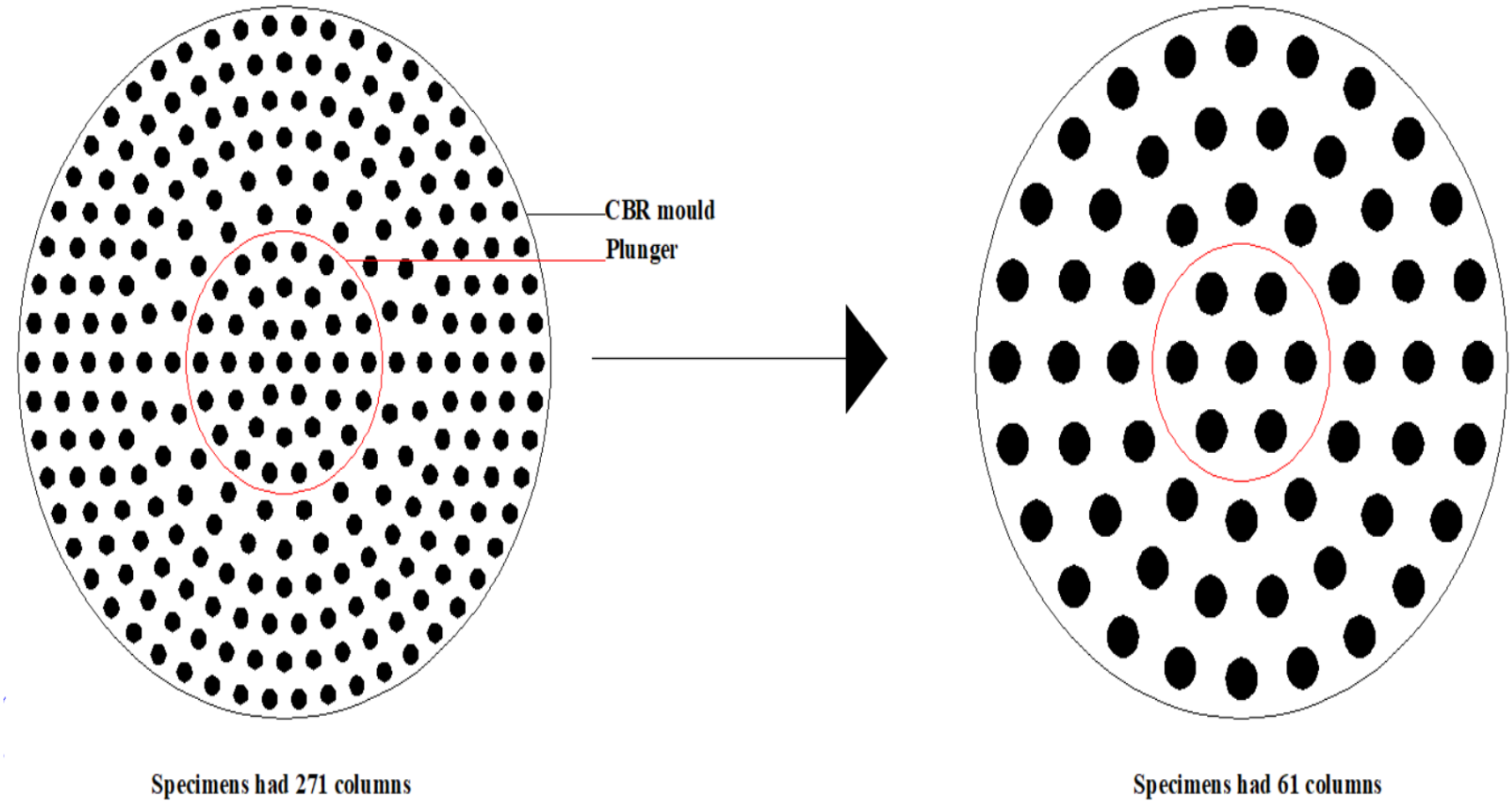

Figure 4.10 Top view of both a specimen which has 271 columns and a specimen which has 61 columns

These specimens have waited in the curing room for 7 days, 28 days, and 90 days due to the lignosulfonate lime column stabilizations process. 7 kPa and 25 kPa surcharge pressures are applied to specimens prepared in this step (Figure 4.11).

a) 7 kPa b) 25 kPa

Figure 4.11The soaking step of the CBR test

The specimen is put into the CBR test machine after the soaking process and the surcharge pressure is applied to the specimen during the test (Figure 4.12).

Figure 4.12 The specimens in the CBR machine

Each specimen is tested to ASTM D1883. The treated specimens prepared in this step are given in Table 4.4.

Table 4.4 The treated specimens prepared in this step

Specimens	Surcharge Pressure	
Specimen A	7 kPa	25 kPa
NaLS LC 7 Days	7 kPa	25 kPa
NaLS LC 28 Days	7 kPa	25 kPa
NaLS LC 90 Days	7 kPa	25 kPa
CaLS LC 7 Days	7 kPa	25 kPa
CaLS LC 28 Days	7 kPa	25 kPa
CaLS LC 90 Days	7 kPa	25 kPa

The data given from tests in this step is shown in Table 4.5 to determine of CBR parameter. Δh is a value related to the change of specimen height that is measured after 4 days of soaked condition. As loads which are measured at both 2.5 mm displacement and 5 mm displacement are necessary for calculating of CBR value.

Table 4.5 The test data obtained from the soaked CBR tests

	7 kPa surcharge pressure			25 kPa surcharge pressure		
Specimens	Swell Δh (mm)	Load (kN) at 2.5 mm	Load (kN) at 5 mm	Swell Δh (mm)	Load (kN) at 2.5 mm	Load (kN) at 5 mm
Specimen A	46.75	0.177	0.233	33.13	0.289	0.381
NaLS 7 Days	14.73	0.530	0.736	11.77	0.770	1.015
NaLS 28 Days	10.47	0.900	1.345	8.44	1.220	1.605
NaLS 90 Days	6.53	1.332	1.675	4.66	1.622	2.012
CaLS 7 Days	14.24	0.654	0.856	10.96	0.901	1.186
CaLS 28 Days	9.41	1.209	1.504	7.11	1.473	1.890
CaLS 90 Days	5.12	1.469	1.753	3.58	1.918	2.234

4.3 Physical Properties

A test procedure that is called a methylene blue test has been followed to observe the alteration of physical properties of soil placed between the columns. This test is that some properties of treated soil, which are cation exchange capacity and specific surface, have been determined with this test procedure. Detailed information about these properties mentioned above is given in subtitles.

4.3.1 Methylene Blue Test

The alteration of both cation exchange capacity and the specific surface of treated specimens has been observed by doing the methylene blue test. Three different specimens for both sodium and calcium lignosulfonate lime column method have been separately prepared for this process. Then, test specimens have been taken from a point that is the center of the distance between two columns (Figure 4.13).

Figure 4.13 The example of the location of the specimen for these tests

The correlation-treated specimens with lignosulfonate lime columns were prepared before the methylene blue test. All specimens have waited in the humid room for 90 days. The properties of the stabilized specimens are given in Table 4.6.

Table 4.6 The properties of the stabilized specimens used for the methylene blue tests

Specimen Name	The diameter of the lignosulfonate lime columns
COR2-NaLS	7 mm
COR4-NaLS	7 mm
COR6-NaLS	14 mm
COR2-CaLS	14 mm
COR4-CaLS	21 mm
COR6-CaLS	21 mm

Test data of methylene blue tests in this step are given in Figures 4.14-4.19.

Figure 4.14 Methylene blue test data obtained from NaLS specimen had 7 mm diameter lime column

Figure 4.15 Methylene blue test data obtained from CaLS specimen had 7 mm diameter lime column

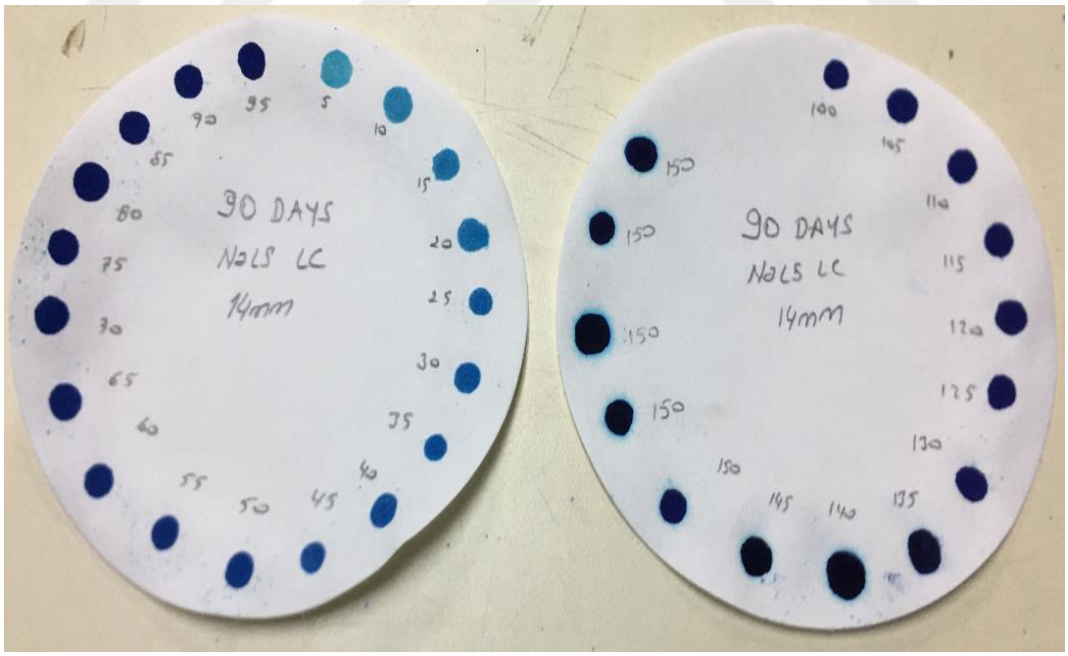

Figure 4.16 Methylene blue test data obtained from NaLS specimen had 14 mm diameter lime column

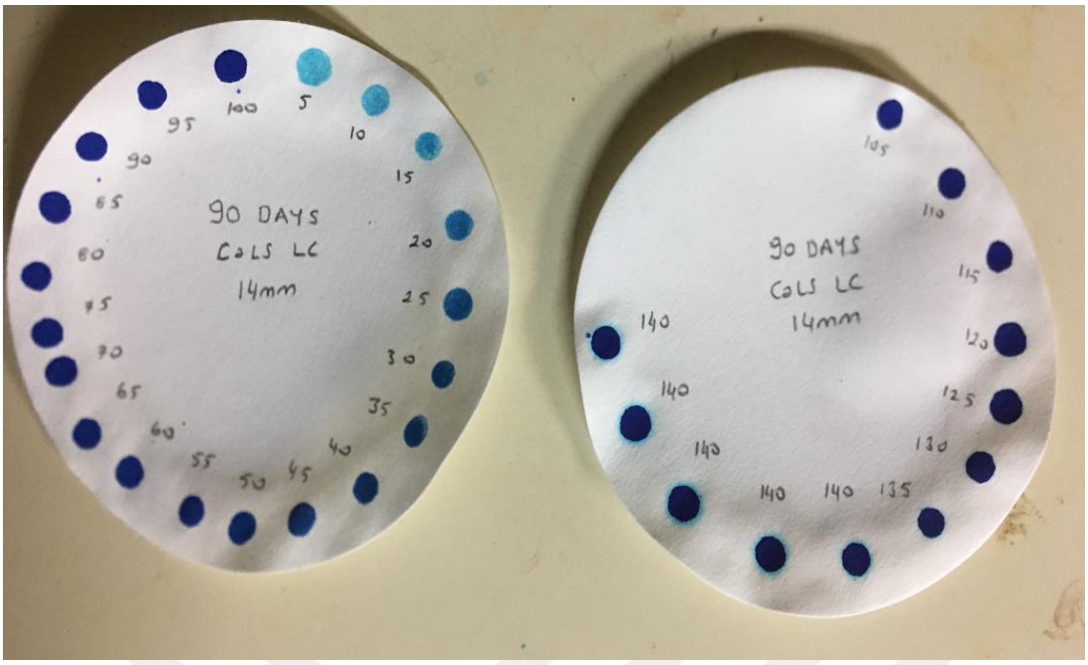

Figure 4.17 Methylene blue test data obtained from CaLS specimen had 14 mm diameter lime column

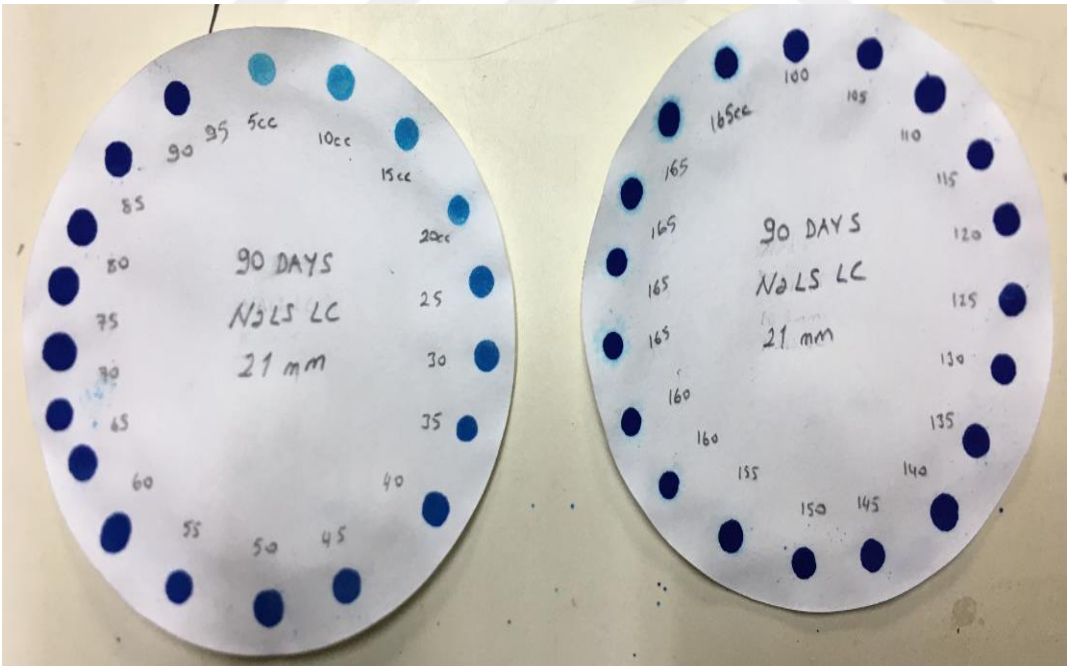

Figure 4.18 Methylene blue test data obtained from NaLS specimen had 21 mm diameter lime column

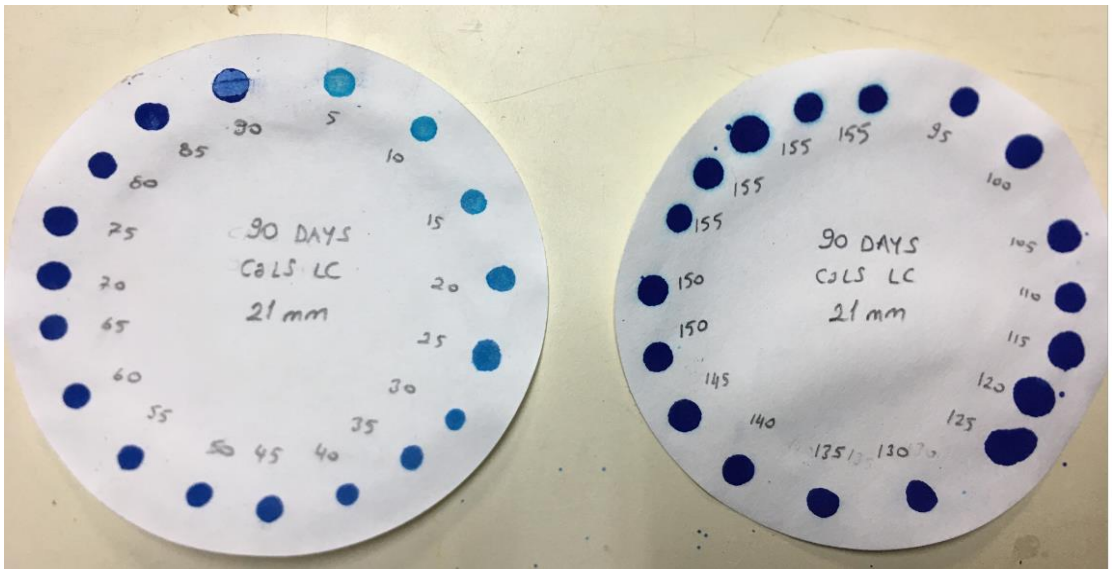

Figure 4.19 Methylene blue test data obtained from CaLS specimen had 7 mm diameter lime column

4.4 SEM-EDX analysis

Detailed information about the microstructure of treated soils and the change in microstructure for chemically treated soils can be obtained by using the scanning electron microscope (SEM). SEM images of soil fabric is a preferable technique to investigate the soil microstructure.

SEM-EDX analysis has been made to investigate and identify the mechanisms of both lime column applications and lignosulfonate lime column applications in this study. The swelling potentials of these treated specimens are reference parameters for the selection of specimens used for this analysis.

Swelling potentials of Specimen A under 7 kPa and 25 kPa are respectively measured as 43.95% and 29.47%. The swelling potentials of the treated specimens with both lime columns (LC) and lignosulfonate lime columns (NaLS and CaLS) under two surcharge pressures applied in this study are different from each other even though these treated specimens have waited in the humid room for the same period (Table 4.7).

Table 4.7 The swelling potentials of treated specimens under 7 kPa surcharge pressure

Curing period (days)	Swelling Potential (%) under 7 kPa surcharge pressure			Swelling Potential (%) under 25 kPa surcharge pressure		
	LC (30%)	NaLS	CaLS	LC (30%)	NaLS	CaLS
0	35	27.37	26.32	23.1	16.32	15.26
28	13.95	7.89	7.11	9.17	4.26	3.16
90	15.26	4.74	4.21	10.01	1.32	0.95
180	15.89	2.37	1.84	10.35	0.53	0.32

The swelling potentials of all treated specimens given in Table 4.7 decrease with the first 28 days curing period. For the specimens treated with lignosulfonate lime columns, this downtrend continues with curing periods. However, the swelling potentials of treated specimens with lime columns increase after 28 days curing period. Thus, the specimens are selected taking account of this parameter. The specimens used for this analysis are listed in Table 4.8.

Table 4.8 The specimens prepared for SEM-EDX analysis

Specimens	Curing period (days)
Specimen A	-
LC (30%)	28
LC (30%)	180
NaLS	180
CaLS	180

A specimen that has 63.5 mm diameter and 19 mm height was prepared for this analysis. Seven columns had 9 mm were opened into this specimen. The specimen used for this analysis was taken from a point that is the center of the distance between two columns (Figure 4.20).

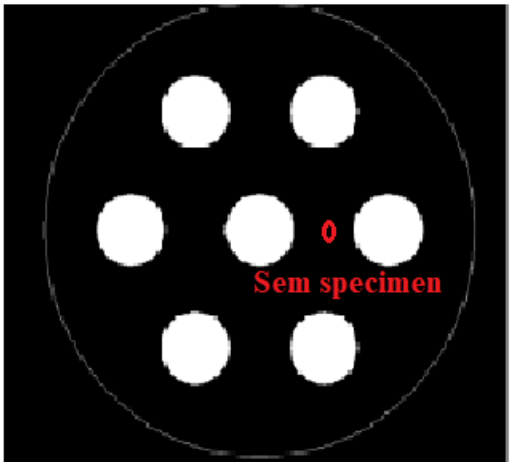

Figure 4.20 The test specimens for SEM-EDX analysis

CHAPTER 5

COMBINED IMPROVEMENT METHOD

5.1 Combined Improvement Method

In previous chapters, soil specimen had swelling potential has been stabilized with either lime column (LC) or lignosulfonate lime columns (LLC). This stabilization process has been investigated in detail. A significant output of this previous study can be said that the achievement of these methods alters with respect to the curing period. Even though these periods take a very long time for the lime column, this period diminishes by adding lignosulfonate to the lime column. Nevertheless, this period is not too short. Some problems can come out during this period when there is a probability that a structure build on the untreated soil with these methods suffers from the volume change of this soil.

A stabilization method consisted of prewetting, lignosulfonate lime column, and geotextile has been applied to untreated soil to solve the problem mentioned above. This stabilization method applied in this study is called as combined improvement method (CIM). When three methods are applied to untreated soil instead of either the lime column method or the lignosulfonate lime column method, this solution is not so economic and easily applicable in regards to the lignosulfonate lime column. This condition firstly means that the stabilization project needs more time and more money. Because of the reduction of both project duration and project cost, nineteen columns instead of thirty-seven columns are built in the untreated soil (Figure 5.1). At this step,

the distance between the columns increases from 0.9D to 2D due to the reduction of column pieces. Therefore, some parameters of columns built in the combined improvement methods such as total borehole area, total borehole surrounding area, and area ratio are naturally reduced with respect to these parameters of the lignosulfonate lime columns method.

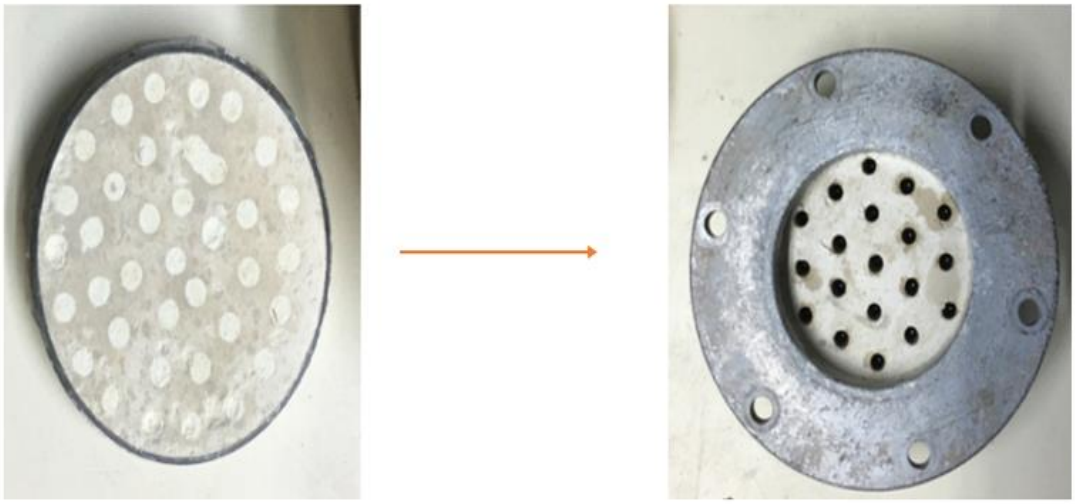

Figure 5.1 Nineteen columns instead of thirty-seven columns installed into the untreated soil

These parameters of columns in both lignosulfonate lime columns and combined improvement methods applied in this step are shown in Table 5.1.

Table 5.1 Parameters of both lignosulfonate lime columns and combined improvement method

Parameters	*4.5mm*37 pieces*	*4.5 mm*19 pieces*
Total Borehole Area (cm^2)	$(\pi * (0.45^2)/4 * 37 = 5.88$	$(\pi * (0.45^2)/4 * 19 = 3.02$
Total Borehole Surrounding Area (cm^2)	$(\pi * (0.45) * 1.9 * 37 = 99.4$	$(\pi * (0.45) * 1.9 * 19 = 51$
Area Ratio (%)	20.91	10
Distance between boreholes	0.9D	2D

Another variable property of columns built in this step is that their location. Although the columns opened in the previous step were circular orbit, the columns opened in the combined improvement method are hexagonal (Figure 5.2). An area ratio calculation of the combined improvement method is given in Appendix D.

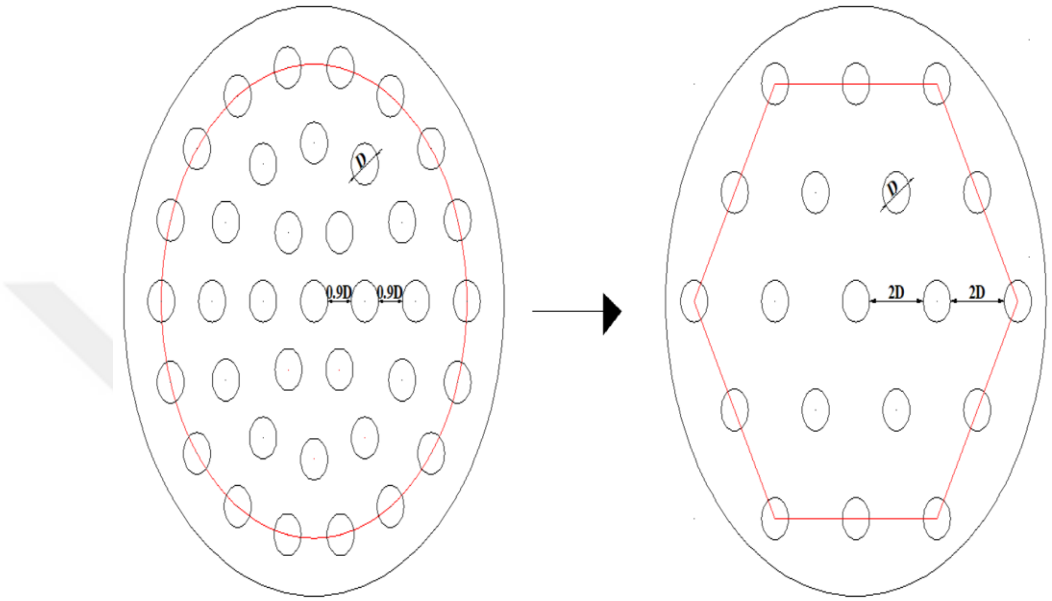

Figure 5.2 A circular orbit and hexagonal structure

These stabilization methods applied to untreated soil in this step are comprehensively explained in the following subtitles;

a) Prewetting: The volume of untreated soils had swelling potential generally changes due to the water content them. Even if the change of soil water content is not usually much in the laboratory condition, this change of this value sometimes reaches up to significant value owing to evaporation in the field. In the literature, Soltani et al. (2002) stated that ammonium lignosulfonate that is a type of lignosulfonate is used to enhance the properties of saline and eroded soils such as physical, chemical, and biological. In addition to this, the water loss of these soils due to the evaporation diminishes by adding this lignosulfonate. While the dry density of untreated soil is maximum dry density, the water content of untreated soil (15%) is too low with respect to its optimum water content (26%). As a result, a mixture consisted of water and calcium lignosulfonate was prepared.

The amount of water into the mixture was determined to increase the water content of untreated soil from 15% to optimum water content (26%). The amount of calcium lignosulfonate in the mixture was found as 2% of untreated soil weight.

Some stages of the prewetting process are given below.

1- Nineteen boreholes are opened into the untreated specimen and these boreholes are filled with the mixture.
2- The amount of this mixture added to each borehole is determined in Appendix E.
3- Untreated soil is absorbed by the water-lignosulfonate mixture. This absorption process takes a while because of the low permeability of the soil.

b) Lignosulfonate lime column: This process is that the filling of boreholes with calcium lignosulfonate lime as in the previous study.

c) Geotextile: Geotextile is a preferable material for soil improvement projects. In this study, a flexible fabric which is named a crystal tulle in the market is utilized as a geotextile in this study (Figure 5.3). When this material is only spread on the untreated soil, it did not resist the volume change of soil. There are two reasons for this condition. The first one is that the weight of this material is very light and the second one is that this material is not anchored.

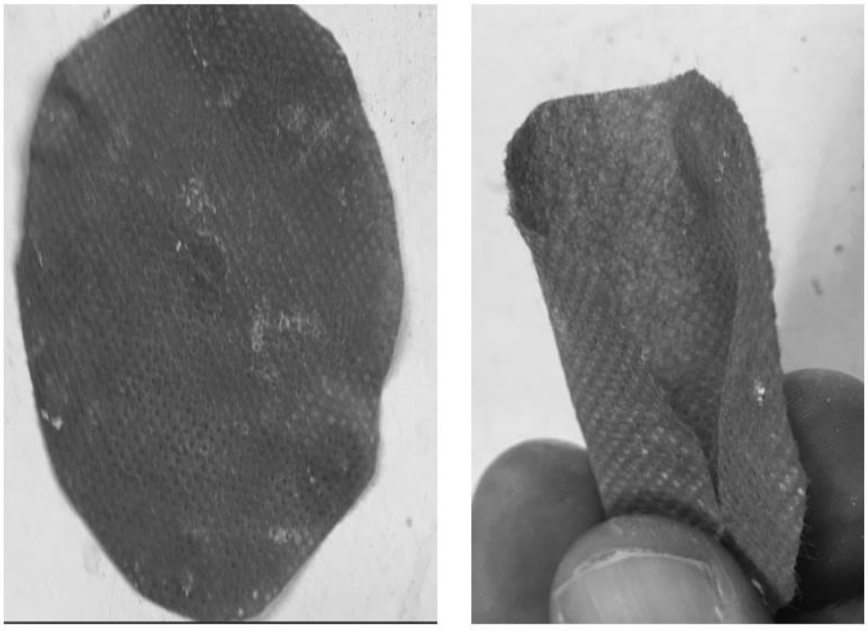

Figure 5.3 A flexible crystal tulle used as a geotextile

An anchorage material is selected as a pin for both the anchorage of geotextile (Figure 5.4).

Figure 5.4 Pins

At the same time, there is more benefit obtained from lignosulfonate lime columns. The height of the pin is two-thirds of the height of the column. This material was not applied for each column and the distance of this material is determined as a 6D. The plan of pins is comprehensively illustrated in Figure 5.5.

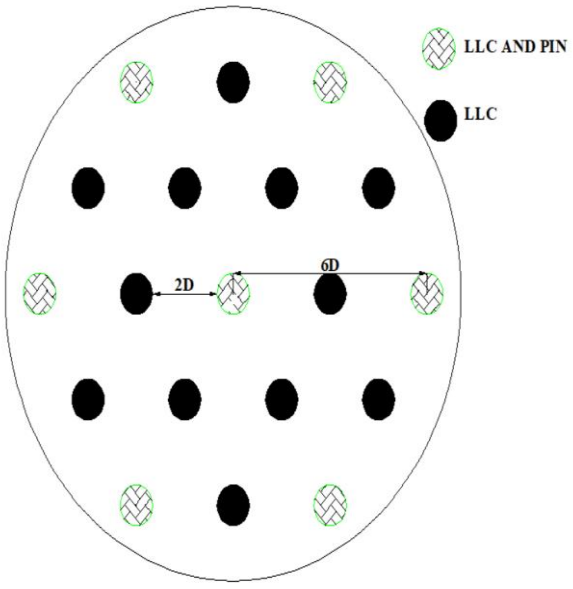

Figure 5.5 A plan of the lignosulfonate lime column + pin in this study

5.2 Free Swell Test On The Oedometer Ring

In this step, an operating logic of the combined improvement method is similar to the lignosulfonate lime columns method even if the installation process of this study is different from the lignosulfonate lime columns method due to the economic solution. These are two parts in this combined improvement method to determine the swelling potential of treated soil.

This chapter is divided into two subtitles that are test specimens in oedometer ring and correlation test specimens.

5.2.1 Test Specimens In Oedometer Ring

The treated specimens used in this study consisted of 19 pieces of calcium lignosulfonate lime columns, six pieces of pins, and a flexible crystal tulle (Figure5.6).

Figure 5.6 The top view of the treated specimens with the CIM stabilization method

The first part is that the treated specimen, which has 6.35 cm diameter and 1.9 cm height, was prepared and a free swell test with this specimen was done under 7 kPa and 25 kPa. The swelling potentials of these treated specimens under two surcharge pressures decrease with curing periods that are 1 day, 7 days, 28 days, 90 days, and 180 days. The swelling potentials of these specimens with CIM were illustrated in

Figures 5.7-5.8. Swelling potential vs. time graphs for treated specimens prepared in this step are presented in Appendix A.

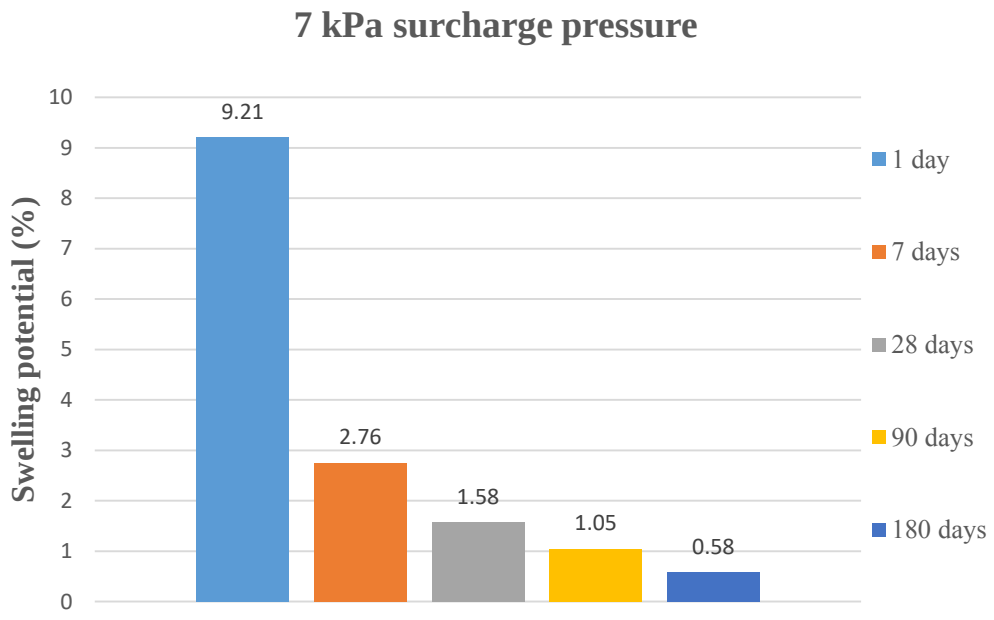

Figure 5.7 The swelling potential of treated specimens that stabilize with CIM with curing under 7 kPa surcharge pressure

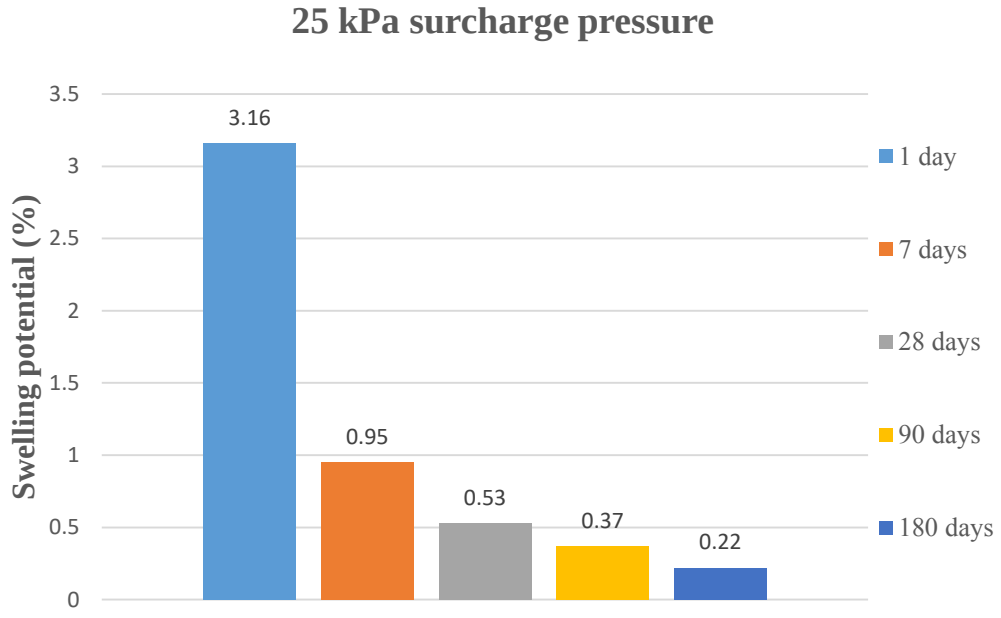

Figure 5.8 The swelling potential of treated specimens that stabilize with CIM with curing under 25 kPa surcharge pressure

5.2.2 Effect of Scale of the Specimens

In the second part, three different diameters of the treated specimen such as 5 cm, 15 cm, and 30 cm were prepared and the swelling potentials of these specimens under two surcharge pressures were determined for a correlation of this method. The parameters related to correlation specimens are mentioned in Table 5.2.

Table 5.2 The parameters of correlation specimen prepared in this study

Specimen name	Specimen diameter (cm)	*Diameter of lime column (D) (mm)*	*The distance between two lime columns (2D) (mm)*	*The distance between the pins (6D) (mm)*
COR1-CIM	5	3.5	7	21
COR2-CIM	15	10.5	21	63
COR3-CIM	30	21	42	126

Four curing periods that are 1 day, 7 days, 28 days, and 90 days were applied to these specimen to observe the curing effect on the swelling potentials of these specimens. After the curing period, the free swell test was under two surcharge pressure for each specimen prepared in this step. Then, the swelling potentials of them were measured under 7 kPa and 25 kPa. The graphs of swelling potentials of correlation specimens are illustrated in Figure 5.9.

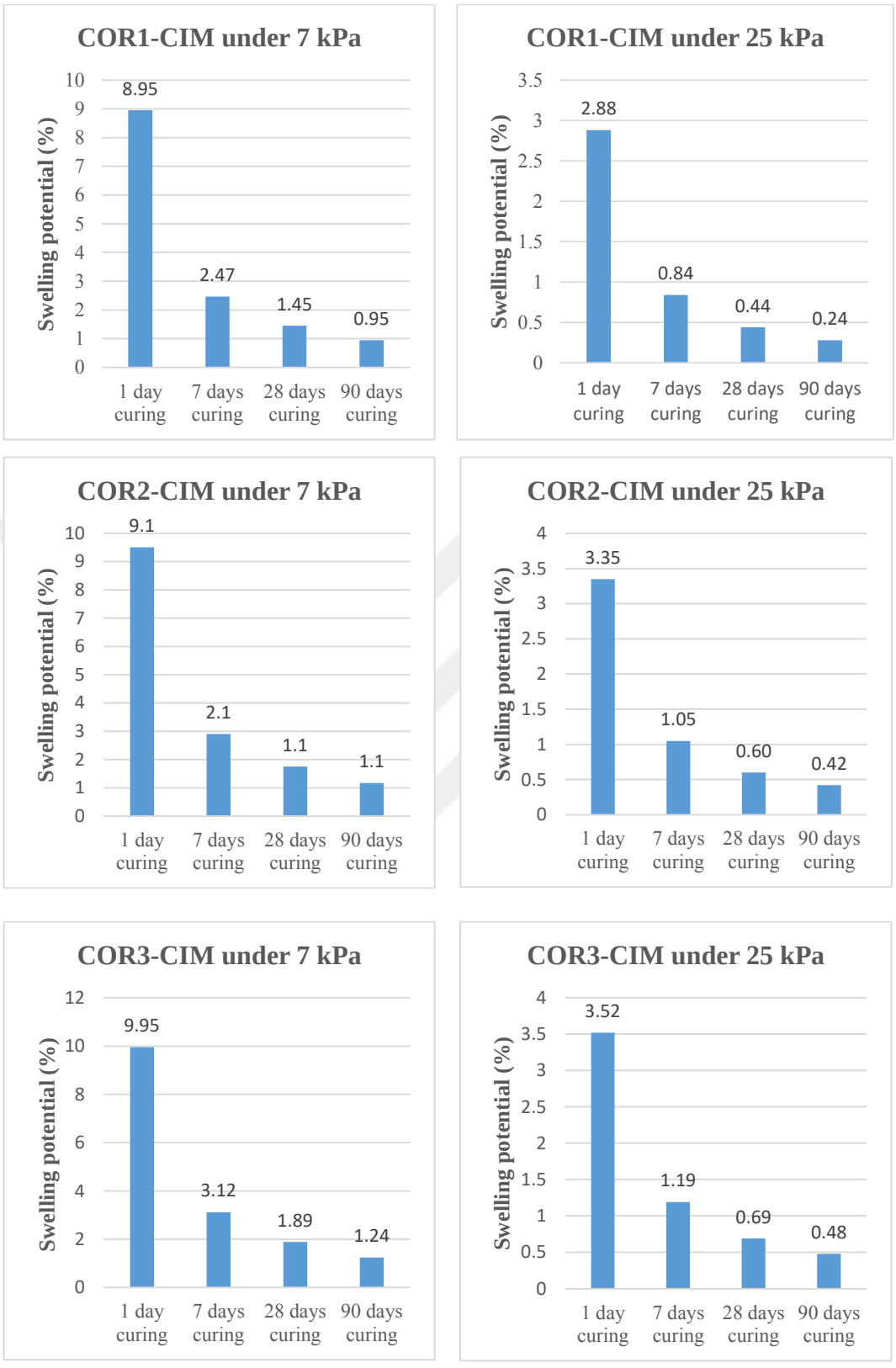

Figure 5.9 The swelling potentials of treated specimens with CIM under both 7 kPa and 25 kPa surcharge pressures

5.3 The Strength of the Specimens for Combined Improvement Method

A series of CBR tests were done to determine the strength of the combined improvement method. Like the previous CBR test done in this study, two surcharge pressures, that are 7 kPa and 25 kPa, are applied in these tests.

The specimen used in this step has 19 pieces of columns that had 1.05 cm diameter and six pieces of nails had 6 cm length. In addition to this, six pieces of the flat washer are put on the nails to block the tearing of the geotextile. The specimen used in this step is illustrated in Figure 5.10.

Figure 5.10 The specimen used in this step

To observe the curing effect of this improvement method, the specimens waited in the humid room for 7 days, 28 days, 90 days. After the curing period, the CBR swell value and the CBR values of the treated specimens were determined to the data obtained from these tests.

The test data obtained from the soaked CBR tests done on the specimen treated with CIM are given in Table 5.3.

Table 5.3 The test data obtained from the soaked CBR tests done on the specimen treated with CIM

Specimens	7 kPa surcharge pressure			25 kPa surcharge pressure		
	Swell Δh (mm)	Load (kN) at 2.5 mm	Load (kN) at 5 mm	Swell Δh (mm)	Load (kN) at 2.5 mm	Load (kN) at 5 mm
1 day curing	10.90	0.856	1.118	4.00	0.925	1.163
7 days curing	3.47	1.088	1.369	1.24	2.146	2.669
28 days curing	1.97	1.717	2.136	0.73	3.111	3.870
90 days curing	1.32	2.063	2.566	0.46	3.484	4.334

CHAPTER 6

DISCUSSION ON TEST RESULTS

Experimental studies of this thesis consist of three groups that are lime columns, the change of specimen properties during the stabilization process, and combined improvement methods. Thus, this part is divided into five subtitles;

1- Effect of different lime column installation models on swell potential test results
2- The change of unconfined compressive strength, swelling potential, coefficient of permeability, CEC and SSA of the treated specimens during the stabilization process
3- Comparison of sodium lignosulfonate and calcium lignosulfonate added lime columns
4- Combined improvement methods
5- Comparison of the lignosulfonate added lime columns method and combined improvement method

6.1 Effect of Different Lime Column Installation Models on Swell Potential Test Results

The lime column part of this section starts with the interpretation of the column installation model selected in this study. Then, this part typically includes that the evaluation of free swell test results of small specimens in this study. Finally, the scale effect of the test specimens prepared in this study is examined in terms of free swell test results done in this study.

6.1.1 Column Installation Model

The column installation model has generally selected either square or triangle shape (Figure 6.1). The area ratio of the column is calculated with this selection model. The area ratio is a ratio between the shaded area and stabilized area for both column installation models.

A circular column installation model is preferred due to the shape of the oedometer ring in this study.

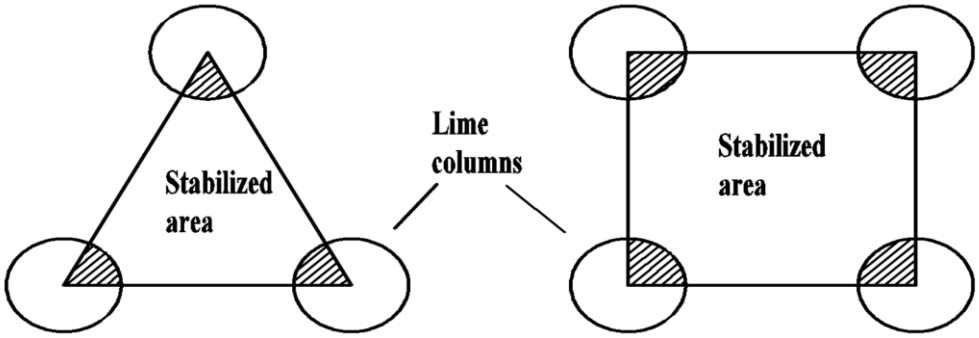

Figure 6.1 Triangle and square column installation model

The column installation model selected in this study is the M2 model had 37 pieces of columns with had 0.45 mm (D) diameter (Figure 6.2). In addition to this, the distance between the columns is 4.05 mm (0.9 D). This model consists of three circular orbits (red line).

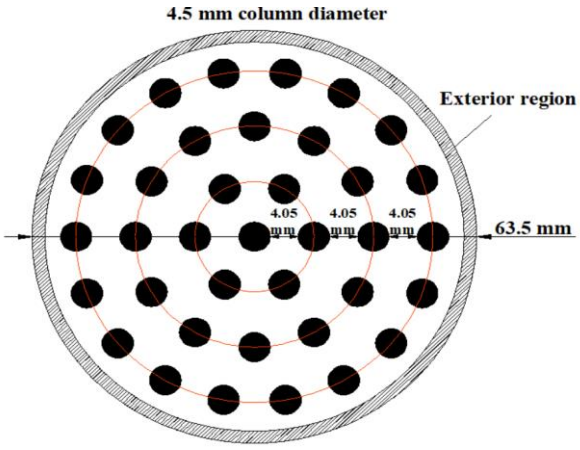

Figure 6.2 M2 model

The calculation of the M2 model area ratio is made this sequences;

1- The stabilized area is an area between the circular orbits (Figure 6.3).

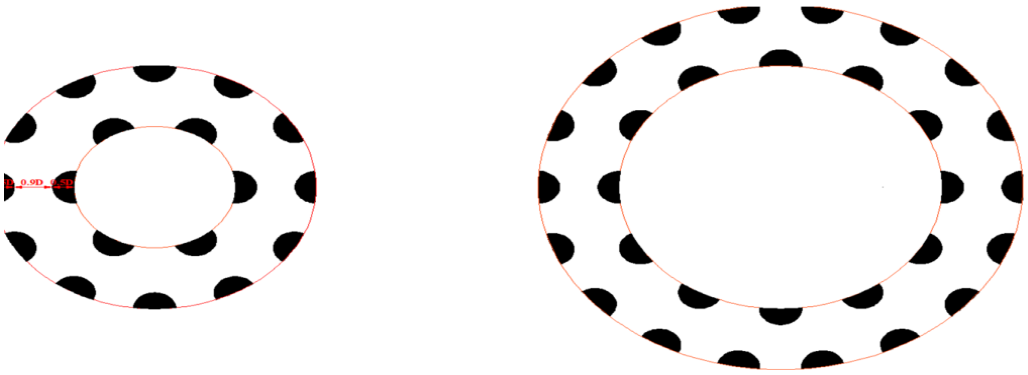

Figure 6.3 Stabilized area

2- The area ratio is calculated at 20.77% for each stabilized area in this model.

3- A column should be placed at the center of this model as the shape of the oedometer ring is a circle. Besides a shaded area of figure 6.2 is an exterior region that diminishes the effect of the oedometer ring. The area ratio change due to the center column and the exterior region. When these two parameters are taken into account of the area ratio, the area ratio of the M2 model is found at 18.58%.

6.1.2 The Height of the Column

The height of Specimen A (h), which is the depth of the active zone in this study, is 19 mm. Two different column heights have been selected as 13 mm (2/3h) and 19 mm (h).

The swelling potential of Specimen A under 7 kPa surcharge pressure was measured as 43.95%. Four treated specimens and Specimen A are given in Table 6.1.

Table 6.1 The swelling potentials of treated specimens with lime column and untreated specimen under 7 surcharge pressure

Treated specimens	The swelling potential of treated specimens under 7 kPa	
	M1-h	M1-2/3h
Without curing	34.64	37.58
7 days curing	30.02	34.42
28 days curing	19.41	27.16

The result of these steps was that the swelling potentials of treated specimens with lime columns had lower than Specimen A and the swelling potentials of them reduced with the curing period. While the swelling potential of the M1-h specimen decreased from 43.95% to 19.41% for 28 days curing, the swelling potential of the M1-2/3h specimen decreased from 43.95% to 27.16% for 28 days curing.

When the M1-2/3h specimen with curing was investigated after the free swell test, these specimens are divided into two groups such as column part and non-column part. For the M1-2/3h specimen waited for 7 days curing, the height of the column part was 13mm and this height was 6 mm for the non-column part before the free swell test. After the test, the height of the column part for M1-2/3h was measured as 17.10 mm, and this height was determined as 8.44 mm for the non-column part (Figure 6.4). As a result, while the increment percentage of the column part was 31.54%, this percentage was found as 40.67% for the non-column part.

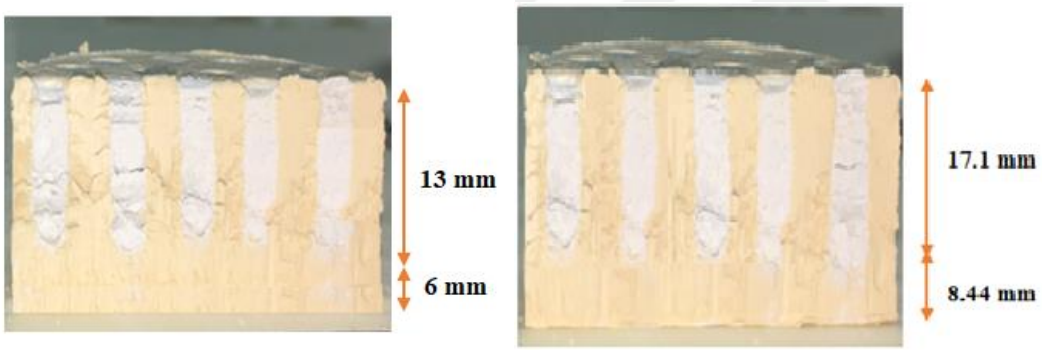

a) Before test b) After test

Figure 6.4 The heights of both column and non-column part of M1-2/3h specimens before/after test

An output of this step is that lime particles diffuse every direction into the untreated soil. However, vertical permeability and horizontal permeability of untreated specimen were measured $9.82*10^{-10}$ cm/s and $4.56*10^{-9}$ cm/s respectively, after the flexible wall permeameter tests. Since the horizontal permeability of untreated specimen is greater than the vertical permeability of this specimen. It means that the diffusion of the lime particles in the horizontal direction is faster than vertical direction.

As a result, the column height should be the height of the specimen. In other words, the height of the lime column should be installed at the depth of the active zone.

6.1.3 The Surrounding Area of all Columns

In this study, two different models are related to the installation of the lime column into Specimen A. These models are named M1 and M2. While the M1 model has consisted of 19 lime columns that have 6.5 mm diameter, the M2 model has consisted of 37 lime columns that have 4.5 mm diameter. These two models are shown in Figure 6.5.

a) Top view of M1-2/3h and M1-h b) Top view of M2-2/3h and M2-h

Figure 6.5 Top view of the treated specimens

The lime column properties of treated specimens that are M1-2/3h, M1-h, M2-2/3h, and M2-h are given in Table 6.2. Although two properties of lime columns, that are total column area and area ratio, are constant for each model in this step, total column volume and total columns surrounding area change with respect to treated specimens prepared in this step. These properties mentioned in Table 6.2 are evaluated for the improvement percentages of treated specimens.

Table 6.2 The lime column properties of treated specimens that are M1-2/3h, M1-h, M2-2/3h, and M2-h

Specimens	*Total Column Area (cm^2)*	*Area Ratio (%)*	*Total Column Volume (cm^3)*	*Total Columns Surrounding Area (cm^2)*
M1-2/3h	6.30	21.05	8.19	50.4
M1-h	6.30	21.05	11.97	73.7
M2-2/3h	5.88	20.91	7.64	68.0
M2-h	5.88	20.91	11.17	99.4

M2 model treated specimens have more total borehole surrounding area than M1 model treated specimens even though the area ratio is approximately similar for them. In addition to this, the total column volume of M1 model treated specimens are greater than M2 model treated specimens. As the achievement of the lime column method is based on lime diffusion into the soil, the total surrounding area is a more considerable property than the other properties. In other words, when an interaction area of lime-clay increases, the improvement percentages of treated specimens rise with curing periods (Table 6.3).

Table 6.3 Improvement percentages of treated specimens in this step under 7 kPa

Specimens	*Total Columns Surrounding Area (cm^2)*	*Improvement percentages (%) without curing*	*Improvement percentages (%) 7 days curing*	*Improvement percentages (%) 28 days curing*
M1-2/3h	50.4	1.01	9.33	28.46
M2-2/3h	68.0	-4.27	13.56	44.86
M1-h	73.7	1.59	14.72	31.39
M2-h	99.4	-6.67	25.94	55.15

Since the total surrounding area of the lime column increases. The result of this condition is that the reaction between the untreated soil and stabilizer material goes effectively up. Another conclusion of this step is that the lime diffusion into the specimen rises with the curing period when the distance between the columns in the M2 model treated specimens, which is 0.9D, is lower than the M1 model treated specimens. As the columns approach each other, the volume of untreated soil reduces.

6.1.4 The Water Percentages of the Water-Lime Mixture

Lime can be either dry or wet at the lime column applications. The water percentage of the lime column affects the achievement of this method. In other words, the water percentage of the lime column in the previous study was zero.

The improvement percentages of treated specimens without curing, which are called M1-2/3h, M1-h, M2-2/3h, and M2-h, are given in Table 6.3. The improvement percentage of both the M2-2/3h specimen and the M2-h specimen without curing was calculated with negative values that are -4.27% and -6.67%. The reason is that these specimens lost some water at the first period of lime column application as there is no water in the lime column. Therefore, the swelling potential of this specimen slightly increased due to a dehydration process.

The water percentages of the lime column should be greater than the water content of Specimen A that is 15%. To solve this problem, water-lime columns were prepared instead of lime columns. Two water percentages of lime columns have been selected as 18% and 30%. The swelling potentials of the M2-h treated specimens are given in Table 6.4.

Table 6.4 The swelling potentials of M2-h treated specimens under 7 kPa surcharge pressure

Specimens	Swelling potential (%) under 7 kPa surcharge pressure			
	Without curing	7 days curing	28 days curing	90 days curing
M2-h (0%)	38.17	26.5	16.05	17.12
M2-h (18%)	35.53	25.77	15.79	16.84
M2-h (30%)	35	22.79	13.95	15.26

The improvement percentages of the M2-h treated specimens are given in Table 6.5.

Table 6.5 The improvement percentages of M2-h treated specimens under 7 kPa surcharge pressure

Specimens	Improvement percentage (%) under 7 kPa surcharge pressure			
	Without curing	7 days curing	28 days curing	90 days curing
M2-h (0%)	-6.67	25.94	55.15	52.16
M2-h (18%)	0.71	27.98	55.87	52.94
M2-h (30%)	2.19	36.31	61.02	57.35

This step concluded that the water percentage of this mixture should be equal to or greater than the water content of the untreated specimen. The optimum curing period of this stabilization process can be said as 28 days.

The result of this step was that all treated specimens had lower swelling potential than untreated specimens. When the water percentages of the water-lime mixture into the columns increased, the swelling potentials of treated specimens went down. Meanwhile, the swelling potentials of treated specimens declined with the curing period, the swelling potentials of treated specimens rise again after 28 days curing period. A problem could be based on ettringite mineral formation during the lime column stabilization process. This mineral is usually formed during the lime or cement stabilizations of soil.

A SEM analysis of this study was done to examine this condition. Three specimens were selected to examine the formation of ettringite minerals. The properties of these specimens properties are given in Table 6.6.

Table 6.6 Specimens selected for SEM analysis

Specimen	Curing period (Days)	Swelling potential under 7 kPa surcharge pressure (%)
Specimen A	-	43.95
M2-h (30%)	28	13.95
M2-h (30%)	180	15.89

The SEM images of them are given in Figures 6.6-6.8.

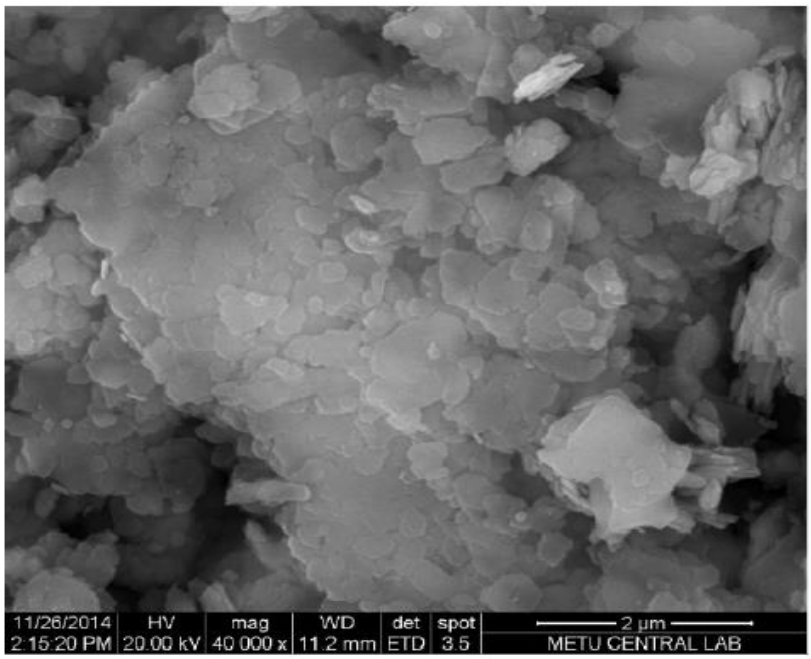

Figure 6.6 SEM image of Specimen A

(magnification factor=40000)

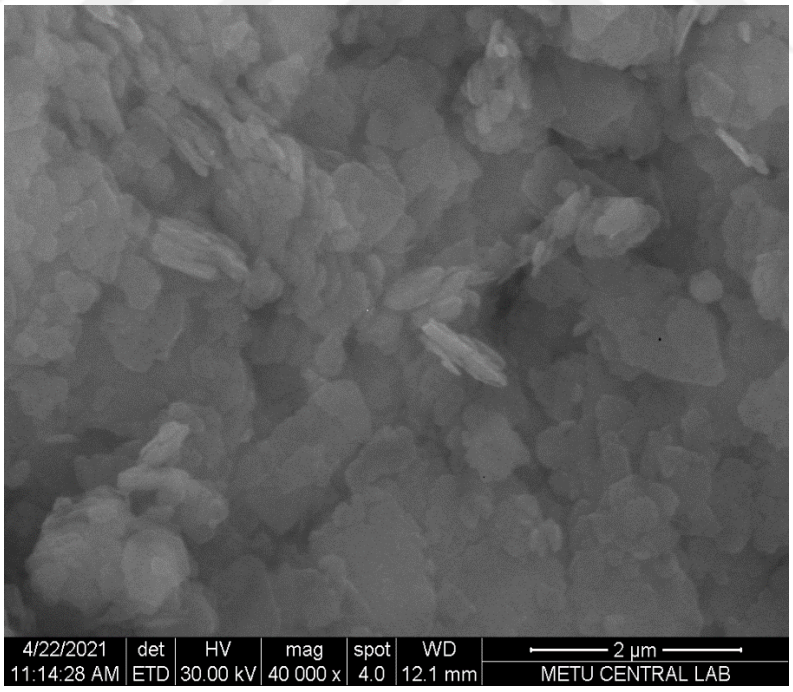

Figure 6.7 SEM image of M2-h (30%) 28 days curing

(magnification factor=40000)

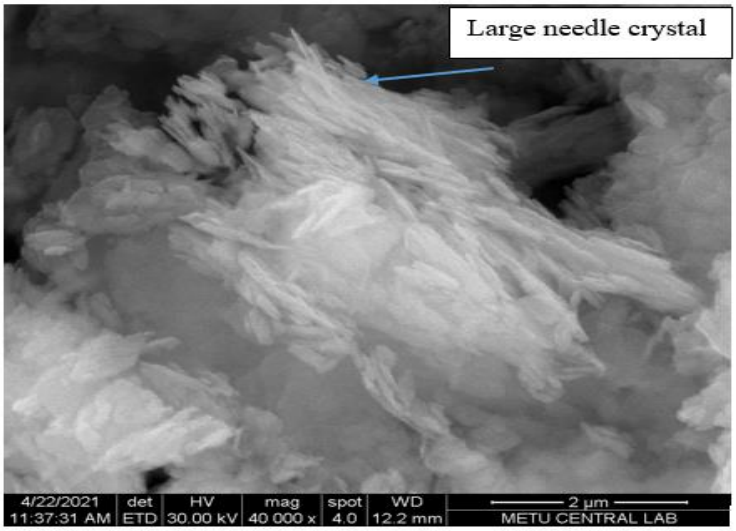

Figure 6.8 SEM image of M2-h (30%) 180 days curing

(magnification factor=40000)

Large needle crystals are shown in Figure 6.8. Thus, ettringite minerals have formed during this stabilization process. The increase of the swelling potential of treated specimens is based on this mineral after 28 days curing period.

In summary, the curing period of treated soils was a problematic case after 28 days due to the formation of ettringite. This step presented two targets following the results of these tests;

1- The swelling potential of treated specimens had to be declined to achieve the goal of a more stable soil. In other words, the lime diffusion into the soil specimens had to be accelerated.
2- The formation of ettringite minerals had to be stopped during the process of lime column stabilizations.

M2-h (30%) treated specimen improved the soil specimen than the other treated specimen. The maximum swelling potential of treated specimens should be 0.5% according to HTS (2013). After the 180 days curing period, the swelling potential of the M2-h (30%) specimen is measured at 15.89% under 7 kPa surcharge pressure. The lime columns consisted of lime and water is not sufficiently stabilized the untreated specimen. Besides, these lime columns cause the formation of ettringite minerals in this study after 28 days curing period. However, the new material should be applied to lime columns to achieve these targets.

6.1.5 Lignosulfonate Added to the Water-Lime Mixture

The next step of this study is that the addition of lignosulfonate into lime-water columns. Sodium lignosulfonate (NaLS) and calcium lignosulfonate (CaLS) have been separately added into lime –water column. The main goal is that the increase the velocity of the lime diffusion into the specimen.

Three different types of specimens are M2-h (30%), NaLS, and CaLS. The swelling potentials of them with curing periods under 7 kPa and 25 kPa surcharge pressure are given in Table 6.7 and Table 6.8.

Table 6.7 The swelling potentials of M2-h (30%), NaLS, and CaLS specimens under both 7 kPa surcharge pressure

Specimens	Swelling potential (%) under 7 kPa surcharge pressure				
	Without curing	7 days curing	28 days curing	90 days curing	180 days curing
M2-h (30%)	35	22.79	13.95	15.26	15.89
NaLS	27.37	10.53	7.89	4.74	2.37
CaLS	26.32	10	7.11	4.21	1.84

Table 6.8 The swelling potentials of M2-h (30%), NaLS, and CaLS specimens under both 25 kPa surcharge pressure

Specimens	Swelling potential (%) under 25 kPa surcharge pressure				
	Without curing	7 days curing	28 days curing	90 days curing	180 days curing
M2-h (30%)	23.1	15.2	9.17	10.01	10.35
NaLS	16.32	9.21	4.26	1.32	0.53
CaLS	15.26	8.3	3.16	0.95	0.32

The optimum curing period was found at 28 days for the M2-h (30%) specimens. The swelling potentials of both the NaLS specimens and the CaLS specimens decrease with curing periods. After the 180 curing periods, the swelling potentials of these specimens

under 7 kPa surcharge pressure were measured at 2.37%, 1.84%, respectively. Under 25 kPa surcharge pressure, while the swelling potential of the NaLS specimen was dropped away from 29.47% to 0.53 after 180 days curing period, this value was determined at 0.32 for the CaLS specimen.

The lignosulfonate addition to the lime-water mixture is the final step of the test program. According to HTS (2013), the main goal of this test program is that the swelling potential of the treated specimen used for the subgrade material in the highway construction should be either equal to 1% or lower than 1%. After the 180 days curing period, the swelling potential of the specimen treated with sodium lignosulfonate lime columns under 25 kPa surcharge pressure has reached this goal. The specimen stabilized with calcium lignosulfonate lime columns under 25 kPa surcharge pressure is a suitable method for HTS (2013).

According to Seed et al. (1962), The classification of both untreated and treated specimens is done by using their swelling potentials (Table 6.9).

Table 6.9 The classification of both untreated and treated specimens according to Seed et al. 1962

Treated specimen	Surcharge pressure (kPa)	Curing period (days)	Swelling potential (%)	Degree of expansion
Specimen A	7	-	43.95	Very high
Specimen A	25	-	29.47	Very high
M2-h (30%)	7	180	15.89	High
M2-h (30%)	25	180	10.35	High
NaLS	7	180	2.37	Medium
NaLS	25	180	0.53	Low
CaLS	7	180	1.84	Medium
CaLS	25	180	0.32	Low

The other subject investigated in this step is the prevention of ettringite formation during this stabilization process. After 28 days curing period, the ettringite minerals have formed during the lime-water column stabilization process. For this reason, the waste material named lignosulfonate was added to the lime-water mixture.

The SEM analysis was done for searching the effect of lignosulfonate addition on the formation of ettringite minerals. The specimens used for this analysis are listed below (Table 6.10).

Table 6.10 The specimens used for the SEM analysis

Treated specimen	Curing period (days)
Specimen A	-
M2-h (30%)	180
NaLS	180
CaLS	180

The SEM images of them are given in Figures 6.9-6.12.

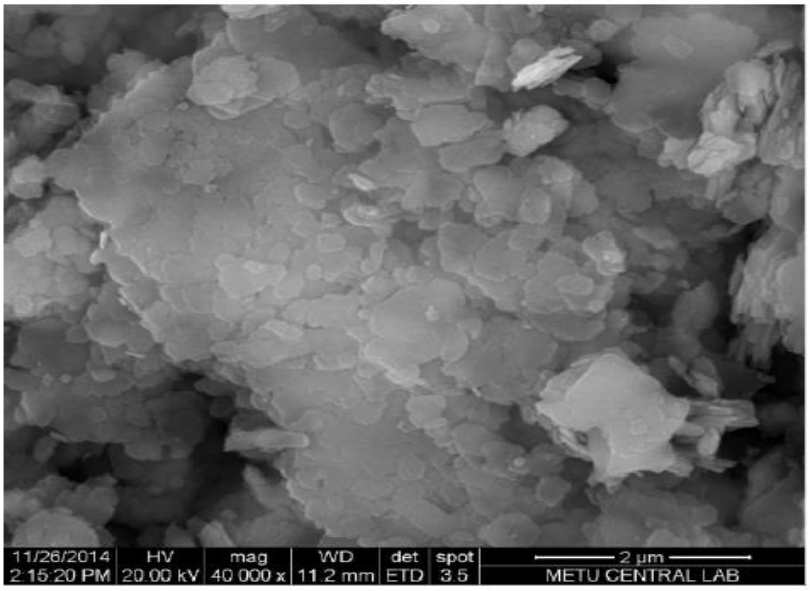

Figure 6.9 SEM image of Specimen A

(magnification factor=40000)

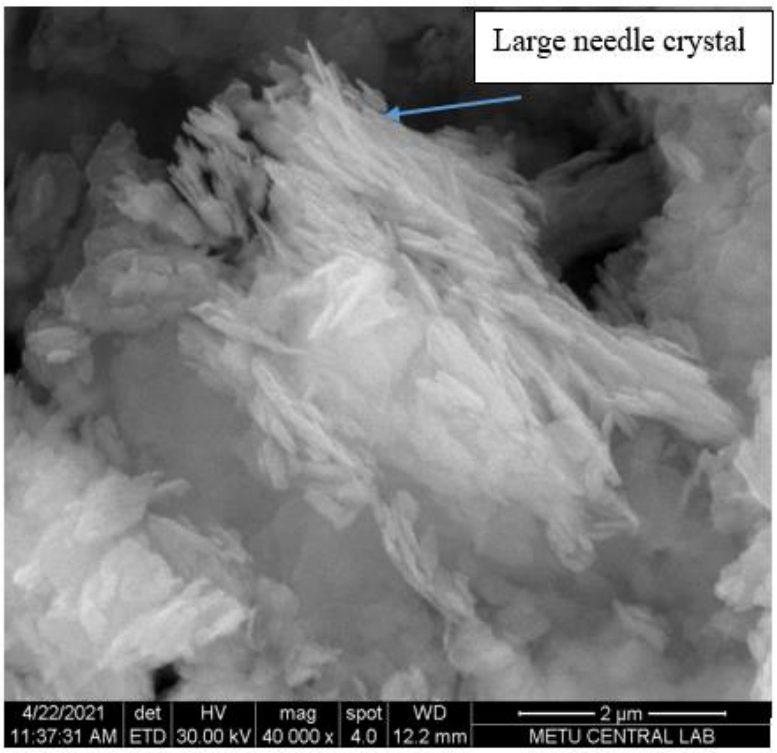

Figure 6.10 SEM image of M2-h (30%) 180 days curing

(magnification factor=40000)

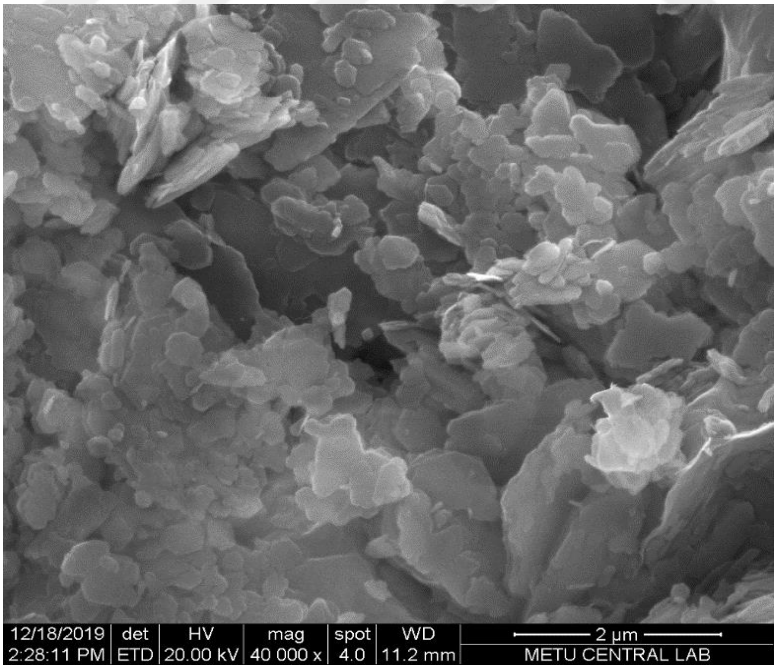

Figure 6.11 SEM image of NaLS specimen 180 days curing

(magnification factor=40000)

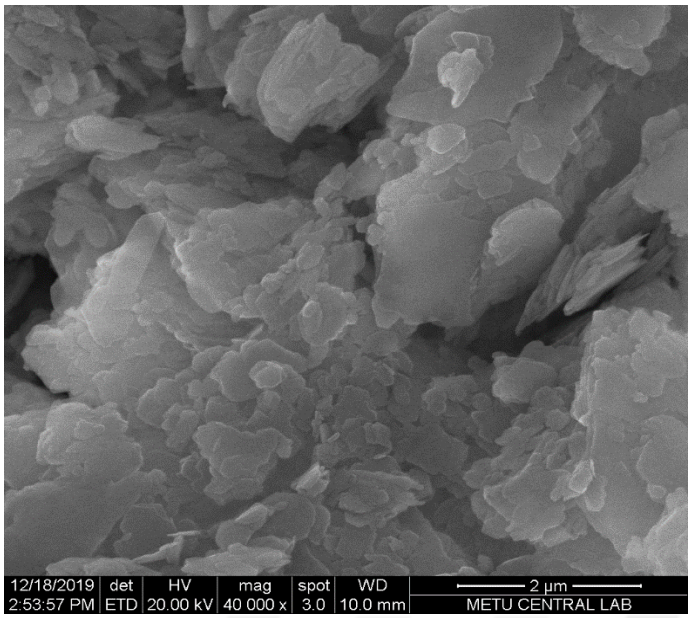

Figure 6.12 SEM image of CaLS specimen 180 days curing

(magnification factor=40000)

The formation of ettringite minerals was not observed in both the NaLS specimen and the CaLS specimen. Thus, the formation of ettringite minerals is blocked due to the addition of lignosulfonate.

6.1.6 Effect of Scale of the Specimens

The dimensions of the specimens influence the improvement percentages of the treated specimens. When the dimensions of the specimens increase, the lime particles placed into columns have to diffuse longer distance to stabilize the untreated specimens. Six different specimens were separately prepared for both the NaLS and the CaLS specimens. The reasons for this step of the study are listed below;

1- The observation of the change of the improvement percentages of the treated specimens

2- The estimation of the swelling potentials of the specimens which had different sizes in this study after this stabilization process

These specimens were waited in the humid room for 7 days, 28 days, and 90 days for observation of the curing effect. The properties of specimens prepared in this step are given in Table 6.11.

Table 6.11 The properties of specimens prepared in this step

Specimen Name	Specimen Diameter (cm)	Borehole Diameter (cm)	Area Ratio (%)
COR1	5	0.35	18.13
COR2	10	0.7	18.13
COR3	15	1.05	18.13
COR4	20	1.4	18.13
COR5	25	1.75	18.13
COR6	30	2.1	18.13

In terms of the curing periods, the swelling potentials of treated specimens tested under 7 kPa prepared in this study are shown in Figure 6.13 and Figure 6.14, respectively.

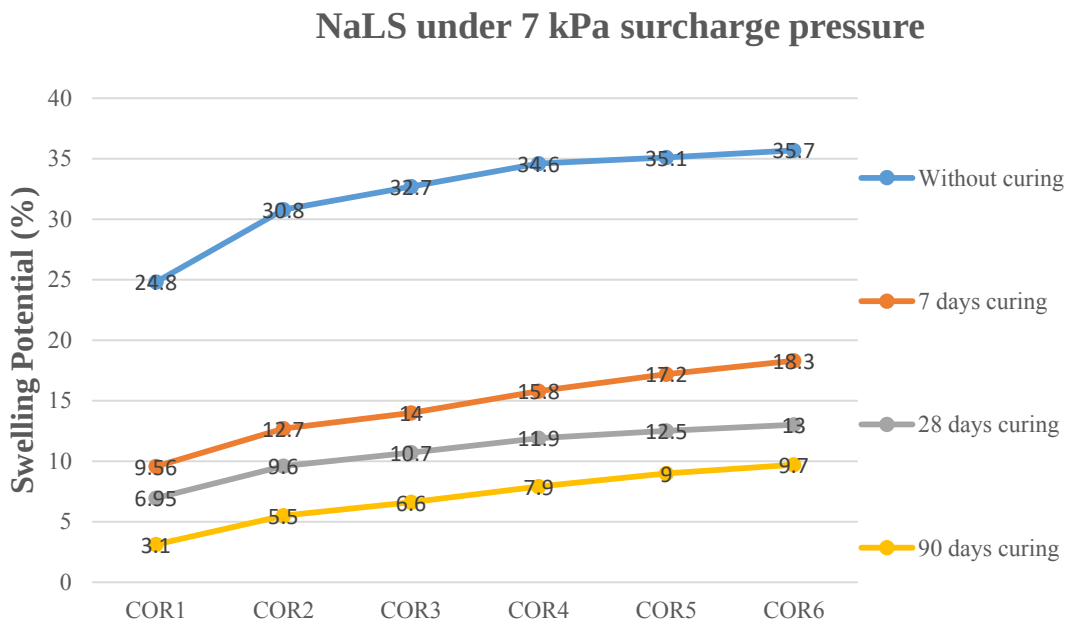

Figure 6.13 The swelling potentials of the treated specimen with sodium lignosulfonate lime column under 7 kPa with respect to curing period

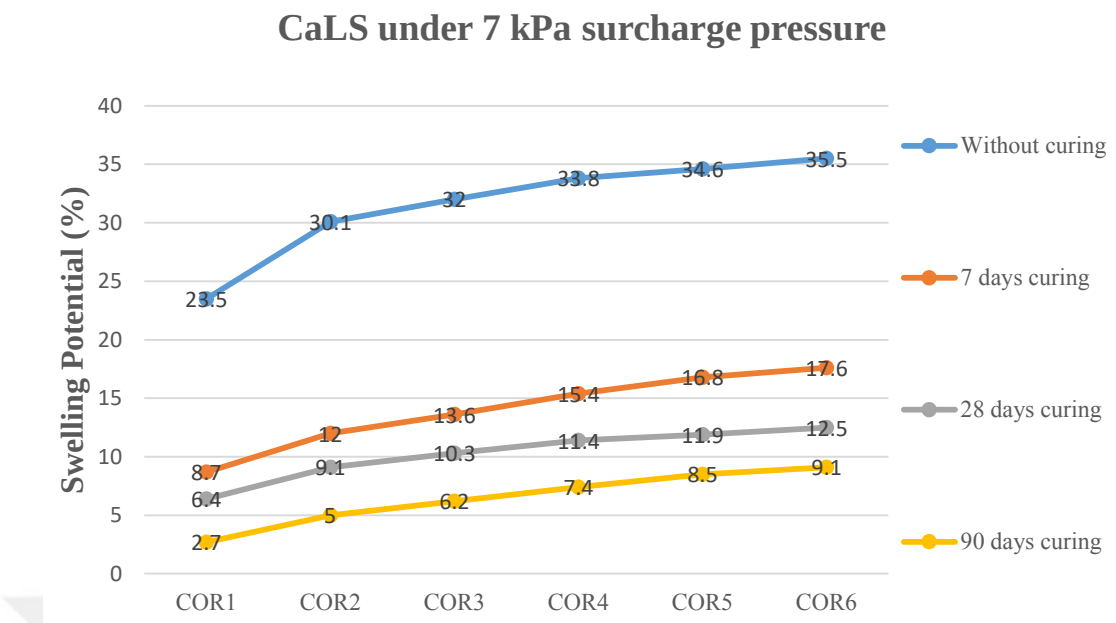

Figure 6.14 The swelling potentials of the treated specimen with calcium lignosulfonate lime column under 7 kPa with respect to curing period

In terms of curing periods, the swelling potentials of treated specimens tested under 25 kPa prepared in this study are shown in Figure 6.15 and Figure 6.16, respectively.

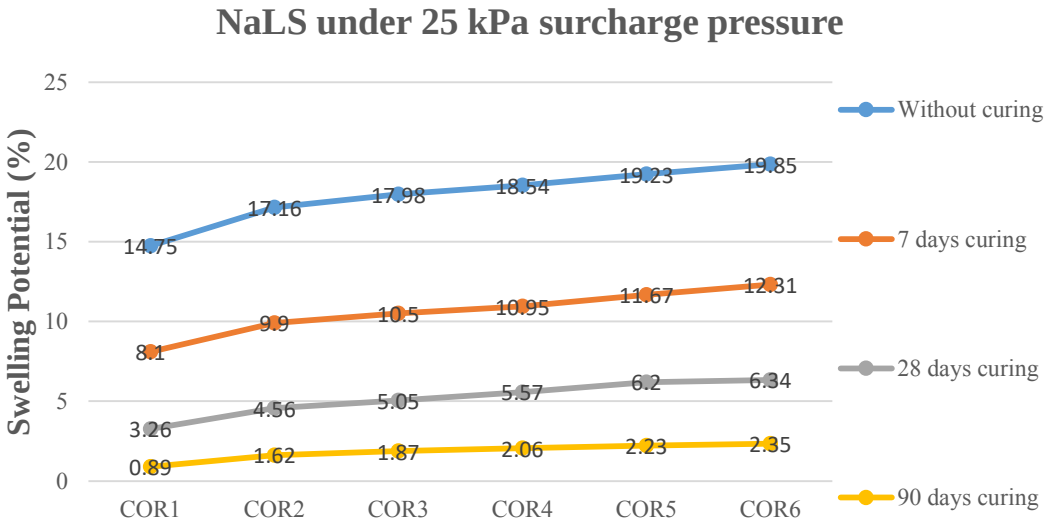

Figure 6.15 The swelling potentials of the treated specimen with sodium lignosulfonate lime column under 25 kPa with respect to curing period

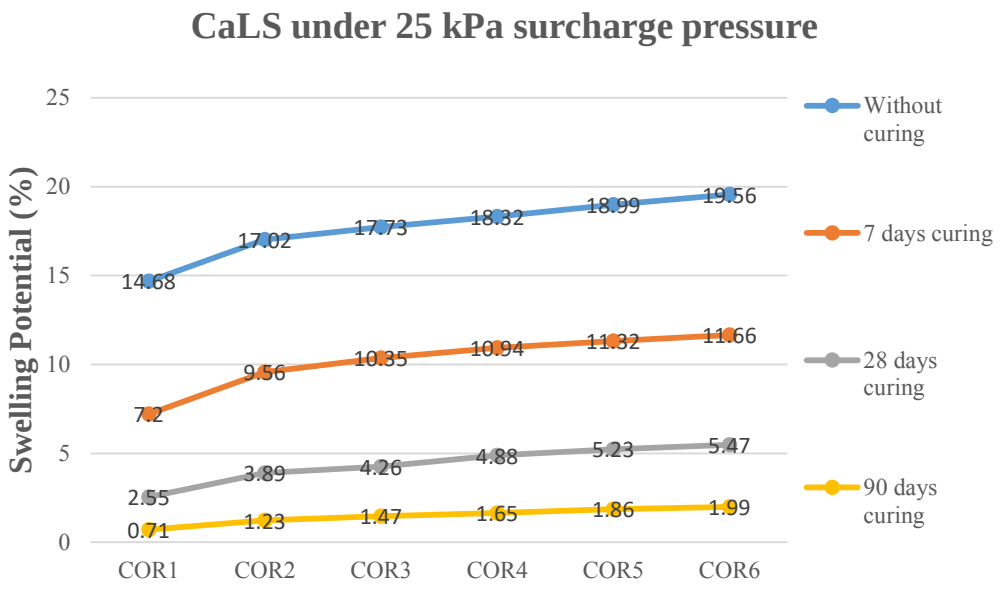

Figure 6.16 The swelling potentials of the treated specimen with calcium lignosulfonate lime column under 25 kPa with respect to curing period

The swelling potentials of both the NaLS specimens and the CaLS specimens are lower than the untreated specimens for each surcharge pressure. The other output is that the curing period is an inducement that is the decrease of the swelling potentials of the treated specimens prepared in this study.

The COR1 specimens have the lowest swelling potentials due to their sizes in this step of the study. Two main reasons for this condition are;

1- Both the diameter of the column and the distance between the column go up owing to the increase of the specimen sizes. Thus the distance, that lime particles have to diffuse, comparatively advances with this increase.
2- The untreated specimen prepared in this study is a low permeable soil. Therefore, this specimen influences from this increase in the specimen sizes.

After 90 days curing period, correlation specimens are classified in regards to Seed et. al. (1962). Table 6.12 shows this classification below.

Table 6.12 Correlation specimens classification

with respect to Seed et. al. (1962)

Specimens	*Surcharge Pressures*	*Swelling Potential (%)*	*Seed et. al. (1962)*
COR1-NaLS	7 kPa	3.1	Medium
COR2-NaLS	7 kPa	5.5	High
COR3-NaLS	7 kPa	6.6	High
COR4-NaLS	7 kPa	7.9	High
COR5-NaLS	7 kPa	9	High
COR6-NaLS	7 kPa	9.7	High
COR1-NaLS	25 kPa	0.89	Low
COR2-NaLS	25 kPa	1.62	Medium
COR3-NaLS	25 kPa	1.87	Medium
COR4-NaLS	25 kPa	2.06	Medium
COR5-NaLS	25 kPa	2.23	Medium
COR6-NaLS	25 kPa	2.35	Medium
COR1-CaLS	7 kPa	2.7	Medium
COR2-CaLS	7 kPa	5	High
COR3-CaLS	7 kPa	6.2	High
COR4-CaLS	7 kPa	7.4	High
COR5-CaLS	7 kPa	8.5	High
COR6-CaLS	7 kPa	9.1	High
COR1-CaLS	25 kPa	0.71	Low
COR2-CaLS	25 kPa	1.23	Low
COR3-CaLS	25 kPa	1.47	Low
COR4-CaLS	25 kPa	1.65	Medium
COR5-CaLS	25 kPa	1.86	Medium
COR6-CaLS	25 kPa	1.99	Medium

The specimens prepared in the laboratory can give some information about the real situation even though they are too small in point of their dimension by comparison with the field application. In this study, six different specimens prepared in the laboratory have been tested for each lime column type to make a consistent estimation of swelling potential. This estimation is based on two parameters that are the diameter of the lime column and the curing period.

The swelling potential of the treated specimen decreases for two reasons for this stabilization process. The first reason is that the influence of the lignosulfonate lime column and the second reason is that the volume of the treated specimen reduces during the installation of these columns. Therefore, a parameter that is named as an improvement percentage has to be produced for the determination of the influence of this stabilization process. As a result, the improvement percentage of the treated specimen is the more accurate parameter with respect to the swelling potential of the treated specimen as long as the use of this estimation. In addition to this, the improvement percentages of these specimen have been calculated owing to these swelling potential in Appendix F.

The relation between the diameter of the lime column and the curing period has to be found by the improvement percentage of the treated specimen with the lignosulfonate lime column applications. Therefore, two graphs show this relation under each pressure applied in this study are drawn for both sodium and calcium lignosulfonate lime column. Finally, a suitable estimation can be individually made using both the diameter of the lime column and the curing period. In a conclusion, the improvement percentage of the treated specimen had a big size in the field can be estimated by using these equations of these curves in the graph (Figure 6.17-6.20).

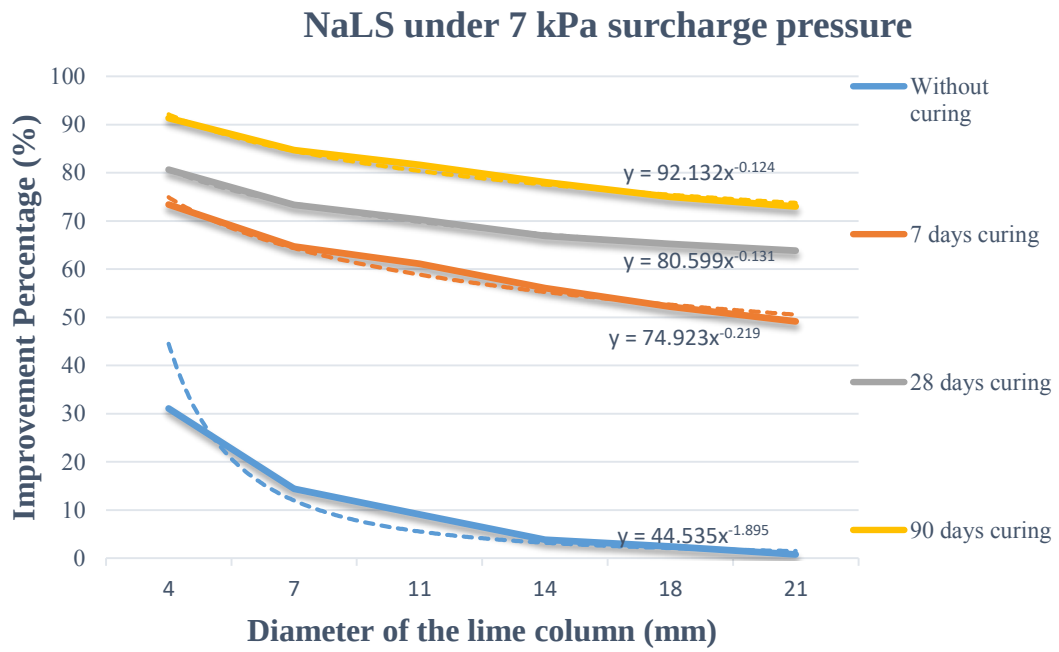

Figure 6.17 The improvement percentages of the treated specimen with sodium lignosulfonate lime column under 7 kPa with respect to both curing period and distance between the boreholes

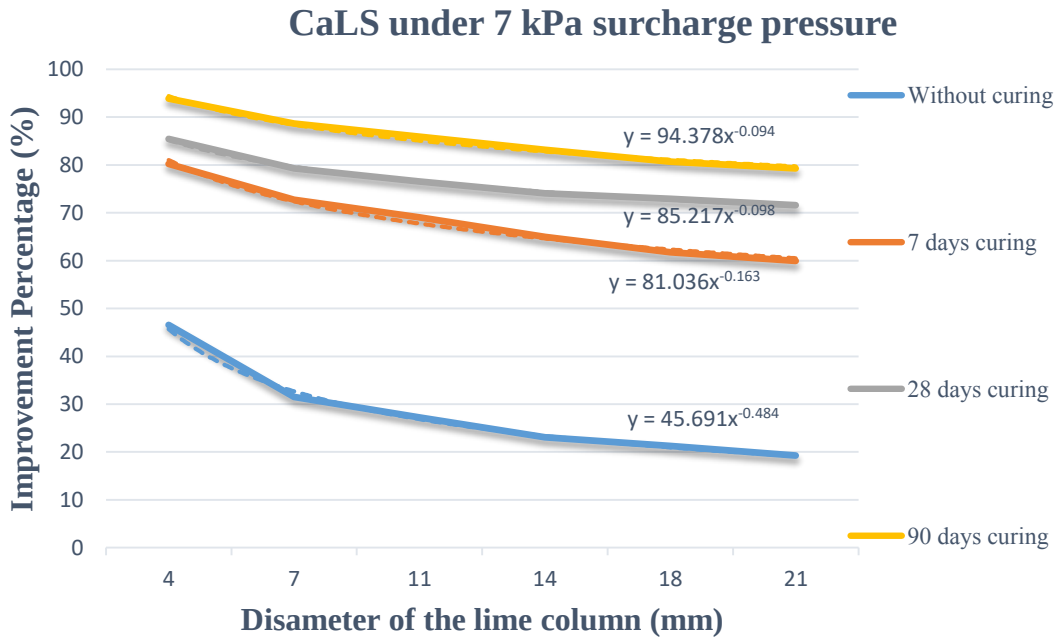

Figure 6.18 The improvement percentages of the treated specimen with calcium lignosulfonate lime column under 7 kPa with respect to both curing period and distance between the boreholes

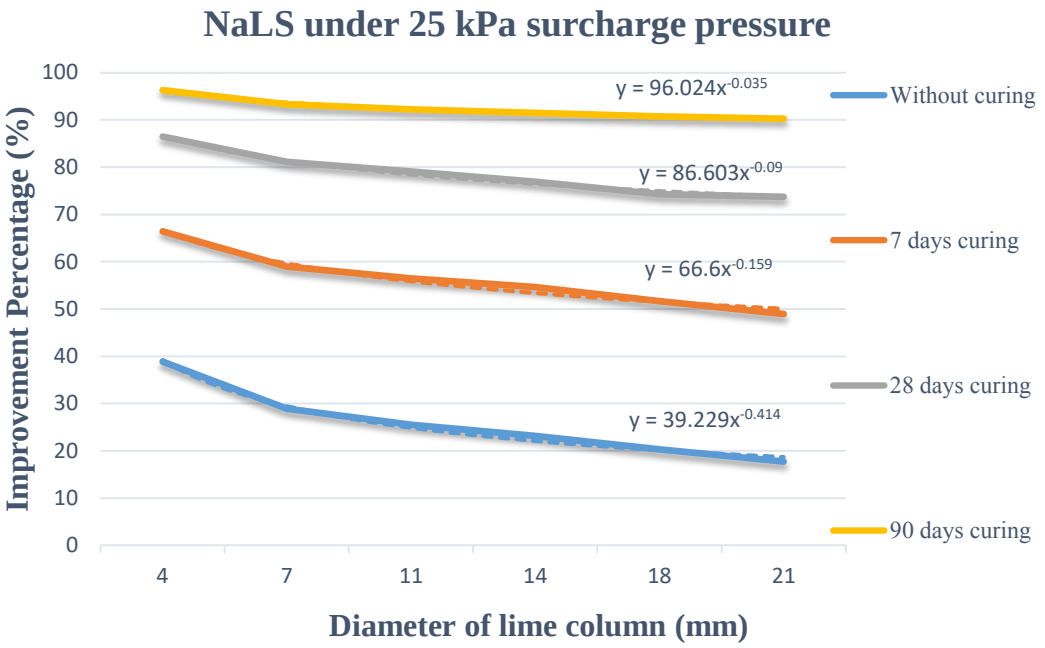

Figure 6.19 The improvement percentages of the treated specimen with calcium lignosulfonate lime column under 25 kPa with respect to both curing period and distance between the boreholes

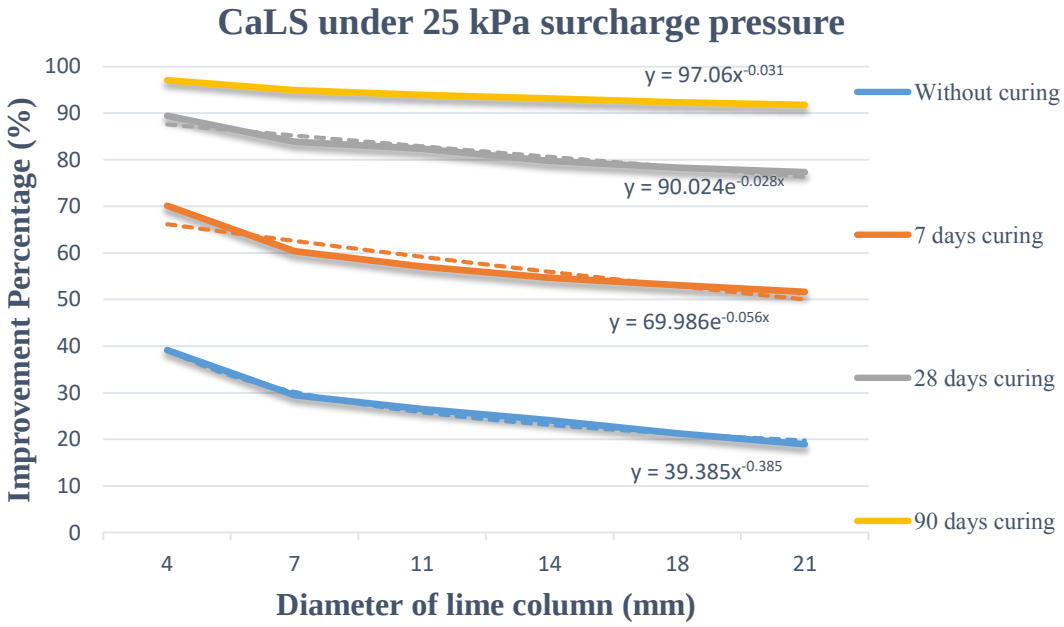

Figure 6.20 The improvement percentages of the treated specimen with calcium lignosulfonate lime column under 25 kPa with respect to both curing period and distance between the boreholes

6.2 The Change of Unconfined Compressive Strength, Swelling Potential, Coefficient of Permeability, CEC And SSA of the Treated Specimen During The Stabilization Process

The lime columns chapter is based on the swelling potentials of the treated specimen prepared in this study. In addition to this, the treated specimens are evaluated as a whole in the previous chapter.

Two different types of treated specimens, which are the NaLS specimen and CaLS specimen have been prepared in this step. The soil specimens placed between the lignosulfonate lime columns are investigated in this chapter. The soil properties examined in this step are listed below (Table 6.13).

Table 6.13 The soil properties examined in this step

Engineering properties	Unconfined compressive strength
	Swelling potential
	Coefficient of permeability
Physical properties	Cation exchange capacity
	Specific surface area

In addition to this, the California bearing ratios of the treated specimens are investigated in this step. However, the specimens used for this property are not taken from a region that is between the columns. The whole treated specimens are tested for this property.

6.2.1 Unconfined Compressive Strength

The undisturbed specimens that had approximately 36 mm diameter and 72 mm height were used for the unconfined compressive strength test. The unconfined compressive strengths of treated specimens and untreated specimen were shown in Figure 6.21.

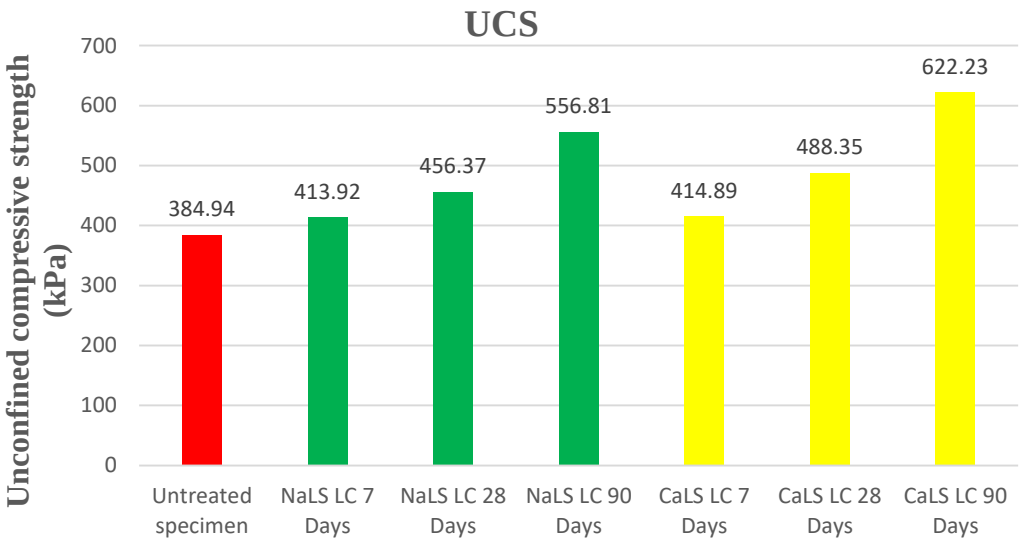

Figure 6.21The unconfined compressive strength for untreated specimen and treated specimens

After the 90 day curing period, the unconfined compressive strength of untreated specimen treated with sodium lignosulfonate lime column increased from 384.94 kPa to 556.81 kPa. In addition to this, the unconfined compressive strength of untreated specimen treated with calcium lignosulfonate lime column at the same curing period reached up to 622.23 kPa. The stress-strain relationship for untreated specimen and treated specimens are given in Figure 6.22.

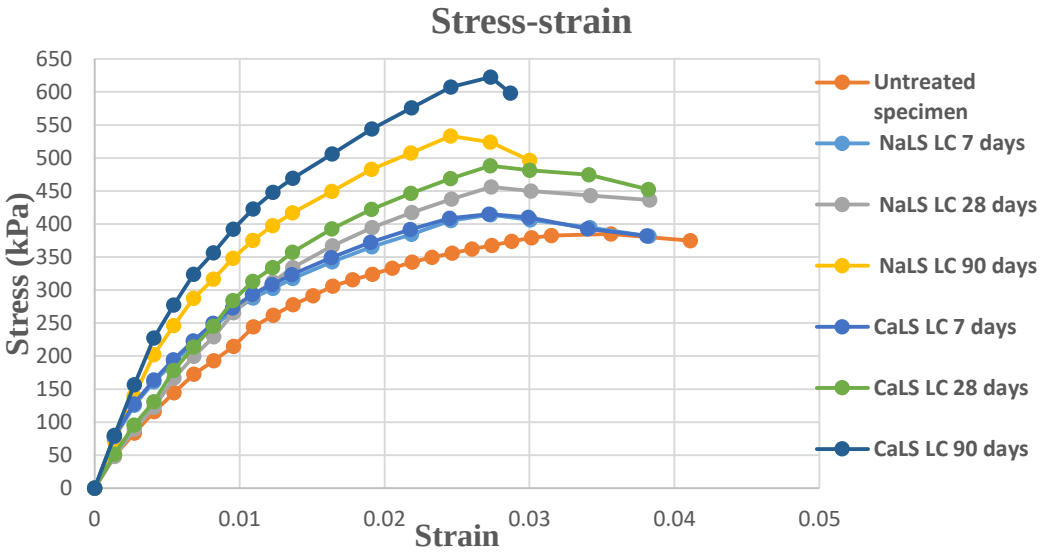

Figure 6.22 Stress-strain relationship for untreated specimen and treated specimens

The untreated specimen is a ductile material according to the result of the unconfined compressive strength test. With the curing period, this specimen treated with either NaLS or CaLS lime columns convert from the ductile material to a brittle material.

6.2.2 Swelling Potential

The swelling potentials of the stabilized specimens with the lignosulfonate lime columns diminish with the curing period. When the curing period increases, the decrease of swelling potentials of the treated specimens increases.

The specimens for this test are given from the region located between three lignosulfonate lime columns. The swelling potentials of the treated specimens under 7 kPa surcharge pressure are illustrated in Figure 6.23.

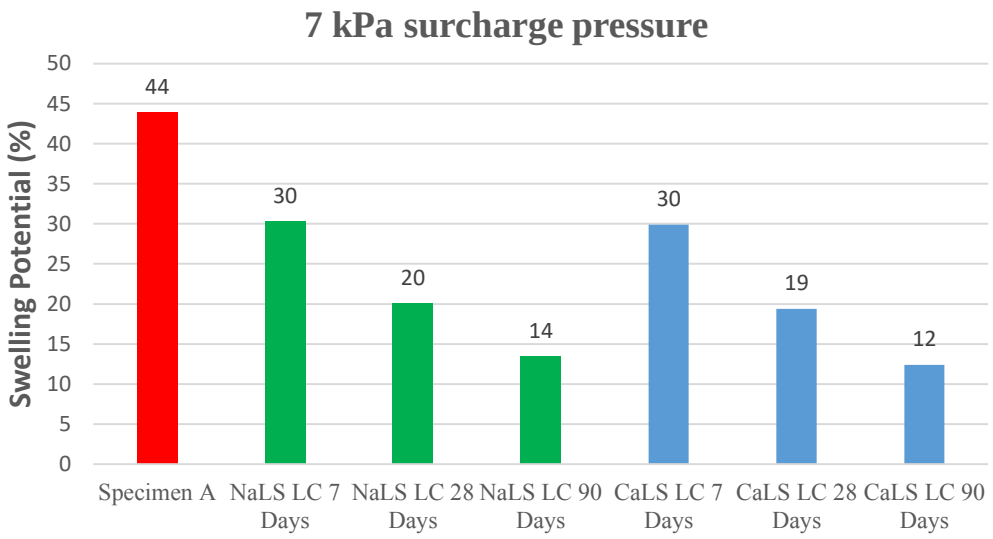

Figure 6.23 The swelling potential of the treated and untreated specimen under 7 kPa

After 90 days curing period, the swelling potentials of the treated specimens with sodium lignosulfonate lime columns and calcium lignosulfonate lime columns under 7 kPa reduced from 43.95% to 13.5 and 12.4%, respectively.

The swelling potentials of the treated specimens under 25 kPa surcharge pressure are illustrated in Figure 6.24.

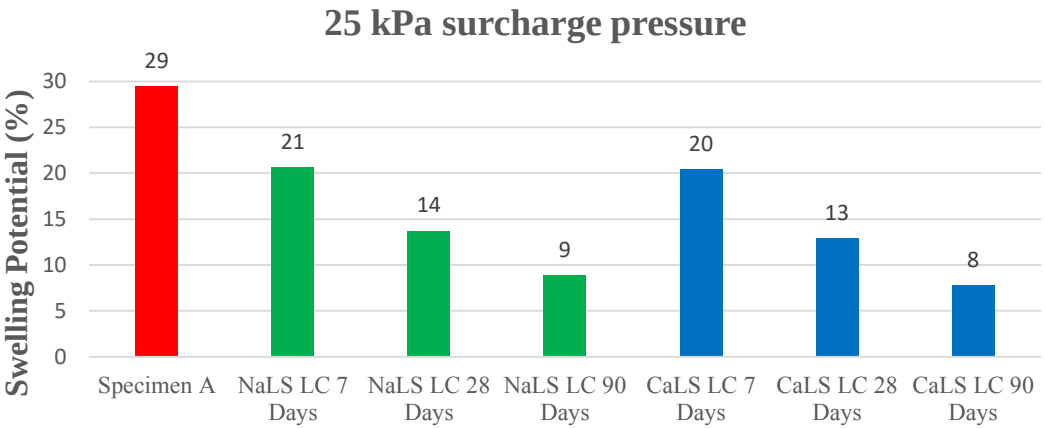

Figure 6.24 The swelling potential of the treated and untreated specimen under 25 kPa

When 25 kPa surcharge pressure is applied instead of 7 kPa surcharge pressure, the swelling potential of the treated specimen with sodium lignosulfonate lime columns is found at 8.8%. The lowest swelling potential value is found at 8.65% that is obtained from CaLS specimen with 90 days curing period.

6.2.3 Coefficient of Permeability

The coefficient permeability values of treated specimens with curing period were given in Table 6.14.

Table 6.14 The coefficient permeability values of untreated and treated specimens with curing period

Specimens	Coefficient of Permeability (cm/s)
Untreated specimen	$6.6 * 10^{-10}$
NaLS LC 7 Days	$5.2 * 10^{-10}$
NaLS LC 28 Days	$1.4 * 10^{-10}$
NaLS LC 90 Days	$5.3 * 10^{-11}$
CaLS LC 7 Days	$4.5 * 10^{-10}$
CaLS LC 28 Days	$9.7 * 10^{-11}$
CaLS LC 90 Days	$3.1 * 10^{-11}$

The coefficient of permeability of treated specimens improved with the curing period. After 90 days curing period, this value reached up to $5.3 * 10^{-11}$ and $3.1 * 10^{-11}$ for sodium lignosulfonate lime columns and calcium lignosulfonate lime columns, respectively.

6.2.4 California Bearing Ratio

The unsoaked CBR value of the untreated specimen is a very stiff material. However, this parameter is measured very low CBR value when this specimen has waited under the soaked condition. For this reason, the soaked CBR tests have been done for treated specimens in this step. All specimens have waited under soaked conditions for 4 days. The CBR swell and CBR values for treated specimens in this step have been determined under both 7 kPa and 25 kPa surcharge pressure.

The change of two outputs that are CBR swell (%) and CBR value is evaluated in this step. After 4 days of soaked condition, the CBR swells values of these specimens are given in Figures 6.25 and 6.26 with respect to surcharge pressure.

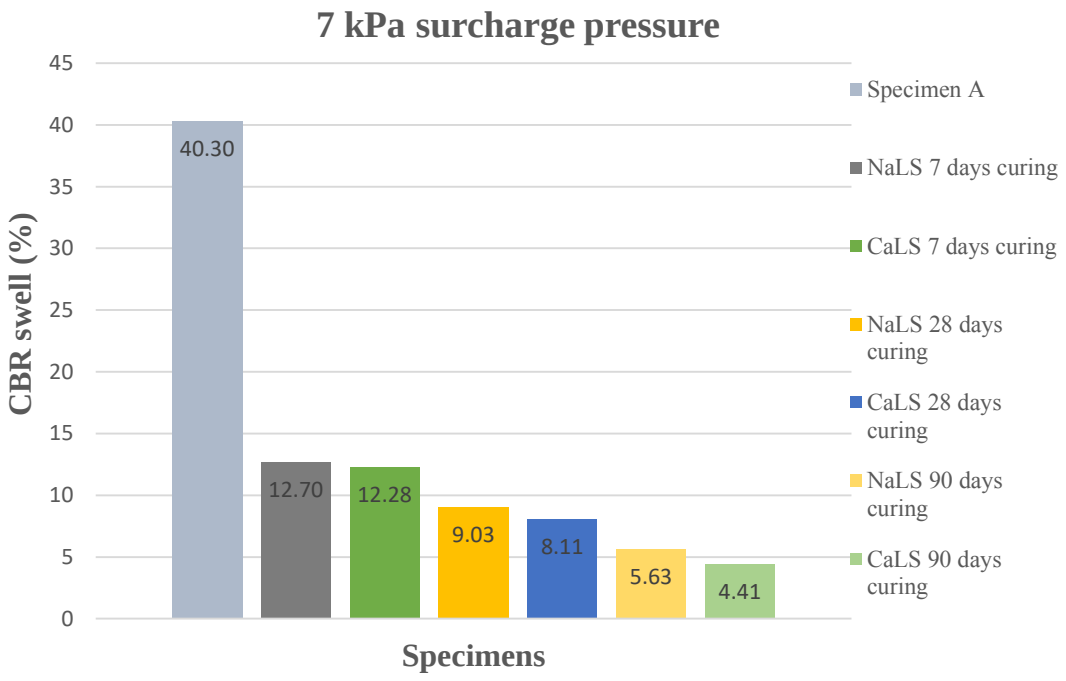

Figure 6.25 CBR swell values of treated specimens under 7 kPa surcharge pressure

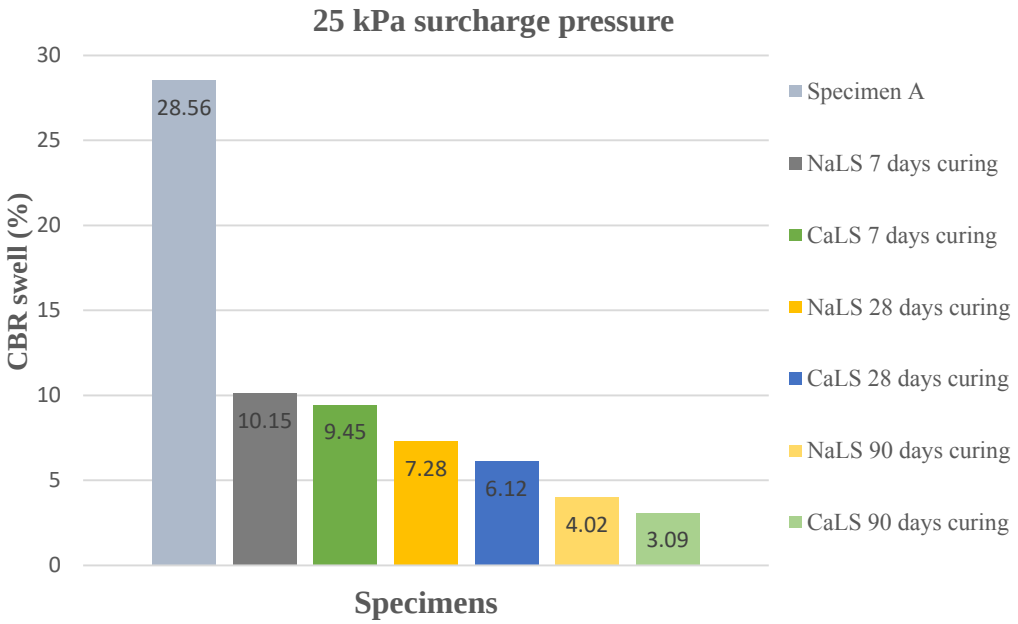

Figure 6.26 CBR swell values of treated specimens under 25 kPa surcharge pressure

Treated specimens prepared in this step have the lower swelling potential of Specimen A because the lignosulfonate lime column stabilizes the untreated part with the curing period. The CBR swell values of treated specimens prepared in this study decrease with the curing period for each surcharge pressure. After 90 days curing period, while the CBR swell of the treated specimen with NaLS is determined 5.63% under 7 kPa surcharge pressure, this parameter for the same specimen is found at 4.02% when 25 kPa surcharge pressure is applied. In addition to this, the treated specimen with CaLS has the lowest CBR swell value for each surcharge pressure. After these specimens waited in the humid room for 90 days, the CBR swell values of this specimen under 7 kPa and 25 kPa surcharge pressure are measured at 4.41%, and 3.02%, respectively.

CBR values of treated specimens have improved during this stabilization method. Under 7 kPa and 25kPa surcharge pressure, Figures 6.27 and 6.28 show the load-penetration curves for both untreated and treated specimens obtained from the soaked CBR tests.

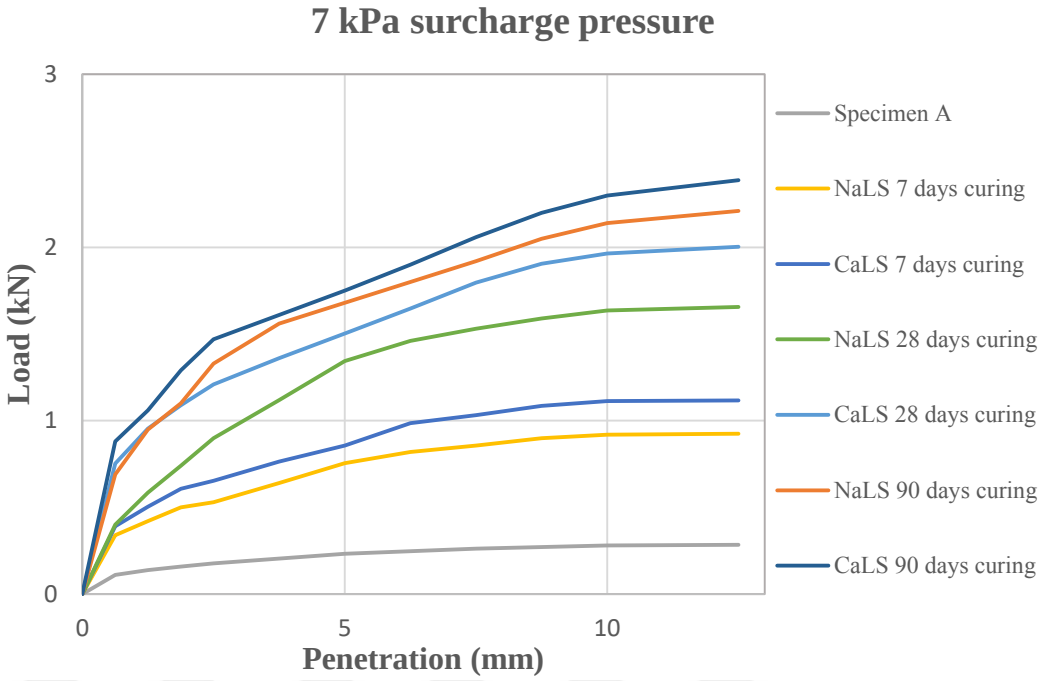

Figure 6.27 The curves of the load-penetration of the treated specimens under 7 kPa surcharge pressure after the soaked CBR test

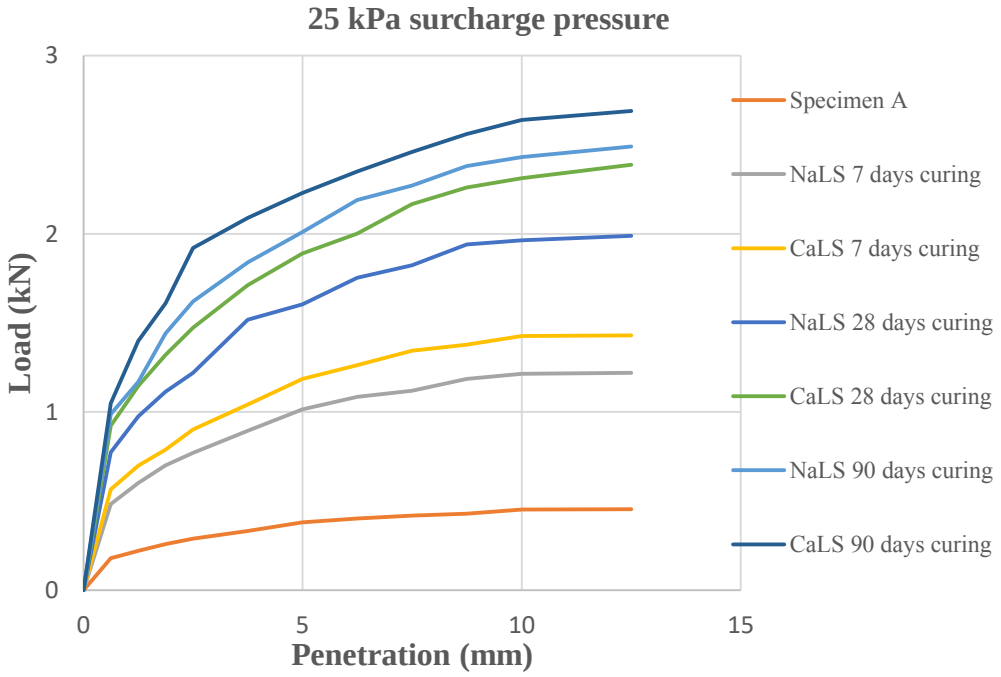

Figure 6.28 The curves of the load-penetration of the treated specimens under 25 kPa surcharge pressure after the soaked CBR test

There is an apparent influence of the lignosulfonate lime column stabilization method when the investigation of each load-penetration curve is obtained from the soaked CBR tests done in this step. Moreover, the plunger load at any penetration is greater in all cases of the treated specimens as compared to the untreated specimen. Besides, this plunger load for the same type of treated soils increases with the curing period. Finally, the plunger load obtained from the treated specimens with CaLS is more than the load measured from the treated specimens with NaLS.

From the load-penetration curves obtained from both untreated and treated specimens, the CBR values of them are calculated to the loads read at 2.50 mm and 5.00 penetration. The CBR value corresponding to 5.00 mm penetration was lower than that obtained for 2.50 mm penetration. Therefore CBR values of them are taken into account by concerning the load at 2.50 mm penetration.

The CBR values of treated specimens, which are calculated from the soaked CBR tests, are given in Figures 6.29-6.30.

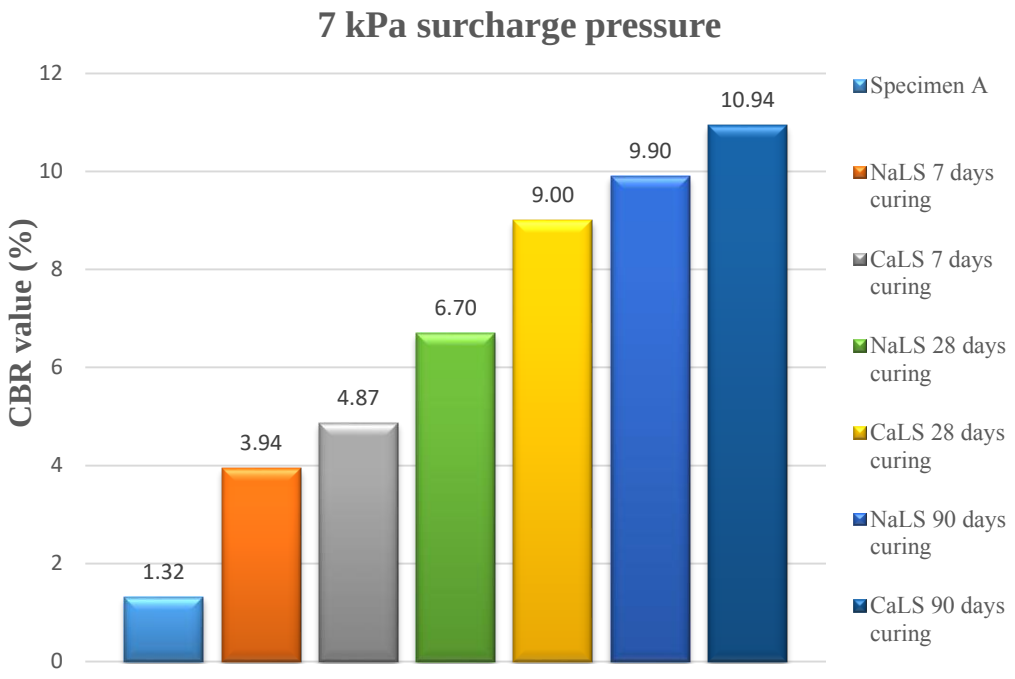

Figure 6.29 The soaked CBR values for treated specimens under 7 kPa surcharge pressure

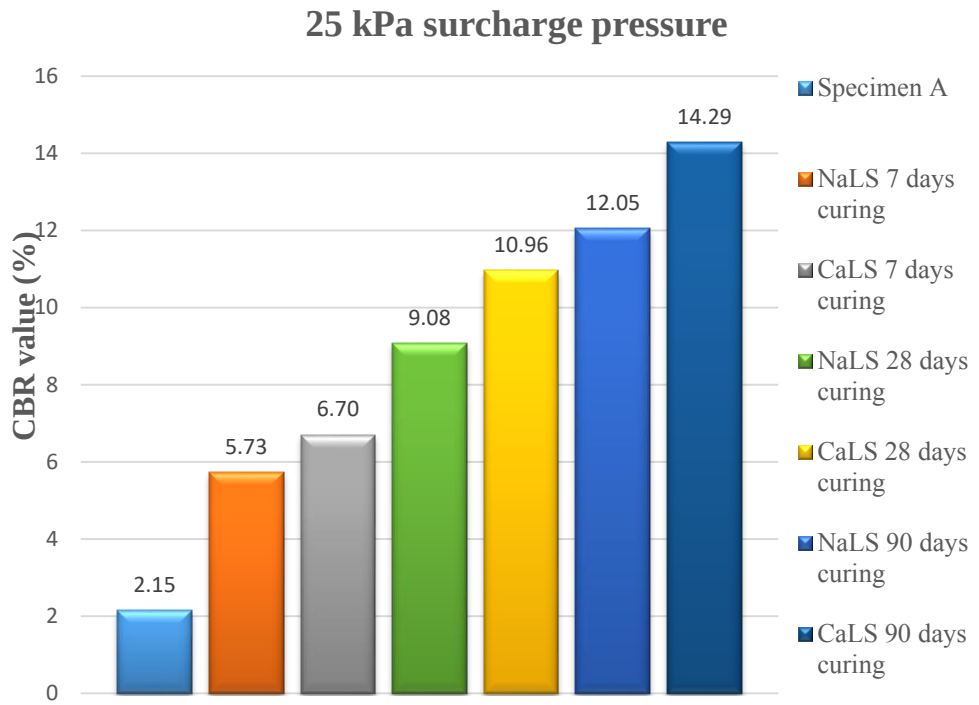

Figure 6.30 The soaked CBR values for treated specimens under 25 kPa surcharge pressure

The main goal of the CBR test done in this study is that;

- The CBR value of the treated specimen utilized as subgrade material should be either equal to or greater than 20% according to HTS (2013).
- The rating of the subgrade material that has either equal to or greater than 10% is fair-good. It means that this soil can be used as a subgrade material (Schaefer et al., 2008).

The test results of the treated specimens waited in the humid room for 90 days are evaluated to be able to reach the goals mentioned above. Table 6.15 is related to the evaluation of the treated specimens in regards to both HTS (2013) and Schaefer et al. (2008).

Table 6.15 The evaluation of the treated specimens in regards to both HTS (2013) and Schaefer et al. (2008)

Specimens	Surcharge pressure (kPa)	Curing period (days)	CBR (%)	HTS (2013)	Schaefer et al. (2008)
NaLS	7	7	3.94	Unsuitable	Unsuitable
NaLS	7	28	6.70	Unsuitable	Unsuitable
NaLS	7	90	9.90	Unsuitable	Unsuitable
NaLS	25	7	5.73	Unsuitable	Unsuitable
NaLS	25	28	9.08	Unsuitable	Unsuitable
NaLS	25	90	12.05	Unsuitable	Suitable
CaLS	7	7	4.87	Unsuitable	Unsuitable
CaLS	7	28	9.00	Unsuitable	Unsuitable
CaLS	7	90	10.94	Unsuitable	Suitable
CaLS	25	7	6.70	Unsuitable	Unsuitable
CaLS	25	28	10.96	Unsuitable	Suitable
CaLS	25	90	14.29	Unsuitable	Suitable

6.2.5 Physical Properties

The change of both specific surface area and cation exchange capacity of treated specimens has been observed by using methylene blue tests. The final readings of the methylene blue tests done in this study are given in Table 6.16.

Final readings of treated specimens are lower than the final reading of Specimen A. Then, both cation exchange capacity and the specific surface of treated specimens are calculated with respect to these final readings for each treated specimen.

Table 6.16 Test specimens and final readings of methylene blue test done in this step

Specimens	*Final reading (cc)*
Specimen A	180
COR2-NaLS 90 Days	125
COR4-NaLS 90 Days	150
COR6-NaLS 90 Days	165
COR2-CaLS 90 Days	110
COR4-CaLS 90 Days	140
COR6-CaLS 90 Days	150

Table 6.17 shows the values of these properties of the treated specimens tested in this step.

Table 6.17 The microchemical properties of both untreated and treated specimen used in this study

Specimens	*Final reading (cc)*	*Methylene Blue value (g/100g)*	*Cation exchange capacity (meq/100g)*	*Specific surface (m^2/g)*
Specimen A	180	6	18.75	146.73
COR2-NaLS 90 Days	125	4.167	13.02	101.89
COR4-NaLS 90 Days	150	5	15.625	122.28
COR6-NaLS 90 Days	165	5.5	17.188	134.50
COR2-CaLS 90 Days	110	3.667	11.458	89.67
COR4-CaLS 90 Days	140	4.667	14.583	114.12
COR6-CaLS 90 Days	150	5	15.625	122.28

Some important properties, which are blue value, cation exchange capacity, and specific surface area of stabilized soil specimens, are determined according to the final readings of the methylene blue tests done in this study. All properties of stabilized soil specimens are lower than the unstabilized soil specimen. Since, the lignosulfonate lime particles have diffused into Specimen A for curing periods applied. The clay particles

have converted from parallel structure to edge-to-face structure after the flocculation process. Thus, both specific surface area and cation exchange capacity have reduced during the stabilization process.

6.3 SEM-EDX analysis

The alteration of microstructure and microchemical of the particles in the treated specimen with both lime columns and lignosulfonate lime columns are followed during the curing period applied in this study to understand the effect of these methods on the untreated specimen.

Specimen A and treated specimens with both lime columns and lignosulfonate lime columns were used for SEM-EDX analysis in this study. Thus, this part of this study is divided into two groups that are SEM analysis and EDX analysis.

6.3.1 SEM Analysis

Specimen A prepared in the laboratory consists of kaolinite (85%) and bentonite (15%). Thus, the main part of this specimen is kaolinite. The shape of the kaolinite crystal is thin plate-like particles (Figure 6.31). The SEM image of the specimen treated with lime columns that has waited in the humid room for 28 days (Figure 6.32)

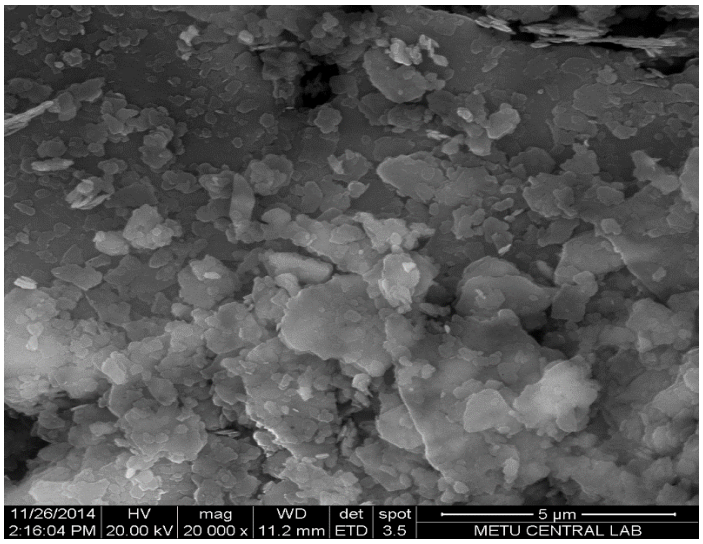

Figure 6.31 SEM image of Specimen A

(magnification factor=20000)

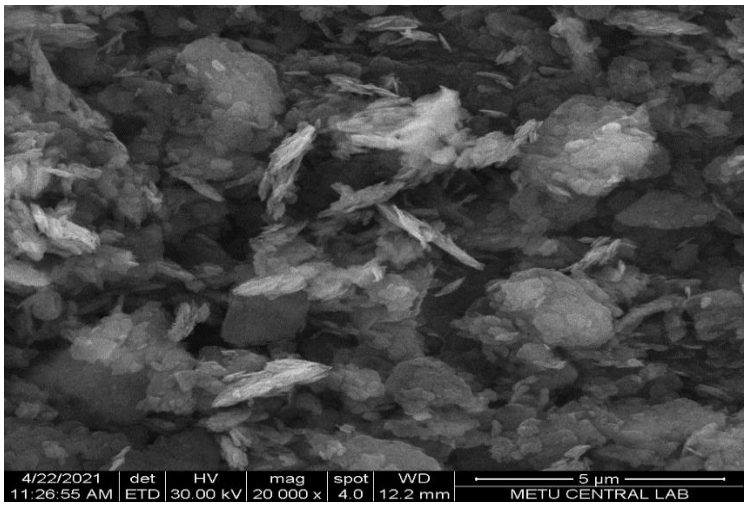

Figure 6.32 SEM image of LC (30%) 28 days curing

(magnification factor=20000)

When Figures 6.31-6.32 are examined in detail, the connection between the clay particles sheets is face to face (Figure 6.31). Then, the structure of Specimen A has changed by stabilizing with lime columns for 28 days curing period. After the reactions between the lime and Specimen A have occurred for this period, the clay particles sheets connected with each other by edge to face orientation (i.e. flocculated structure). Thus, the texture of Specimen A has been significantly modified by stabilizing with lime columns.

Figure 6.33 shows the SEM image of the specimen with lime columns that have waited in the humid room for 180 days curing period.

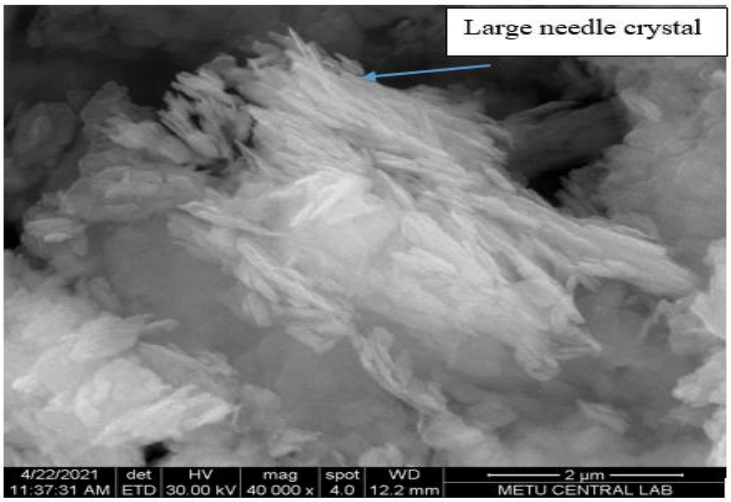

Figure 6.33 SEM image of LC (30%) 180 days curing

(magnification factor=40000)

Highly expansive crystalline ettringite mineral occurred during the lime columns stabilization method in this study after 28 days curing period when the observation of the SEM image of the treated specimen with lime columns that have waited in the humid room for 180 days is done. This mineral is a trouble material that causes the increase of the swelling potential of the treated specimen. Under 7 kPa surcharge pressure, the swelling potential of the specimen treated with lime columns for 28 days was determined at 13.95%. If this specimen has waited in the humid room for 180 days, the swelling potential of this specimen rises 15.89%.

The swelling potentials of the treated specimens used for SEM analysis are given in terms of both surcharge pressures and the curing period in Table 6.18.

Table 6.18 The swelling potentials of the treated specimens used for SEM analysis

Specimens	Swelling potential (%) under 7 kPa surcharge pressure			Swelling potential (%) under 25 kPa surcharge pressure		
	Without curing	28 days curing	180 days curing	Without curing	28 days curing	180 days curing
LC	35	13.95	15.89	23.1	9.17	10.35
NaLS	27.37	7.89	2.37	16.32	4.26	0.53
CaLS	26.32	7.11	1.84	15.26	3.16	0.32

Due to the formation of the ettringite mineral, the decrease of the swelling potential of the treated specimen with lime columns has stopped after 28 days curing period. However, the swelling potentials of the treated specimens with both types of lignosulfonate lime columns in this study have diminished with the curing period. For this reason, SEM images of the treated specimen with both sodium (NaLS) and calcium lignosulfonate (CaLS) lime columns that have waited in the humid room for 180 days are illustrated in Figures 6.34-6.35, respectively.

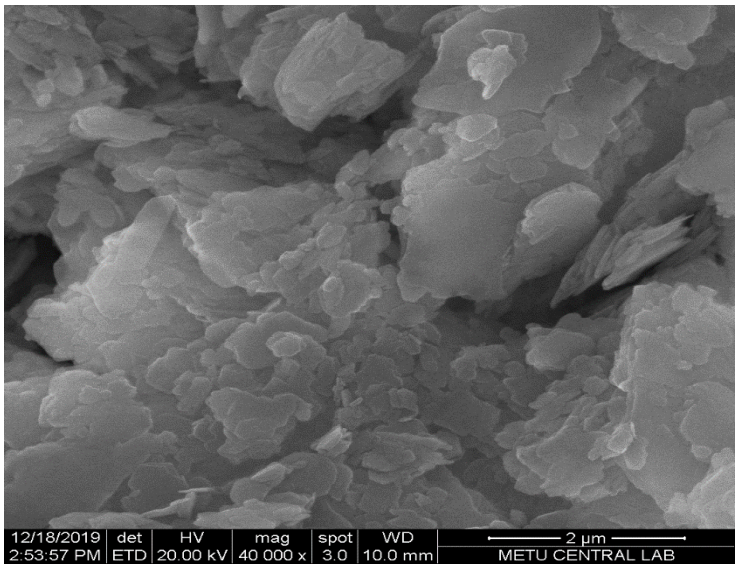

Figure 6.34 SEM image of NaLS (30%) 180 days curing

(magnification factor=40000)

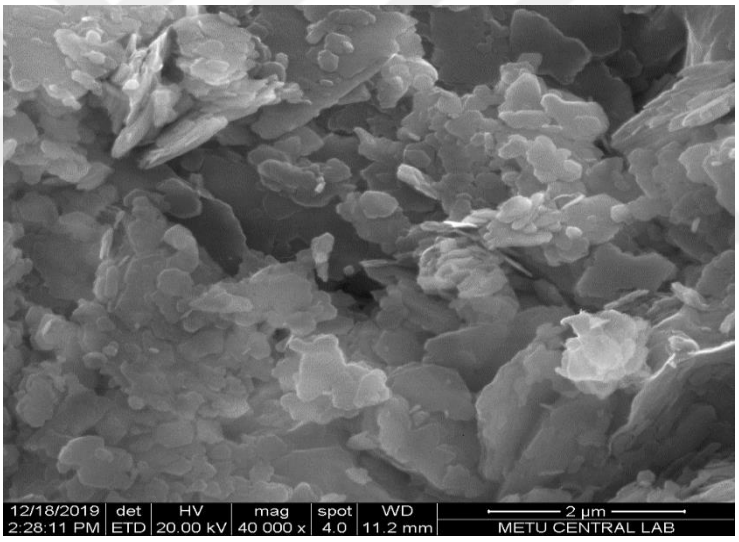

Figure 6.35 SEM image of CaLS (30%) 180 days curing

(magnification factor=40000)

When Figures 6.13-6.14 are examined in detail, SEM images in these figures consist of a high number of small particles. These particles have resulted from the reaction between the clay-lime during the lignosulfonate lime column stabilizations. In addition to this, there is no ettringite mineral in these figures. In conclusion, the addition of the lignosulfonate to lime columns both blocks the formation of the ettringite mineral and accelerates the decrease of the swelling potential of treated specimens in this study.

6.3.2 EDX Analysis

Energy Dispersive X-ray (EDX) analysis is utilized for the chemical characterization of the specimen. This analysis is a technique that determines the compositions of the elements in any material. This analysis may be done during the SEM analysis.

EDX analysis in this study was done for specimens that are given in Table 6.19. EDX diagrams of the treated specimens utilized in this study are given in Appendix G.

Table 6.19 Specimens are used for EDX analysis in this study

Specimens	Curing period (days)
Specimen A	0
LC (30%)	180
NaLS	180
CaLS	180

Table 6.20 shows the microchemical compositions of test specimens obtained from EDX analysis.

Table 6.20 The microchemical compositions of test specimens obtained from EDX analysis

Elements	The weight percentage of the test specimens (%)			
	Specimen A	LC 180 days curing	NaLS 180 days curing	CaLS 180 days curing
Al	15.57	18.25	16.91	18.27
Si	19.39	25.02	27.59	20.81
O	48.68	51.70	45.95	49.69
Ca	0.39	1.60	1.81	3.63
Na	-	0.25	0.94	0.52

As Al, Si, and O are the main elements of Specimen A, they form the major part of this specimen. The weight percentages of these elements change during the stabilization process applied in this study.

Ca ions have diffused into Specimen A during the stabilizations of both lime column and lignosulfonate lime column. The weight percentage of this ion has increased during the curing period. Besides, Na ions have diffused during the NaLS stabilizations method. Thus, the weight percentage of this ion has increased with the curing period.

6.3.2.1 The Diffusion Calculation of Both Ca and CO_3 Ions

The diffusion calculation of both Ca and CO_3 ions is made by using the equation that is based on Fick's first law. The slaked lime ($CaCO_3$) includes Ca^{+2} and $CO_3{}^{-2}$, the diffusion coefficient of these ions are given in Table 6.21.

Table 6.21 The diffusion coefficient of the ions of the slaked lime

Ions	Type	Molecular Diffusion Coefficient, D^0
Ca^{+2}	Cation	$0.793 * 10^{-9}\ m^2/s$
$CO_3{}^{-2}$	Anion	$0.955 * 10^{-9}\ m^2/s$

The concentration at the midpoint placed between the columns is calculated below (Eq. 6.1).

$$\frac{C(x,t)}{C_0} = erfc\left(\frac{x}{2\sqrt{D_L^* * t}}\right) \qquad \text{(Eq. 6.1)}$$

Where x (m) is the distance of the Diffussion, t is the time (second).

The parameters of this equation are determined for the treated specimen which had 37 pieces of calcium lignosulfonate lime columns (Figure 6.36).

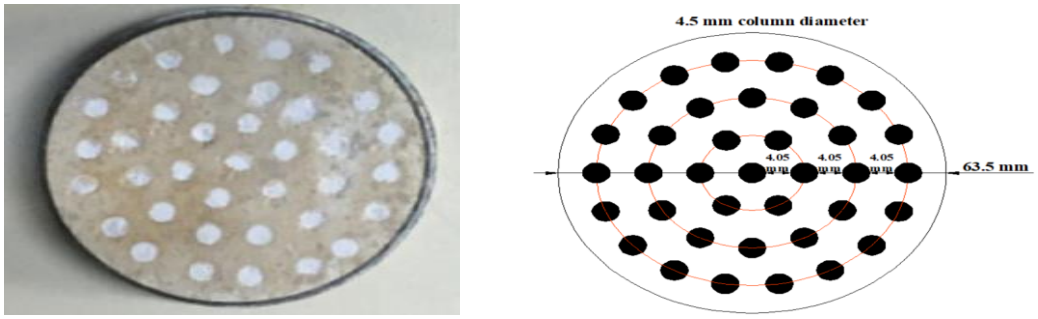

Figure 6.36 The top view of the treated specimens consists of thirty-seven calcium lignosulfonate lime columns

The diameter of the columns and distance between the columns are 4.5 mm and 4.05 mm, respectively. The diffusion distance of the ions is the half of the distance between the columns that is 2.025 mm.

D^0 is the free solution diffusion coefficient that is no soil present. The effective diffusion coefficient (D^*)is related to the molecular diffusion coefficient D^0 [m^2/s] by the following relation (Eq. 6.2):

$$D^* = \omega D^0 \qquad (Eq. 6.2)$$

Freeze and Cherry (1979) suggest values between 0.5 and 0.01 for different geomaterials. As the value of ω for Specimen A is not known, the value of ω is firstly tried to found for Specimen A.

The improvement percentages of treated specimens with calcium lignosulfonate lime columns are used as the rate of the concentration to determine the value of ω for Specimen A prepared in this study (Figure 6.37).

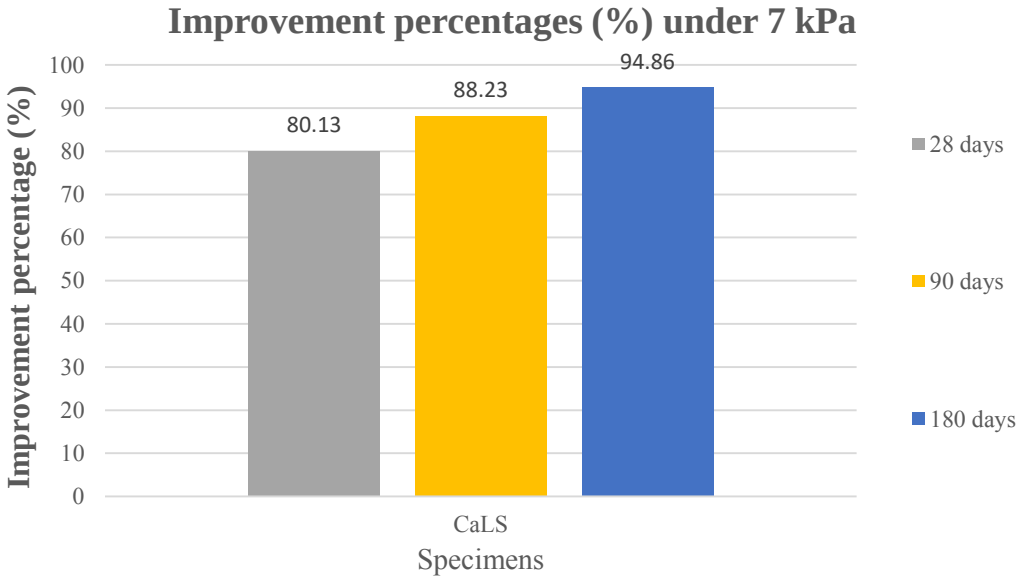

Figure 6.37 The improvement percentages of treated specimens with calcium lignosulfonate lime columns

The other parameters related to the concentrations equation are given in Table 6.22. The unknown value of this equation is ω. For this reason, Eq. 1 is solved to determine the value of the ω. The solution of concentration equation is presented in Table 6.23.

According to literature, the value of the ω should be between the 0.01-0.5 for geomaterials. The value of the ω is calculated between the 0.015-0.040 (Figure 6.38).

Table 6.22 The parameters of the concentration equations

Specimens	Improvement percentages (%)	C/C_0	Time (second)
CaLS 28 days curing	80.13	0.8013	2419200
CaLS 90 days curing	88.23	0.8823	7776000
CaLS 180 days curing	94.86	0.9486	15552000

Table 6.23 The solution of concentration equation

Specimens	$\frac{C(x,t)}{C_0}$	$D^*\left(\frac{m^2}{s}\right)$	$D^0{}_{Ca^{+2}}\left(\frac{m^2}{s}\right)$	ω
CaLS 28 days curing	(0.002025, 2419200)= 0.8013	$1.203 * 10^{-11}$	$0.793 * 10^{-9}$	0.015
CaLS 90 days curing	(0.002025, 7776000)= 0.8823	$1.339 * 10^{-11}$	$0.793 * 10^{-9}$	0.017
CaLS 180 days curing	(0.002025, 15552000)= 0.9486	$2.648 * 10^{-11}$	$0.793 * 10^{-9}$	0.033

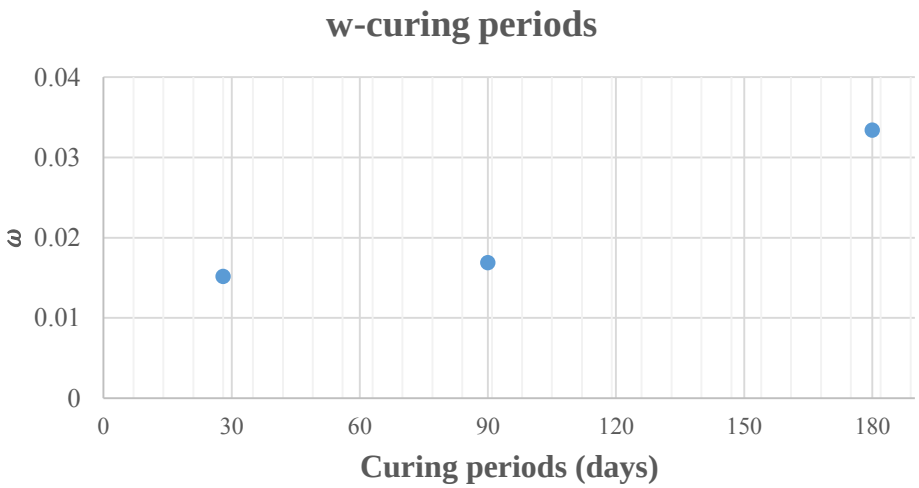

Figure 6.38 The graph of the ω versus curing periods

This graph is used for the determination of the value of the ω for Specimen A. The value of the ω is assumed as 0.025 with respect to this graph.

After the value of the ω is determined, the EDX analysis of this study is evaluated according to these parameters.

$$D^*_{Ca^{+2}} = \omega D^0 = 0.025 * 0.793 * 10^{-9} = 1.983 * 10^{-11}\, m^2/s$$

$$D^*_{CO_3{}^{-2}} = \omega D^0 = 0.025 * 0.955 * 10^{-9} = 2.388 * 10^{-11}\, m^2/s$$

The treated specimen prepared for SEM-EDX analysis in this study consists of seven columns had 9 mm diameter. The distance between the columns is 0.9D (equal to 8.1 mm). x is equal to 0.45D (equal to 4.05 mm).

The concentration of the midpoint placed between the columns is calculated below.

For Ca^{+2} ions;

$$C_{Ca^{+2}}(4.05\ mm, 180\ days) = C_0 \left[erfc\left(\frac{4.05 * 10^{-3}}{2\sqrt{1.983 * 10^{-11} * 180 * 24 * 60 * 60}}\right)\right]$$

$$C_{Ca^{+2}}(4.05\ mm, 180\ days) = C_0[erfc(0.115)]$$

$$C_{Ca^{+2}}(4.05\ mm, 180\ days) = C_0 * 0.870$$

For CO_3^{-2} ions;

$$C_{CO_3^{-2}}(4.05\ mm, 180\ days) = C_0 \left[erfc\left(\frac{4.05 * 10^{-3}}{2\sqrt{2.388 * 10^{-11} * 180 * 24 * 60 * 60}}\right)\right]$$

$$C_{CO_3^{-2}}(4.05\ mm, 180\ days) = C_0[erfc(0.151)]$$

$$C_{CO_3^{-2}}(4.05\ mm, 180\ days) = C_0 * 0.881$$

The results of these calculations are that the concentration of the ions of the slaked lime is approximately 87%. It means that the diffusion process in this study has almost finished at the rate of 87%.

The EDX analysis of both Specimen A and treated specimen with calcium lignosulfonate lime columns were made and the results of this analysis are given in Figures 6.39-6.40.

Specimen A is treated with calcium lignosulfonate lime columns during 180 days curing period. The weight ratio of calcium ions in Specimen A increased from 0.39% to 3.63%. The increase of the weight ratio of the calcium ions in Specimen A is approximately 9.3 times.

The lignosulfonate added to lime columns causes to speed up the diffusion velocity of these ions. In conclusion, the lime particles covered with lignosulfonate have diffused faster than the lime particles.

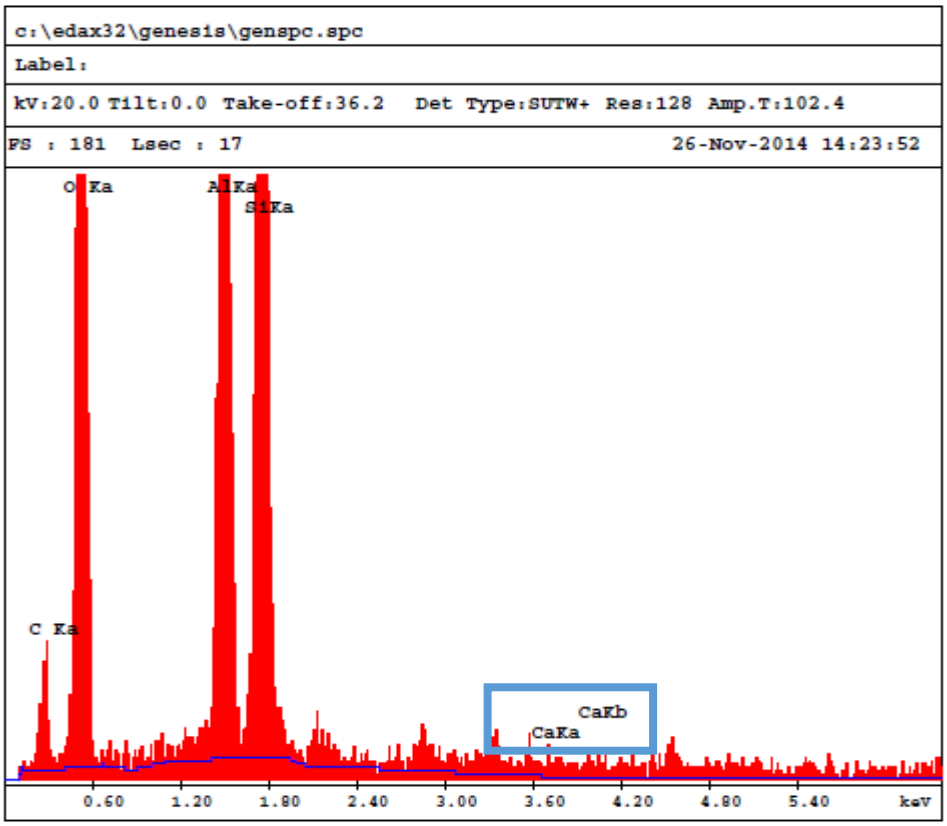

EDAX ZAF Quantification (Standardless)
Element Normalized
SEC Table : Default

Element	Wt %	At %	K-Ratio	Z	A	F
C K	15.97	23.53	0.0270	1.0334	0.1634	1.0005
O K	48.68	53.86	0.1543	1.0161	0.3119	1.0004
AlK	15.57	10.21	0.1084	0.9465	0.7307	1.0072
SiK	19.39	12.22	0.1284	0.9741	0.6796	1.0000
CaK	0.39	0.17	0.0035	0.9445	0.9493	1.0000
Total	100.00	100.00				

Element	Net Inte.	Bkgd Inte.	Inte. Error	P/B
C K	8.72	1.01	8.92	8.61
O K	130.62	1.35	2.10	96.79
AlK	130.39	3.15	2.13	41.41
SiK	143.89	3.54	2.02	40.62
CaK	2.42	0.73	19.32	3.31

Figure 6.39 The EDX analysis of Specimen A

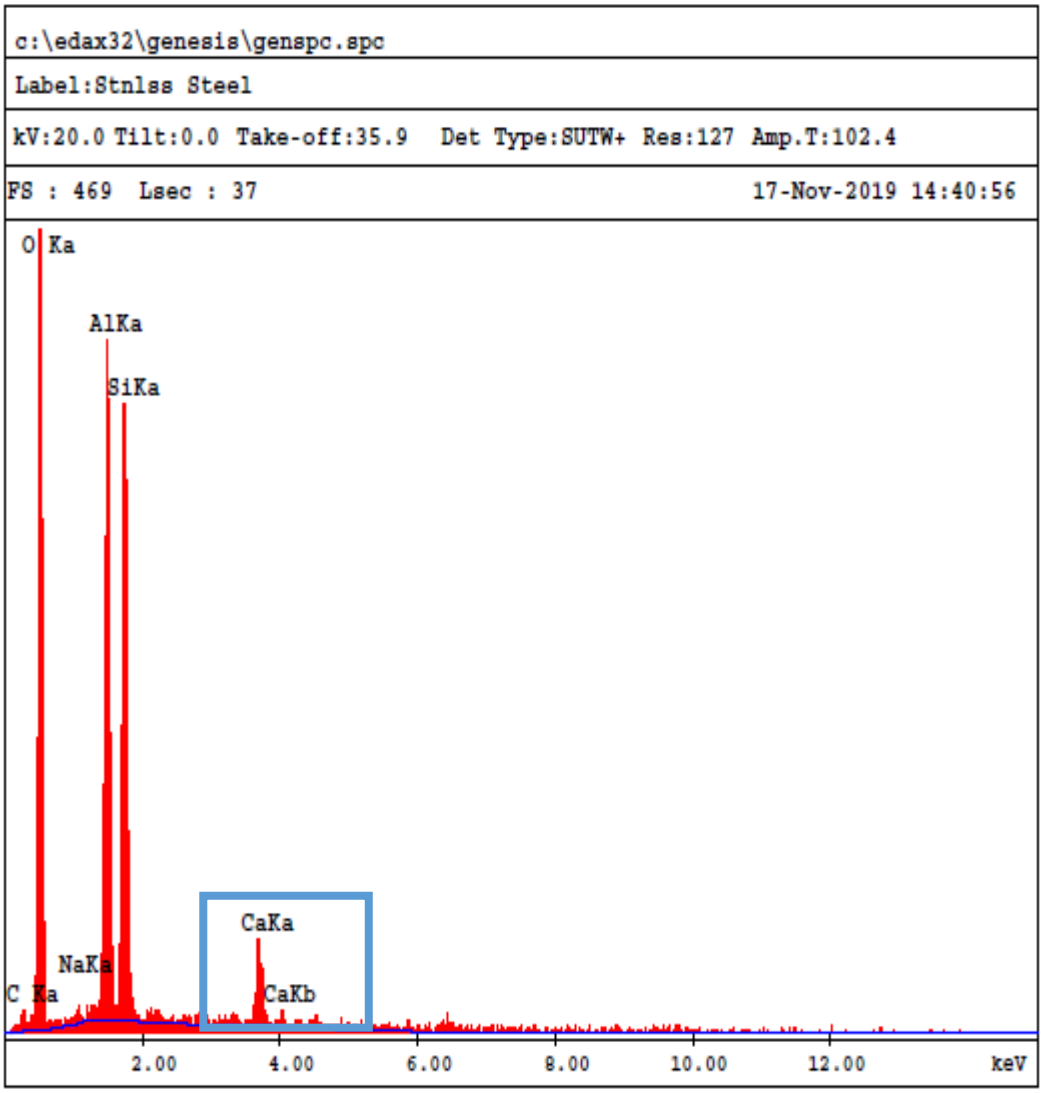

EDAX ZAF Quantification (Standardless)
Element Normalized
SEC Table : Default

Element	Wt %	At %	K-Ratio	Z	A	F
C K	7.08	11.28	0.0110	1.0401	0.1489	1.0006
O K	49.69	59.42	0.1579	1.0227	0.3105	1.0004
NaK	0.52	0.43	0.0020	0.9572	0.4112	1.0045
AlK	18.27	12.96	0.1253	0.9525	0.7144	1.0074
SiK	20.81	14.18	0.1318	0.9803	0.6455	1.0004
CaK	3.63	1.73	0.0324	0.9510	0.9380	1.0000
Total	100.00	100.00				

Figure 6.40 The EDX analysis of treated specimen with calcium lignosulfonate lime columns 180 days curing

6.4 Comparison of the Effect of Sodium Lignosulfonate and Calcium lignosulfonate Addition to the Lime Columns

There are different types of lignosulfonate in the market. In this study, two types of this material are added to the lime column to improve the effectiveness of this stabilization method on the expansive soil. These materials are sodium lignosulfonate and calcium lignosulfonate.

These materials are separated from each other in terms of their chemical compositions. The achievement of the lignosulfonate lime column stabilization method is based on the chemical reactions between the lignosulfonate lime column and expansive clay.

The chemical composition of these materials is generally similar to each other. While the basic element of sodium lignosulfonate is sodium, calcium lignosulfonate consists constitutively of calcium. These basic elements of these materials affect the chemical reactions occurred during the stabilization method. Since the sodium ion has one electrovalent, the electrovalent of the calcium ion has two.

This section of this study is related to the comparison of both sodium and calcium lignosulfonate added to lime columns. Divalent ion such as Ca^{+2} ion tends to beyond replace with respect to monovalent ion such as Na^{+1}. Since, The diffusion of the calcium lignosulfonate lime particles has rapidly occurred than the diffusion of the sodium lignosulfonate lime particles.

According to SEM-EDX analysis done in this study, both the microchemical compositions and the microstructure of treated specimen's particles with lignosulfonate lime columns have changed due to the diffusion of Ca^{+2}, Na^{+1} ions during the curing period. As a result, the expansive soil specimen has lost plasticity properties and the structures of these soil particles have flocculated. The diffusion of these ions through into the expansive soil specimen ends up with both reduction of the swelling potential and the increase of the strength of this specimen.

Ca^{+2} ions of the lignosulfonate lime particles are replaced with monovalent ions in a medium that has a high pH environment. This case results in the flocculation process that decrease the swelling potential of expansive soil. After this process, the soil specimen has higher volumetric stability and strength.

The evaluation process of the lime column method could be divided into two groups. These groups are explained below.

1- The change of the block specimen: This subject is interested in the whole specimen that consisted of expansive soil and lignosulfonate lime columns. The assessment of this subject in this study is based on the free swell test results from the whole specimen.

2- The change of the stabilized soil specimen: The change of the properties of the soil specimen placed between the lignosulfonate lime columns is a considerable parameter for the judgment of the lime column technique. Thus this issue is related to the alteration of some properties of soil specimens taken from a location between the lime columns.

6.4.1 The Change of the Swelling Potentials, CBR Swell, and CBR Values of the Stabilized Block Soil Specimens with both Sodium and Calcium Lignosulfonate Lime Columns

The block stabilized soil specimen consisted of expansive clay and lignosulfonate lime columns were tested in both free swell test and CBR test during this study. In this chapter, the results obtained from these tests are investigated and two lignosulfonate types are compared to each other.

The first part of this chapter is interested in the outputs of the free swell tests. The lignosulfonate lime column stabilization method of this study is initially focused on the small expansive soil specimens that had 63.5 mm diameter and 19 mm height. These specimens stabilized with both sodium and calcium lignosulfonate lime columns were tested to determine their swelling potentials. This part deals with the change of the swelling potentials of these stabilized soil. Finally, these stabilized soil specimens are evaluated as a whole.

These stabilized soil specimens were tested both under two different surcharge pressures and particular curing periods. According to surcharge pressures applied in these tests, the change of the swelling potentials of them are given in Figures 6.41-6.42.

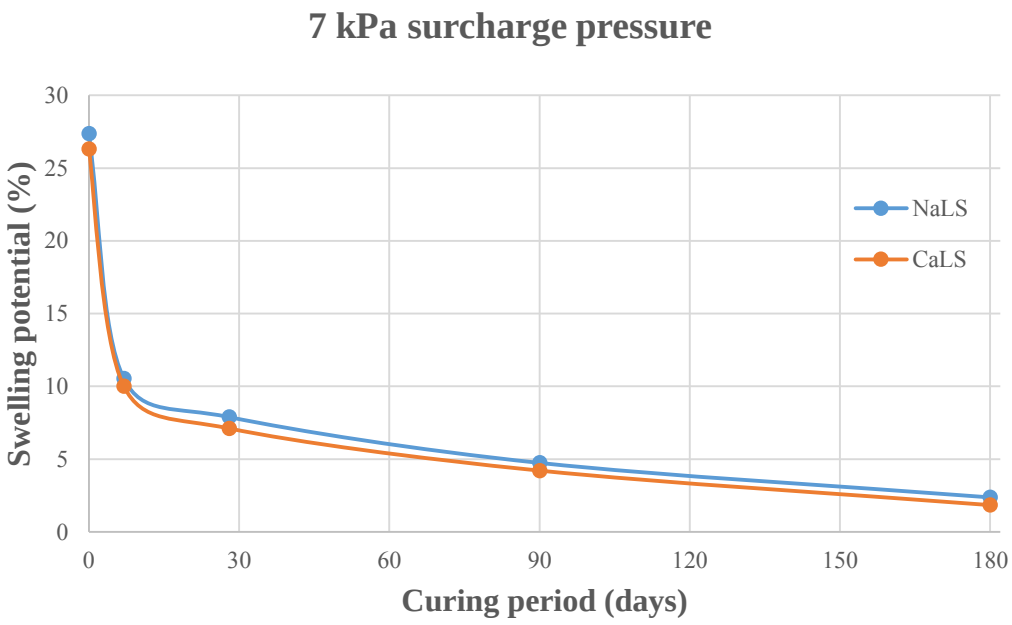

Figure 6.41 The swelling potentials of the stabilized soil specimens with both sodium and calcium lignosulfonate lime columns under 7 kPa surcharge pressure

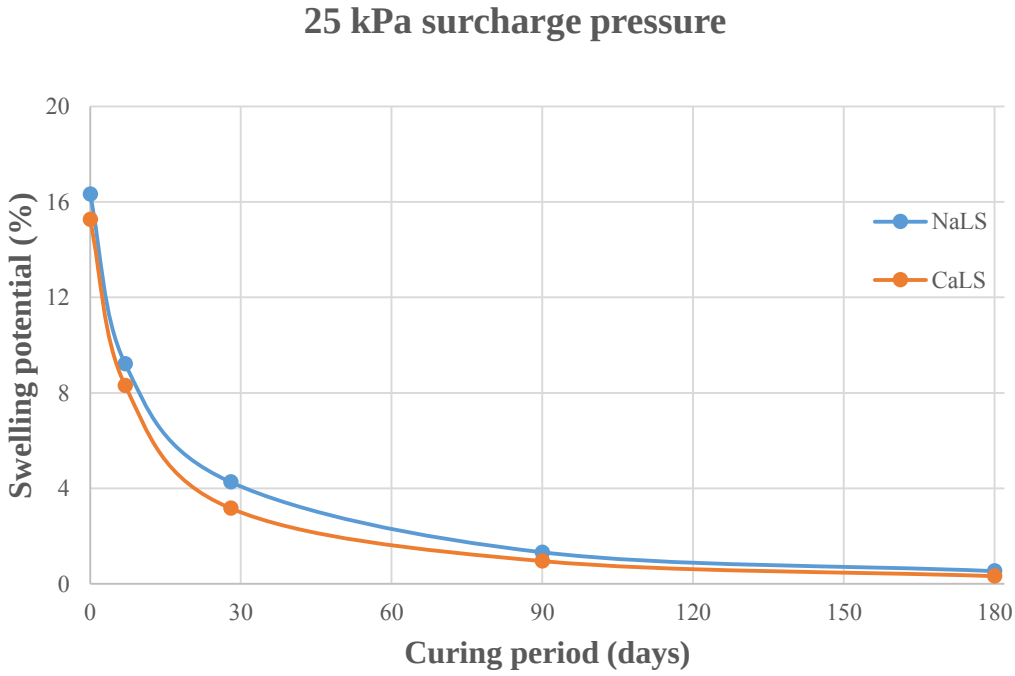

Figure 6.42 The swelling potentials of the stabilized soil specimens with both sodium and calcium lignosulfonate lime columns under 25 kPa surcharge pressure

The swelling potentials of these stabilized soil decrease with curing periods under both surcharge pressures applied in this study. The addition of these lignosulfonates to the lime column strengthens the achievement of this method. However, the CaLS specimen has a lower swelling potential than the NaLS specimen for each curing period of this study. In conclusion, calcium lignosulfonate is more suitable for the increase of the effectiveness of the lime columns on the swelling potentials of expansive soil due to the ion exchange capacity.

The CBR parameters of the stabilized soil specimen with lignosulfonate lime columns are based on the final part of this section. Figure 6.43 and Figure 6.44 show a graph that shows the relationship between the CBR swell value of stabilized soil specimens and the curing periods applied in this study.

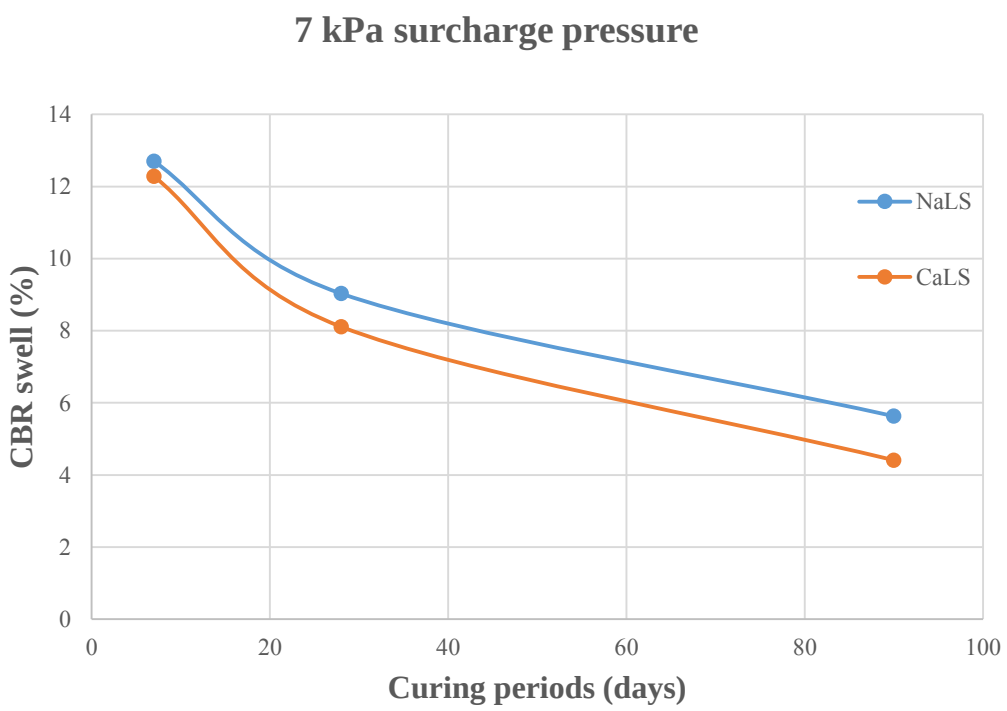

Figure 6.43 Effect of Curing Time on the CBR swell value for both NaLS and CaLS specimens under 7 kPa surcharge pressure

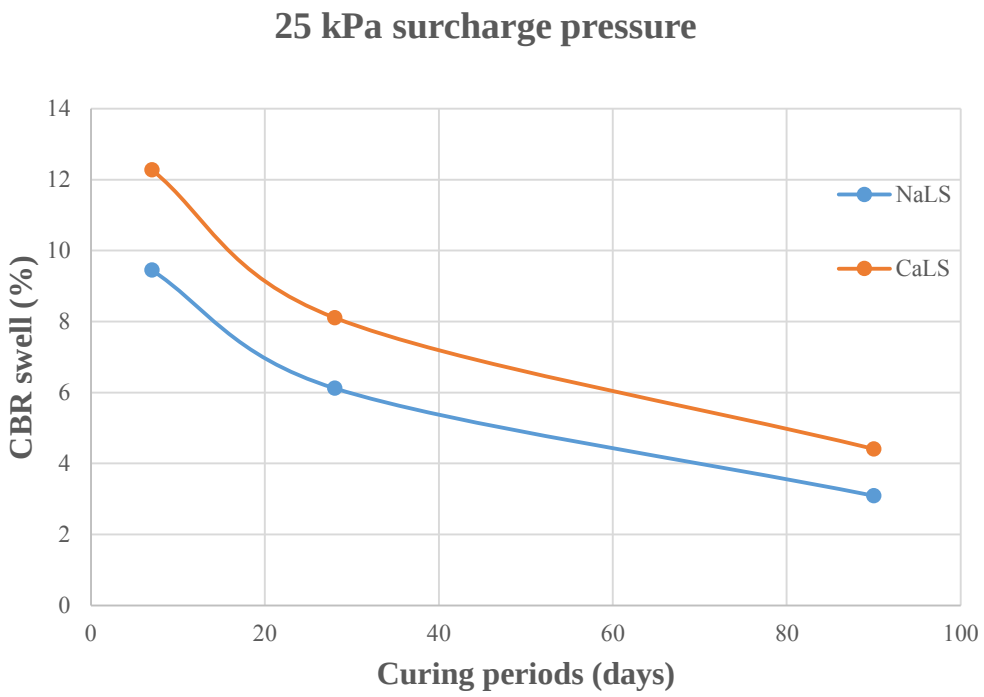

Figure 6.44 Effect of Curing Time on the CBR swell value for both NaLS and CaLS specimens under 25 kPa surcharge pressure

The treated specimens that included 61 pieces of lignosulfonate lime columns have lower swelling potential than the untreated specimen. The swelling potential of the treated specimen decreases with the curing period for each lignosulfonate lime column. The CaLS specimens have both lower swelling potential and higher CBR values than the NaLS specimens for each curing period.

The graphs related to the CBR values of these stabilized specimens and the curing periods are given in Figure 6.45- Figure 6.46. With the increase of the curing periods, the CBR values of these stabilized specimens in this study rise. In addition to this, the stabilized soil specimens with calcium lignosulfonate lime columns have higher CBR values than the stabilized soil specimens with sodium lignosulfonate lime columns.

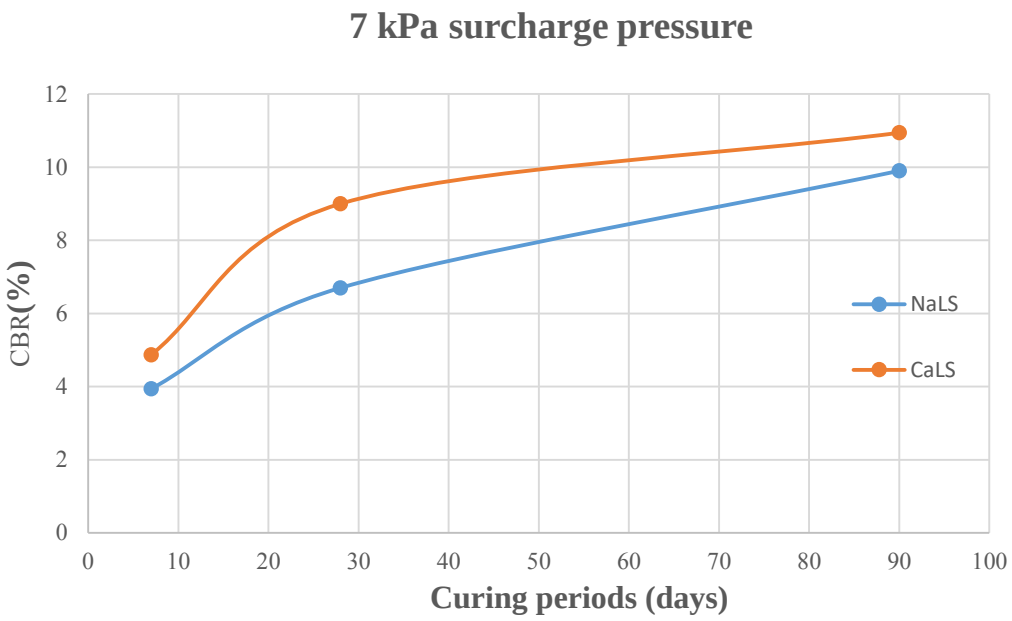

Figure 6.45 Effect of Curing Time on the CBR for both NaLS and CaLS specimens under 7 kPa surcharge pressure

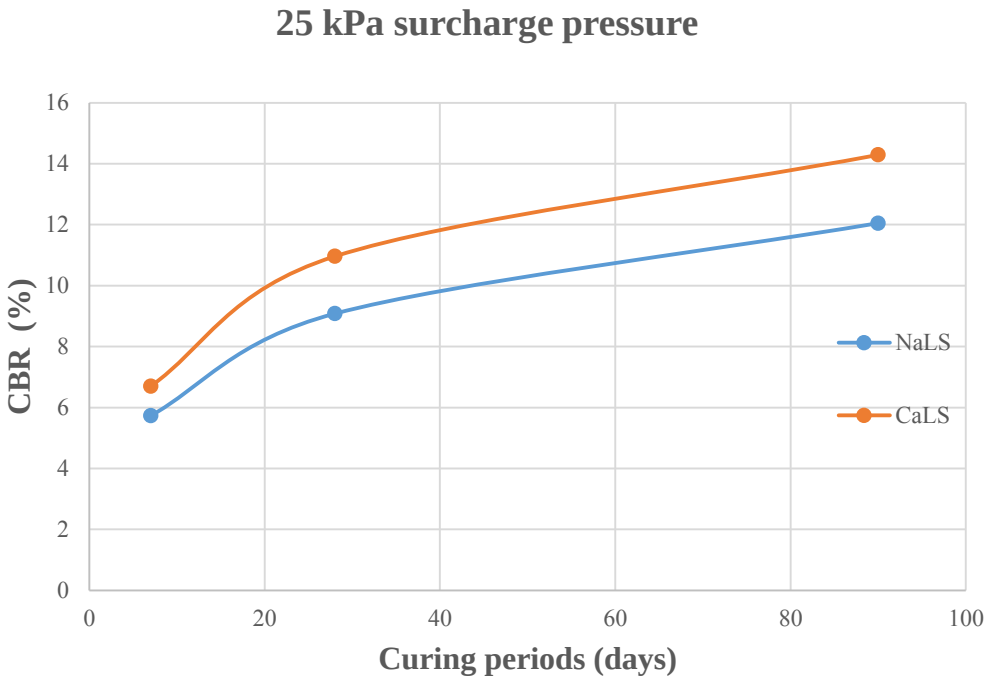

Figure 6.46 Effect of Curing Time on the CBR for both NaLS and CaLS specimens under 25 kPa surcharge pressure

6.4.2 The Change of the Unconfined Compressive Strength, Swell Potential and CBR Values of the Stabilized Soil Specimens (between the lignosulfonate lime columns)

The stabilized soil specimens were taken from a location between the lignosulfonate lime columns for the observation of the alteration of some engineering properties.

The first part is that the relationship between the unconfined compressive strengths of these stabilized specimens and curing periods. The graph of the relationship between the UCS and the curing period is given in Figure 6.47.

Figure 6.47 shows that the unconfined compressive strength of stabilized soils for treated specimens increases with curing time days. The treated specimens treated with calcium lignosulfonate lime columns have a higher unconfined compressive strength than the specimens treated with sodium lignosulfonate lime columns when an equal curing period is applied to them.

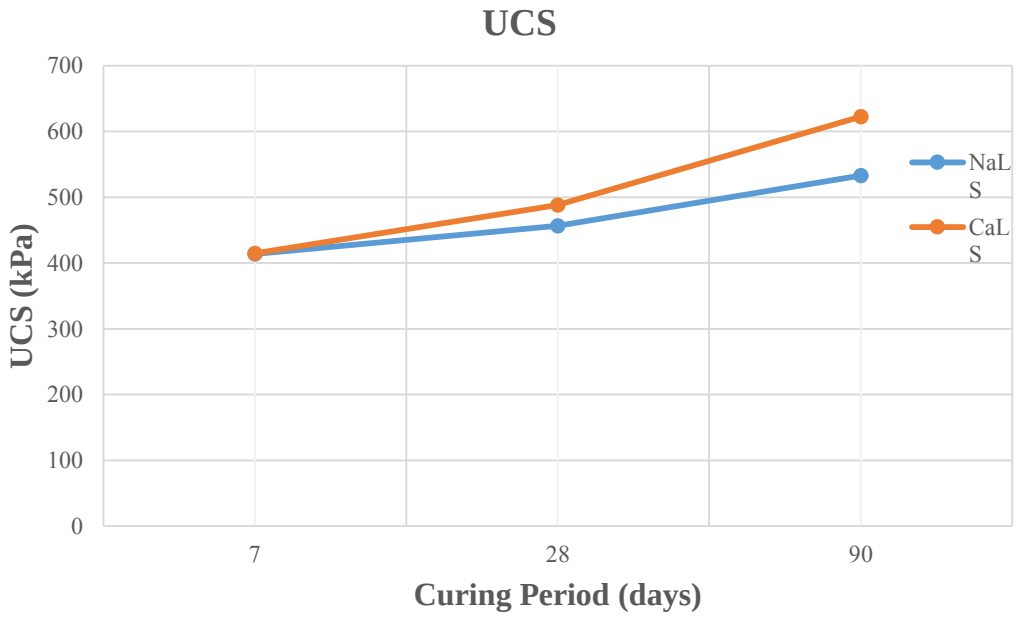

Figure 6.47 Effect of Curing Time on the UCS for specimens treated with both NaLS and CaLS lime columns

There is a fall of the swelling potentials of the stabilized specimens with curing periods applied in this study for each surcharge pressure. The swelling potentials of the stabilized soil specimens are given in Figures 6.48-6.49.

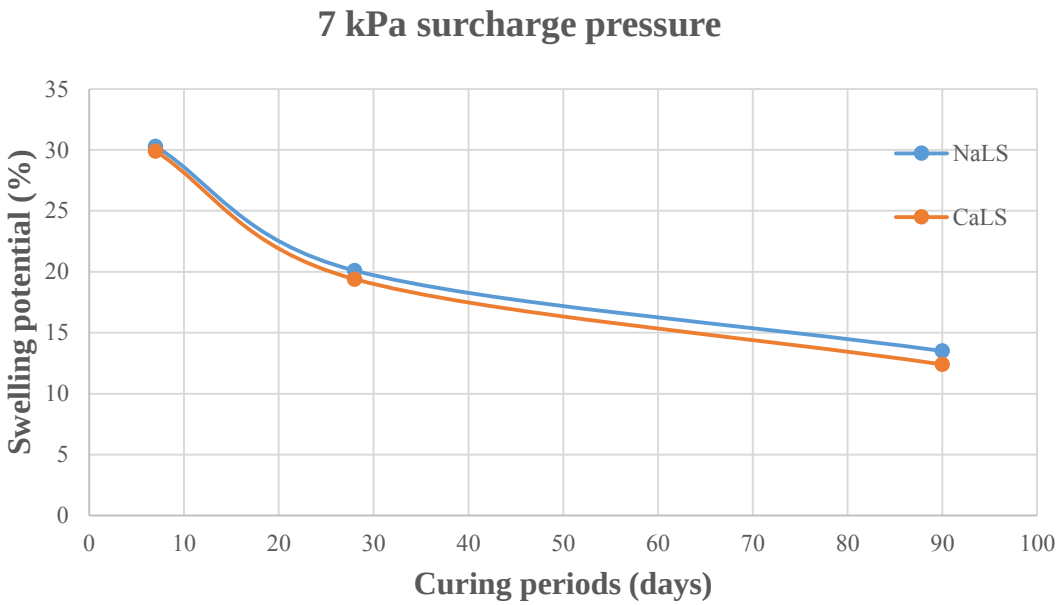

Figure 6.48 Effect of Curing Time on the swelling potential for specimens stabilized with both NaLS and CaLS lime columns under 7 kPa surcharge pressure

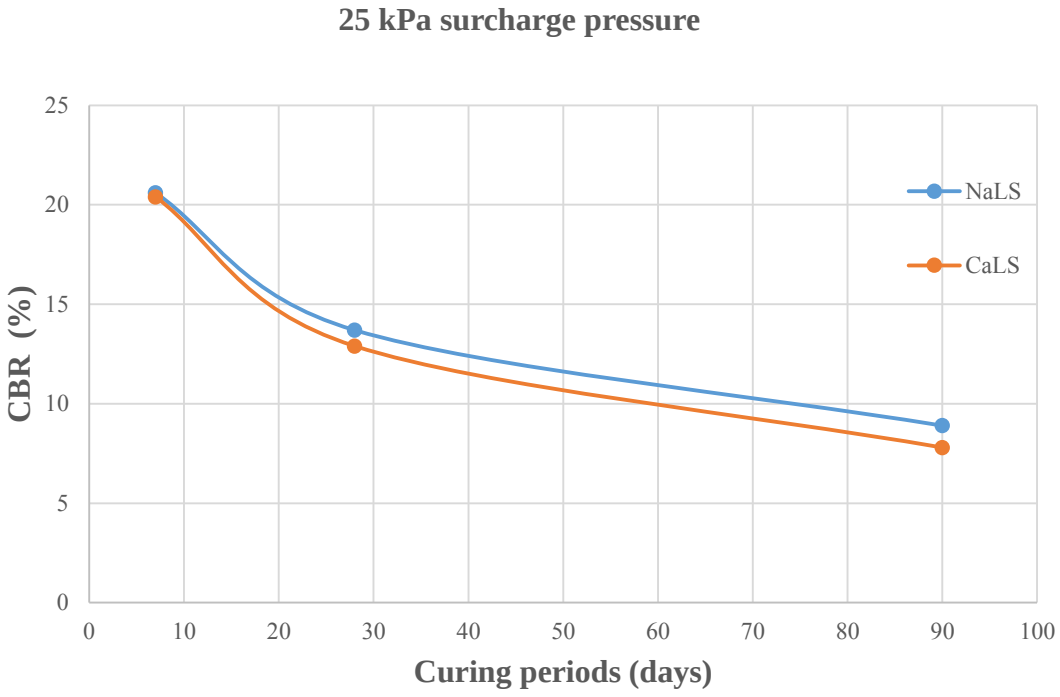

Figure 6.49 Effect of Curing Time on the swelling potential for specimens stabilized with both NaLS and CaLS lime columns under 25 kPa surcharge pressure

6.4.3 The Correlation Between The Soil Bearing Capacity (CBR) and Unconfined Compressive Strength (UCS) of Specimens

The performance of a pavement depends on the quality of the subgrade which can be measured by CBR value of subgrade. The correlation between the soil bearing capacity (CBR) under 7kPa and 25kPa pressure and unconfined compressive strength (UCS) of specimens between the NaLs and CaLS lime columns were determined (Figures 6.50-6.53). The results of the tests show that the unconfined compressive strength and CBR values increase linearly.

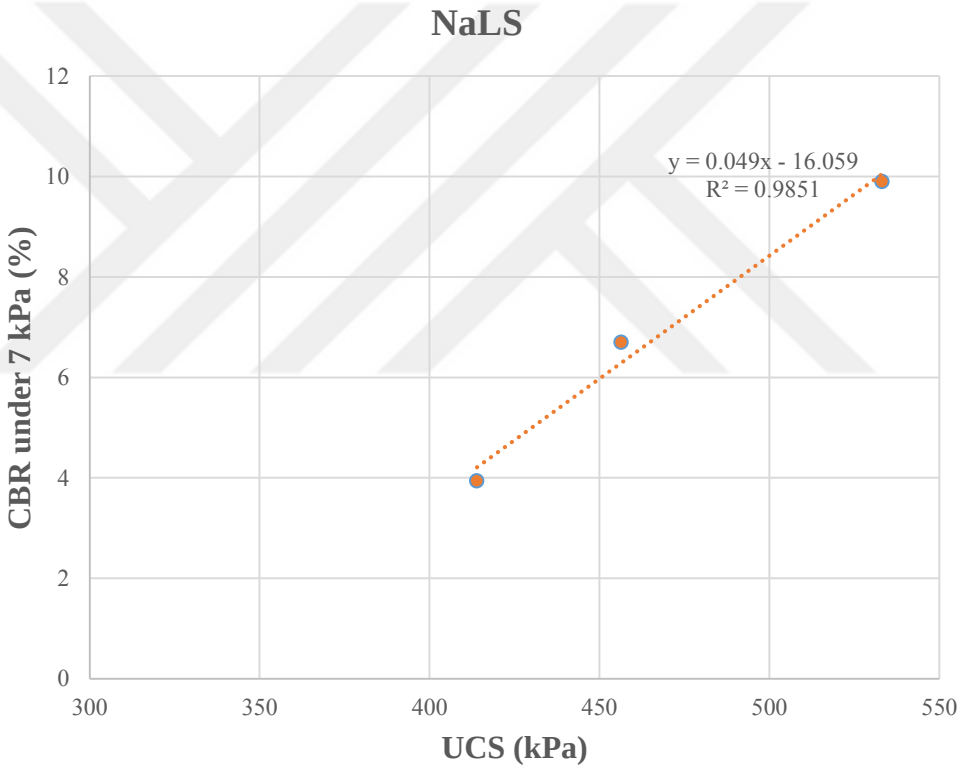

Figure 6.50 CBR test under 7 kPa pressure (NaLS)

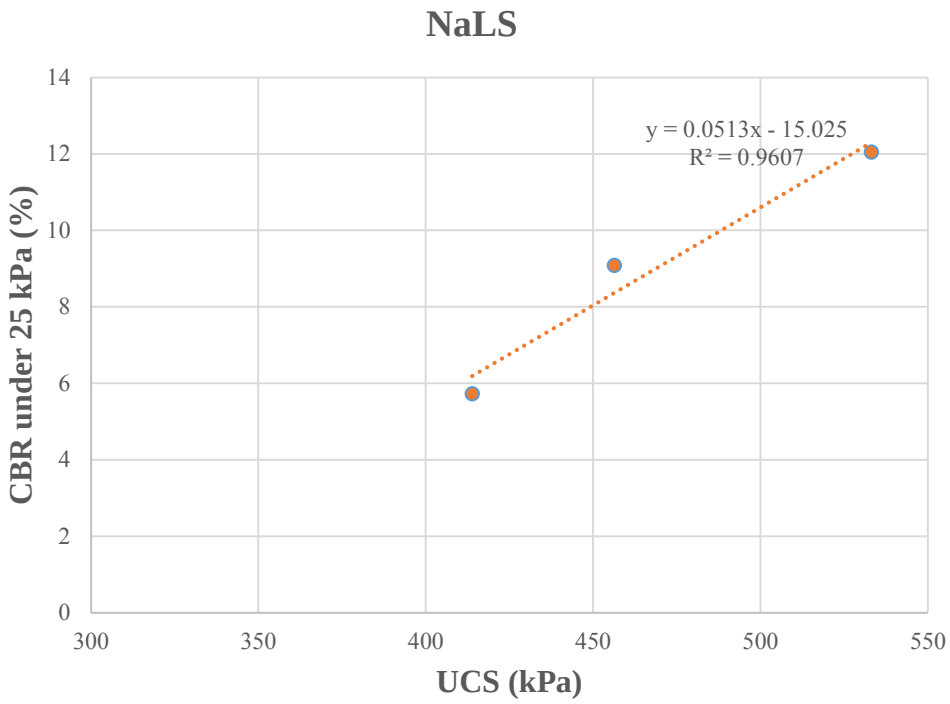

Figure 6.51 CBR test under 25 kPa pressure (NaLS)

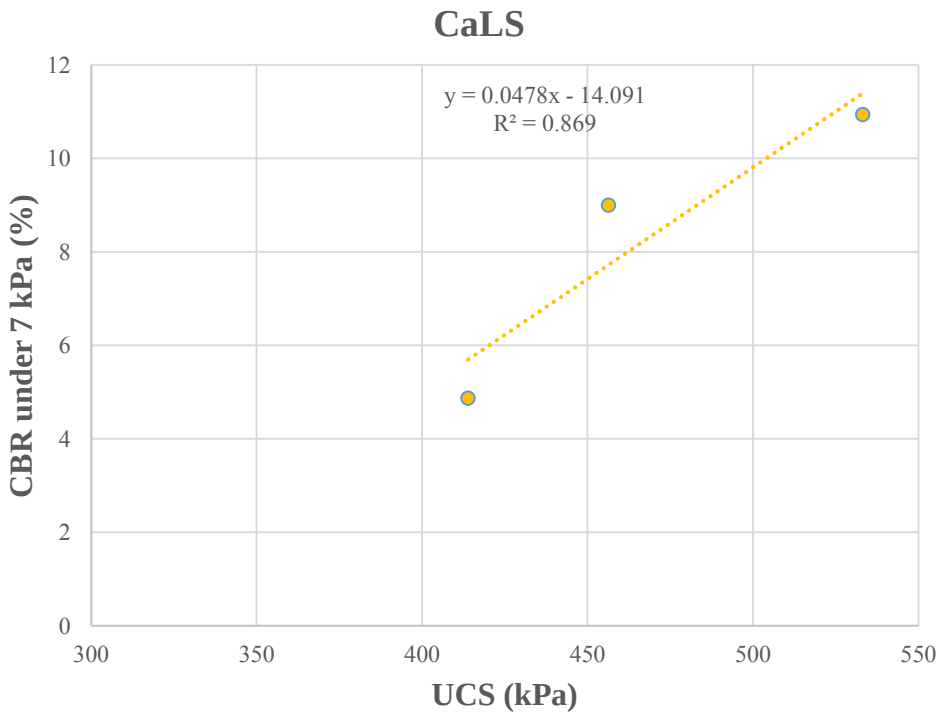

Figure 6.52 CBR test under 7 kPa pressure (CaLS)

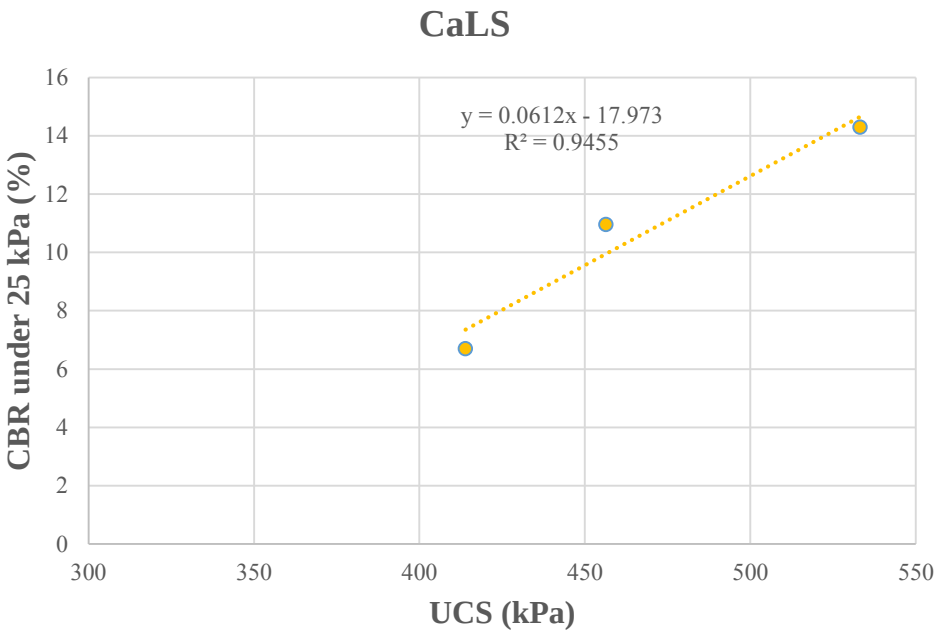

Figure 6.53 CBR test under 25 kPa pressure (CaLS)

Based on that regression analysis, R^2 value for CBR-qu correlations were found as 86.6% for CBR tests under 7kPa pressure and 92.8% for CBR tests under 25kPa pressure (Figures 6.54-6.55).

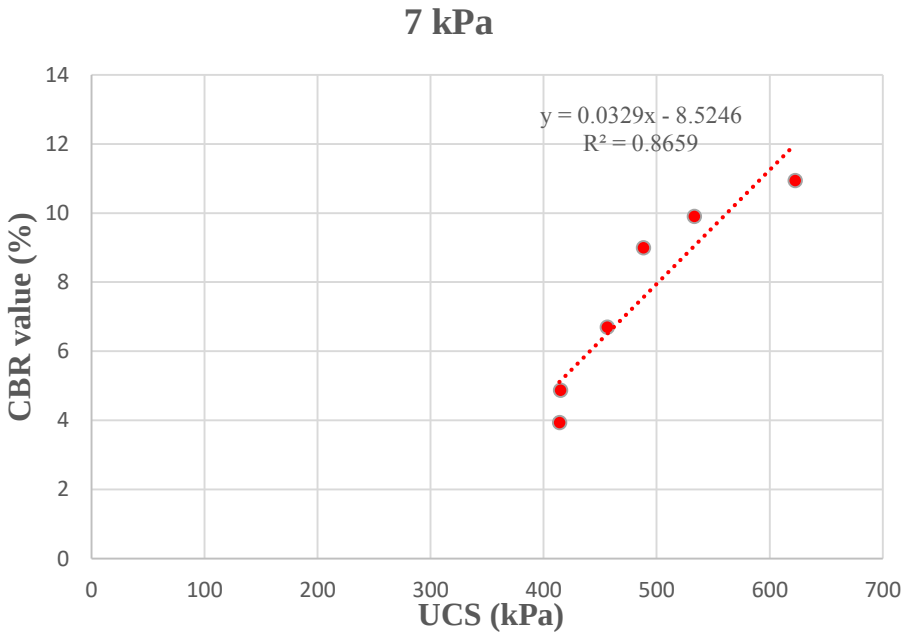

Figure 6.54 NaLS ve CaLS samples together (under 7 kPa)

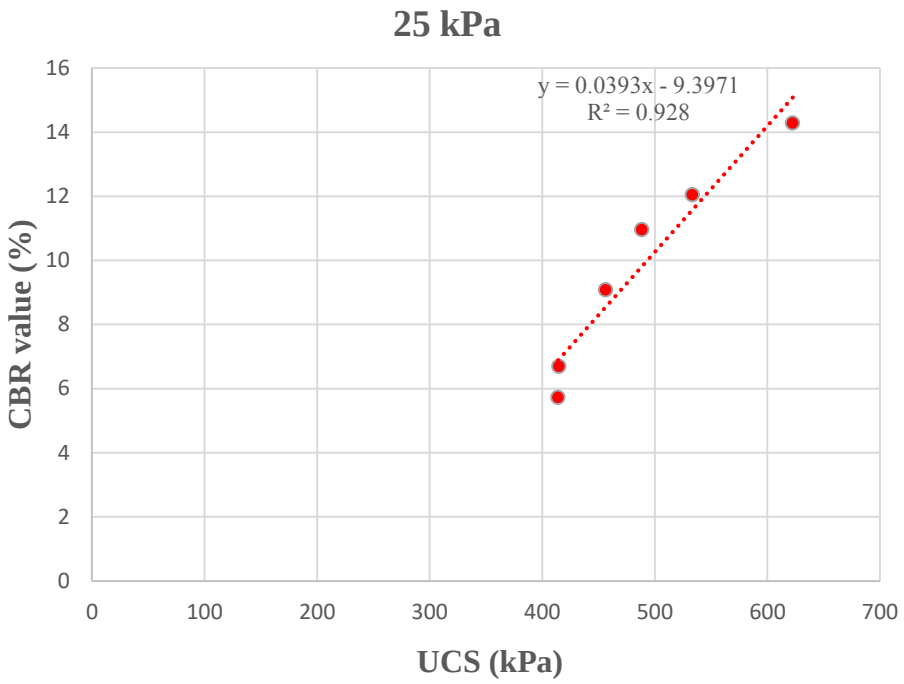

Figure 6.55 NaLS ve CaLS samples together (under 25 kPa)

6.5 Combined Improvement Method

The lignosulfonate lime column method applied in this study is useful for the stabilization of the expansive soil. However, this treatment method improves the expansive soil with a curing period that should be a minimum of 180 days in this study to be able to reach the goals of this study. Thus, the combined improvement method (CIM) has been applied to shorten this period.

The experimental works that related to the treated specimens with CIM are listed below;

- Free swell test on the oedometer ring
- Scale effect of the specimens
- CBR test

The experimental works listed above are explained in detail. Moreover, the treated specimens have waited in the humid room for some different curing periods applied in this study.

6.5.1 Free Swell Test on the Oedometer Ring

The swelling potentials of the specimens stabilized with CIM were measured under both 7 kPa and 25 kPa surcharge pressures by doing free swell tests. Table 6.24 shows the swelling potentials of these specimens treated with the combined improvement method given in regards to the curing period.

Table 6.24 The swelling potential of the specimens treated with the combined improvement method

Curing period	Swelling potential (%)	
	7 kPa	25 kPa
1 day	9.21	3.16
7 days	2.76	0.95
28 days	1.58	0.53
90 days	1.05	0.37
180 days	0.58	0.22

The swelling potential of the treated specimen with CIM was measured at 9.21% under 7 kPa surcharge pressure after this specimen waited in the humid room for one day. When 25 kPa surcharge pressure is applied to this specimen, the swelling potential of this specimen decreased by 3.16%.

The fall of the swelling potential of this specimen continues with the curing period. After 180 days curing period, the swelling potential of this specimen that was applied 7 kPa surcharge pressure was determined at 0.58%. Under 25 kPa surcharge pressure, the swelling potential of this specimen was found 0.22%.

According to Seed et al. (1962), The classification of treated specimens with CIM is done by using their swelling potentials (Table 6.25).

Table 6.25 The classification of treated specimens with CIM according to Seed et al. 1962

	Surcharge pressure (kPa)	Curing period (days)	Swelling potential (%)	Degree of expansion
Treated specimen with CIM	7	1	9.21	High
	7	7	2.76	Medium
	7	28	1.58	Medium
	7	90	1.05	Medium
	7	180	0.58	Medium
	25	1	3.16	Medium
	25	7	0.95	Medium
	25	28	0.53	Medium
	25	90	0.37	Low
	25	180	0.22	Low

According to HTS (2013), the main goal of this test program is that the swelling potential of the treated specimen used for the subgrade material in the highway construction should be either equal to 0.5% or lower than 0.5%. After the 180 days curing period, the swelling potential of the specimen treated with CIM under 7 kPa surcharge pressure has almost reached this goal. Under 25 kPa surcharge pressure, the specimen stabilized with CIM is a suitable subgrade material for 28 days curing period.

6.5.2 Effect of Scale of the Specimens

Three specimens had different diameters and heights were prepared to investigate the scale effect of the specimens on their swelling potentials. These specimens also waited in the humid room for 1 day, 7 days, 28 days, 90 days. In terms of the curing periods, the swelling potentials of treated specimens tested under both 7 kPa and 25 kPa surcharge pressures prepared in this study are shown in Figure 6.56 and Figure 6.57, respectively.

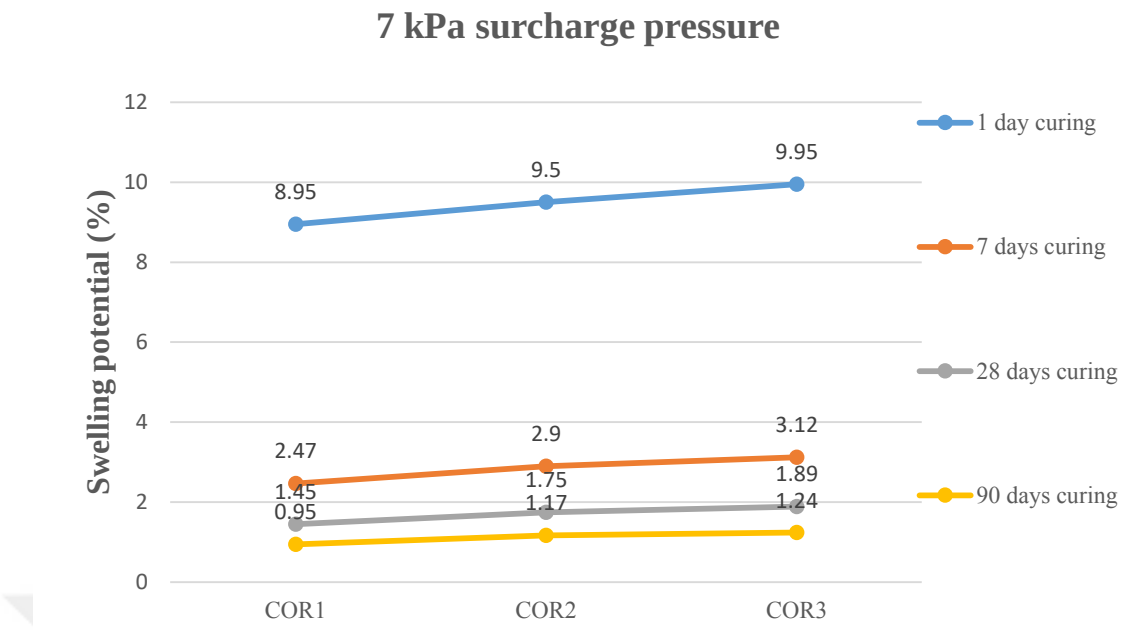

Figure 6.56 The swelling potentials of the treated specimen with CIM under 7 kPa surcharge pressure

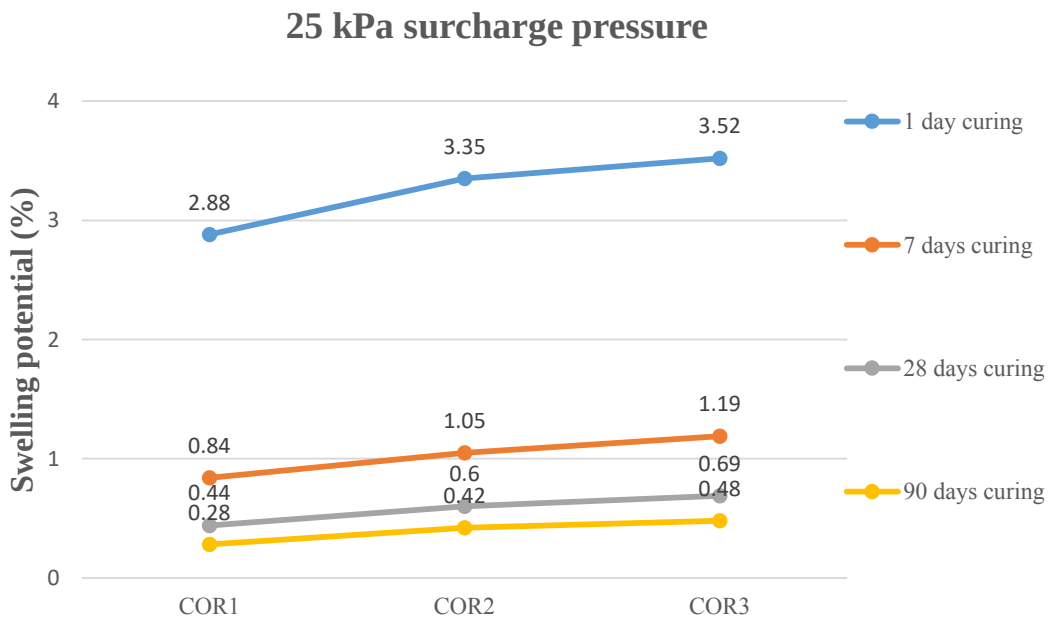

Figure 6.57 The swelling potentials of the treated specimen with CIM under 25 kPa surcharge pressure

Correlation specimens treated with CIM are classified in regards to Seed et. al. (1962). Table 6.26 shows this classification below.

Table 6.26 Correlation specimens classification with respect to Seed et. al. (1962)

Specimens	*Surcharge Pressures*	*Curing Period*	*Swelling Potential (%)*	*Seed et. al. (1962)*
COR1	7 kPa	1 day	8.95	High
COR1	7 kPa	7 days	2.47	Medium
COR1	7 kPa	28 days	1.45	Medium
COR1	7 kPa	90 days	0.95	Medium
COR2	7 kPa	1 day	9.5	High
COR2	7 kPa	7 days	2.9	Medium
COR2	7 kPa	28 days	1.75	Medium
COR2	7 kPa	90 days	1.17	Medium
COR3	7 kPa	1 day	9.95	High
COR3	7 kPa	7 days	3.12	Medium
COR3	7 kPa	28 days	1.89	Medium
COR3	7 kPa	90 days	1.24	Medium
COR1	25 kPa	1 day	2.88	Medium
COR1	25 kPa	7 days	0.84	Medium
COR1	25 kPa	28 days	0.44	Low
COR1	25 kPa	90 days	0.28	Low
COR2	25 kPa	1 day	3.35	Medium
COR2	25 kPa	7 days	1.05	Medium
COR2	25 kPa	28 days	0.6	Medium
COR2	25 kPa	90 days	0.42	Low
COR3	25 kPa	1 day	3.52	Medium
COR3	25 kPa	7 days	1.19	Medium
COR3	25 kPa	28 days	0.69	Medium
COR3	25 kPa	90 days	0.48	Low

The relation between the diameter of the lime column and the curing period has to be found by the improvement percentage of the treated specimen with the combined improvement method application in this study. Therefore, two graphs show this relation under both 7 kPa and 25 kPa surcharge pressure applied in this study are drawn. Finally, a suitable estimation can be individually made using both the diameter of the lime column and the curing period. In a conclusion, the improvement percentage of the treated specimen had a big size in the field can be estimated by using the equation of these curves in the graph (Figure 6.58-6.59).

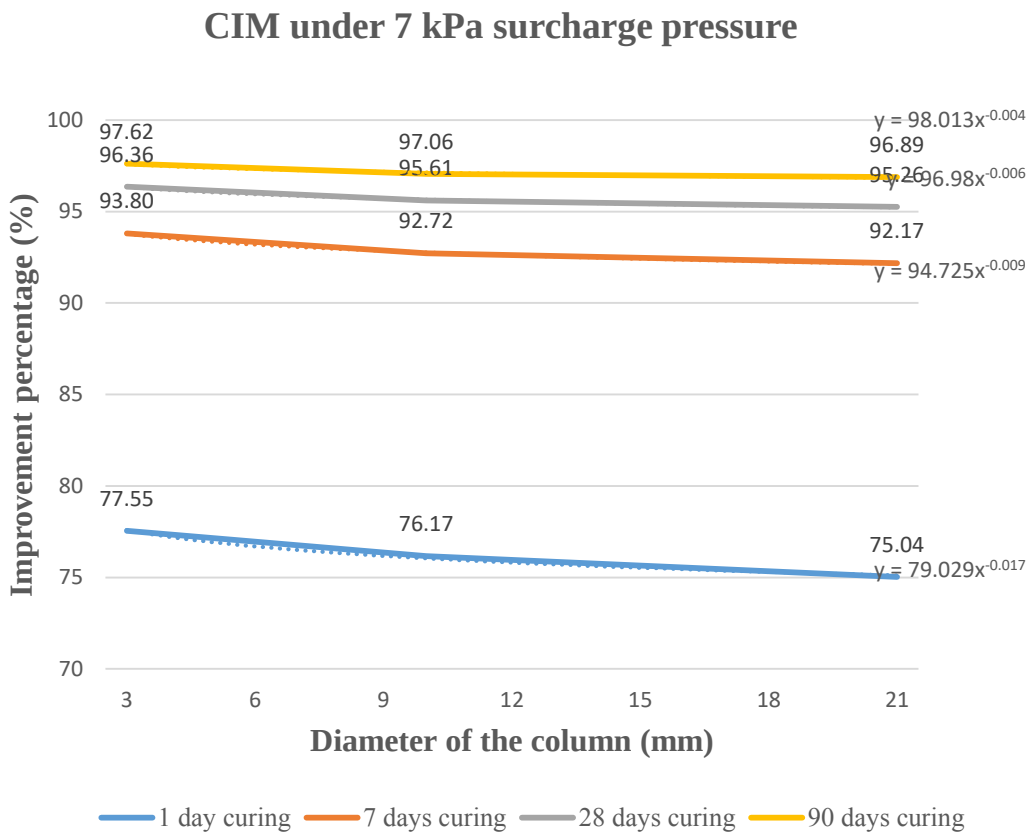

Figure 6.58 The improvement percentages of the treated specimen with CIM under 7 kPa with respect to both curing period and distance between the boreholes

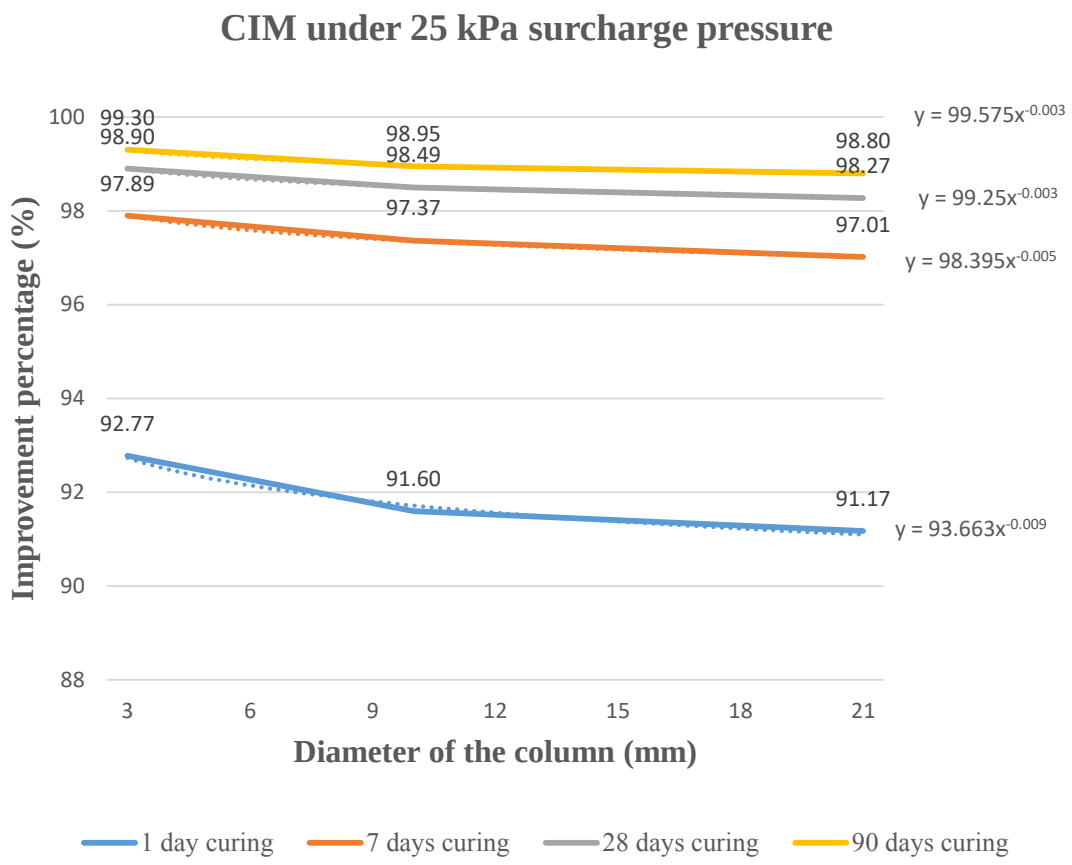

Figure 6.59 The improvement percentages of the treated specimen with CIM under 25 kPa with respect to both curing period and distance between the boreholes

6.5.3 California Bearing Ratio

The soaked CBR values of the treated specimens with the combined improvement method under two surcharge pressures have been determined with curing periods.

The CBR swells of these treated specimens with respect to surcharge pressures are illustrated in Figures 6.60-6.61.

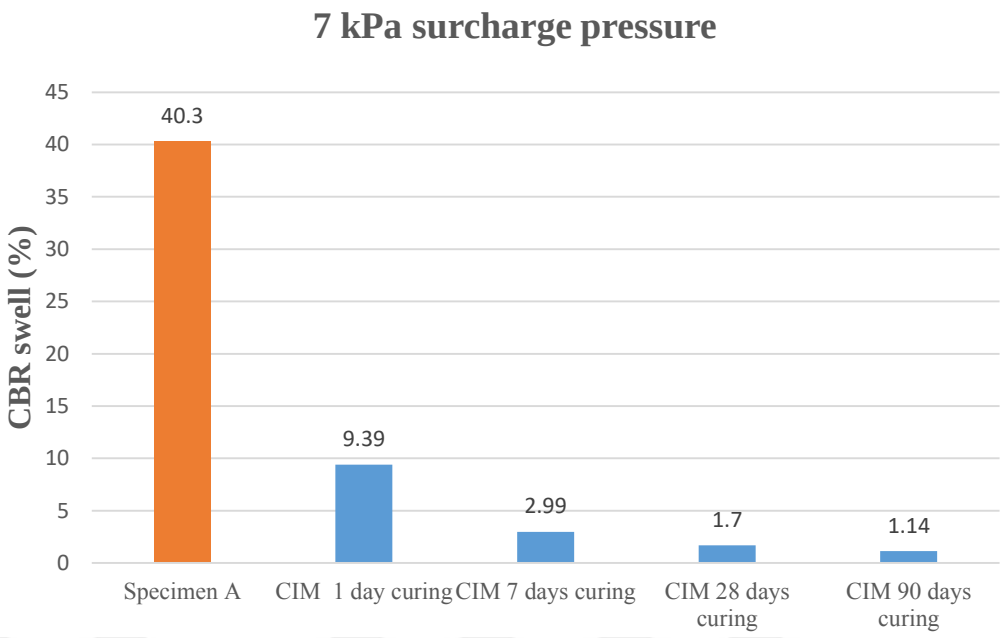

Figure 6.60 CBR swell values of treated specimens under 7 kPa surcharge pressure

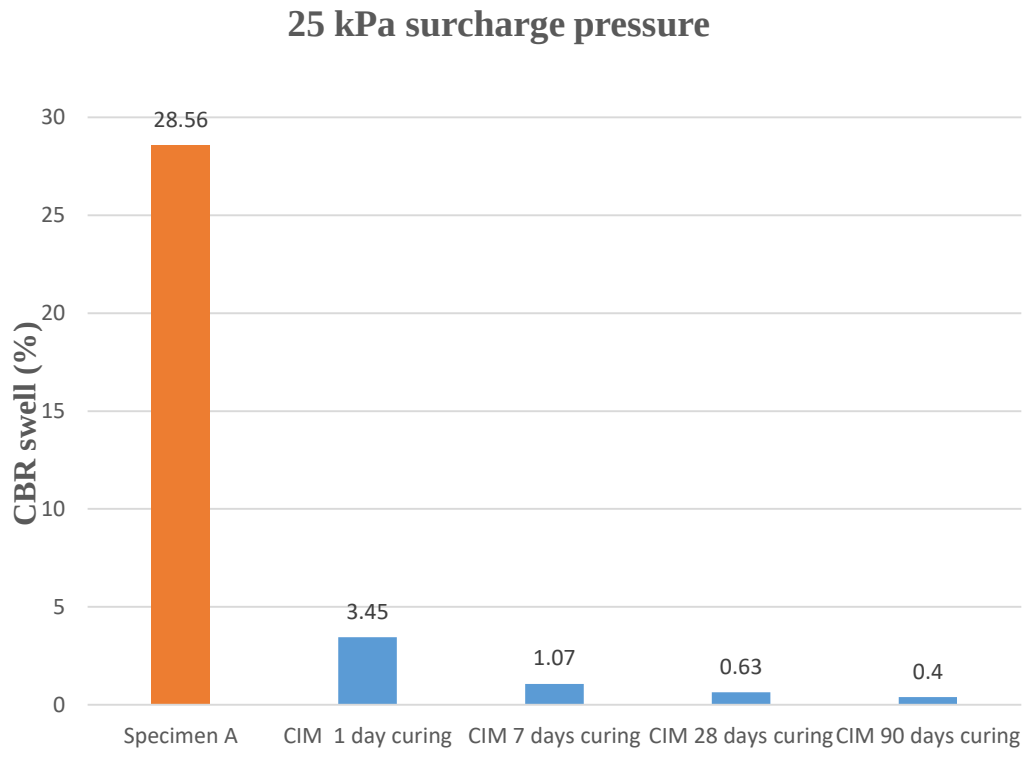

Figure 6.61 CBR swell values of treated specimens under 25 kPa surcharge pressure

Treated specimens with the CIM have the lower swelling potential of both Specimen A and the treated specimens with lignosulfonate lime columns. The CBR swell values of treated specimens with CIM decrease with the curing period for each surcharge pressure. After 90 days curing period, while the CBR swell of the treated specimen with CIM is determined 1.14% under 7 kPa surcharge pressure.Besides, this parameter of the same specimen is found at 0.4% when 25 kPa surcharge pressure is applied.

CBR values of treated specimens have improved during this stabilization method. Under 7 kPa and 25kPa surcharge pressure, Figures 6.62 and 6.63 show the load-penetration curves for both untreated and treated specimens obtained from the soaked CBR tests.

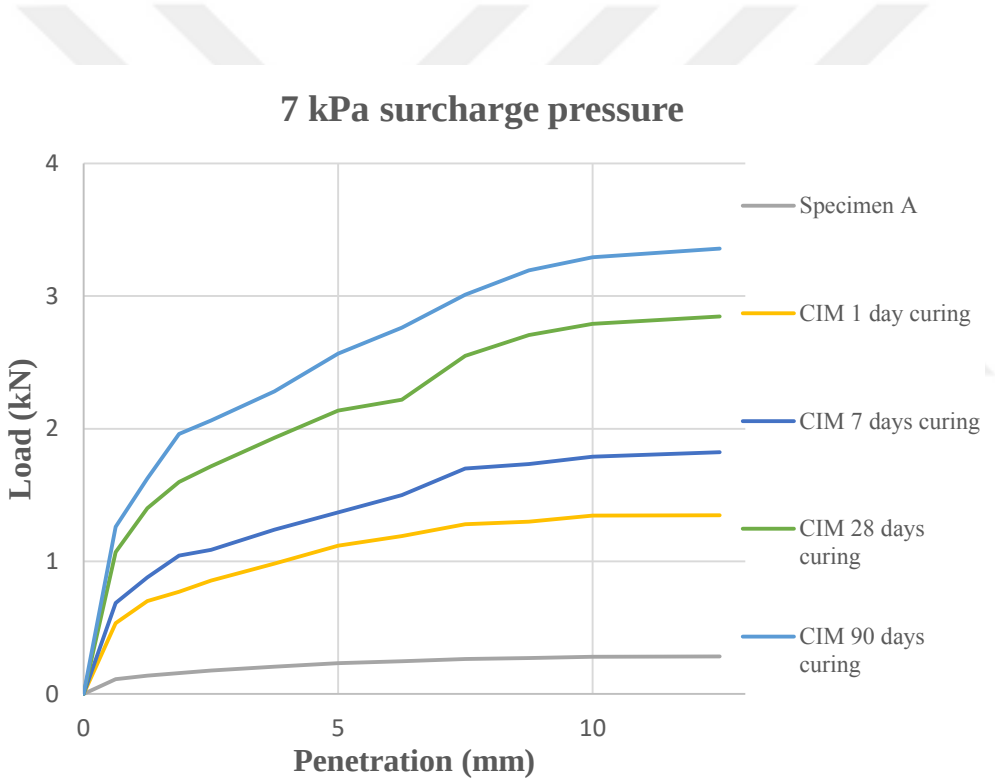

Figure 6.62 The curves of the load-penetration of the treated specimens under 7 kPa surcharge pressure after the soaked CBR test

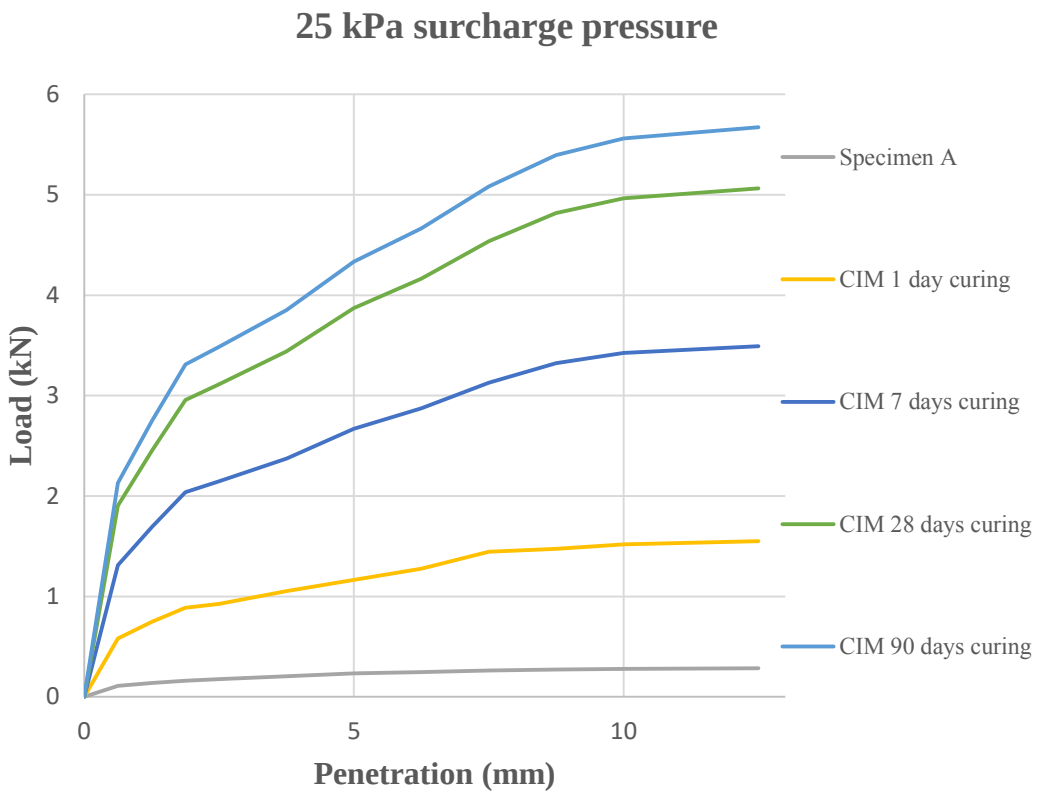

Figure 6.63 The curves of the load-penetration of the treated specimens under 25 kPa surcharge pressure after the soaked CBR test

The specimens stabilized with CIM are stiffer material than both Specimen A and the treated specimens with lignosulfonate lime columns when the investigation of each load-penetration curve is obtained from the soaked CBR tests done in this step.

From the load-penetration curves obtained from both untreated and treated specimens, the CBR values of them are calculated from the loads read at 2.50 mm and 5.00 penetration. The CBR value corresponding to 5.00 mm penetration was lower than that obtained for 2.50 mm penetration. Therefore CBR values of them are counted concerning the load at 2.50 mm penetration.

The CBR values of treated specimens, which are calculated from the soaked CBR tests, are given in Figures 6.64-6.65.

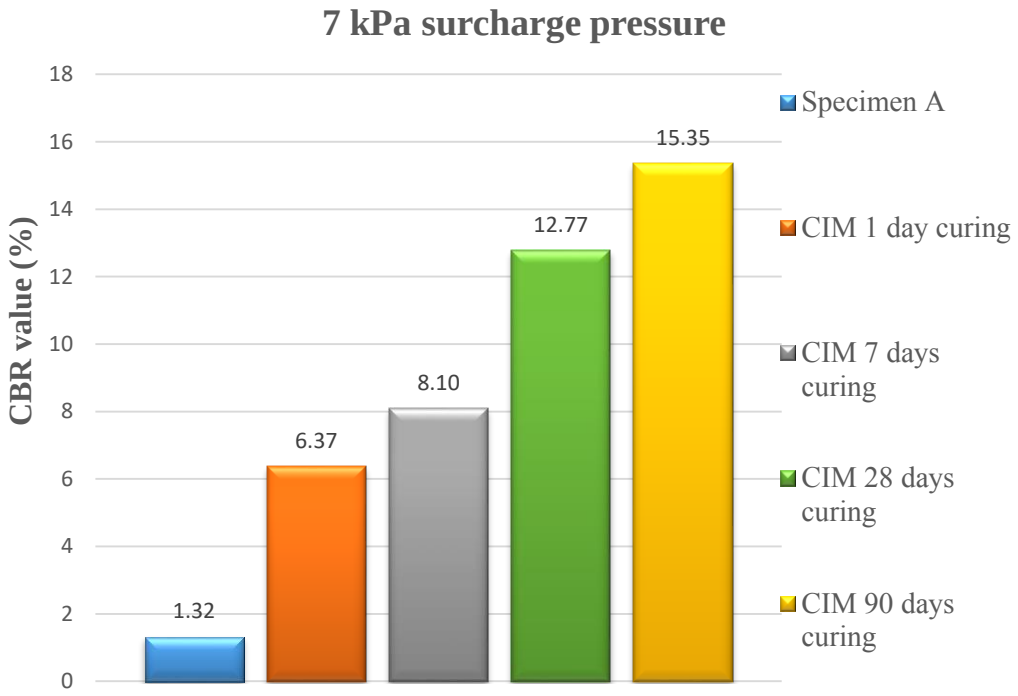

Figure 6.64 The CBR values for treated specimens under 7 kPa surcharge pressure

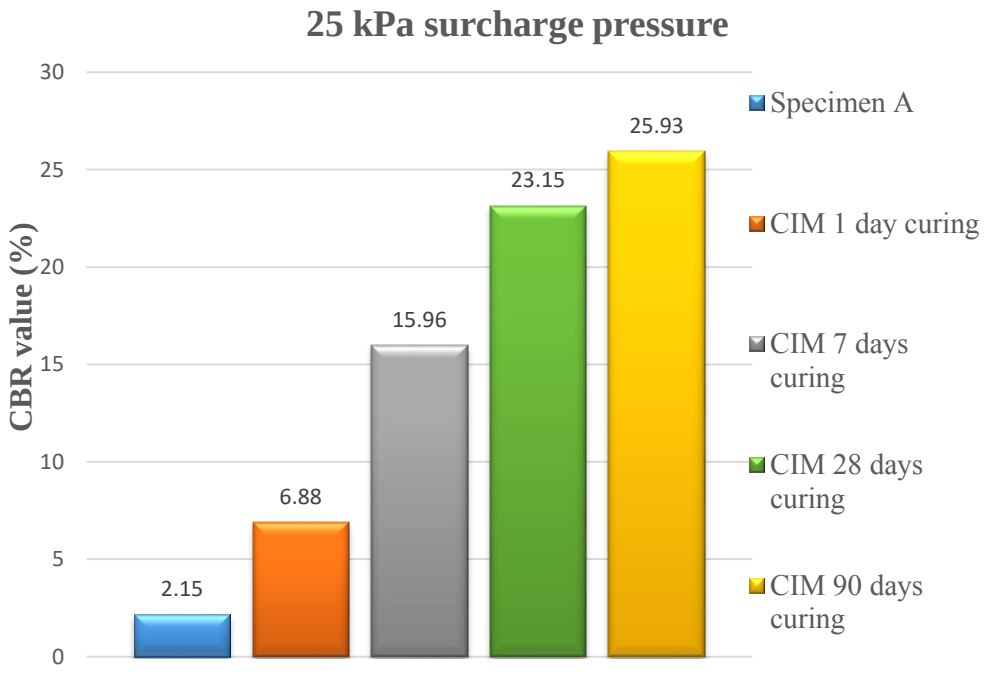

Figure 6.65 The CBR values for treated specimens under 25 kPa surcharge pressure

Under 7 kPa surcharge pressure, the CBR values of t the treated specimens with CIM waited in the humid room for 90 days are measured at 15.35%. The CBR value for the treated specimens with CIM is approximately 26%. For each surcharge pressure, the CBR values for treated specimens increase with the curing period.

After 90 days curing period, the CBR value of the treated specimens with CIM tested under 25 kPa surcharge pressure is a sutiable material for the subgrade material specified in both HTS (2013) and Scheafer et al. (2008).

6.6 Comparison of the Lignosulfonate Lime Columns method and Combined Improvement Method

The expansive soil specimen prepared in this study have been stabilized with both the lignosulfonate lime column method (NaLS and CaLS) and the combined improvement method (CIM). In the previous section of this study, CaLS is a more effective method than NaLS. Thus, this part compares CaLS and CIM. As two different types of improvement methods have been applied in this study, detailed discussions on the comparisons of these improvement methods are done in this section of this study.

The swelling potentials, CBR swell and CBR values of treated specimens with CIM are lower than the treated specimens with CaLS for each curing period applied in this study. The reason of this case is that while the expansive soil specimen treated with CaLS is enveloped in the only horizontal direction, this soil treated with CIM is confined in both vertical and horizontal directions. To sum up, the improvement process of the CIM method is faster than the lignosulfonate lime columns method. In conlusion, the treated specimens with CIM are more stable than the treated specimen with CaLS under the same curing period.

This section is divided into two groups that are listed below;

- The change of the swelling potential of the treated specimens
- The change of the strength properties of the treated specimens

These subtitles given above are discussed in more detail.

6.6.1 The change of the swelling potential of the treated specimens

The swelling potentials of the treated specimens are important parameters to observe the improvement process of these techniques applied in this study. This parameter was determined for specimens prepared in the oedometer ring. Furthermore, this parameter was measured in two different surcharge pressures that are 7 kPa and 25 kPa.

The comparison of the swelling potential of the treated specimens with both CaLS and CIM is illustrated for each surcharge pressure applied in this study in Figures 6.66-6.67.

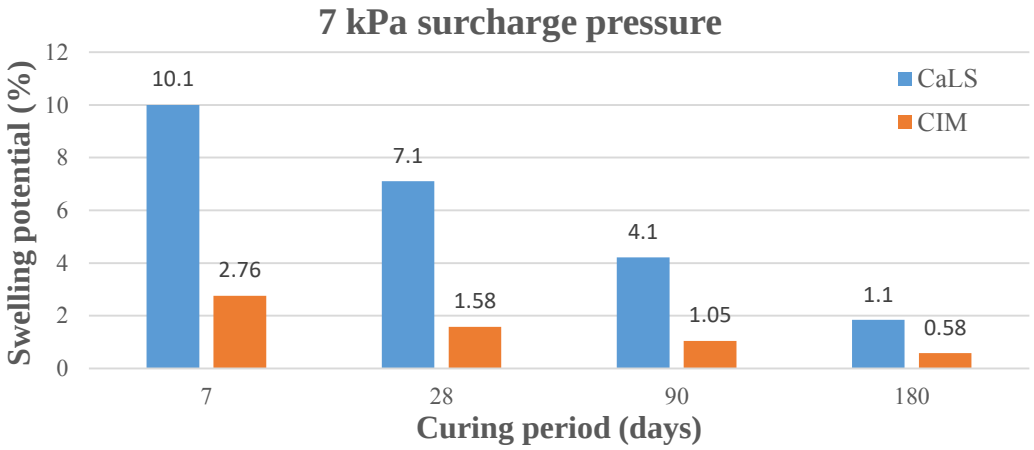

Figure 6.66 The swelling potentials of the stabilized soil specimens with both CaLS and CIM under 7 kPa surcharge pressure

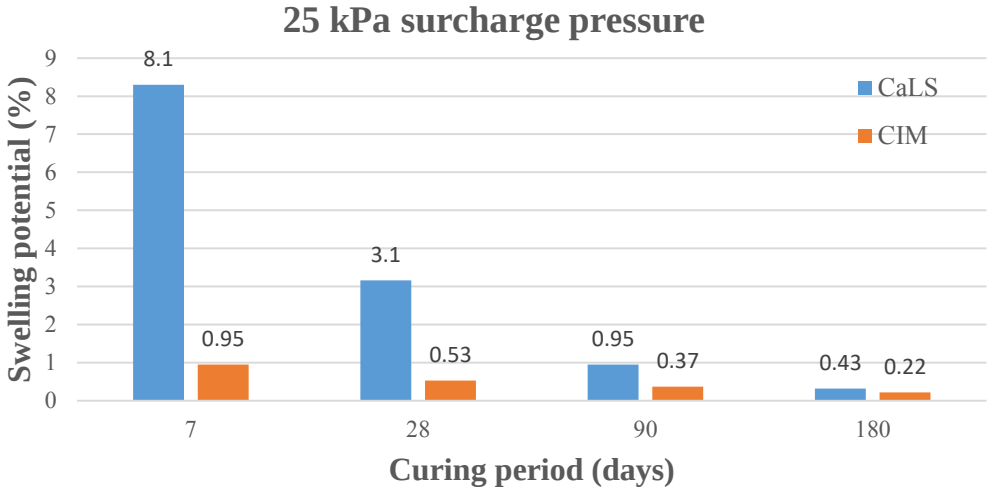

Figure 6.67 The swelling potentials of the stabilized soil specimens with both CaLS and CIM under 25 kPa surcharge pressure

According to HTS (2013), the swelling potential of improvement material used as a subgrade in highway construction should be either equal to 1% or lower than 1%. Under 7 kPa surcharge pressure, while the swelling potentials of the treated specimens with CaLS have not reached this goal during 180 days curing period, the treated specimens with CIM that waited in the humid room for 90 days have almost reached this goal. When 25 surcharge pressure has been applied to these treated specimens instead of 7 kPa surcharge pressure, the treated specimen with CIM has 0.95% swelling potential after only 7 days curing period. In conclusion, as the curing period and the surcharge pressure increase, swelling potential of the treated specimen with CIM, decrease to less than 1%.

6.6.2 The Change of the Strength Properties of the Treated Specimens

The specimens tested in the CBR tests are the stabilized soil specimen with both calcium lignosulfonate lime columns and the combined improvement method during this study. While the treated specimens with CaLS include 61 pieces column which has 10.5 mm diameter, the number of the columns for the treated specimens with CIM is only 19. In addition to this, the geotextile and seven anchors were used for the CIM method. In this section, the results obtained from these tests are evaluated and two techniques are compared with each other.

The CBR parameters of the stabilized soil specimen with both CaLS and CIM are illustrated in Figure 6.68 and Figure 6.69 These graphs show the relationship between the CBR swell value of stabilized soil specimens and the curing periods applied in this study.

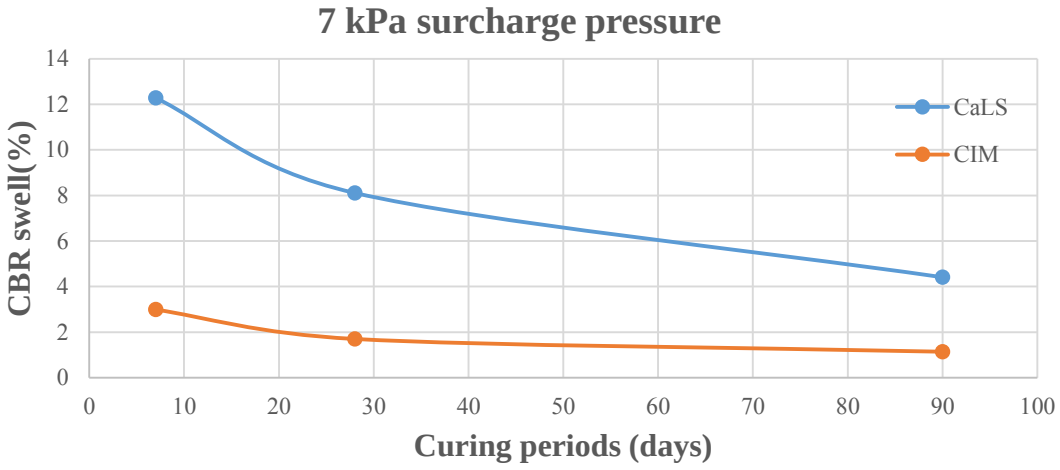

Figure 6.68 Effect of Curing Time on the CBR swell value for both CaLS and CIM specimens under 7 kPa surcharge pressure

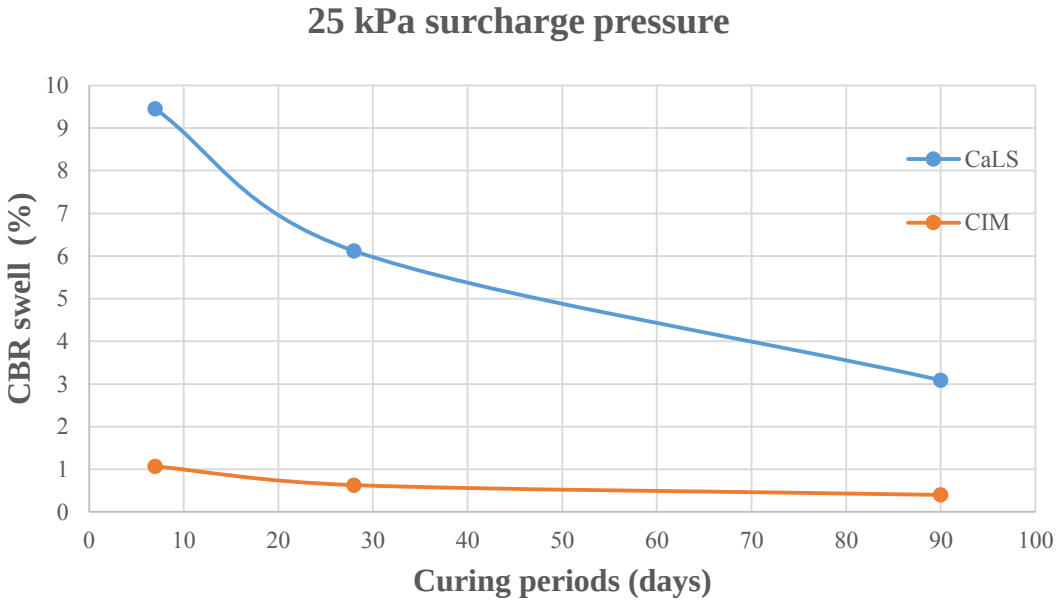

Figure 6.69 Effect of Curing Time on the CBR swell value for both CaLS and CIM specimens under 25 kPa surcharge pressure

The graphs related to the CBR values of these stabilized specimens and the curing periods are given in Figure 6.70- Figure 6.71.

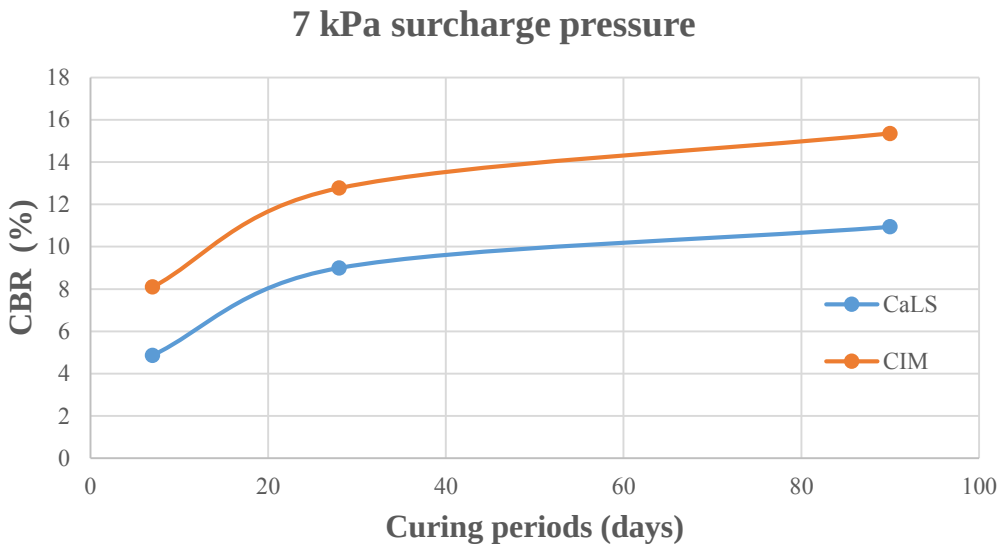

Figure 6.70 Effect of Curing Time on the CBR for both NaLS and CaLS specimens under 7 kPa surcharge pressure

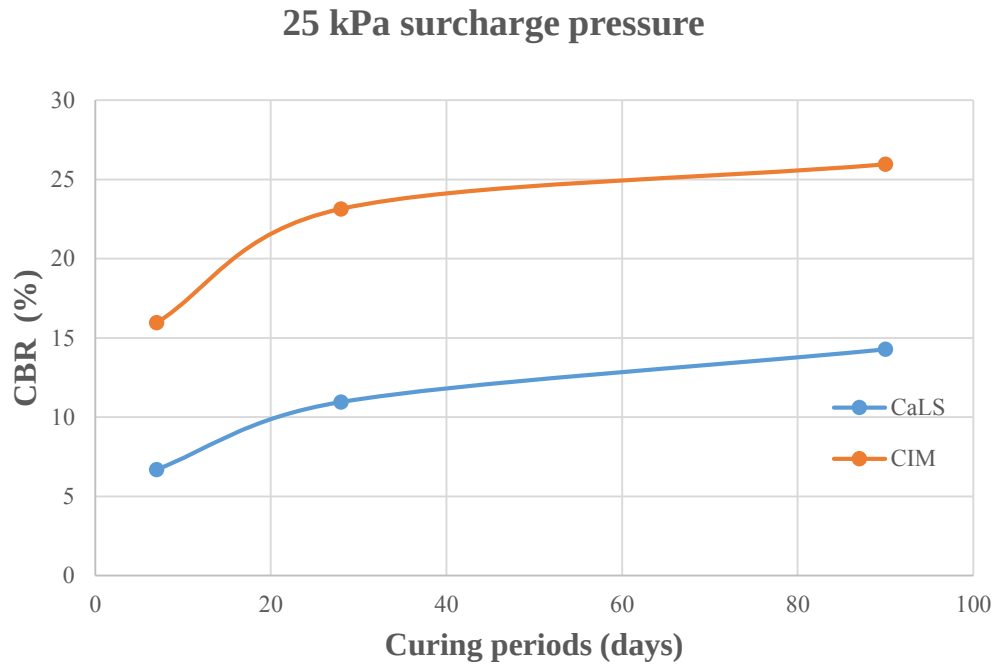

Figure 6.71 Effect of Curing Time on the CBR for both NaLS and CaLS specimens under 25 kPa surcharge pressure

CHAPTER 7

CONCLUSIONS

The main aim of this study is that the addition of the lignosulfonate to the lime column method during the stabilization of the expansive soil which is the subgrade material in the highway constructions. The effects of addition of the lignosulfonate to the lime column on physical and engineering properties of expansive soil was investigated, the influence of parameters such as lime column heights, lime column diameters, space between the lime columns, scale of the lab model test, ... etc on the improvement were studied. The change of unconfined compressive strength, swelling potential, coefficient of permeability, CEC and SSA of the treated specimen during the stabilization process were studied.

Some parameters related to lime columns that are area ratio, surrounding area, the height of the column, and water content have been investigated in detail in this study. Two different models prepared in this study are M1 and M2; while the M1 model consists of 19 pieces of 6.5 mm diameter lime columns, the M2 model includes 37 pieces of 4.5 mm diameter lime columns. Although the area ratio of the M1-h model (21.05%) is greater than the area ratio of the M2-h model (20.91%), the swelling potential of the treated specimens with the M2-h model are lower than the treated specimens with the M1-h model, since the surrounding area is a more effective parameter than the area ratio (i.e. surrounding area of M1-h model is 73.7cm^2 and surrounding area of M2-h model is 99.4 cm^2). In conclusion, the lime columns that had small diameters should be selected instead of the lime columns that had bigger diameters during the lime column stabilization.

The height of the lime column should be the depth of the active zone during the lime stabilization. Since the horizontal permeability of the expansive soil specimen prepared in this study is greater than the vertical permeability of this soil. Thus, the diffusion of the lime particles into the soil specimens is faster in the horizontal direction than in the vertical direction.

The water content of the lime column affects the improvement percentages of the treated specimens prepared in this study. When the water content of the lime columns is lower than the water content of the expansive soil, this soil loses some water due to the hydraulic balance of the medium during the first period of the lime column stabilization. The swelling potential of the treated specimen with the lime column method decreases as the water content of the lime columns increase. When the water content of the lime columns is greater than 30%, the mixture consisted of lime and water is not practicable material due to its sticky structure.
The ettringite minerals have formed during the lime column stabilization method in this study. This mineral causes the increase of the swelling potential of the treated specimens due to its needle structure. The addition of the lignosulfonate to lime columns blocks the formation of the ettringite minerals into the expansive soil specimen prepared in this study.

The addition of the lignosulfonate to lime columns increases the diffusion rate of the lime particles into the expansive soil specimen prepared in this study. After the lignosulfonate particles cover the surface of the clay particles, the electrostatic repulsion force occurs between the particles. According to the result of the EDX analysis done in this study, the amount of Ca^{+2} ions diffused through the expansive soil specimen is the highest in the treated specimens with lignosulfonate lime columns.

Two lignosulfonate types, which are sodium and calcium, were selected for the additive materials of the lime columns. The calcium lignosulfonate type is more effective than the sodium lignosulfonate type as the calcium ions are prone to the ion Exchange in regards to sodium ions.

The cation exchange capacity and the specific surface area are significant properties for the expansive soil specimens. The stabilized specimens with lignosulfonate lime columns decreased these properties than the untreated specimens. As a result, the stabilized specimens have lower swelling potentials than untreated specimens.

The strength properties of the treated specimens in this study have been measured by two laboratory tests that are unconfined compressive strength (UCS) and California bearing ratio (CBR).

Firstly, the UCS test is used for the specimens located between the columns. The unconfined compressive strengths of the treated specimens with lignosulfonate lime columns are greater than the untreated specimens. The UCS values of treated specimens increase with the curing period applied. The UCS of the treated specimens is higher than the untreated specimens. For example, the UCS of the treated specimens with calcium lignosulfonate lime columns has increased from 385 kPa to 622 kPa.

Secondly, the whole specimen that consists of the untreated specimens and lignosulfonate lime columns are tested by using the test equipment of the CBR test. The CBR swell and CBR value are considerable outputs obtained from this test. The CBR swell values of treated specimens have lower than the untreated specimens. For instance, although the CBR swell of the untreated specimens was determined at 40.30%, the CBR swell of the treated specimen with calcium lignosulfonate lime columns under 7 kPa surcharge pressure was measured 4.41% after 90 days curing period. The CBR value of this treated specimen has reached from 1.32% to 10.94% after 90 days curing period.

The combined improvement method (CIM) includes three techniques that are prewetting, lignosulfonate lime columns, and geotextile+anchor. The aim of the prewetting technique is that the saturation step of the soil specimen with the mixture consists of calcium lignosulfonate and water. The lignosulfonate lime column technique is applied after the prewetting technique. The final step is that a geotextile is spread over the soil specimen and anchors are used for the connection between the geotextile and soil specimen. The geotextile provides both the uniform pressure and a more stable layer placed over the expansive soil. Also, the anchors provide that the connection between the lignosulfonate lime columns and geotextile. Thus, the expansive soil is trapped in both vertical and horizontal directions.

The improvement process of the combined improvement method in this study is faster than the lignosulfonate lime columns although the work steps of the combined improvement method are more excessive than the lignosulfonate lime columns. To

reduce the workload of the combined improvement method, the number of columns decreased from 37 to 19.

The treated specimen with CIM is more stable and resistant to volumetric change than both the other treated specimens and untreated specimens prepared in this study. Also, the improvement process of the CIM method is faster than the other methods applied in this study.

In this study, a design method (CIM) was developed and it has been shown that the high swelling potential of subgrade clay layers, in the active depth, can be reduced to low swelling potential values by this method.

Recommendations for Future Researches

This study has focused on the improvement of expansive soil by using the lime column method that includes sodium and calcium lignosulfonates. As many types of lignosulfonate may be found in the market, these lignosulfonate types can be added to the lime columns during the expansive soil treatment. Thus, the alterations of the expansive soil properties can be observed in detail.

The selected distance between the columns was constant for this study. This distance could be either shortened or stretched for the optimum value of this parameter.

The combined improvement method applied in this study can be further thought as the swelling potentials and CBR parameters of the treated specimens with CIM were investigated. The geotextiles used in this method can be varied and tested to determine the most suitable model.

CIM can be applied at field scale and diffusion of lime through the expansive soil can be observed and compared with the theoretical diffusion calculations.

Effect of freezing-thawing and wetting-drying cycles on the test specimens can be studied.

REFERENCES

Ashok, P., Reddy, G.S. (2015), Lime Pile Technique for the Improvement of Properties of Clay Soil, International Journal of Science and Research (IJSR), Vol. 5, Pp. 1204 -1210.

ASTM Standard D422, (2007), Standard Test Method for Particle-Size Analysis of Soils. ASTM International, West Conshohocken, PA.

ASTM Standard D5102, (2009), Standard Test Methods for Unconfined Compressive Strength of Compacted Soil-Lime Mixtures. ASTM International, West Conshohocken, PA.

ASTM Standard D4546, (2014), Standard Test Methods for One- Dimensional Swell or Collapse of Soils. ASTM International, West Conshohocken, PA.

ASTM Standard D4318, (2017), Standard Test Method for Liquid Limit, Plastic Limit and Plasticity Index of Soils. ASTM International, West Conshohocken, PA.

ASTM Standard D854, (2014), Standard Test Methods for Specific Gravity of Soil Solids by Water Pycnometer. ASTM International, West Conshohocken, PA.

Barker J.E., Rogers C.D.F., Boardman D.I., (2006), Physio-chemical changes in clay caused by ion migration from lime-piles Journal of Materials in Civil Engineering, pp. 182-189

Beetham, P., Dijkstra, T., Dixon, N., Fleming, P., Hutchison, R., & Bateman, J., (2015), Lime stabilisation for earthworks: a UK perspective. Proceedings of the Institution of Civil Engineers - Ground Improvement, 168(2), 81–95.

Bhuvaneswari S., Thyagaraj T., Robinson R. G., and Gandhi S. R., (2010), Alternative technique to induce faster lime stabilization reaction in deeper expansive strata, in Proceedings of the Indian Geotechnical Conference (GEOtrendz '10), pp. 609–612, Mumbai, India

Boardman, D.I., Glendinning, S. and Rogers, C.F.D. (2001) Development of stabilisation and solidification in lime-clay mixes, Geotechnique, 533–543.

Broms, B., and Boman, P. (1975), Lime stabilized columns, Proc., 5th Asian Regional Conf. on SMFE, Bangalore, India, (1), 227-234.

Celik, A. O., (2014), Evaluation of hydrated lime stabilization of sulfate bearing expansive soils. Ph. D. Thesis, Eastern Mediterranean University, North Cyprus, 114 pages.

Chen, F. H., (1988), Foundations on Expansive Soils, Elsevier Scientific Pub. Co., Amsterdam.

Chen QS and Indraratna B., (2014), Deformation behavior of lignosulfonate-treated sandy silt under cyclic loading, Journal of Geotechnical and Geoenvironmental Engineering 141(1).

Chen, Q., & Indraratna, B. (2015). Shear behaviour of sandy silt treated with lignosulfonate. Canadian Geotechnical Journal, 52(8), 1180–1185.

Cherian, C., Arnepalli, D. N., (2013), Role of Lime Diffusion in Stabilization of Fine Grained Soils: A Critical Review, Fourth Indian Young Geotechnical Engineer's Conference-2013, 17-18th May, Indian Institute of Technology Madras, India, pp1-10.

Cokca, E., (1991), Swelling potential of expansive soils with a critical appraisal of the identification of swelling of Ankara soils by methylene blue tests. PhD Thesis, Department of Civil Engineering, Middle East Technical University, Ankara, Turkey.

Dafalla, M. A., & Shamrani, M. A. (2011). Road Damage Due to Expansive Soils: Survey of the Phenomenon and Measures for Improvement. Design, Construction, Rehabilitation, and Maintenance of Bridges

Ekinci C. E., Ay S., Baykuş N., Ay. A., Examination of the impact of lignin sulfonate based structure chemicals on fresh and hardened concrete. Pamukkale Univ Muh Bilim Derg. 2016; 22(6): 478-485

Erguler Z.A., Ulusay R., (2003), Engineering characteristics and environmental impacts of the expansive Ankara clay, and swelling maps for central and SW parts of the Ankara (Turkey) metropolitan area Environmental Geology, 44 , pp. 979-992
EM 1110-1-1904. 1990. Settlement Analysis. U.S. Army Corps of Engineers.

Federal Highway Administration, FHWA NHI-05-037 (2006) Geotechnical Aspects of Pavements.

Freeze, R. A., Cherry J. A., (1979), Groundwater, 604 pp., Prentice-Hall, Englewood Cliffs, N. J.

Goud, G.N., Hyma, A.; Chandra, V.S., Rani, R.S., (2017), Expansive soil stabilization with coir waste and lime for flexible pavement subgrade. In Proceedings of the International Conference on Recent Advances in Materials, Mechanical and Civil Engineering, Hyderabad, India, 1–2 June 2017; IOP Publishing: Bristol, UK, 2018; Volume 330, p. 012130.

Hunter D., (1988), Lime-induced heave in sulfate-bearing clay soils, International Journal of Rock Mechanics and Mining Sciences & Geomechanics Abstracts, 25(5), 217

Indraratna, B., Mahamud, M., Vinod, J.S., and Wijeyakulasuriya, V. (2010). Stabilization of an erodible soil using a chemical admixtures, In Bouassida, M, Hamdi, E & Said, I (eds), ICGE'10: Proceedings, 2nd International Conference on Geotechnical Engineering: 45-54.

Jungnickel C, Smith D., Fityus S., (2004), Coupled multi-ion electrodiffusion analysis for clay soils. Canadian Geotechnical Journal 41(2): 287–298.

Karayolları Teknik Şartnamesi (2013), Yol altyapısı, sanat yapıları, köprü ve tüneller, üstyapı ve çeşitli işler, Karayolları Genel Müdürlüğü yayınları, Ankara.

Chiappone, A., Marello, S., Scavia, C., & Setti, M., (2004), Clay mineral characterization through the methylene blue test: comparison with other experimental techniques and applications of the method. Canadian Geotechnical Journal, 41(6), 1168–1178.

Masia, M. J., Totoev, Y. Z., & Kleeman, P. W. (2004). Modeling Expansive Soil Movements Beneath Structures. Journal of Geotechnical and Geoenvironmental Engineering, 130(6), 572–579.

Murray H.H., (2007), Applied Clay Mineralogy: Occurrences, Processing and Application of Kaolins, Bentonites, Palygorskite-Sepiolite, and Common Clays Elsevier Press

Nelson, J. D., Overton, D. D., & Durkee, D. B. (2001). Depth of Wetting and the Active Zone. Expansive Clay Soils and Vegetative Influence on Shallow Foundations, ASCE Geotechnical special publications No.116., 95-109.

Muntohar, A. S., (2005), The Influence of Molding Water Content and Lime Content on the Strength of Stabilized Soil with Lime and Rice Husk Ash. Civil Engineering Dimension, 7(1), Pp. 1-5.

Muntohar, A. S., (2010), A laboratory Test on the Strength and Load-Settlement Characteristic of Improved Soft Soil Using Lime-Column, Dinamika Teknık Sıpıl

Nelson J.D., Chao K.C., Overton D.D., Nelson E.J., (2015) Foundation Engineering for Expansive Soils Foundation Engineering for Expansive Soils

Nelson, J. and Miller, D. J., , (1992) Expansive Soils: Problems and Practice in Foundation and Pavement Engineering, John Wiley & Sons, New York

NF P 94-068. (1998), Soils: Investigation and testing—Measuring of the methylene blue adsorption capacity of a rock soil—Determination of the methylene blue of a soil by means of the stain test. Paris: Association Française de Normalisation.

Orszulik, S.T. (2013). Environmental Technology in the Oil Industry, Springer Science and Business Media, Netherlands, Also available at; https://books.google.com.au/books?id=QDjpCAAAQBAJ, accessed on July 12 2021.

Parhi, P.S., Garanayak, L., Mahamaya, M., Das, S.K. Stabilization of an expansive soil using alkali activated fly ash based geopolymer. In Advances in Characterization and Analysis of Expansive Soils and Rocks; Hoyos, L., McCartney, J., Eds.; Springer: New York, NY, USA, 2017; pp. 36–50.

Pearl, I. A. (1967), The Chemistry of Lignin, Publisher; Marcel Dekker, INC., New York.

Perkins, T. K., Johnston, O. C., (1963), A Review of Diffusion and Dispersion in Porous Media. Society of Petroleum Engineers Journal, 3(01), 70–84.

Prusinski, J., Bhattacharja, S., (1999), Effectiveness of Portland Cement and Lime in Stabilizing Clay Soils. Transportation Research Record: Journal of the Transportation Research Board, 1652, 215–227

Puppala, A. J., Du, Y.-J., Jiang, N.-J., Liu, S.-Y., Jin, F., Singh, D. N., (2014), Engineering properties and microstructural characteristics of cement-stabilized zinc-contaminated kaolin. Canadian Geotechnical Journal, 51(3), 289–302.

Rajasekaran, G., Narasimha Rao, S., (2005), Sulphate Attack in Lime-Treated Marine Clay. Marine Georesources & Geotechnology, 23(1-2), 93–116.

Rakaraddi, P.G., and Vijay, G., (2015), Establishing Relationship between CBR with Different Soil Propertie, International Journal of Research in Engineering and Technology, Vol.4, Issue 2, 2014, pp26-30.

Rana D., Neale G.H., Hornof V.,(2002), Surface tension of mixed surfactant systems: lignosulfonate and sodium dodecyl sulfate. Colloid & Polymer Science, 280(8), 775–778.

Rogers, C.D.F. and Glendinning, S. (1996), Modification of clay soils using lime, Proceedings, Seminar on Lime Stabilization, Loughborough University, Civil and Building Engineering Department, London, pp. 99–114.

Rogers, C. D. ., & Glendinning, S., (1997), Improvement of clay soils in situ using lime piles in the UK. Engineering Geology, 47(3), 243–257.

Rowe, R.K., Caers, CJ. and Barone, F., (1988), Laboratory determination of diffusion and distribution coefficients of contaminants using undisturbed clayey soils. Canadian Geotech. J., 25: 108-I 18.

Schaefer, V. R., Phan T. H., Cushman M., White D. J., Jahren C. T., Sharma, R. S., (2008), Case Study of Seasonal Variation in the Subgrade and Subbase Layers of Highway US 20. Iowa Department of Transportation, Ames.

Seed, H. B., Woodward, R. J., Jr. and Lundgren, R., (1962) Prediction of swelling potential for compacted clays: J. ASCE, Soil Mechanics and Foundation Division, Vol. 88, No. SM-3, Part 1, pp. 53–87.

Shaqour, F., Ismeik, M., Esaifan, M. (2017). Alkali activation of natural clay using a $Ca(OH)_2/Na_2CO_3$ alkaline mixture. Clay Minerals, 52(04), 485–496.

Sudhakar M. R and Shivananda P, (2005), Compressibility Behaviour of Lime-Stabilized Clay, Geotechnical and Geological Engineering 23: 309–319.

Sulphite Pulp Manufacturers Research League, (1963). A Bulletin about Spent Sulphite Liquor, Appleton, Wisconsin, USA.

Snethen, D. R. 1986. “Expansive Soils: Where Are We? Ground Failure.” National Research Council Communication on Ground Failure Hazards 12–16. Washington, DC:National Research Council.

Theng, B.K.G. (1979). Formation and properties of clay-polymer complexes, Elsevier Scientific Publishing Company, Amsterdam, The Netherlands.

Tingle, J.S., Newman, J.K., Larson, S.L., Weiss, C.A., and Rushing J.F. (2007). Stabilization mechanisms of non-traditional additives, Transportation Research Record: Journal of the Transportation Research Board, No. 1989, 2, Transportation Research Board of the National Academics, Washington, D.C., 59 – 67.

Tingle, J., Santoni, R., (2003), Stabilization of Clay Soils with Nontraditional Additives. Transportation Research Record: Journal of the Transportation Research Board, 1819, 72–84.

Tonoz M.C., Gokceoglu C. , Ulusay R. (2003), A laboratory scale experimental investigation on the performance of lime columns in expansive Ankara (Turkey) clay Bulletin of Engineering Geology and the Environment, 62 (2), pp. 91-106

Vakili A.H., M. Kaedi, M. Mokhberi, M.R. bin Selamat, M. Salimi, (2018), Treatment of highly dispersive clay by lignosulfonate addition and electroosmosis application, Appl. Clay Sci. 152 1–8.

Vinod, J.S., Indraratna, B., and Mahamud M.A.A. (2010), Stabilization of an erodible soil using a chemical admixture, Journal of Ground Improvement, Vol. 163: 43 – 51.

Vinod, J. S., Hussaini, S. K. K., Indraratna, B., (2016), A laboratory investigation to assess the functioning of railway ballast with and without geogrids. Transportation Geotechnics, 6, 45–54.

Yang, D., Qiu, X., Zhou, M., & Lou, H., (2007), Properties of sodium lignosulfonate as dispersant of coal water slurry. Energy Conversion and Management, 48(9), 2433–2438.

APPENDICES

A. Swelling Potential Versus Time Graphs For Treated Specimen In This Study

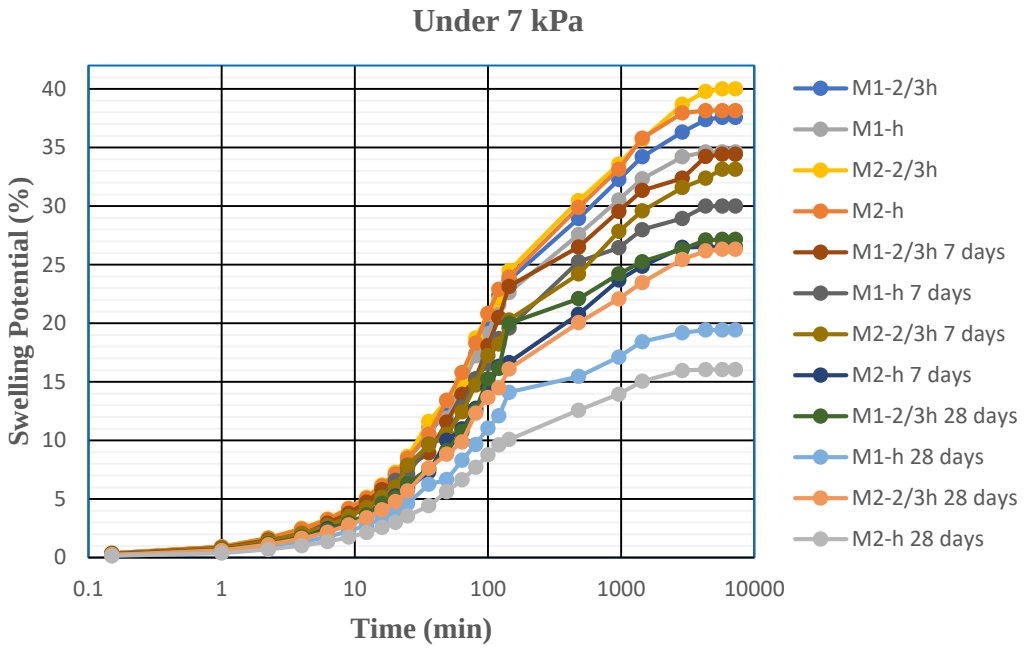

Figure A.1 Swelling potential versus Time Graph for Treated Samples with lime column

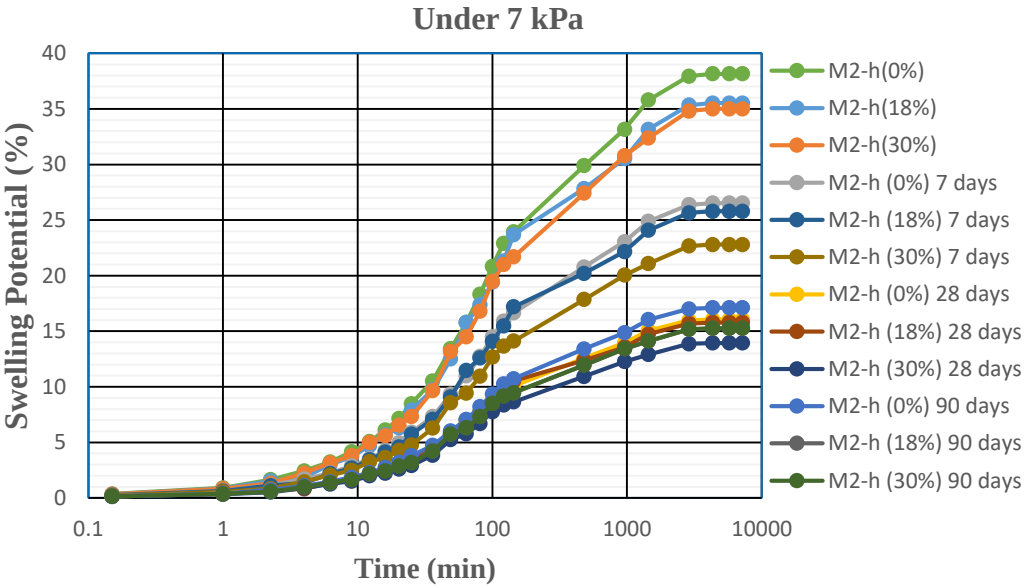

Figure A.2 Swelling potential versus Time Graph for Treated Samples with lime column

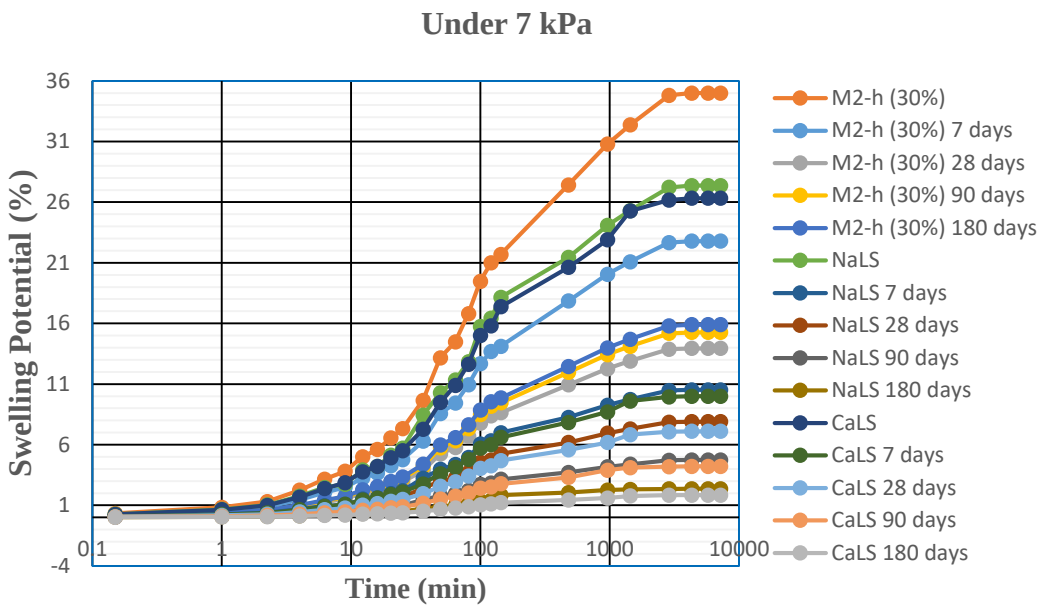

Figure A3 Swelling potential versus Time Graph for Treated Samples with both lime column and lignosulfonate lime column under 7 kPa

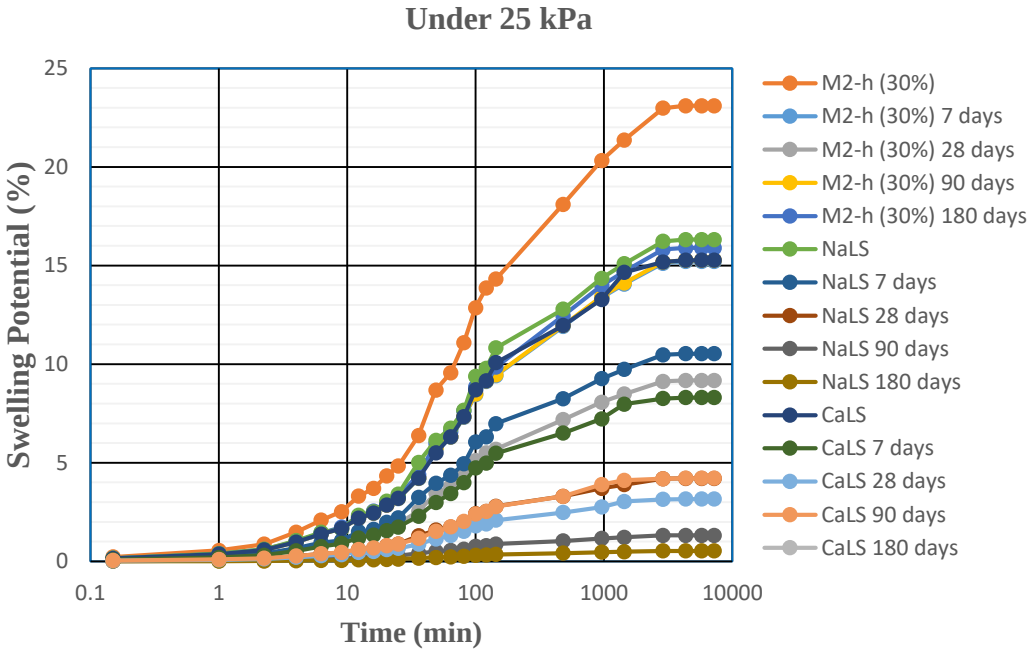

Figure A.4 Swelling potential versus Time Graph for Treated Samples with both lime column and lignosulfonate lime column under 25 kPa

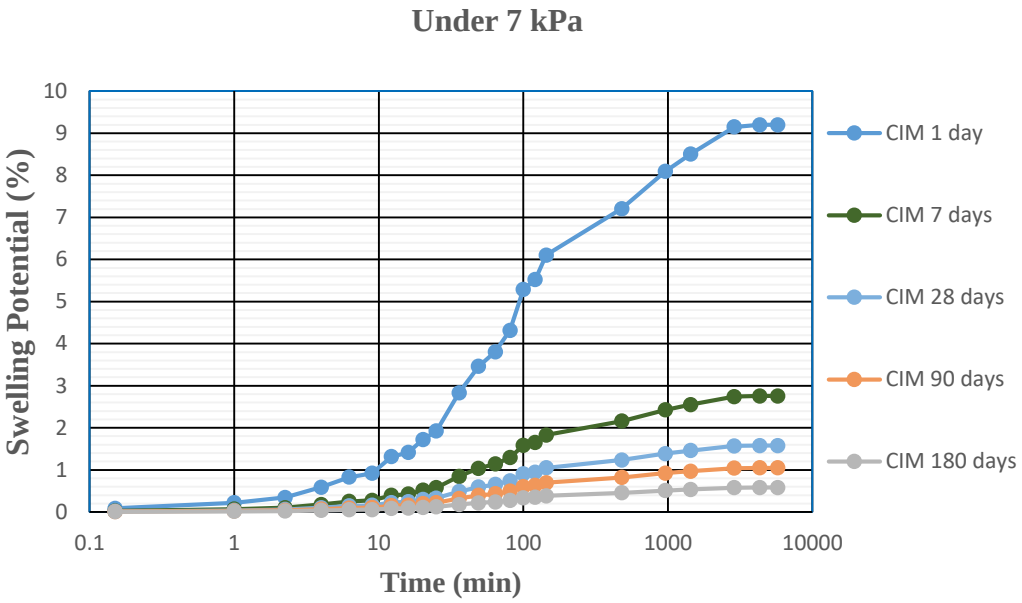

Figure A.5 Swelling potential versus Time Graph for Treated Samples with CIM under 25 kPa

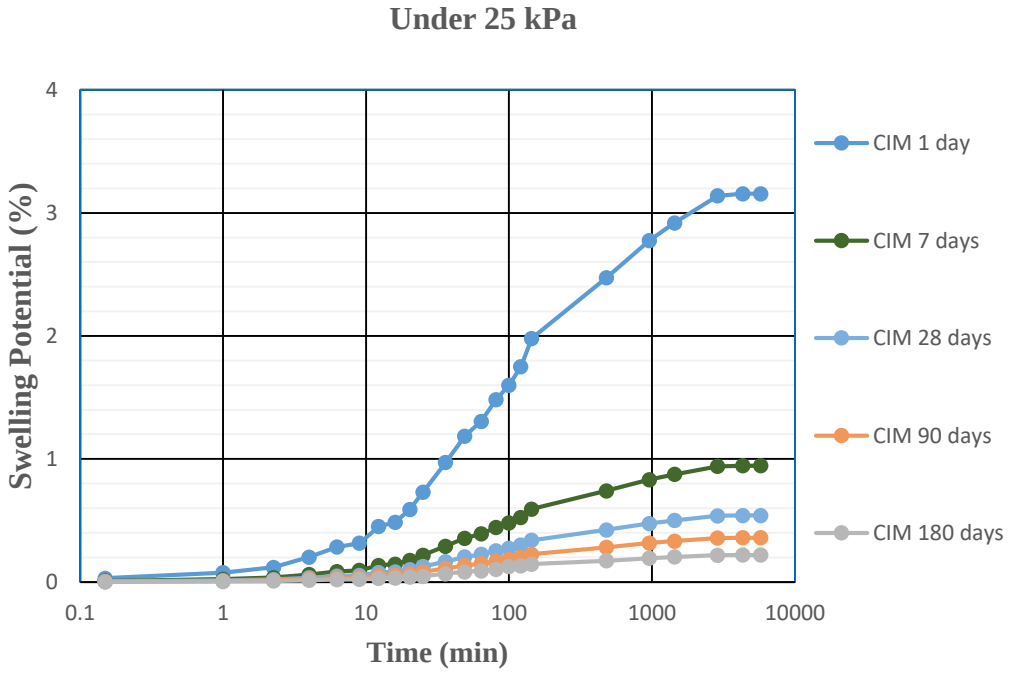

Figure A.6 Swelling potential versus Time Graph for Treated Samples with CIM under 7 kPa

B. The Calculation of the Improvement Percentages of the Treated Specimens that are M1-2/3h, M1-h, M2-2/3h, and M2-h under 7 kPa surcharge pressure

✓ **<u>The calculation of improvement percentage of the M1-2/3h treated specimen under 7 kPa</u>**

Specimens	**Swelling potential (%) under 7 kPa**
Untreated Specimen	43.95
M1-2/3h	27.16

$$The\ swelling\ potential\ of\ untreated\ specimen\ under\ 7\ kPa = 43.95\%$$

$$The\ volume\ of\ treated\ specimen$$

$$\pi * \frac{6.35^2}{4} * 1.9 = 60.17\ cm^3$$

$$The\ volume\ of\ all\ lime\ columns\ of\ treated\ specimen$$

$$19 * \pi * \frac{0.65^2}{4} * 1.3 = 8.20\ cm^3$$

$$The\ volume\ of\ expansive\ soil\ into\ the\ treated\ specimen$$

$$60.17 - 8.20 = 51.97\ cm^3$$

$$The\ expected\ swelling\ potential\ of\ treated\ specimen\ under\ 7\ kPa$$

$$\frac{51.97}{60.17} * 43.95 = 37.96\%$$

$$The\ measured\ swelling\ potential\ of\ treated\ specimen\ under\ 7\ kPa$$

$$= 27.16\%$$

$$The\ improvement\ percentage\ of\ treated\ specimen\ under\ 7\ kPa$$

$$\frac{37.96 - 27.16}{37.96} * 100 = 28.46\%$$

✓ **The calculation of improvement percentage of the M1-h treated specimen under 7 kPa**

Specimens	Swelling potential (%) under 7 kPa
Untreated Specimen	43.95
M1-h	19.41

$$The\ swelling\ potential\ of\ untreated\ specimen\ under\ 7\ kPa$$
$$= 43.95\%$$

$$The\ volume\ of\ treated\ specimen$$
$$\pi * \frac{6.35^2}{4} * 1.9 = 60.17\ cm^3$$

$$The\ volume\ of\ all\ lime\ columns\ of\ treated\ specimen$$
$$19 * \pi * \frac{0.65^2}{4} * 1.9 = 11.98\ cm^3$$

$$The\ volume\ of\ expansive\ soil\ into\ the\ treated\ specimen$$
$$60.17 - 11.98 = 48.19\ cm^3$$

$$The\ expected\ swelling\ potential\ of\ treated\ specimen\ under\ 7\ kPa$$
$$\frac{48.19}{60.17} * 43.95 = 35.20\%$$

$$The\ measured\ swelling\ potential\ of\ treated\ specimen\ under\ 7\ kPa$$
$$= 19.41\%$$

$$The\ improvement\ percentage\ of\ treated\ specimen\ under\ 7\ kPa$$
$$\frac{35.2 - 19.41}{35.20} * 100 = 44.86\%$$

✓ **The calculation of improvement percentage of the M2-2/3h treated specimen under 7 kPa**

Specimens	Swelling potential (%) under 7 kPa
Untreated Specimen	43.95
M2-2/3h	26.32

$$The\ swelling\ potential\ of\ untreated\ specimen\ under\ 7\ kPa = 43.95\%$$

$$The\ volume\ of\ treated\ specimen$$

$$\pi * \frac{6.35^2}{4} * 1.9 = 60.17\ cm^3$$

$$The\ volume\ of\ all\ lime\ columns\ of\ treated\ specimen$$

$$37 * \pi * \frac{0.45^2}{4} * 1.3 = 7.65\ cm^3$$

$$The\ volume\ of\ expansive\ soil\ into\ the\ treated\ specimen$$

$$60.17 - 7.65 = 52.52\ cm^3$$

$$The\ expected\ swelling\ potential\ of\ treated\ specimen\ under\ 7\ kPa$$

$$\frac{52.52}{60.17} * 43.95 = 38.36\%$$

$$The\ measured\ swelling\ potential\ of\ treated\ specimen\ under\ 7\ kPa$$

$$= 26.32\%$$

$$The\ improvement\ percentage\ of\ treated\ specimen\ under\ 7\ kPa$$

$$\frac{38.36 - 26.32}{38.36} * 100 = 31.39\%$$

✓ **The calculation of improvement percentage of the M2-h treated specimen under 7 kPa**

Specimens	Swelling potential (%) under 7 kPa
Untreated Specimen	43.95
M2-h	16.05

$$The\ swelling\ potential\ of\ untreated\ specimen\ under\ 7\ kPa = 43.95\%$$

$$The\ volume\ of\ treated\ specimen$$

$$\pi * \frac{6.35^2}{4} * 1.9 = 60.17\ cm^3$$

$$The\ volume\ of\ all\ lime\ columns\ of\ treated\ specimen$$

$$37 * \pi * \frac{0.45^2}{4} * 1.9 = 11.18\ cm^3$$

$$The\ volume\ of\ expansive\ soil\ into\ the\ treated\ specimen$$

$$60.17 - 11.18 = 48.99\ cm^3$$

$$The\ expected\ swelling\ potential\ of\ treated\ specimen\ under\ 7\ kPa$$

$$\frac{48.99}{60.17} * 43.95 = 35.78\%$$

$$The\ measured\ swelling\ potential\ of\ treated\ specimen\ under\ 7\ kPa$$

$$= 16.05\%$$

$$The\ improvement\ percentage\ of\ treated\ specimen\ under\ 7\ kPa$$

$$\frac{35.78 - 16.05}{35.78} * 100 = 55.14\%$$

C. The Graph Used To Calculate The Coefficient Permeability Of Both Specimen A And Treated Specimen

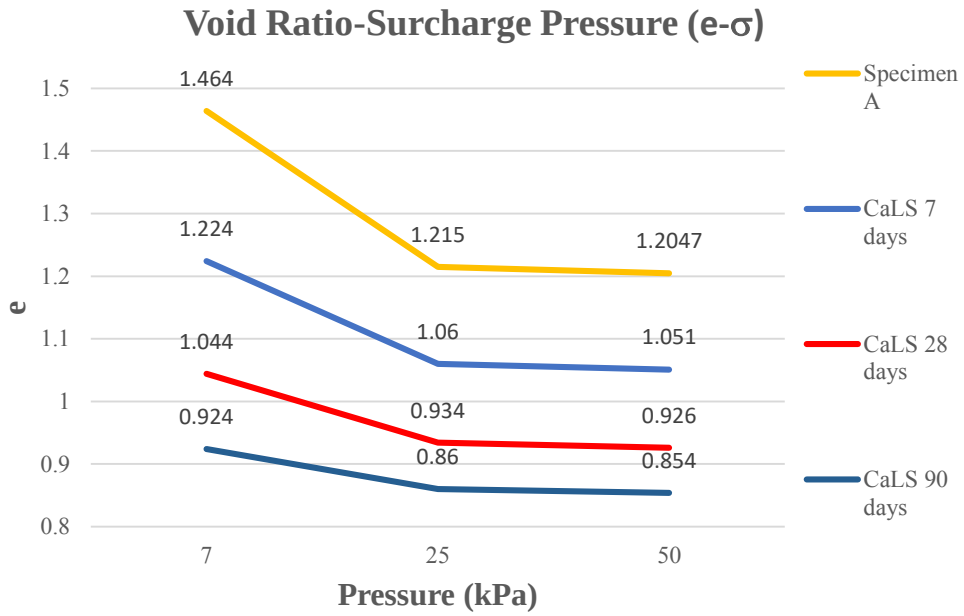

Figure C.1 Void ratio versus consolidation pressure graph for Specimen A and treated specimen with NaLS

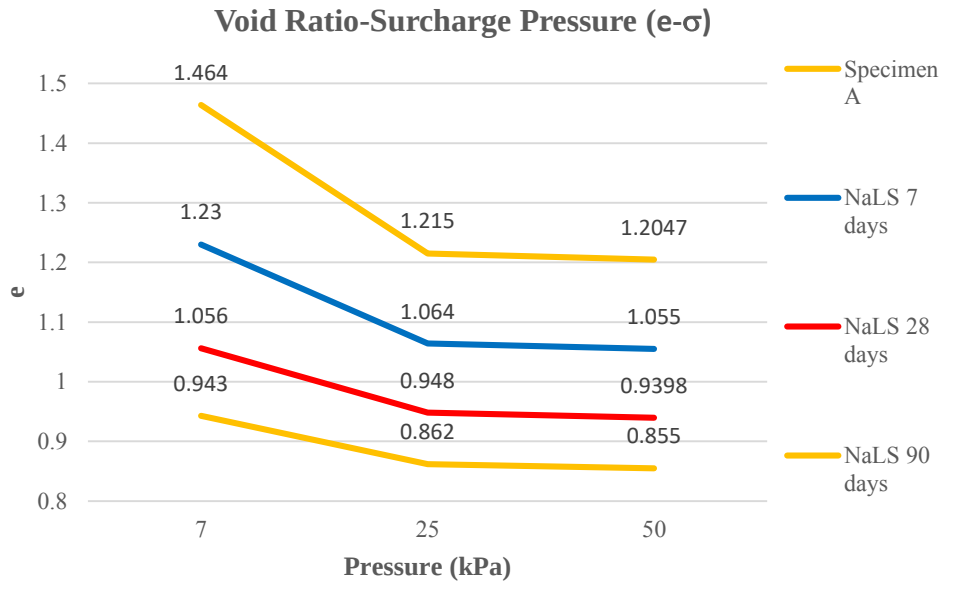

Figure C.2 Void ratio versus consolidation pressure graph for Specimen A and treated specimen with CaLS

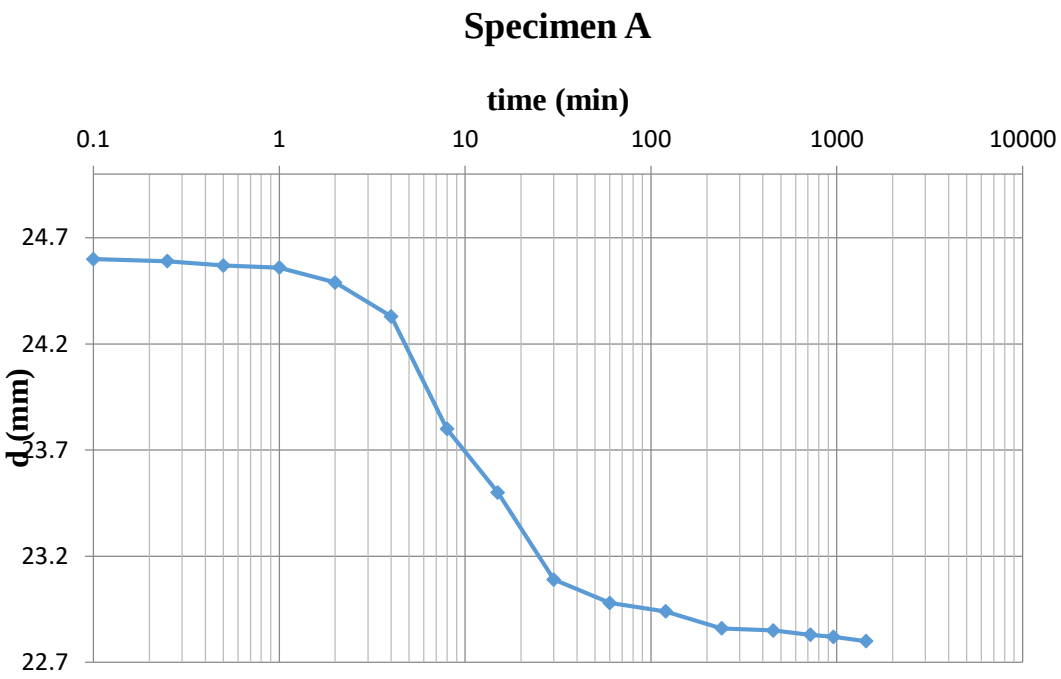

Figure C.3 Displacement versus time graph for Specimen A under 25 kPa

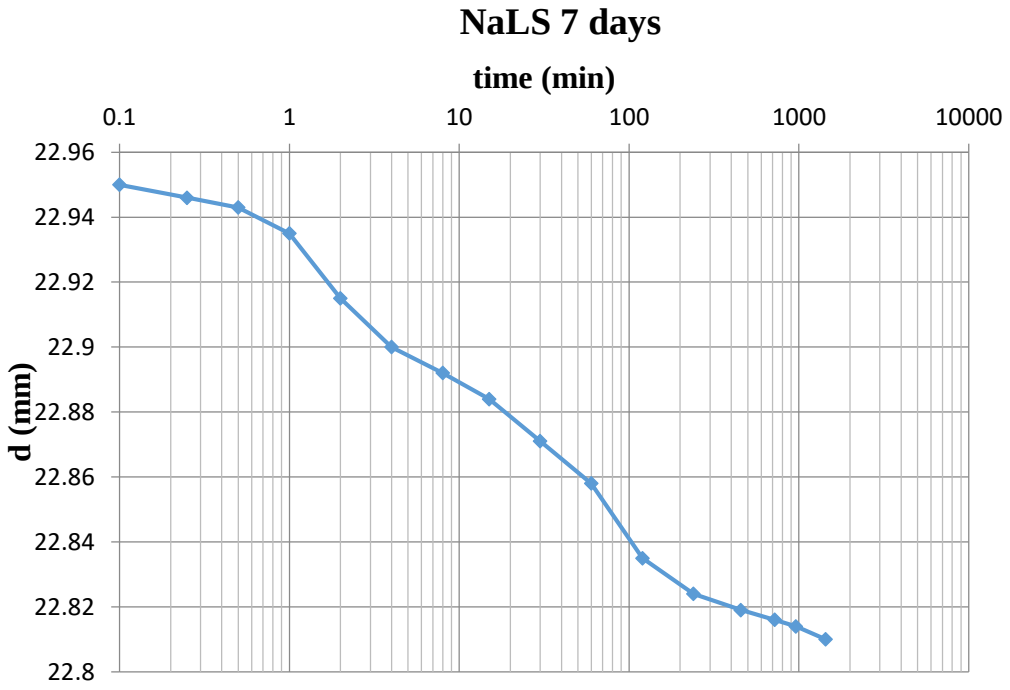

Figure C.4 Displacement versus time graph for treated specimen with NaLS (7 days curing) under 25 kPa

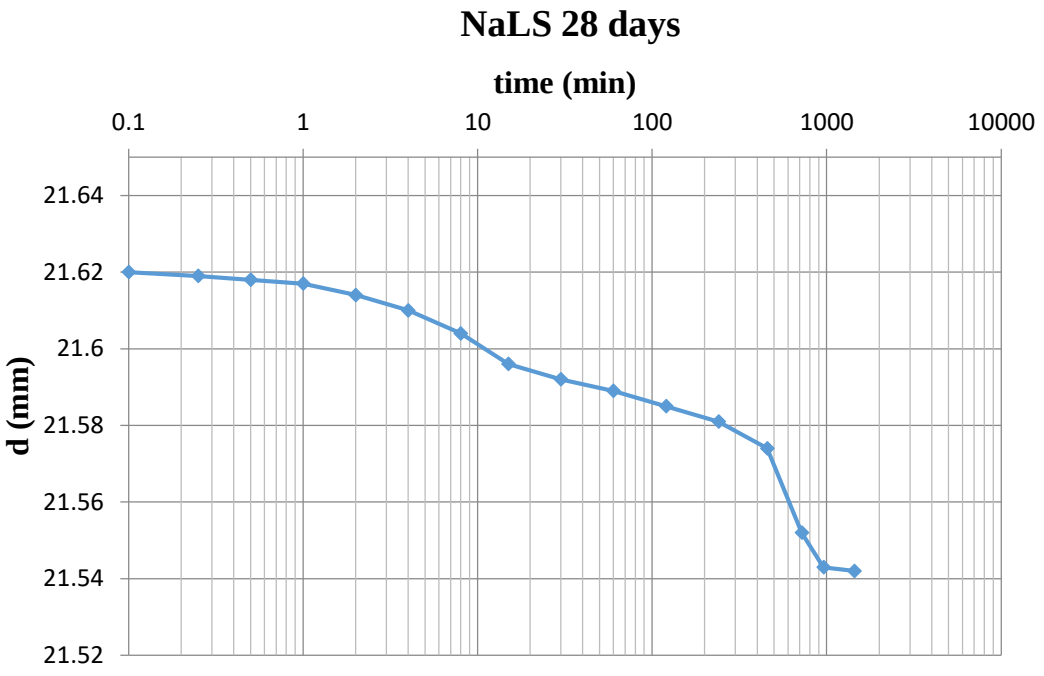

Figure C.5 Displacement versus time graph for treated specimen with NaLS (28 days curing) under 25 kPa

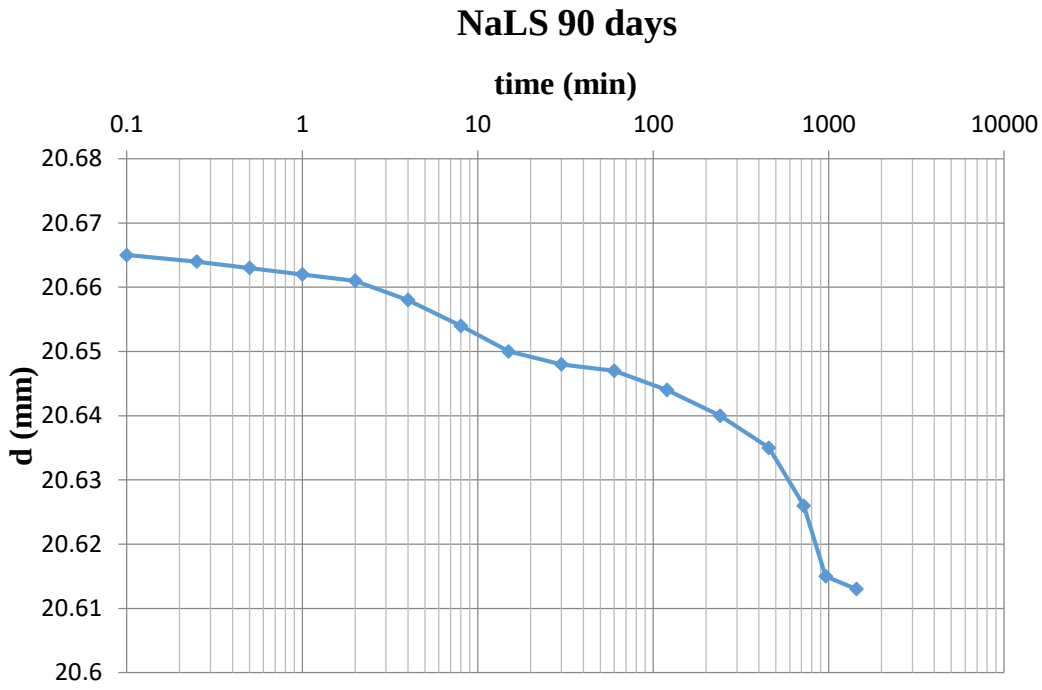

Figure C.6 Displacement versus time graph for treated specimen with NaLS (90 days curing) under 25 kPa

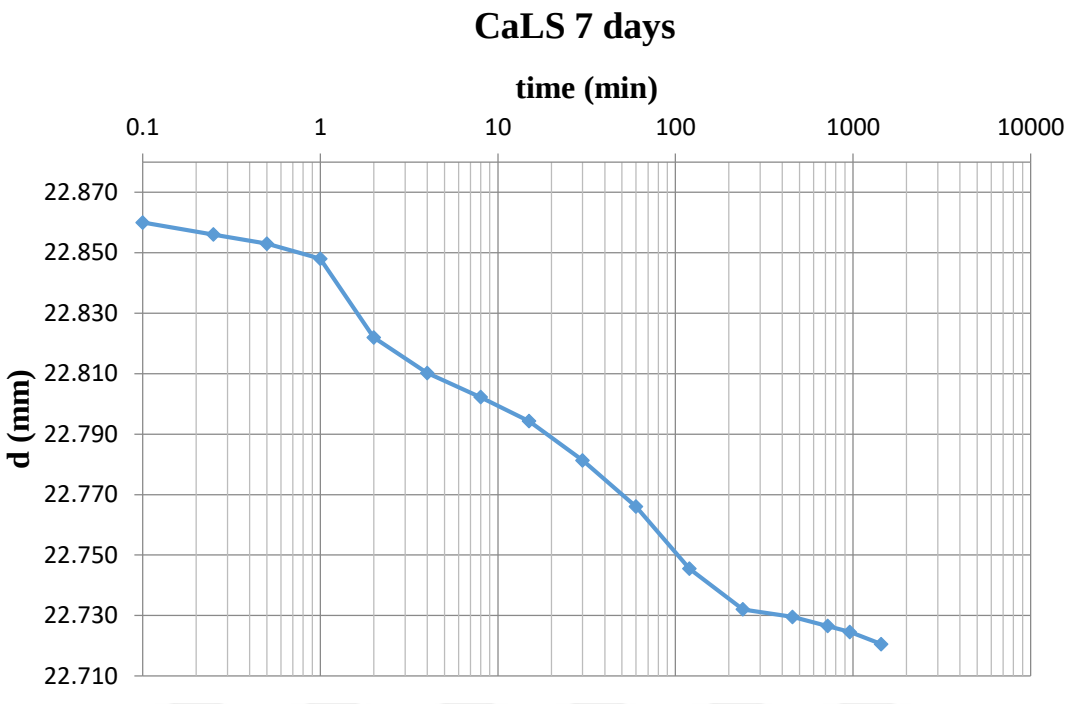

Figure C.7 Displacement versus time graph for treated specimen with CaLS (7 days curing) under 25 kPa

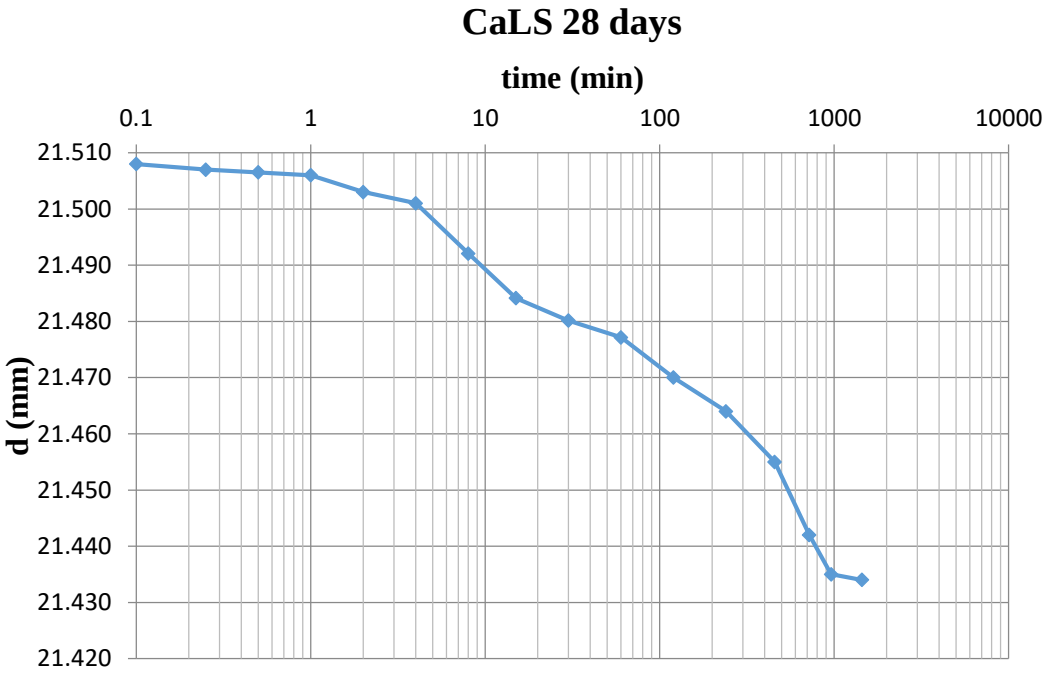

Figure C.8 Displacement versus time graph for treated specimen with CaLS (28 days curing) under 25 kPa

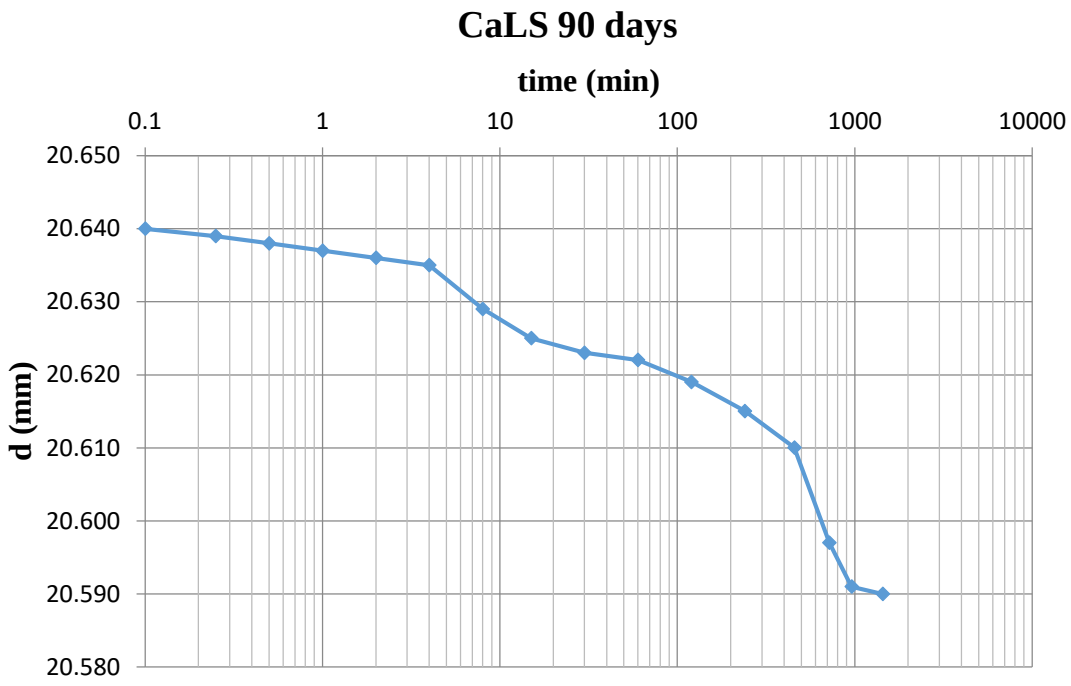

Figure C.9 Displacement versus time graph for treated specimen with CaLS (90 days curing) under 25 kPa

D. The Calculation of the Area Ratio of Combined Improvement Method

✓ This area ratio calculation is based on hexagonal area

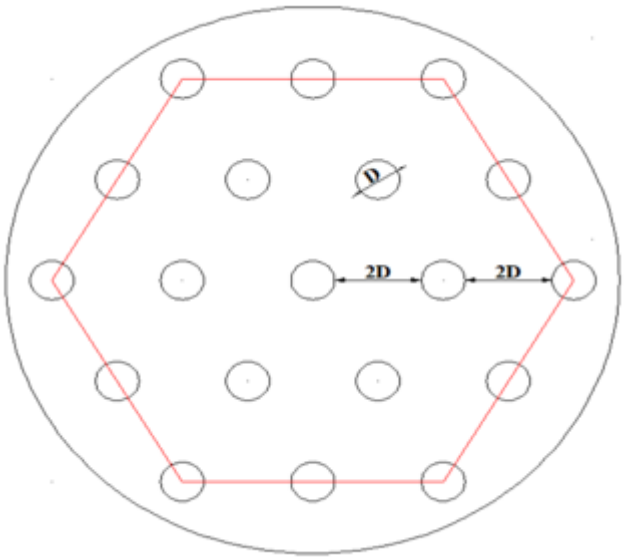

$$Hexagonal\ area$$

$$\frac{6 * (6D^2) * \sqrt{3}}{4} = \frac{6 * (6 * 0.45^2) * \sqrt{3}}{4} = 18.94\ cm^2$$

$$Total\ column\ area$$

$$7 * \left(\frac{\pi * D^2}{4}\right) + 6 * \frac{1}{2} * \left(\frac{\pi * D^2}{4}\right) + 6 * \frac{1}{3} * \left(\frac{\pi * D^2}{4}\right)$$

$$7 * \left(\frac{\pi * 0.45^2}{4}\right) + 6 * \frac{1}{2} * \left(\frac{\pi * 0.45^2}{4}\right) + 6 * \frac{1}{3} * \left(\frac{\pi * 0.45^2}{4}\right) = 1.91\ cm^2$$

$$Area\ Ratio$$

$$\frac{Total\ column\ area}{Hexagonal\ area} = \frac{1.91}{18.94} \cong 0.10\ (10\%)$$

E. The Calculation of the Amount of the Water-Lignosulfonate Mixture for Each Column

The layout of the column installation into the untreated soil is hexagonal. There are many equilateral trigonal prisms formed into this layout (Figure 1).

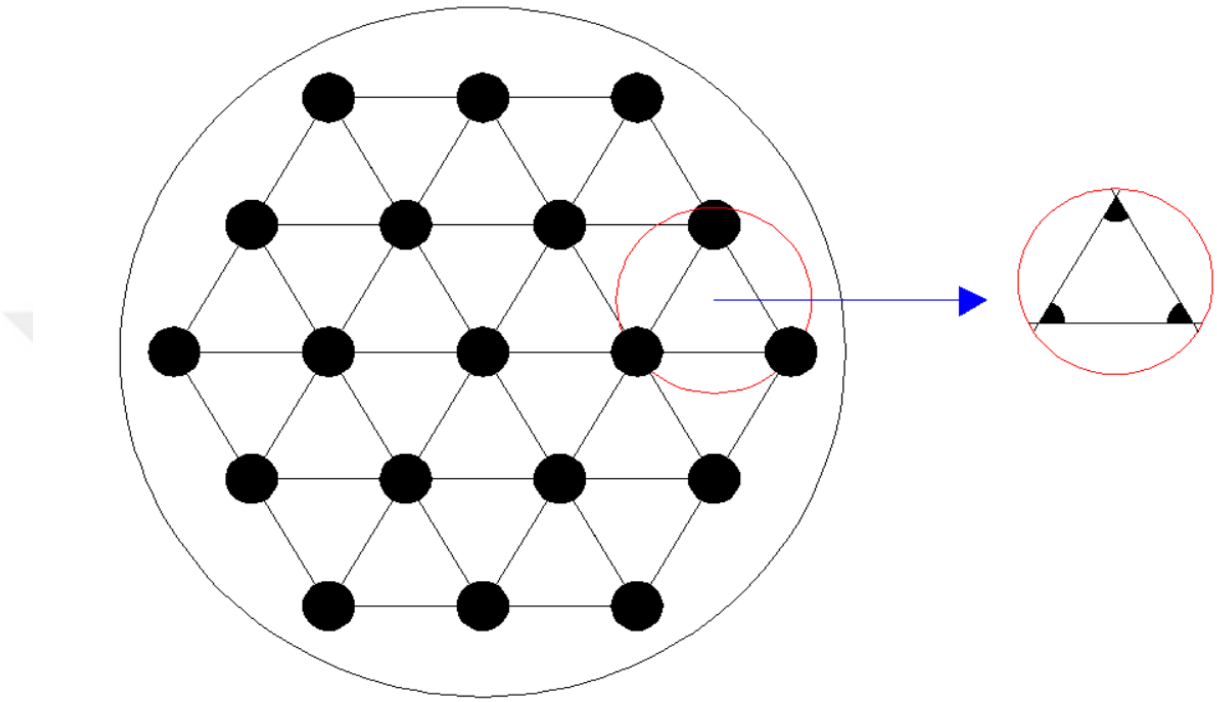

Figure 1. A top view of both hexagonal structure and an equilateral trigonal prism

- The calculation is done with respect to an equilateral trigonal prism. The half of the column supports an equilateral trigonal prism so one column supports two equilateral trigonal prisms.

The water content of untreated soil has to be increased from 15% to the optimum water content of this soil (26%). The dry density of untreated soil is $1.495\ g/cm^3$.

- The calculation of the amount of water-lignosulfonate mixture added to one column is given below. Besides that, one column supports two equilateral trigonal prisms. This calculation is done for soil specimens that had 6.35 cm diameter and 1.9 cm height. The diameter and height of the column at this specimen are 0.45 cm and 1.9 cm, respectively.

$Volume\ of\ two$ equilateral trigonal prisms

$$V_{total} = ((a^2 * \sqrt{3})/4) * h * 2 = ((1.35^2 * \sqrt{3})/4) * 1.9 * 2 = 2.998\ cm^3$$

$Volume\ of\ six\ columns\ had\ 60°\ into\ two$ equilateral trigonal prisms

$$V_c = \left(\frac{\pi * D^2}{4} * \frac{1}{6}\right) * h * (3 * 2) = \left(\frac{\pi * 0.45^2}{4} * \frac{1}{6}\right) * 1.9 * (3 * 2) = 0.302\ cm^3$$

$Volume\ of\ untreated\ soil\ into\ an$ equilateral trigonal prisms

$$V_{us} = V_{total} - V_c = 2.998 - 0.302 = 151 = 2.696\ cm^3$$

$An\ amount\ of\ water\ of\ untreated\ soil\ into\ two$ equilateral trigonal prisms

$$w = 15\% \rightarrow M_{w,0.15} = \rho_d * V_{us} = 1.495 * 2.696 * 0.15 = 0.604\ gram$$

$An\ amount\ of\ water\ of\ untreated\ soil\ had\ optimum\ water\ content\ into\ two$ equilateral trigonal prisms

$$w = 26\% \rightarrow M_{w,0.26} = \rho_d * V_{us} * w = 1.495 * 2.696 * 0.26 = 1.048\ gram$$

$The\ amount\ of\ water\ into\ the\ mixture\ that\ increases\ water\ contentof\ untreated\ soil\ from\ 15\%\ to\ 26\%$

$$M_{w,0.26} - M_{w,0.15} = 1.048 - 0.604 = 0.444\ gram$$

$The\ amount\ of\ calcium\ lignosulfonate\ into\ the\ mixture$

$$M_{CaLS} = \rho_d * V_{us} * 0.02 = 1.495 * 2.696 * 0.02 = 0.08\ gram$$

F. The Calculation of the Improvement Percentages of the Correlation Treated Specimens

✓ **The improvement percentage of the treated specimen is calculated under 7 kPa and 25 kPa, respectively. The data relating to the COR1-NaLS specimen is used for this calculation.**

The calculation of improvement percentage of the treated specimen under 7 kPa

Specimens	Swelling potential (%) under
Untreated Specim	43.95
COR1- NaLS	24.8

$$The\ swelling\ potential\ of\ untreated\ specimen\ under\ 7\ kPa = 43.95\%$$

$$The\ volume\ of\ treated\ specimen$$

$$\pi * \frac{5^2}{4} * 1.9 = 37.30\ cm^3$$

$$The\ volume\ of\ all\ lime\ columns\ of\ treated\ specimen$$

$$37 * \pi * \frac{0.35^2}{4} * 1{,}9 = 6.76\ cm^3$$

$$The\ volume\ of\ expansive\ soil\ into\ the\ treated\ specimen$$

$$37.30 - 6.76 = 30.54\ cm^3$$

$$The\ expected\ swelling\ potential\ of\ treated\ specimen\ under\ 7\ kPa$$

$$\frac{30.54}{37.30} * 43.95 = 35.98\%$$

$$The\ measured\ swelling\ potential\ of\ treated\ specimen\ under\ 7\ kPa$$

$$= 24.8\%$$

$$The\ improvement\ percentage\ of\ treated\ specimen\ under\ 7\ kPa$$

$$\frac{35.98 - 24.8}{35.98} * 100 = 31.07\%$$

✓ **The calculation of improvement percentage of the treated specimen under 25 kPa**

Specimens	**Swelling potential (%) under 7 kPa**
Untreated Specimen	29.47
COR1- NaLS	14.75

$$The\ swelling\ potential\ of\ untreated\ specimen\ under\ 25\ kPa = 29.47\%$$

$$The\ volume\ of\ treated\ specimen$$

$$\pi * \frac{5^2}{4} * 1.9 = 37.30\ cm^3$$

$$The\ volume\ of\ all\ lime\ columns\ of\ treated\ specimen$$

$$37 * \pi * \frac{0.35^2}{4} * 1{,}9 = 6.76\ cm^3$$

$$The\ volume\ of\ expansive\ soil\ into\ the\ treated\ specimen$$

$$37.30 - 6.76 = 30.54\ cm^3$$

$$The\ expected\ swelling\ potential\ of\ treated\ specimen\ under\ 25\ kPa$$

$$\frac{30.54}{37.30} * 29.47 = 24.13\%$$

$$The\ measured\ swelling\ potential\ of\ treated\ specimen\ under\ 25\ kPa$$

$$14.75\%$$

$$The\ improvement\ percentage\ of\ treated\ specimen\ under\ 7\ kPa$$

$$\frac{24.13 - 14.75}{24.13} * 100 = 38.87\%$$

G. EDX diagrams

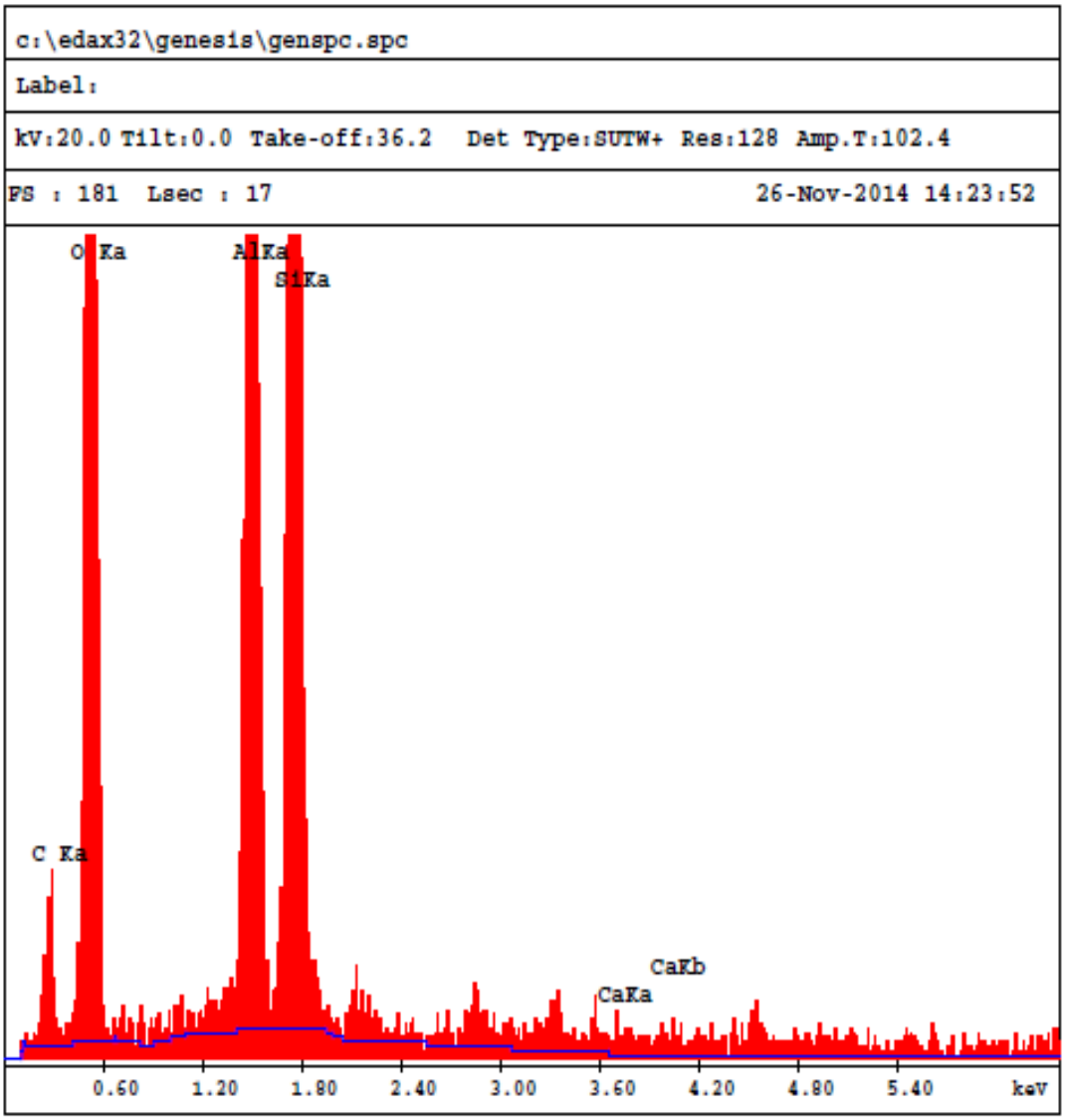

EDAX ZAF Quantification (Standardless)
Element Normalized
SEC Table : Default

Element	Wt %	At %	K-Ratio	Z	A	F
C K	15.97	23.53	0.0270	1.0334	0.1634	1.0005
O K	48.68	53.86	0.1543	1.0161	0.3119	1.0004
AlK	15.57	10.21	0.1084	0.9465	0.7307	1.0072
SiK	19.79	12.22	0.1284	0.9741	0.6796	1.0000
CaK	0.39	0.17	0.0035	0.9445	0.9493	1.0000
Total	100.00	100.00				

Figure G.1 EDX diagram of Specimen A

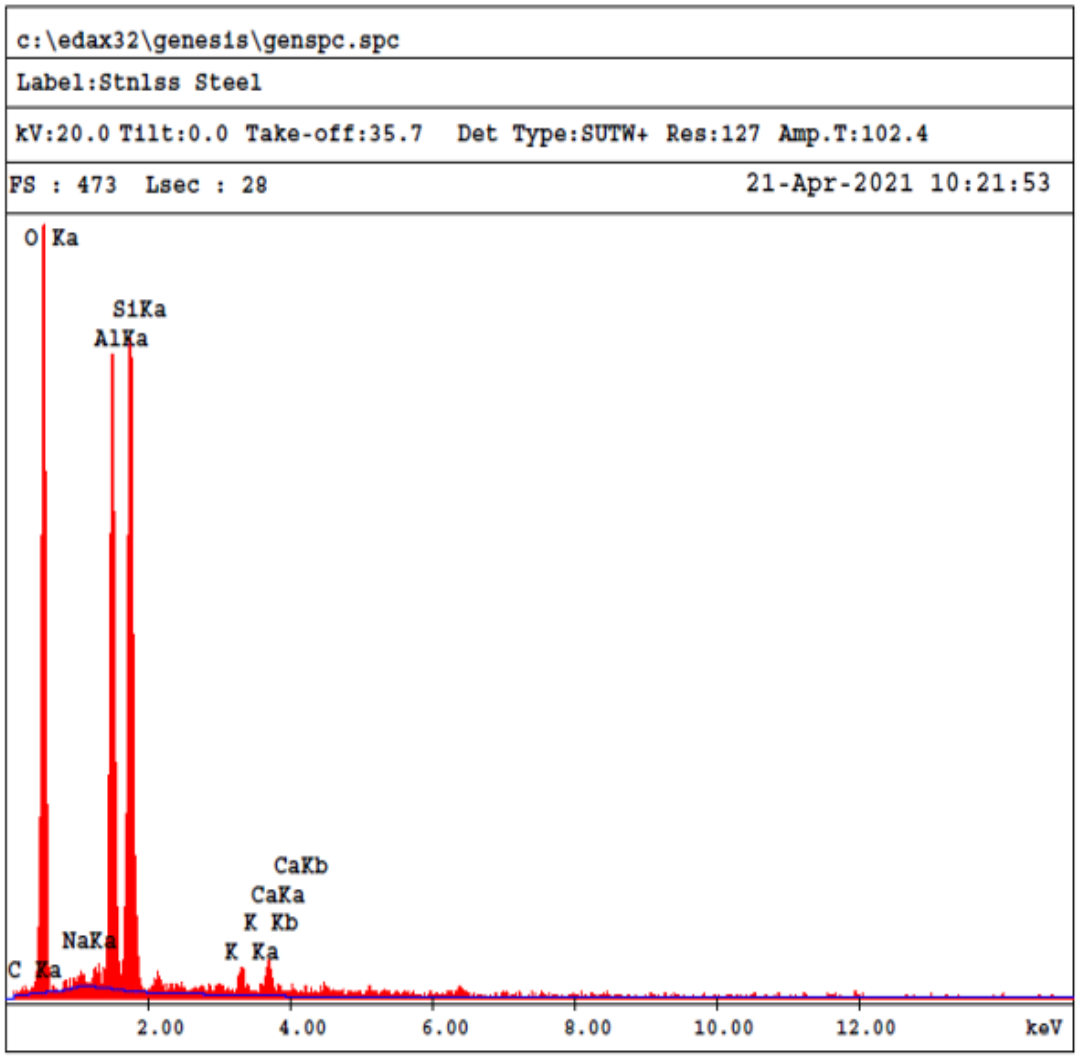

EDAX ZAF Quantification (Standardless)
Element Normalized
SEC Table : Default

Element	Wt %	At %	K-Ratio	Z	A	F
C K	2.25	3.71	0.0032	1.0422	0.1369	1.0006
O K	51.70	63.86	0.1814	1.0247	0.3421	1.0004
NaK	0.25	0.21	0.0010	0.9591	0.4112	1.0049
AlK	18.25	13.36	0.1259	0.9544	0.7168	1.0088
SiK	25.02	17.60	0.1589	0.9822	0.6464	1.0003
K K	0.93	0.47	0.0077	0.9309	0.8908	1.0024
CaK	1.60	0.79	0.0141	0.9530	0.9237	1.0000
Total	100.00	100.00				

Figure G.2 EDX diagram of treated specimen with lime columns

consists of 70% lime and 30% water

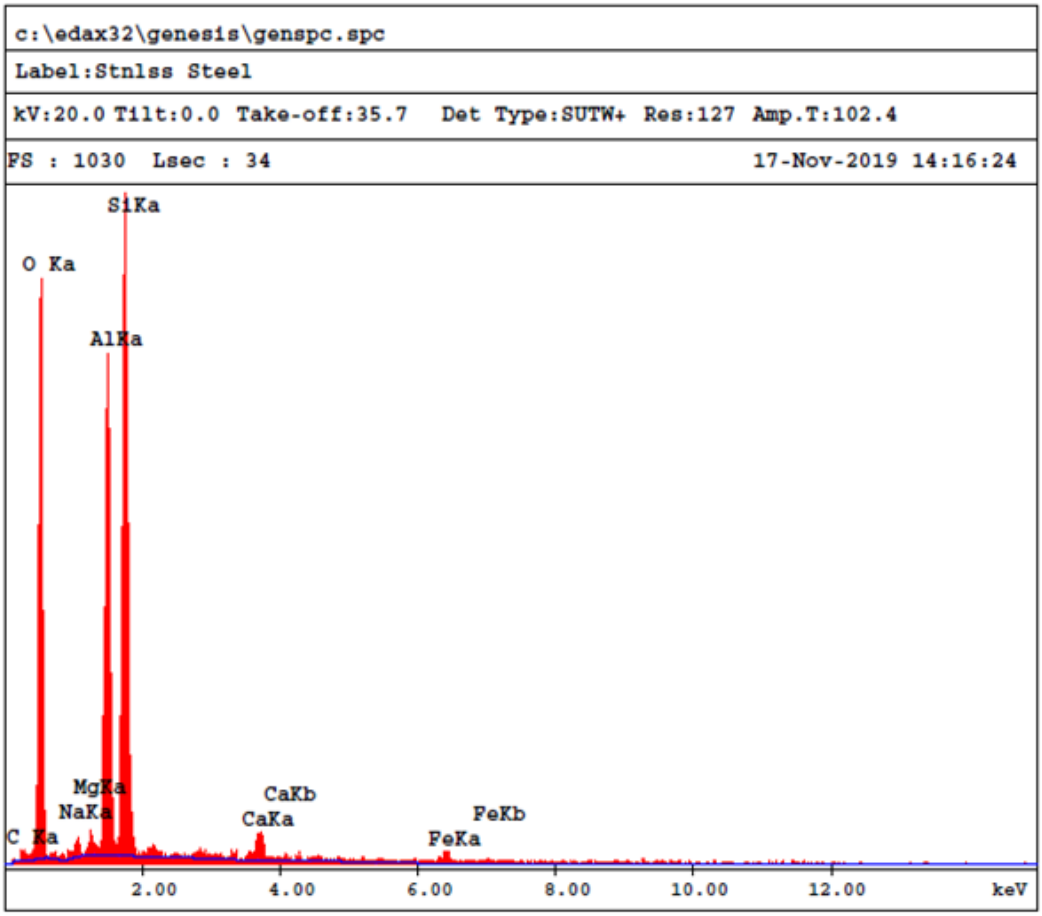

EDAX ZAP Quantification (Standardless)
Element Normalized
SEC Table : Default

Element	Wt %	At %	K-Ratio	Z	A	F
C K	4.34	7.23	0.0060	1.0444	0.1315	1.0005
O K	45.95	57.53	0.1521	1.0269	0.3222	1.0005
NaK	0.94	0.82	0.0038	0.9611	0.4180	1.0050
MgK	0.84	0.69	0.0048	0.9853	0.5690	1.0099
AlK	16.91	12.56	0.1151	0.9564	0.7051	1.0096
SiK	27.59	19.68	0.1767	0.9843	0.6506	1.0002
CaK	1.81	0.91	0.0160	0.9552	0.9225	1.0008
FeK	1.62	0.58	0.0141	0.8674	1.0005	1.0000
Total	100.00	100.00				

Figure G.3 EDX diagram of treated specimen with sodium lignosulfonate lime columns with 180 days curing period

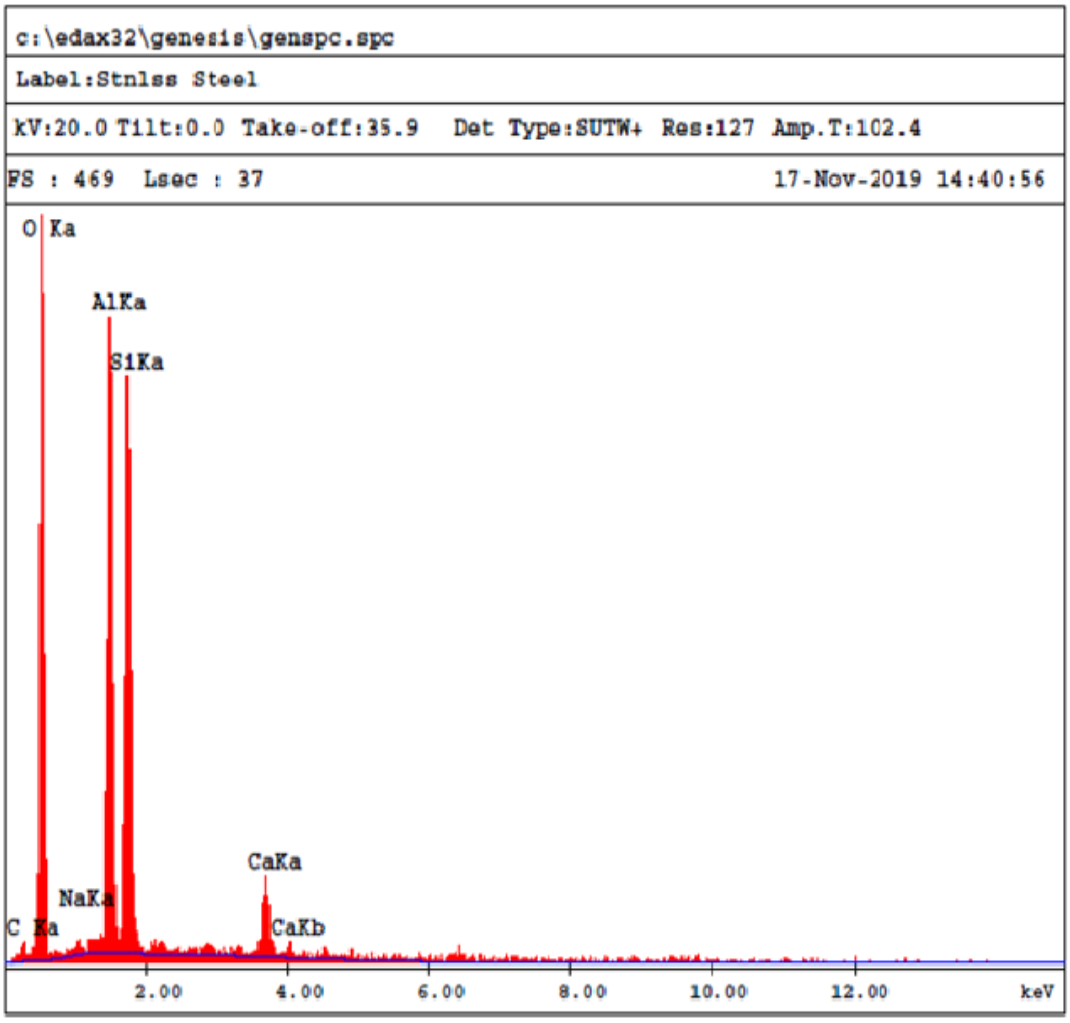

EDAX ZAF Quantification (Standardless)
Element Normalized
SEC Table : Default

Element	Wt %	At %	K-Ratio	Z	A	F
C K	7.08	11.28	0.0110	1.0401	0.1489	1.0006
O K	49.69	59.42	0.1579	1.0227	0.3105	1.0004
NaK	0.52	0.43	0.0020	0.9572	0.4112	1.0045
AlK	18.27	12.96	0.1253	0.9525	0.7144	1.0074
SiK	20.81	14.18	0.1318	0.9803	0.6455	1.0004
CaK	3.63	1.73	0.0324	0.9510	0.9380	1.0000
Total	100.00	100.00				

Figure G.4 EDX diagram of treated specimen with calcium lignosulfonate lime columns with 180 days curing period